Physics Beyond the Standard Model, LHC, and Cosmology

A thesis submitted in partial fulfillment of

the requirements for the degree of

Doctor of Philosophy

by

Chandan Hati

(Roll No. 13330005)

Thesis Supervisor

Prof. Utpal Sarkar

Thesis Co-supervisor

Dr. Namit Mahajan

Theoretical Physics Division

Physical Research Laboratory, Ahmedabad, India.

DISCIPLINE OF PHYSICS

INDIAN INSTITUTE OF TECHNOLOGY GANDHINAGAR

2016

to

My parents

for their selfless love and support

Declaration

I declare that this written submission represents my ideas in my own words and where others' ideas or words have been included, I have adequately cited and referenced the original sources. I also declare that I have adhered to all principles of academic honesty and integrity and have not misrepresented or fabricated or falsified any idea/data/fact/source in my submission. I understand that any violation of the above will be cause for disciplinary action by the Institute and can also evoke penal action from the sources which have thus not been properly cited or from whom proper permission has not been taken when needed.

Signature

Name: Chandan Hati

(Roll No: 13330005)

Date:

CERTIFICATE

It is certified that the work contained in the thesis titled **"Physics Beyond the Standard Model, LHC, and Cosmology"** by **Mr. Chandan Hati** (Roll No. 13330005), has been carried out under our supervision and that this work has not been submitted elsewhere for a degree.

Prof. Utpal Sarkar
(Thesis Supervisor)
Theoretical Physics Division
Physical Research Laboratory,
Ahmedabad, India.

Date:

Dr. Namit Mahajan
(Thesis Co-supervisor)
Theoretical Physics Division
Physical Research Laboratory,
Ahmedabad, India.

Date:

Acknowledgments

First and foremost, I would like to express my sincere gratitude to my Ph.D. advisor, Utpal Sarkar, for taking me as his student and for his guidance, mentoring and especially his unending support and enthusiasm. He is an exceptional physicist and needless to say, I have learned a lot from him over the past three years. His vast knowledge of the subject, simple and intuitive approach to any research problem have influenced me a lot. Not only as a physicist but as a person as well, he has been exceptionally humble, kind, supportive and encouraging. Though he was extremely busy with enormous administrative workload while acting as the Director, PRL, for the last two years, he made time for me whenever I wanted to meet and discuss physics with him. He has been a constant source of encouragement and motivation for me. He patiently listened to my ideas with great enthusiasm and gave me complete freedom and encouragement to take up new research problems. He also often encouraged me to work on independent research problems and gave me the confidence and support to do it. It has been truly a great privilege to be his student.

Next, I would like to thank Namit Mahajan and Raghavan Rangarajan, who have played key parts in completion of this thesis. I am immensely grateful to them for being my DSC committee members and for taking the pain of being my thesis experts. Their valuable comments, criticisms and feedback have immensely helped me in improving my understanding of the subject and this thesis. I am very grateful to Namit for being my thesis co-supervisor and for being a wonderful collaborator. He encouraged my interest in flavor physics, which resulted in a number of collaborative projects on the field. His insights and understanding of the subject have helped me learn many things. I have really enjoyed many long physics and non-physics discussions with him. I am thankful to him for his patience and encouragement. My interaction with Raghu started with a coursework project on cosmology when he introduced me to the beautiful world of cosmology and "Kolb and Turner". He is an excellent teacher and I have learned a lot from him. We have also collaborated on a number of research projects. His basic approach in writing and critical scrutiny of the physics details have taught me a lot. I thank him for his immense patience and many many useful physics and non-physics discussions.

I am very grateful to Frank F. Deppisch and Jose W. F. Valle for giving me the opportunity to collaborate with them and to learn from them. They have taught me a lot of physics. Numerous discussions with them over coffee, sometimes while walking the streets of Valencia, and over Skype made doing physics so much fun. Their great insights into the subject and research styles have influenced and taught me a lot. I hope to continue learning from them in future.

I am thankful to Sudhanwa Patra, Mansi Dhuria, Girish Kumar, Diganta Das, and Arnab Dasgupta for many wonderful collaborations. I am really grateful to them for their enthusiasm and countless stimulating discussions. I sincerely thank them for all the things that I have learned from them.

I must thank Srubabati Goswami for her encouragement and guidance during my M.Sc. summer project, which greatly motivated me to take up a research career in high energy physics. I will always be grateful to her. I am also grateful to Subhendra Mohanty, Partha Konar, Dilip Angom, Bijaya K Sahoo, Navinder Singh for teaching various theoretical courses during my Ph.D. tenure. I also thank all the other (present and past) faculty members of Theoretical Physics Division, PRL, including Anjan S. Joshipura, Saurabh D. Rindani, Hiranmay Mishra, Jitesh Bhatt for their help and support. I must also thank Mr. Raza-ahmed Maniar, Ms. Bhagyashree Jagirdar, and Mrs. Sujata Krishna for numerous help in official matters related to the Division. I sincerely thank the whole Theoretical Physics Division, PRL, for providing a free and fertile research environment.

I thank Jay Banerji, Goutam K. Samanta, Ravindra P. Singh, M. G. Yadava, J. S. Ray, Som K. Sharma, Smitha V. Thampi, Shashikiran Ganesh, Sachindra Naik, N. M. Ashok, Bhuwan Joshi, Ramitendranath Bhattacharyya, Brajesh Kumar, Shibu K. Mathew for teaching me various courses (other then theoretical physics) during the coursework. This gave me an unique opportunity to learn about different research activities going on at PRL.

I thank Arko Roy for helping me with the formatting of this thesis and Ujjal Dey for carefully proofreading the introduction. They have helped and guided me in several ways throughout the whole course of preparation of this thesis. I am thankful to Avdesh Kumar, Girish Kumar, Chandan Gupta, and Arko Roy for sharing office space with me. I thank them for bearing with my gossips and for keeping an energizing working atmosphere at the office.

I remain grateful to the Director, Dean, Academic Committee for the academic & non-academic support and for all the help I got throughout my Ph.D. tenure of three years. Thank you for providing all the necessary facilities and a healthy atmosphere. I am thankful to Bhushit G. Vaishnav for his continuous support since I joined PRL as a Ph.D. student. I would also like to thank all the academic and administrative staff at PRL and IIT Gandhinagar (IIT-GN) for their numerous help. I am deeply indebted to the PRL and IIT-GN Library staff for all the facilities. I thank all the members of the Computer Center, PRL for their endless advice, support and cooperation.

In these three years spent at PRL I have grown close to many wonderful people and certainly it is impossible to do justice in properly acknowledging all of them. So before I start, I apologize for that.

I must start with Arko Roy, Monojit Ghosh, Tanmoy Chattopadhyay, Naveen Negi, and Ujjal Dey, who are like big brothers to me. I treasure and cherish countless amazing and fun hours spent with them. The late night hangouts and parties at Thaltej Hostel with Arko da, Mono da, Tanmoy da and Naveen bhaiya were something that kept me going during hard and tiring times. The amazing company of Ujjal da, Nabyendu da and Sudip da during countless feasts, parties and trips is something that I am really grateful for. I thank Girish Kumar for innumerable cups of coffee and chats over my unannounced visits. I also thank Arvind Singh for hosting many amazing parties and for many interesting discussions over cocktails; Gautam Samanta for his sports enthusiasm and amazing mutton parties; Priyanka Chaturvedi and Shweta Srivastava for inviting me to many cooking parties. I must also mention my juniors Subir and Kaustav, who are fun to be around. Thank you guys for all the fun, thrill and excitement.

Next, I would like to thank my batch mates at PRL, Navpreet, Rukmani, Rupa, Ali, Jabir, Kuldeep, Kumar, Prahlad, and Satish who made Thaltej Hostel feel like home and are nothing less than my second family. I will always cherish countless happy memories spent with you guys. It has been a privilege to be a part of such an amazing group of wonderful people. Without your support and encouragement this thesis would not have been possible.

There are many other wonderful people at PRL with whom I have had the opportunity to interact with. An incomplete list consists of my seniors Soumya Rao, Bhaswar Chatterjee, Tanushree Basak, Susanta K. Bisoi, Sunil Chandra, Amarendra Pandey, Arun Awasthy, Gulab Bhambaniya, Girish Chakravarty, Gaurav Tomar, Wageesh Mishra, Dillip K. Nandy, Yashpal Singh, Bhavya PS., Salla Gangi Reddy, A Aadhi, Shashi Prabhakar, Upendra K. Singh, Abhaya Swain, Tanmoy Mondal, Arun K. Pandey, Gaurav Jaiswal, Manu George, Kuldeep Suthar, Guruprasad Kadam, Chithrabhanu P., Ikshu Gautam, Shraddha Band, Anirban Chatterjee, Alok R. Tiwary, Sanjay Kumar, Bivin G. George, Venkatesh Chinni, Deepak K. Karan, Dipti R. Raut, Newton Nath, Pankaj Bhalla, Apurv Chaitanya N., Jiniya Sikhdar, Chandana K. R., Lalit K. Shukla, Rahul Yadav; my juniors Bhavesh, Bharti, Aman, Vishnudath, Pradeep, Soumik, Niharika, Anil, Nijil, Akanksha, Arvind, Balbeer, Aarthy, Archita, Shivangi, Nidhi, Shefali, Varun; and postdocs at theoretical physics division Anant Mishra, Gaveshna Gupta, Gaurav Goswami, Abhishek Atreya, Ila Garg, Manpreet Singh, Laxmi, Rahul Srivastava.

I feel privileged to acknowledge my dear friend Sumanta Chakraborty, IUCAA, for his enthusiastic friendship. He has been a constant source of motivation and inspiration to me. Thank you for being there and for all the things I have learned from you. I also thank Soumyajit Roy for his wonderful company during M.Sc. and afterwards. Thank you for being the mature guy; without you our triangle is not complete. I would like to also thank Pritish K. Mishra, NCRA, for his support and friendship since my B.Sc. days. Thank you for patiently listening to all my nonsense blabbering. I also thank my home-squad friends Indranil, Niladri and Kuntal. Without you life at home would have been very boring. Thank you for your never ending friendship. I am grateful to Sudha for her continuous support and immense patience. Thank you for making me smile during the hard times.

Last but not the least, I express my deepest thanks and gratitude to my parents, Uttam Hati and Tripti Rani Hati, for their never ending support and love. Thank you for letting me chase my dreams. Without your selfless sacrifices this thesis would not have been a reality. Thank you for always being there for me. I am immensely grateful to my choto mama, Sujit K. Ghosh, for his support and enthusiasm throughout my career. Thanks for always standing by me. Finally, I would like to remember my deceased grandparents Anadi Hati, Durga Rani Hati, Adyanath Ghosh and express my deepest thanks to my grandmother Pratima Rani Ghosh for their unconditional love and affection.

Chandan

Abstract

The Standard Model (SM) of particle physics has been highly successful in explaining most of the experimental measurements in elementary particle physics. It has survived decades of precision tests at highest available energies and with the discovery of the Higgs boson in 2012 at the Large Hadron Collider (LHC) the last missing piece of the SM was confirmed. However, the SM suffers from a number of shortcomings, which strongly suggest that the SM is only an effective limit of a more fundamental theory of interactions. The aim of this thesis is to study various aspects of the physics beyond the SM ranging from the phenomenological implications of viable models to cosmological implications such as the matter-antimatter asymmetry of the universe, dark matter, and dark energy.

In this thesis we study several models beyond the SM in the contexts of LHC phenomenology, neutrino masses, flavor anomalies associated with B-decays and gauge coupling unification. We also study the possibilities of explaining the matter-antimatter asymmetry via baryogenesis (leptogenesis) mechanisms in these models. We also touch upon the issues of potential candidates for dark matter and the realization of dark energy in models beyond the SM.

We study the implications of a right handed charged gauge boson $W_R^\pm$ with mass of around a few TeV for leptogenesis. We point out how the discovery of a TeV scale $W_R^\pm$ will rule out all possibilities of leptogenesis in all classes of the left-right symmetric extensions of the SM due to the unavoidable fast gauge mediated $B-L$ violating interactions. We also study the framework of LRSM with additional scalar singlets and vector-like fermions in the context of the recent LHC excess signals and the phenomenological implications for the fermion masses and mixing. We also discuss how the introduction of a real bi-triplet scalar, which contains a potential DM candidate, can allow gauge coupling unification. Furthermore, we point out that the existence of new vector-like fermions can also have interesting implications for baryogenesis and the dark matter sector.

The effective low energy left-right symmetric subgroups of the superstring inspired E_6 model provide a rich phenomenology, thanks to many additional exotic fields including leptoquarks. We systematically study these low energy subgroups in the con-

text of the LHC excess signals reported by the CMS collaboration, and high scale leptogenesis. We also study the left-right symmetric low energy subgroups of E_6 in the context of recent experimental results from the LHCb, BaBar and Belle collaborations on the decays of the B mesons: $\bar{B} \to D^{(*)}\tau\bar{\nu}$ and $\bar{B} \to \bar{K}ll$, showing significant deviations from the SM, which hint towards a new physics scenario beyond the SM. We use the leptonic decays $D_s^+ \to \tau^+\bar{\nu}$, $B^+ \to \tau^+\bar{\nu}$, $D^+ \to \tau^+\bar{\nu}$ and D^0-$\bar{D}^0$ mixing to constrain the couplings involved in explaining the enhanced B decay rates. We also study the E_6 motivated $U(1)_N$ extension of the supersymmetric SM in the context of the LHC excess signals and the baryon asymmetry of the universe. In light of the hint, from short-baseline neutrino experiments, of the existence of one or more light sterile neutrinos, we also study the neutrino mass matrices, which are dictated by the discrete symmetries in the variants of this model.

We study a cogenesis mechanism in which the observed baryon asymmetry of the universe and the dark matter abundance can be produced simultaneously at a low reheating temperature without violating baryon number in the fundamental interactions. This mechanism can also provide a natural solution for the cosmic coincidence problem. We also present a realization of mass varying neutrino dark energy in two simple extensions of the SM, where the SM is extended to include new TeV scale triplet scalars and fermions, respectively. We also discuss the possible leptogenesis mechanisms for simultaneously generating the observed baryon asymmetry of the universe in both the scenarios and the collider signatures for the new TeV scale fields.

Contents

Acknowledgments **1**

Abstract **5**

Contents **7**

List of Figures **11**

List of Tables **17**

1 Introduction **19**

1.1 The Standard Model of particle physics 19

1.1.1 Spontaneous symmetry breaking and masses of the gauge bosons 22

1.1.2 Fermion masses and mixing 24

1.1.3 Limitations of the Standard Model 25

1.2 Physics beyond the Standard Model 27

1.2.1 Neutrino masses 27

1.2.2 Left-Right Symmetric Models 32

1.2.3 Grand unified theory 36

1.2.4 Supersymmetry 44

1.3 Cosmological implications of physics beyond the Standard Model . . 50

1.3.1 Baryon Asymmetry of the universe and baryogenesis 51

1.3.2 Dark matter and dark energy 63

1.4 Potential hints of new physics from the LHC and flavor physics 65

1.4.1 Potential signals of new physics at the LHC 66

1.4.2 Flavor anomalies pointing to new physics beyond the SM . . . 68

1.5 Objectives and overview of the chapters 69

2 Probing Left-Right Symmetric Models at the LHC and implications for leptogenesis 73

2.1 Falsifying leptogenesis with a TeV-scale $W_R^{\pm}$ at the LHC 75

2.1.1 Wash out of lepton asymmetry for $T > M_{W_R}$ 80

2.1.2 Wash out of asymmetry for $T < M_{W_R}$ 81

2.2 Summary of the chapter 83

3 Left-Right Symmetric Model in light of the diphoton excess, unification and baryogenesis 85

3.1 Left-Right Symmetric Model framework with vector-like fermions . . 87

3.2 Diphoton signal from a scalar resonance 90

3.3 Gauge coupling unification 93

3.4 Implications for baryogenesis and dark matter 95

3.5 Summary of the chapter 99

4 Left-Right Symmetric low-energy subgroups of E_6 in light of LHC and baryogenesis 101

4.1 Left-right symmetric low-energy subgroups of E_6 104

4.1.1 Conventional Left-Right Symmetric Model like case 105

4.1.2 Alternative Left-Right Symmetric Model 106

4.1.3 Neutral Left-Right Symmetric Model 110

4.2 Exotic sparticle(s) production leading to an $eejj(e\not{p}_T jj)$ signal 115

4.3 Explaining the diphoton excess in Alternative Left-Right Symmetric Model 117

4.4 Leptogenesis in supersymmetric low energy E_6-subgroups 122

4.5 Summary of the chapter 125

5 Explaining the B-decay anomalies in the left-right symmetric low energy subgroups of E_6 127

5.1 Explaining $\overline{B} \to D^{(*)}\tau\overline{\nu}$ excesses in Alternative Left-Right Symmetric Model 128

5.1.1 The effective Hamiltonian for $\overline{B} \to D^{(*)}\tau\overline{\nu}$ decay 129

5.1.2 Analysis of the operators mediating $\overline{B} \to D^{(*)}\tau\overline{\nu}$ in ALRSM . 130

5.1.3 Constraints from B, D decays and $D^0 - \overline{D}^0$ oscillations . . . 131

5.1.4 λ_{33j}-λ_{32j} parameter space explaining both R_{D^*} and R_D data . 136

5.2 Explaining $R_{D^{(*)}}$, R_K and $(g-2)_\mu$ anomalies in the Neutral Left-Right Symmetric Model 137

5.2.1 Explaining $R_{D^{(*)}}$ anomalies in NLRSM 138

5.2.2 Explaining R_K anomaly and constraints from $B_s^0 - \overline{B}_s^0$ mixing 140

5.2.3 Explaining anomalous muon magnetic moment 141

5.3 Summary of the chapter 142

6 Addressing the LHC excesses, baryogenesis and neutrino masses in E_6 motivated $U(1)_N$ model 143

6.1 $U(1)_N$ extension of supersymmetric Standard Model 144

6.2 Discrete symmetries and variants of $U(1)_N$ model 146

6.2.1 Model 1 148

6.2.2 Model 2 149

6.2.3 Model 3 150

6.2.4 Model 4 150

6.2.5 Model 5 and 6 151

6.2.6 Model 7 and 8 152

6.3 Explaining the CMS $eejj$ (and $e\not{p}_T jj$) excess(es) 153

6.4 ATLAS and CMS diboson and dijet excesses 154

6.5 Baryogenesis (via leptogenesis) in $U(1)_N$ models 156

6.6 Neutrino masses 160

6.7 Summary of the chapter 164

7 Correlating the baryon asymmetry of the universe with the dark matter abundance 167

7.1 Cogenesis of baryon asymmetry and dark matter from moduli decay . 168

7.1.1 Cogenesis mechanism 171

7.1.2 Annihilation of the symmetric dark matter component 176

7.2 Summary of the chapter . . . 178

8 Neutrino dark energy and leptogenesis with TeV scale triplets 179
8.1 Neutrino masses and the dark energy connection . . . 181
8.1.1 Model A . . . 182
8.1.2 Model B . . . 183
8.1.3 Realization of neutrino dark energy . . . 185
8.2 Leptogenesis . . . 187
8.3 Collider signatures . . . 191
8.4 Summary of the chapter . . . 193

9 Scope for future studies 195

10 Epilogue 197

Bibliography 199

List of Publications 233

Publications attached with thesis 235

List of Figures

1.1 one-loop correction to the Higgs squared mass parameter due to a Dirac fermion f. . . . 26

1.2 (left) one-loop diagram diagram generating neutrino mass in Zee model. (right) Two loop diagram generating neutrino mass in Zee-Babu model. 31

1.3 The one-loop evolution of the gauge coupling constants in the minimal $SU(5)$ grand unified theory. . . . 42

1.4 An example of gauge boson mediated proton decay $p \to e^+\pi^0$. 43

1.5 One-loop correction to the Higgs squared mass parameter due to a scalar s. . . . 46

1.6 Tree level and one-loop vertex diagrams contributing to the vertex type CP violation in models with right handed neutrinos. . . . 58

1.7 Tree level and one-loop self-energy diagrams contributing to the CP violation in models with right handed neutrinos. . . . 59

1.8 Tree level and one-loop self-energy diagrams contributing to the CP violation in a model with triplet Higgs. . . . 62

2.1 Feynman diagrams for $e_R^- W_R^+ \to e_R^+ W_R^-$ scattering mediated by N_R and Δ_R^{++} fields. The Feynman diagrams for $e_R^- e_R^- \to W_R^- W_R^-$ are the same as above with appropriate change in direction of the external lines. 79

2.2 Plot showing K as a function of temperature (T) with $M_{W_R} = 2.1$ TeV for the scattering processes $e_R^\pm W_R^\mp \to e_R^\mp W_R^\pm$ and $e_R^\pm e_R^\pm \to W_R^\pm W_R^\pm$ (including both Δ_R^{++} and N_R mediated diagrams) for $v_R > T > M_{W_R}$. 81

2.3 Plots showing the out-of-equilibrium temperature (T) of the scattering process $e_R^{\pm} W_R^{\mp} \to e_R^{\mp} W_R^{\pm}$ (mediated via Δ_R^{++} and N_R fields) as a function of M_{W_R} for three different values of M_{Δ_R} and $M_{N_R} \sim M_{W_R}$. 82

3.1 Gauge coupling running in the considered model accommodating the diphoton excess, demonstrating successful gauge unification at the scale $M_{\rm GUT} = 10^{17.75}$ GeV with an intermediate left-right symmetry breaking scale at 10 TeV. The dashed lines correspond to one loop RGE of gauge couplings while the two loop effects are displayed in solid lines. 95

4.1 Box diagrams in the ALRSM contributing to $D^0 - \bar{D}^0$ mixing. 108

4.2 s- and t-channel Feynman diagrams for the process: $g + u \to h + W_{R'}$. 109

4.3 Tree level flavor changing neutral-current processes due to mixing of the six quarks, d, s, b and exotic quarks: h_i $(i = 1, 2, 3)$. 112

4.4 Box diagrams leading to $\bar{d}s - \bar{s}d$ mixing if only exotic $h_i (i = 1, 2, 3)$ mix. 112

4.5 Loop diagrams involving exotic fermions and W_N leading to $\mu \to e\gamma$. 113

4.6 s- and t-channel Feynman diagrams for the process: $g + d \to h + W_N$. 113

4.7 s- and t-channel Feynman diagrams for the process: $e^+e^- \to W_N^+ W_N^-$. 115

4.8 R-parity conserving Feynman diagrams for a single exotic particle $\tilde{E}$ production leading to both $eejj$ and $e\not{p}_T jj$ signals. 116

4.9 $pp \to \tilde{n}$ production cross section in gluon fusion at $\sqrt{s} = 13\,\text{TeV}$ as function of scalar leptoquark mass and $\lambda_3^{\tilde{h}}$. The numbers in the boxes are the production cross sections corresponding to the contours. . . . 119

4.10 The branching fraction as a function of slepton mass $M_{\tilde{E}}$ and scalar leptoquark mass $M_{\tilde{h}}$ with $\lambda_3^{\tilde{h}} = \lambda_5^{\tilde{E}} = 14$. The numbers in the boxes are the branching fractions corresponding to the contours. 121

4.11 The production cross section times branching ratio $\sigma(pp \to \tilde{n}) \times \mathrm{BR}(\tilde{\mathrm{n}} \to \gamma\gamma)$ as a function of scalar leptoquark mass $M_{\tilde{h}}$ (for three different values of slepton mass $M_{\tilde{E}}$) with $\lambda_3^{\tilde{h}} = \lambda_3^{\tilde{E}} = 14$, $\theta_{\tilde{h}} = \theta_{\tilde{E}} = \pi/4$. The pink band corresponds to the observed value of $\sigma(pp \to \tilde{n}) \times \mathrm{BR}(\tilde{\mathrm{n}} \to \gamma\gamma) = 2 - 8$ fb, corresponding to 95% CL upper limit on the allowed cross section at 13 TeV. 122

4.12 Loop diagrams for N_k decay. 124

5.1 Feynman diagrams for the decays $\bar{B} \to D^{(*)}\tau\bar{\nu}$ induced by the exchange of scalar leptoquark ($\tilde{h}^*$) and slepton ($\tilde{E}$). 131

5.2 A plot showing the dependence of the observables $R_{D^{(*)}}$ on $C^{\tau}_{S_L}$: red (blue) curve corresponds to R_D (R_{D^*}) corresponding to $C^{\tau}_{S_L}$, and the horizontal red (blue) band corresponds to the experimentally allowed 1σ range. No common region exists for $C^{\tau}_{S_L}$ which can simultaneously explain both R_D and R_{D^*} data. 132

5.3 A plot showing the dependence of the observables $R_{D^{(*)}}$ on $C^{\tau}_{V_L}$: red (blue) curve corresponds to R_D (R_{D^*}) corresponding to $C^{\tau}_{V_L}$, and the horizontal red (blue) band corresponds to the experimentally allowed 1σ range. $C^{\tau}_{V_L}$ can simultaneously explain both R_D and R_{D^*} data. . . 133

5.4 Feynman diagram for the decay $B \to \tau\nu$ induced by the exchange of the scalar leptoquark $\tilde{h}^{j*}$. 133

5.5 Feynman diagram for the decay $D_s^+ \to \tau\nu$ induced by scalar leptoquarks. The diagram for the decay $D^+ \to \tau\nu$ can be obtained by replacing the s quark by a d quark. 134

5.6 Feynman diagrams inducing $D^0 - \bar{D}^0$ mixing in ALRSM. 136

5.7 The parameter space of λ_{33j}-λ_{32j} explaining the experimental data on $\mathcal{R}(D^{(*)})$ for $m_{\tilde{h}^{j}*} = 1000\,\mathrm{GeV}$. The deep blue band corresponds to the allowed parameter space from R_D data, and the orange band shows the allowed parameter space explaining both R_{D^*} and R_D data simultaneously. The light blue shaded rectangles correspond to λ_{33j}-λ_{32j} parameter space for different values of λ_{31j} (marked on top of the allowed upper boundary shown in dashed lines) allowed by the current measurement of the decay rates of $B \to \tau\nu$, $D_s \to \tau\nu$, $D^+ \to \tau\nu$, and $D - \bar{D}$ mixing. 137

5.8 $\lambda^6_{33k} - \lambda^6_{23k}$ parameter space compatible with $R_{D^{(*)}}$ data and constraints from $B \to \tau\nu$, $D_s^+ \to \tau\nu$ and $D^0 - \bar{D}^0$ mixing. 140

5.9 Representative diagrams for $b \to s\ell\ell$ transition. 141

6.1 Feynman diagram for a single exotic particle $\tilde{E}$ production leading to $eejj$ signal. 153

6.2 Feynman diagram for exotic slepton $\tilde{E}$ production leading to both $eejj$ and $e\not{p}_T jj$ signal 153

6.3 One-loop diagrams for N_k decay which interferes with the tree level decay to provide CP violation. 157

6.4 The tree level and one-loop diagrams for N_3 decay giving rise to baryogenesis in model 5. 158

6.5 n-$\bar{n}$ oscillation induced by effective six-quark interaction. 159

6.6 One-loop diagrams for N_a decay which interferes with the tree level decay to provide CP violation. 160

7.1 A cartoon showing decay of the modulus into color triplet and singlet superfields. 173

7.2 Feynman diagrams contributing to the baryon asymmetry and the dark matter asymmetry via a baryon number conserved interaction vertex. . 173

8.1 Diagram realizing the effective nonrenormalizable operator generating right handed neutrino mass $M_R = (F_2\Omega)M_\Sigma^{-1}(F_2^T\Omega)$. 185

8.2 The tree level (left) and one-loop (right) decay diagrams for $\xi^{++} \to l^+l^+$. A lepton asymmetry is generated by the CP violation occurring due to the interference between them. 188

List of Tables

1.1 The transformation of the Standard Model fermions under the gauge group $\mathcal{G}_{\rm SM} \equiv SU(3)_c \times SU(2)_L \times U(1)_Y$. 21
1.2 Relations among chemical potential arising from interactions in chemical equilibrium. 56

3.1 LRSM representations of extended field content. 88

6.1 Transformations of the various superfields of the 27 representation under $SU(3)_C \times SU(2)_L \times U(1)_Y \times U(1)_N$. 146
6.2 Possible transformations of h, h^c and N^c under Z_2^B and the allowed superpotential terms. 148

Chapter 1

Introduction

1.1 The Standard Model of particle physics

The Standard Model of particle physics is a theory based on local gauge symmetries describing the strong, the electromagnetic and the weak interactions. The symmetry gauge group $\mathcal{G}_{\rm SM} \equiv SU(3)_c \times SU(2)_L \times U(1)_Y$ governs these interactions. The $SU(3)_c$ gauge theory governs the strong interactions dictating the interactions among the quarks of six flavors having three colors each, mediated by eight gauge bosons, called gluons, corresponding to the eight generators of the group $SU(3)_c$. Colored states are confined (today) and only color singlet states such as baryons (consisting of three quarks forming a color singlet) or mesons (consisting of quark-antiquark forming a color singlet) are allowed to exist as free particles in nature. The weak interactions responsible for nuclear beta decay can be described by a dimension six effective four fermion interaction leading to a coupling constant with a dimension of inverse mass squared. This effective theory emerges from a renormalizable theory, called electroweak theory [1–3], which describes both the weak and electromagnetic interactions at around 100 GeV. The electroweak theory based on the gauge group $SU(2)_L \times U(1)_Y$ is spontaneously broken at around 100 GeV with the symmetry breaking pattern

$$SU(2)_L \times U(1)_Y \longrightarrow U(1)_Q, \tag{1.1}$$

such that the electric charge Q and hyper charge Y are related by

$$Q = T_{3L} + Y, \tag{1.2}$$

where T_{3L} is the diagonal generator of $SU(2)_L$. There are three gauge bosons corresponding to $SU(2)_L$ with electric charges $\pm 1, 0$, where the gauge bosons with electric charges ± 1 corresponds to the raising and lowering generators of $SU(2)_L$. There is another electrically neutral gauge boson corresponding to $U(1)_Y$. Before the electroweak symmetry breaking all four generators are massless; and after the symmetry is spontaneously broken, three of the gauge bosons $W^{\pm}, Z$ become massive, leaving behind a massless combination of the two neutral gauge bosons, which is identified with the photon corresponding to $U(1)_Q$. The electromagnetic interactions governing the interactions of charged particles is described by a $U(1)_Q$ gauge theory, where Q corresponds to the electric charge. The electromagnetic interaction is mediated via the photon, which is the gauge boson corresponding to the only generator of $U(1)_Q$. The heavy $W^{\pm}, Z$ bosons appear as internal propagators in the effective four fermion interactions and mediate the weak interaction.

In the Standard Model the quarks and the leptons are the only fermionic fields. The left handed fermions transform as doublets under $SU(2)_L$, while all the right handed fermions transform as singlets. Once the $SU(2)_L$ transformations are assigned to a particle, the hypercharge quantum number can be determined from the electrical charge using the relation given in Eq. (1.2). The left handed up type quarks (${u_i^\alpha}_L$) and down type quarks (${d_i^\alpha}_L$) form a doublet ${Q_i^\alpha}_L$, where $\alpha = 1, 2, 3$ is the $SU(3)_c$ index and $i = 1, 2, 3$ is the generation index. In the leptonic sector the left handed neutrinos $\nu_{\ell_i L}$ and the leptons ℓ_{iL}^- form a doublet under $SU(2)_L$. There are no right handed neutrinos in the Standard Model. The $SU(3)_c \times SU(2)_L \times U(1)_Y$ quantum numbers of the fields in the Standard Model are summarized in Table. 1.1.

Other than the fermions and gauge bosons, the Standard Model also includes the doublet Higgs scalar which is responsible for breaking the electroweak symmetry [4–8]. The Higgs scalar transforms as a doublet under $SU(2)_L$ with a charged and a neutral component. The transformation of the Higgs scalar under $SU(3)_c \times SU(2)_L \times U(1)_Y$ is given by

$$\phi \equiv \begin{pmatrix} \phi^+ \\ \phi^0 \end{pmatrix} \equiv (1, 2, 1/2). \tag{1.3}$$

	1st generation	2nd generation	3rd generation	$(SU(3)_c, SU(2)_L, U(1)_Y)$ transformations
Q^α_{iL}	$\begin{pmatrix} u^\alpha_L \\ d^\alpha_L \end{pmatrix}$	$\begin{pmatrix} c^\alpha_L \\ s^\alpha_L \end{pmatrix}$	$\begin{pmatrix} t^\alpha_L \\ b^\alpha_L \end{pmatrix}$	(3,2,1/6)
u^α_{iR}	u^α_R	c^α_R	t^α_R	(3,1,2/3)
d^α_{iR}	d^α_R	s^α_R	b^α_R	(3,1,−1/3)
ψ_{iL}	$\begin{pmatrix} \nu_{eL} \\ e^-_L \end{pmatrix}$	$\begin{pmatrix} \nu_{\mu L} \\ \mu^-_L \end{pmatrix}$	$\begin{pmatrix} \nu_{\tau L} \\ \tau^-_L \end{pmatrix}$	(1,2,−1/2)
e^-_{iR}	e^-_R	μ^-_R	τ^-_R	(1,1,−1)

Table 1.1: The transformation of the Standard Model fermions under the gauge group $\mathcal{G}_{\rm SM} \equiv SU(3)_c \times SU(2)_L \times U(1)_Y$.

The renormalizable gauge invariant Lagrangian for the gauge interactions is given by

$$\begin{aligned}
\mathcal{L} = \; & - \; \frac{1}{4}G^p_{\mu\nu}G^{\mu\nu}_p - \frac{1}{4}W^m_{\mu\nu}W^{\mu\nu}_m - \frac{1}{4}B_{\mu\nu}B^{\mu\nu} \\
& + \; \bar{Q}^\alpha_{aL} i\gamma^\mu \Big[\delta_{\alpha\beta}\delta_{ab}\partial_\mu + ig_s\delta_{ab}(T_{\alpha\beta})^p G^p_\mu \\
& + \; ig\delta_{\alpha\beta}(\sigma_{ab})^m W^m_\mu + i\frac{g'}{6}\delta_{\alpha\beta}\delta_{ab}B_\mu\Big] Q^\beta_{bL} \\
& + \; \bar{u}^\alpha_R i\gamma^\mu \Big[\delta_{\alpha\beta}\partial_\mu + ig_s(T_{\alpha\beta})^p G^p_\mu + i\frac{2g'}{3}\delta_{\alpha\beta}B_\mu\Big] u^\beta_R \\
& + \; \bar{d}^\alpha_R i\gamma^\mu \Big[\delta_{\alpha\beta}\partial_\mu + ig_s(T_{\alpha\beta})^p G^p_\mu - i\frac{g'}{3}\delta_{\alpha\beta}B_\mu\Big] d^\beta_R \\
& + \; \bar{\psi}_{aR} i\gamma^\mu \Big[\delta_{ab}\partial_\mu + ig(\sigma_{ab})^m W^m_\mu - i\frac{g'}{2}\delta_{ab}B_\mu\Big] \psi_{bR} \\
& + \; \bar{e}_R i\gamma^\mu \left[\partial_\mu - ig'B_\mu\right] e_R \; ;
\end{aligned} \tag{1.4}$$

where we have dropped the generation indices i for simplicity; $a, b = 1, 2$ are the $SU(2)_L$ indices and $\alpha, \beta = 1, 2, 3$ are the $SU(3)_c$ indices in the fundamental representations; g_s, g and g' are the gauge couplings for the groups $SU(3)_c$, $SU(2)_L$, and $U(1)_Y$, respectively. $G^p_{\mu\nu}$, $W^m_{\mu\nu}$ and $B_{\mu\nu}$ are the field strength tensors for $SU(3)_c$,

$SU(2)_L$, and $U(1)_Y$ groups, respectively. T^p, σ^m are the generators of the groups $SU(3)_c$ and $SU(2)_L$, respectively.

1.1.1 Spontaneous symmetry breaking and masses of the gauge bosons

The Lagrangian involving the Higgs scalar can be written as

$$\mathcal{L}_\phi = \mathcal{L}_{\phi\text{Kin}} + \mathcal{L}_\text{Y} - V(\phi), \tag{1.5}$$

where the first term on the right hand side $\mathcal{L}_{\phi\text{Kin}}$ is the kinetic energy term given by

$$\mathcal{L}_{\phi\text{Kin}} = -\frac{1}{2}\left|\partial_\mu\phi + ig\sigma^m W_\mu^m\phi + i\frac{g'}{2}B_\mu\phi\right|^2 ; \tag{1.6}$$

the second term $\mathcal{L}_\text{Y}$ contains the Yukawa interactions

$$-\mathcal{L}_\text{Y} = h^u_{ij}\bar{Q}_{iL}u_{jR}\tilde{\phi} + h^d_{ij}\bar{Q}_{iL}d_{jR}\phi + h^e_{ij}\bar{\psi}_{iL}e_{jR}\phi + \text{h.c.}, \tag{1.7}$$

where $i, j = 1, 2, 3$ are the generation indices and $\tilde{\phi}$ is defined as

$$\tilde{\phi} = i\tau_2\phi^* = \begin{pmatrix} \phi_0^* \\ -\phi^- \end{pmatrix} \equiv (1, 2, -1/2), \tag{1.8}$$

where τ_2 is the second Pauli matrix. The last term in Eq. (1.5) corresponds to the scalar potential given by

$$V(\phi) = -\frac{\mu^2}{2}\phi^\dagger\phi + \frac{\lambda}{4}\left(\phi^\dagger\phi\right)^2 . \tag{1.9}$$

Taking the mass parameter μ^2 to be positive-definite, it is straightforward to find the vacuum expectation value (VEV) of the Higgs scalar

$$\langle\phi^\dagger\phi\rangle = v^2 = \mu^2/\lambda. \tag{1.10}$$

Note that the manifold of points, at which $V(\phi)$ is minimized, is $SU(2)$ invariant and one must perturb ϕ about a particular choice of minimum to break the symmetry spontaneously. Now in the unitary gauge [1] where

$$\langle\phi\rangle = \begin{pmatrix} 0 \\ v \end{pmatrix}, \tag{1.11}$$

[1] The unitary gauge is a particular gauge choice in a gauge theory with a spontaneous symmetry breaking, such that the scalar field responsible for the spontaneous symmetry breaking is transformed into a basis in which the Goldstone components are set to zero. In the unitarity gauge choice the manifest number of scalar degrees of freedom is minimal.

it is easy to verify that the generators of $SU(2)_L$ and $U(1)_Y$ no longer annihilate the vacuum state; however, the linear combination $T_{3L} + Y \equiv Q$ does. Thus, the spontaneous symmetry breaking leaves the subgroup $U(1)_Q$ unbroken, which governs the quantum electrodynamics.

The interactions of the Higgs scalar ϕ with the gauge bosons of the broken groups given in the kinetic energy term [Eq. (1.6)] make the gauge bosons massive. The charged gauge bosons corresponding to $SU(2)_L$ given by,

$$W_\mu^\pm = \frac{1}{\sqrt{2}}(W_\mu^1 \mp W_\mu^2), \tag{1.12}$$

and a combination of neutral gauge bosons,

$$Z_\mu = \cos\theta_w W_\mu^3 - \sin\theta_w B_\mu, \tag{1.13}$$

where $\sin\theta_w = g'/(g^2 + g'^2)^{1/2}$, get masses

$$m_W = \frac{1}{2}vg, \quad m_Z = \frac{1}{2}v\sqrt{g^2 + g'^2}, \tag{1.14}$$

respectively, while the other remaining neutral gauge boson, identified as the photon,

$$A_\mu = \sin\theta_w W_\mu^3 + \cos\theta_w B_\mu, \tag{1.15}$$

remains massless.

Comparing the effective four-fermion interaction describing muon decay obtained in this theory with the $(V - A)$ theory gives the relation

$$g^2/m_W^2 = 4\sqrt{2}G_F, \tag{1.16}$$

where the Fermi constant $G_F = 1.16639 \times 10^{-5}\text{GeV}^{-2}$. One obtains the value of the VEV of ϕ given by

$$v = \frac{2m_W}{g} \simeq 246 \text{ GeV}. \tag{1.17}$$

The interactions of the physical gauge bosons with the fermions is given by

$$\mathcal{L}_{\text{gauge}} = -\frac{g}{\sqrt{2}}(j_{CC}^\mu W_\mu^+ + j_{CC}^\mu{}^\dagger W_\mu^-) - \frac{g}{\cos\theta_w} j_{NC}^\mu Z_\mu - e j_Q^\mu A_\mu, \tag{1.18}$$

where

$$\begin{aligned} j_{CC}^\mu &= \bar{\psi}_{fL}\gamma^\mu \frac{1}{2}(\tau_1 + i\tau_2)\psi_{fL}, \\ j_{NC}^\mu &= \bar{\psi}_{fL}\gamma^\mu \frac{1}{2}(c_V - c_A\gamma^5)\psi_{fL}, \\ j_Q^\mu &= \bar{\psi}_{fL}\gamma^\mu Q\psi_{fL}, \end{aligned} \tag{1.19}$$

are the charged current, the neutral current and the electromagnetic current respectively. τ_1 and τ_2 are the first and the second Pauli matrices, $c_V = T_{3L} - 2Q\sin^2\theta_w$ and $c_A = T_{3L}$.

The relative strengths of the neutral and charged current weak interactions is often expressed as the ρ-parameter defined as,

$$\rho = \frac{m_W^2}{m_Z^2\cos^2\theta_w}, \tag{1.20}$$

which is experimentally constrained to be very close to unity within a small uncertainty, which matches with the value given by the Standard Model.

1.1.2 Fermion masses and mixing

After the symmetry is broken by the VEV of ϕ the fermions acquire masses through the Yukawa couplings in Eq. (1.7)

$$\begin{aligned} -\mathcal{L}_{\mathrm{Y}} &= h^u_{ij}\bar{Q}_{iL}u_{jR}\begin{pmatrix} v \\ 0 \end{pmatrix} + h^d_{ij}\bar{Q}_{iL}d_{jR}\begin{pmatrix} 0 \\ v \end{pmatrix} + h^e_{ij}\bar{\psi}_{iL}e_{jR}\begin{pmatrix} 0 \\ v \end{pmatrix} + \mathrm{h.c.} \\ &= m^u_{ij}\bar{u}_{iL}u_{jR} + m^d_{ij}\bar{d}_{iL}d_{jR} + m^e_{ij}\bar{e}_{iL}e_{jR} + \mathrm{h.c.}, \end{aligned} \tag{1.21}$$

where the up type quark, down type quark and the charged lepton mass matrices are given by

$$m^u_{ij} = h^u_{ij}v; \quad m^d_{ij} = h^d_{ij}v; \quad m^e_{ij} = h^e_{ij}v; \tag{1.22}$$

respectively. The neutrinos are massless in the Standard Model. We will discuss the issue of neutrino masses in more detail in the following section.

Note that the quark and lepton mass matrices are in general non-diagonal. Since the neutrinos are massless in the Standard Model, it is possible to make a unitary transformation to a basis where charged leptons are diagonal without affecting the charged current interactions. However, the case of the quark sector is nontrivial and will be discussed below.

In the weak basis the quark masses can be written in the matrix form as

$$-\mathcal{L}_{\mathrm{M}} = \bar{U}_L M_u U_R + \bar{D}_L M_d D_R, \tag{1.23}$$

where $U_{L(R)}$ and $D_{L(R)}$ are the matrices corresponding to $u_{iL(R)}$ and $d_{iL(R)}$; and the mass matrix $M_{u(d)}$ has the elements $m_{u(d)_{ij}}$. The mass matrices $M_{u(d)}$ are not diagonal in the weak basis, in which the charged current interaction can be written as

$$\mathcal{L}_{CC} = \frac{g}{\sqrt{2}}(\bar{u}_{kL}\gamma^{\mu}d_{kL}W_{\mu}^{+} + \bar{d}_{kL}\gamma^{\mu}u_{kL}W_{\mu}^{-}). \tag{1.24}$$

Now one can diagonalize the mass matrices $M_{u(d)}$ to obtain the physical or mass eigenstates $U'_{L(R)}$ and $D'_{L(R)}$. Noting that M_u and M_d are in general not Hermitian, a biunitary transformation is required to diagonalize them

$$\mathcal{U}_{uL}^{\dagger}M_u\mathcal{U}_{uR} = \hat{M}_u, \quad \mathcal{U}_{dL}^{\dagger}M_d\mathcal{U}_{dR} = \hat{M}_d, \tag{1.25}$$

where $\hat{M}_{u(d)}$ are diagonal matrices; $\mathcal{U}_{uL(R)}$ and $\mathcal{U}_{dL(R)}$ are unitary matrices. The mass eigenstates are related to weak eigenstates by the relations

$$U'_{L(R)} = \mathcal{U}_{uL(R)}U_{L(R)}, \quad D'_{L(R)} = \mathcal{U}_{dL(R)}D_{L(R)}. \tag{1.26}$$

In the mass basis the quark masses can be written as

$$\mathcal{L}_{\mathrm{M}} = \bar{U}'_L\hat{M}^u U'_R + \bar{D}'_L\hat{M}^d D'_R. \tag{1.27}$$

In a weak interaction the particles are created in weak basis, but their time evolution occurs as physical or mass eigenstates. In other words, a down type quark produced in a weak interaction, can propagate as an admixture of down and strange quarks, and can become a strange quark at a certain time when detected in the weak basis. The charged current interaction can be written in the mass basis as

$$\mathcal{L}_{CC} = \frac{g}{\sqrt{2}}(\bar{u}'_{iL}\gamma^{\mu}V_{ij}d_{jL}W_{\mu}^{+} + \bar{d}'_{jL}\gamma^{\mu}V_{ij}^{*}u'_{iL}W_{\mu}^{-}), \tag{1.28}$$

where the unitary matrix

$$V_{ij} = [\mathcal{U}_{uL}]_{ik}[\mathcal{U}_{dL}^{\dagger}]_{jk}, \tag{1.29}$$

is called the Cabibbo-Kobayashi-Maskawa (CKM) mixing matrix [9, 10]. The neutral current interaction is diagonal in both bases; and so is the neutral Higgs couplings. The current values of the CKM elements can be found in Ref. [11].

1.1.3 Limitations of the Standard Model

Although the Standard Model (SM) is highly successful in explaining the low energy phenomenology of fundamental particles, it suffers from a number of shortcomings, which strongly suggests that the SM is only an effective limit of a more fundamental theory of interactions. In what follows we will try to highlight some of the shortcomings of the SM.

Neutrinos are massless in the SM. Due to the absence of right handed neutrinos one cannot write a Dirac mass term, and a Majorana mass term of the form $\frac{1}{2}\overline{\nu}_L^c m_\nu \nu_L$ is also not allowed by the $SU(2)_L \times U(1)_Y$ gauge invariance. However, the discovery of neutrino oscillations have established that neutrinos have nonzero masses. This implies that the SM is incomplete. Consequently, the evidence of neutrino masses coming from neutrino oscillation experiments provides a strong evidence of physics beyond the SM.

In addition to the fact that gravity is completely left out in the SM, the strong interaction is not unified with weak and electromagnetic interactions. In fact, even in the electroweak "unification" one still has two coupling constants, g and g' corresponding to $SU(2)_L$ and $U(1)_Y$. Thus, one is tempted to seek for a more complete theory where the couplings g_s, g, and g' unify at some higher energy scale giving a unified description of the fundamental interactions.

Given that the ratio $m_{\rm Pl}/m_W$ is so large, where $m_{\rm Pl} = 1.2 \times 10^{19}$ GeV is the Planck scale, another major issue in the SM is the infamous "hierarchy problem". The discovery of the Higgs boson with a mass around 125 GeV has the consequence that, if one assumes the Standard Model as an effective theory, then in Eq. (1.9) $\lambda \sim \mathcal{O}(0.1)$ and $\mu^2 \sim (\mathcal{O}(100)\ \text{GeV})^2$ (including the effects of 2-loop corrections). The problem is that every particle that couples, directly or indirectly, to the Higgs field yields a correction to μ^2 resulting in an enormous quantum correction. For instance, let us consider a one-loop correction to μ^2 coming from a loop containing a Dirac fermion f, as shown in Fig. 1.1, with mass m_f. If f couples to the Higgs boson via the coupling

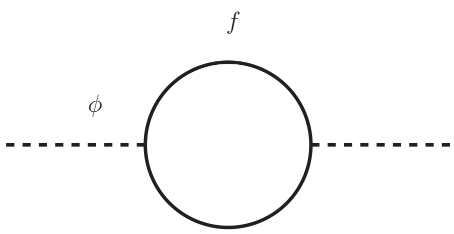

Figure 1.1: one-loop correction to the Higgs squared mass parameter due to a Dirac fermion f.

term $(-\lambda_f \phi \bar{f} f)$, then the correction coming from the one-loop diagram is given by

$$\Delta\mu^2 = \frac{\lambda_f^2}{8\pi^2}\Lambda_{\rm UV}^2 + \cdots \,, \tag{1.30}$$

where $\Lambda_{\rm UV}$ is the ultraviolet momentum cutoff and the ellipses are the terms proportional to m_f^2, growing at most logarithmically with $\Lambda_{\rm UV}$. Each of the quarks and leptons in the SM plays the role of f, and if $\Lambda_{\rm UV}$ is of the order of $m_{\rm Pl}$, then the quantum correction to μ^2 is about 30 orders of magnitude larger than the required value of $\mu^2 = 92.9\ {\rm GeV}^2$. Since all the SM quarks, leptons, and gauge bosons obtain masses from $\langle\phi\rangle$, the entire mass spectrum of the Standard Model is sensitive to $\Lambda_{\rm UV}$. Thus one expects some new physics between m_W and $m_{\rm Pl}$ addressing this problem.

There are also other questions such as why the fermion families have three generations; is there any higher symmetry that dictates different fermion masses even within each generation; in the CKM matrix the weak mixing angles and the CP violating phase are inputs of the theory, instead of being predicted by the SM.

Finally, in the cosmic arena, the observed baryon asymmetry of the universe cannot be explained within the SM. Also there are no suitable candidates for dark matter and dark energy in the SM. These also points towards the existence of physics beyond the SM.

1.2 Physics beyond the Standard Model

1.2.1 Neutrino masses

The atmospheric, solar and reactor neutrino experiments have established that the neutrinos have small nonzero masses which are predicted to be orders of magnitude smaller than the charged lepton masses from cosmology and nuclear β decay experiments. However, in the SM the left handed neutrinos ν_{iL}, $i = e, \mu, \tau$, transform as $(1, 2, -1)$ under the gauge group $SU(3)_c \times SU(2)_L \times U(1)_Y$. Consequently, one cannot write a gauge singlet Majorana mass term for the neutrinos. On the other hand, there are no right handed neutrinos in the SM which would allow a Dirac mass term. The simplest way around this problem is to add singlet right handed neutrinos ν_{iR} with the transformation $(1, 1, 0)$ under the SM gauge group. Then one can straightaway write the Yukawa couplings giving Dirac mass to the neutrinos

$$-\mathcal{L}_{\text{mass}} = \frac{1}{2} h_{ij} \bar{\psi}_{iL} \nu_{jR} \phi, \tag{1.31}$$

such that once ϕ acquires a VEV, the neutrinos get Dirac mass $m_{Dij} = h_{ij} v$. However, to explain the lightness of the neutrinos one needs to assume a very small Yukawa coupling for neutrinos in comparison to charged leptons and quarks, which is rather ad-hoc and unnatural. One way out is to consider the dimension-5 effective lepton number violating operator [12–15] of the form

$$\mathcal{L}_{\text{dim-5}} = \frac{(\nu\phi^0 - e\phi^+)^2}{\Lambda}, \tag{1.32}$$

where Λ is the scale corresponding to some new extension of the SM violating lepton number. This dimension-5 term can induce small Majorana masses to the neutrinos after the eletroweak symmetry breaking

$$-\mathcal{L}_{\text{mass}} = m_\nu \nu_{iL}^T C^{-1} \nu_{jL}, \tag{1.33}$$

with $m_\nu = v^2/\Lambda$. Here, C is the charge conjugation matrix. Consequently, lepton number violating new physics at a high scale Λ would naturally explain the smallness of neutrino masses. In what follows, we discuss some of the popular mechanisms of realizing the same.

Seesaw mechanism: type-I

The type-I seesaw mechanism[2] [16–22] is the simplest mechanism of obtaining tiny neutrino masses. In this mechanism, three singlet right handed neutrinos N_{iR} are added to the SM; and one can write a Yukawa term similar to Eq. (1.31) and a Majorana mass term for the right handed neutrinos since they are singlets under the SM gauge group. The relevant Lagrangian is given by

$$-\mathcal{L}_{\text{type-I}} = h_{i\alpha} \bar{N}_{iR} \phi l_{\alpha L} \phi + \frac{1}{2} M_{ij} N_{iL}^{c\,T} C^{-1} N_{jL}^c + \text{h.c.} \quad . \tag{1.34}$$

Note that, the Majorana mass term breaks the lepton number explicitly and since the right handed neutrinos are SM gauge singlets, there is no symmetry protecting M_{ij}

[2] The seesaw mechanisms generically require a new heavy scale (as compared to the electroweak scale) in the theory, inducing a small neutrino mass (millions of times smaller than the charged lepton masses). Hence the name "seesaw".

and it can be very large. Now after the symmetry breaking, combining the Dirac and Majorana mass matrices we can write

$$
\begin{aligned}
-2\mathcal{L}_{\rm mass} &= m_{D\alpha i}\nu_{\alpha L}^T C^{-1} N_{iL}^c + M_i {N_{iL}^c}^T C^{-1} N_{jL}^c + \text{h.c.} \\
&= \begin{pmatrix} \nu_\alpha & N_i^c \end{pmatrix}_L^T C^{-1} \begin{pmatrix} 0 & m_{D\alpha i} \\ m_{D\alpha i}^T & M_i \end{pmatrix} \begin{pmatrix} \nu_\alpha \\ N_i^c \end{pmatrix}_L + \text{h.c.}\,, \qquad (1.35)
\end{aligned}
$$

where $m_{D\alpha i} = h_{D\alpha i} v$. Now assuming that the eigenvalues of m_D are much less than those of M one can block diagonalize the mass matrix to obtain the light Majorana neutrinos with masses $m_{\nu ij} = -m_{D\alpha i} M_i^{-1} m_{D\alpha i}^T$ and heavy neutrinos with mass $m_N = M_i$. Note that if any of the right handed neutrino mass eigenvalues (M_i) vanish then some of the left handed neutrinos will combine with the right handed neutrinos to form Dirac neutrinos. For n generations, if the rank of M is r, then there will be $2r$ Majorana neutrinos and $n-r$ Dirac neutrinos. The type-I seesaw mechanism not only generates tiny neutrino masses, but also provides the necessary ingredients for explaining the baryon asymmetry of the universe via leptogenesis, which we will discuss in length in the next section.

Seesaw mechanism: type-II

In type-II seesaw mechanism [23–26], the effective operator given in Eq. (1.32) is realized by extending the SM to include an $SU(2)_L$ triplet Higgs scalar ξ which transforms under the SM gauge group $SU(3)_c \times SU(2)_L \times U(1)_Y$ as $(1,3,1)$. For simplicity we assume that there are no right handed neutrinos in this model and only one triplet scalar is present. The Yukawa couplings of the triplet Higgs scalar with the left handed lepton doublet (ν_i, l_i) are given by

$$
-\mathcal{L}_{\text{type-II}} = f_{ij}\left[\xi^0 \nu_i \nu_j + \xi^+ (\nu_i l_j + \nu_j l_i)/\sqrt{2} + \xi^{++} l_i l_j\right]. \qquad (1.36)
$$

Now a nonzero VEV acquired by ξ^0 ($\langle \xi^0 \rangle = u$) gives Majorana masses to the neutrinos. Note that u has to be less than a few GeV to not affect the electroweak ρ-parameter. The most general Higgs potential with a doublet and a triplet Higgs has the form

$$
V = m_\phi^2 \phi^\dagger \phi + m_\xi^2 \xi^\dagger \xi + \frac{1}{2}\lambda_1 (\phi^\dagger\phi)^2 + \frac{1}{2}\lambda_2 (\xi^\dagger \xi)^2 + \lambda_3 (\phi^\dagger\phi)(\xi^\dagger\xi) + \lambda_4 \phi^T \xi^\dagger \phi. \quad (1.37)
$$

We assume $\lambda_4 \neq 0$, which manifests explicit lepton number violation and the mass of the triplet Higgs scalar $M_\xi \sim \lambda_4 \gg v$. The mass matrix of the scalars $\sqrt{2}\,\mathrm{Im}\phi^0$ and $\sqrt{2}\,\mathrm{Im}\xi^0$ is given by

$$\mathcal{M}^2 = \begin{pmatrix} -4\lambda_4 u & 2\lambda_4 v \\ 2\lambda_4 v & -\lambda_4 v^2/u \end{pmatrix}, \tag{1.38}$$

which tells us that one combination of these fields remains massless, which becomes the longitudinal mode of the Z boson; while the other combination becomes massive with a mass of the order of triplet Higgs scalar and hence the danger of Z decaying into Majorons [3] is absent in this model. The minimization of the scalar potential yields

$$u = -\frac{\lambda_4 v^2}{M_\xi^2}, \tag{1.39}$$

giving a seesaw mass to the left handed neutrinos

$$m_{\nu ij} = f_{ij} u = -f_{ij}\frac{\lambda_4 v^2}{M_\xi^2}. \tag{1.40}$$

Note that in the left-right symmetric extension of the SM , which we will discuss in the next subsection, both type-I and type-II seesaw mechanisms are present together. The type-II seesaw mechanism can also provide a very attractive solution to leptogenesis, which we will discuss in the next section.

Seesaw mechanism: type-III

In type-III seesaw mechanism [27, 28] the SM is extended to include $SU(2)_L$ triplet fermions to realize the effective operator given in Eq. (1.32) [4]. The Yukawa interactions in Eq. (1.34) are generalized straightforwardly to $SU(2)_L$ triplet fermions Σ with hypercharge $Y = 0$. The corresponding interaction Lagrangian is given by

$$-\mathcal{L}_{\text{type-III}} = h_{\Sigma i\alpha}\bar{\Psi}_{iL}\left(\vec{\Sigma}_\alpha \cdot \vec{\tau}\right)\tilde{\phi} + \frac{1}{2}M_{\Sigma\alpha\beta}\vec{\Sigma}_\alpha^{c\,T} C^{-1}\vec{\Sigma}_\beta^c + h.c. \quad , \tag{1.41}$$

where $\alpha = 1, 2, 3$. In exactly similar manner as in the case of type-I seesaw, one obtains for $M_\Sigma \gg v$, the left handed neutrino mass

$$m_{\nu ij} = -v^2 h_{\Sigma i\alpha} M^{-1}_{\Sigma\beta\alpha} h^T_{\Sigma j\beta}. \tag{1.42}$$

[3]Majorons correspond to Goldstone bosons associated with the spontaneous breaking of a global lepton number symmetry.

[4]Ref. [28] established the nomenclature Types I, II, III, for the three and only three tree-level seesaw mechanisms.

Radiative models of neutrino mass

Small neutrino masses can also be induced via radiative corrections. The advantage of these models is that without introducing a very large scale into the theory the smallness of the neutrino masses can be addressed. In fact, several of these models can explain naturally the smallness of the neutrino masses with only TeV scale new particles. Thus new physics scale in these models can be as low as TeV, which can be probed in current and next generation colliders.

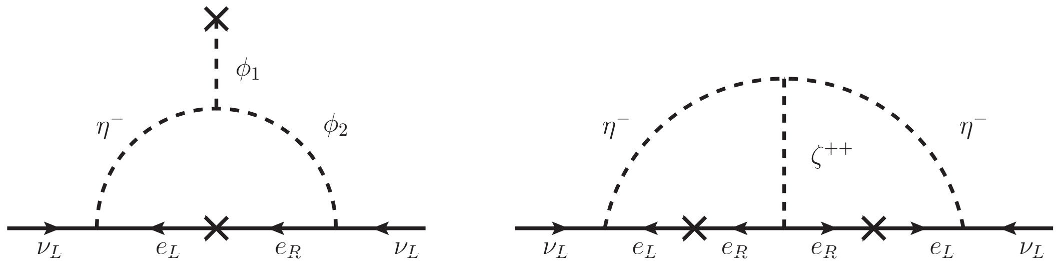

Figure 1.2: (left) one-loop diagram diagram generating neutrino mass in Zee model. (right) Two loop diagram generating neutrino mass in Zee-Babu model.

One realization of this idea is the so-called Zee model [29, 30], where one extends the SM to have two (or more) Higgs doublets ϕ_1 and ϕ_2, and a scalar η^+ which transforms under the SM gauge group $SU(3)_c \times SU(2)_L \times U(1)_Y$ as $(1, 1, 1)$. The lepton number violating Yukawa couplings are given by

$$\mathcal{L}_{\text{Zee}} = f_{ij}\psi_{iL}^T C^{-1}\psi_{jL}\eta^+ + \mu\varepsilon_{ab}\phi_a\phi_b\eta^- + \text{h.c.} \ , \tag{1.43}$$

where f_{ij} is antisymmetric in the family indices i, j and ε_{ab} is the totally antisymmetric tensor. Now, the VEV of the SM Higgs doublet allows mixing between the singlet charged scalar and the charged component of the second Higgs doublet, resulting in a neutrino mass induced through the one-loop diagram showed in Fig. 1.2 (left). The antisymmetric couplings of η^+ with the leptons make the diagonal terms of the mass matrix vanish, with the non-diagonal entries given by

$$m_{ij}^\nu(i \neq j) = A f_{ij}(m_i^2 - m_j^2) \ , \tag{1.44}$$

where $i, j = e, \mu, \tau$ and A is a numerical constant. In the Zee model, if the second Higgs doublet is replaced by a doubly charged singlet scalar ζ^{++}, then one gets what is called Zee-Babu Model [31, 32]. In this model a Majorana neutrino mass can be obtained through a two loop diagram shown in Fig. 1.2 (right). In fact, there are several other radiative models of Majorana neutrino mass such as the Ma model [33] connecting the Majorana neutrino mass to dark matter at one-loop; Krauss-Nasri-Trodden model [34] and Aoki-Kanemura-Sato model [35] giving neutrino mass at the three loop level with a dark matter candidate in the loop; Gustafsson-No-Rivera model [36] involving a three loop diagram with a dark matter candidate and the W boson; and Kanemura-Sugiyama model [37] utilizing an extension of the Higgs triplet model. There are also models for radiative Dirac neutrino masses such as the Nasri-Moussa model [38] utilizing a softly broken symmetry; Gu-Sarkar model [39] with dark matter candidates in the loop; Kanemura-Matsui-Sugiyama model [40] utilizing an extension of the two Higgs doublet model, etc.

1.2.2 Left-Right Symmetric Models

The SM gauge group $\mathcal{G}_{\rm SM} \equiv SU(3)_c \times SU(2)_L \times U(1)_Y$ explains the $(V-A)$ structure of the weak interaction and parity violation, which is reflected by the trivial transformation of all right handed fields under $SU(2)_L$. However, the origin of parity violation is not explained within the SM, and it is natural to seek an explanation for parity violation starting from a parity conserved theory at some higher energy scale. This motivated a left-right symmetric extension of the SM gauge theory, called the Left-Right Symmetric Model (LRSM) [41–46], in which the Standard Model gauge group is extended to

$$\mathcal{G}_{LR} \equiv SU(3)_c \times SU(2)_L \times SU(2)_R \times U(1)_{B-L}$$

where $B-L$ is the difference between baryon (B) and lepton (L) numbers. In LRSM all left handed fermions transform trivially under $SU(2)_R$, while all right handed fermions transform trivially under $SU(2)_L$. The quarks and the leptons transform under the gauge group $SU(3)_c \times SU(2)_L \times SU(2)_R \times U(1)_{B-L}$ as

$$\begin{aligned} Q_L &= \begin{pmatrix} u \\ d \end{pmatrix}_L : (3,2,1,\frac{1}{3}), \;\; Q_R = \begin{pmatrix} u \\ d \end{pmatrix}_R : (3,1,2,\frac{1}{3}) \\ l_L &= \begin{pmatrix} \nu \\ e \end{pmatrix}_L : (1,2,1,-1), \;\; l_R = \begin{pmatrix} N \\ e \end{pmatrix}_R : (1,1,2,-1). \end{aligned} \tag{1.45}$$

The electric charge Q and the SM electroweak quantum numbers T_{3L} and Y are related to the quantum numbers corresponding to $SU(2)_R$ and $U(1)_{B-L}$ through the charge equation

$$Q = T_{3L} + Y = T_{3L} + T_{3R} + \frac{B-L}{2}. \tag{1.46}$$

Note that $B-L$ is a local gauge symmetry in LRSM, and any $B-L$ violating process such as generation of Majorana neutrino mass or neutron-antineutron oscillation can occur only after the $U(1)_{B-L}$ symmetry is broken spontaneously.

In LRSM, the invariance of the Lagrangian under parity ensures that the gauge coupling constants $g_{L(R)}$ corresponding to $SU(2)_{L(R)}$ are the same before the $SU(2)_R$ is broken at a scale M_R; and after the left-right symmetry breaking the two gauge coupling constants canbe different. In some variants of LRSM the parity symmetry is broken spontaneously along with $SU(2)_R$ or before $SU(2)_R$ breaking; while in some other variants parity is broken explicitly: for example in some superstring inspired models it is also possible that parity breaks down during the compactification.

The most popular choice of the Higgs sector for the LRSM consists of one bi-doublet Φ and two triplet $\Delta_{L,R}$ complex scalar fields with the transformations

$$\begin{aligned} \Phi &= \begin{pmatrix} \Phi_1^0 & \Phi_1^+ \\ \Phi_2^- & \Phi_2^0 \end{pmatrix} : (1,2,2,0), \\ \Delta_L &= \begin{pmatrix} \frac{\Delta_L^+}{\sqrt{2}} & \Delta_L^{++} \\ \Delta_L^0 & -\frac{\Delta_L^+}{\sqrt{2}} \end{pmatrix}_L : (1,3,1,2), \\ \Delta_R &= \begin{pmatrix} \frac{\Delta_R^+}{\sqrt{2}} & \Delta_R^{++} \\ \Delta_R^0 & -\frac{\Delta_R^+}{\sqrt{2}} \end{pmatrix}_R : (1,1,3,2). \end{aligned} \tag{1.47}$$

The left-right symmetry is spontaneously broken to reproduce the Standard Model, where the symmetry breaking pattern follows the scheme

$$\begin{aligned} SU(3)_c \times SU(2)_L \times SU(2)_R \times U(1)_{B-L} &\equiv \mathcal{G}_{LR} \\ \xrightarrow{\langle\Delta_R\rangle} SU(3)_c \times SU(2)_L \times U(1)_Y &\equiv \mathcal{G}_{SM} \\ \xrightarrow{\langle\Phi\rangle} SU(3)_C \times U(1)_Q &\equiv \mathcal{G}_{EM} \end{aligned} \tag{1.48}$$

In the first stage of symmetry breaking the right handed triplet Δ_R acquires a Vacuum Expectation Value (VEV) $\langle\Delta_R\rangle = v_R \sim M_R$ which breaks the $SU(2)_R$ symmetry and gives masses to the $W_R^\pm$, Z_R bosons. The electroweak symmetry is broken by the VEVs of the bidoublet Higgs Φ, which gives masses to the charged fermions and the gauge bosons $W_L^\pm$ and Z_L. For simplicity we assume a hierarchy between the VEVs of the two neutral components of Φ, $v \gg v'$, so that we can neglect v'. The Δ_L gets an induced tiny seesaw VEV $\langle\Delta_L\rangle = v_L \ll m_W$, which is constrained to be less than a few eV by the electroweak precision measurements. To see this explicitly, we write down the scalar potential with the fields replaced by their VEVs

$$\begin{aligned} V(v_L, v_R, v) &= -\mu^2 v^2 - \lambda_\Delta^2 (v_L^2 + v_R^2) + \lambda_1 (v_L^4 + v_R^4) + \lambda_2 v_L^2 v_R^2 + \lambda_3 v^4 \\ &\quad + \lambda_4 v^2 (v_L^2 + v_R^2) + \lambda v^2 v_L v_R, \end{aligned} \tag{1.49}$$

which can be minimized with respect to v_L and v_R to obtain

$$(v_L^2 - v_R^2)\left[(4\lambda_1 - 2\lambda_2) v_L v_R - \lambda v^2\right] = 0, \tag{1.50}$$

which has two solutions. The parity conserving solution $v_L = v_R$ is inconsistent with low-energy parity violation; and the other solution gives the induced seesaw VEV

$$v_L = \frac{\lambda v^2}{(4\lambda_1 - 2\lambda_2) v_R}. \tag{1.51}$$

The Lagrangian corresponding to Yukawa couplings can be split into Dirac and Majorana parts

$$\begin{aligned} -\mathcal{L}_{\text{Dir}} &= h_{i\alpha} \bar{Q}_{Li} Q_{R\alpha} \Phi + f_{i\alpha} \bar{l}_{Li} l_{R\alpha} \Phi, \\ -\mathcal{L}_{\text{Maj}} &= f_{Lij} l_{Li}^T C^{-1} l_{Lj} \Delta_L + f_{R\alpha\beta} l_{R\alpha}^T C^{-1} l_{L\beta} \Delta_R, \end{aligned} \tag{1.52}$$

where $i, j(\alpha, \beta) = 1, 2, 3$ are left (right) handed generation indices. After the electroweak symmetry is broken by the VEVs of the bidoublet Higgs Φ the quarks and charged leptons get masses. The neutrinos also get a Dirac mass of the same order of magnitude as the charged leptons $m_D \sim f_{i\alpha} v$. The neutrinos also get Majorana masses once Δ_R acquires a Vacuum Expectation Value (VEV) $\langle \Delta_R \rangle = v_R$, also inducing $\langle \Delta_L \rangle = v_L$ as given by Eq. (1.52). The neutrino mass matrix including both Dirac and Majorana contributions can be written in the basis (ν_L, N_R) as

$$M_\nu = \begin{pmatrix} f_{Lij} v_L & f_{i\alpha} v \\ f^T_{j\beta} v & f_{R\beta\alpha} v_L \end{pmatrix}. \tag{1.53}$$

Now for a nonvanishing $f_{R\alpha\beta}$, we have three heavy Majorana neutrinos with masses $\sim \mathcal{O}(v_R)$ and three light neutrinos with masses

$$m^\nu_{Lij} = \left(-f_{i\alpha} f^{-1}_{R\beta\alpha} f^T_{j\beta} + \frac{\lambda f_{Lij}}{4\lambda_1 - 2\lambda_2} \right) \frac{v^2}{v_R}, \tag{1.54}$$

where the first term corresponds to type-I seesaw and the second term corresponds to type-II seesaw.

In another variant of the LRSM, one considers doublet Higgs scalars instead of triplet Higgs scalars [47–51]. Here the Higgs sector consists of doublet scalars

$$\Phi : (1,2,2,0), \quad H_L : (1,2,1,1), \quad H_R : (1,1,2,1), \tag{1.55}$$

and there is one additional singlet fermion field S (1,1,1,0) in addition to the fermions mentioned in Eq. (1.45). The doublet Higgs scalar H_R acquires a VEV $\langle H_R \rangle = u_R$ to break $SU(2)_R \times U(1)_{B-L}$ symmetry and H_L acquires a small VEV $\langle H_L \rangle = u_L$. The bidoublet scalar breaks the electroweak symmetry and generates charged fermion masses like before. The relevant Lagrangian corresponding to the Yukawa interactions of the neutrinos and S is given by

$$\mathcal{L}_{\rm S} = f_{i\alpha} \bar{l}_{Li} l_{R\alpha} \Phi + f_{Li} \bar{l}_{Li} S H_L + f_{R\alpha} \bar{l}_{R\alpha} S H_R + M_S S S. \tag{1.56}$$

After the Higgs scalars acquire VEVs, the neutrino mass matrix can be written in the basis (ν_L, N_R, S) as

$$M_\nu = \begin{pmatrix} 0 & f_{i\alpha} v & f_{Li} u_L \\ f^T_{j\beta} v & 0 & f_{R\beta} u_R \\ f^T_{Lj} u_L & f^T_{R\alpha} u_R & M_S \end{pmatrix}. \tag{1.57}$$

The right handed neutrinos get an effective Majorana mass

$$M^{N_R}_{\beta\alpha} \simeq \frac{v^2}{M_S} f_{R\beta} f^T_{R\alpha}; \tag{1.58}$$

while the left handed neutrinos acquire a light mass

$$m^{\nu_R}_{ij} = -f_{i\alpha} {f^T_{R\alpha}}^{-1} f^T_{Lj} \frac{v u_L}{u_R} + f_{i\alpha} {f^T_{R\alpha}}^{-1} f^{-1}_{R\beta} f^T_{j\beta} \frac{M_S v^2}{u_R^2}, \tag{1.59}$$

where the second term is the so-called double seesaw contribution [27, 52–56]. Note that, although we have considered only one singlet fermion for simplicity, in a general case three singlets S_p, $p = 1, 2, 3$, are required to have a rank-3 light neutrino mass matrix. In this model, parity can be broken spontaneously by an additional singlet Higgs scalar. Alternatively, parity can be broken explicitly by giving different masses to H_L and H_R. A natural hierarchy between VEVs of the Higgs scalars is $v_L \lesssim v \ll v_R$. Depending on the hierarchy between M_S and v_R one can have pseudo-Dirac or Majorana heavy neutrinos.

One of the key features of LRSM is the prediction of two charged right handed gauge bosons ($W^\pm_R$) with mass $M_{W_R} \sim v_R$ and one combination of neutral gauge bosons, Z_R, corresponding to $SU(2)_R$ and $U(1)_{B-L}$ with mass $M_{Z_R} \sim v_R$. Although low energy phenomenology gives a lower bound on M_R of only about a TeV a left-right symmetry breaking scale M_R at around 10^9 GeV or higher is required to explain neutrino masses in the conventional models and to have high scale leptogenesis. However, using the resonant scheme the lower bound on M_R from leptogenesis can be reduced quite significantly. The seesaw texture can also be engineered to have correct neutrino masses for relatively low M_R. There has been some keen interest in TeV scale left-right symmetry breaking in recent times due to the potential hint of W_R detection at the Large Hadron Collider (LHC) reported by the CMS collaboration. However, the detection of a TeV scale W_R can have very severe implications for leptogenesis, which we will discuss at length in the next chapter.

1.2.3 Grand unified theory

The essential idea behind grand unified theories is to embed the SM gauge group $\mathcal{G}_{\rm SM} \equiv SU(3)_c \times SU(2)_L \times U(1)_Y$ into one bigger gauge group with only one coupling constant. At some higher energy, called the unification scale M_U, the unified group $\mathcal{G}_U$ breaks down to the SM gauge group followed by different evolution of the different couplings g_s, g, and g' leading to their SM values at the electroweak symmetry breaking scale. Note that it is possible to have several intermediate scales between M_U and m_W corresponding to multi-stage breaking of $\mathcal{G}_U$ to $\mathcal{G}_{\rm SM}$. The first attempt to find a symmetry that unifies all the SM symmetries was made by Pati and Salam [41,42], who proposed a partially unified $SU(4)_c \times SU(2)_L \times SU(2)_R$ gauge theory with leptons as a fourth color. This model unified the quarks and leptons in the same representation treating them in the same footing at higher energies and explained the quantization of the electric charge. In fact, the number of coupling constants in the original Pati-Salam gauge group can be reduced from three to two by making the theory left right symmetric so that the two $SU(2)$ couplings become equal [44, 45]. Following this Georgi and Glashow [57] pointed out that the SM can be embedded into the rank-4 simple Lie group $SU(5)$ leading to a unification of all coupling constants. In what follows, we will discuss the $SU(5)$ unification briefly and then make some general remarks about the $SO(10)$ unification.

$SU(5)$ grand unification

In the SM the first generation contains 15 fermions: the left handed up and down type quarks $u_L^{1,2,3}$ and $d_L^{1,2,3}$, the right handed up and down type quarks $u_R^{1,2,3}$ and $d_R^{1,2,3}$, the left handed and right handed electrons e_L, e_R, and the left handed neutrinos ν_{eL}. In grand unified theories, often it is convenient to include the left handed particles (ψ_L) and the CP conjugates of the right handed particles $({\psi^c}_L)$ in a particular representation. The right handed particles and the CP conjugates of the left handed particles are assumed to be in a different representation of the group. Following this convention we have the SM fermions

$$\begin{aligned} Q_L &= \begin{pmatrix} u \\ d \end{pmatrix}_L \equiv (3,2,1/6); \quad {u^c}_L \equiv (\bar{3},1,-2/3); \quad {d^c}_L \equiv (\bar{3},1,1/3); \\ l_L &= \begin{pmatrix} \nu \\ e^- \end{pmatrix}_L \equiv (1,2,-1/2); \quad {e^c}_L \equiv (1,1,1); \end{aligned} \tag{1.60}$$

which we want to assign to $SU(5)$ representations. Before we do that, we note that the simple group $SU(5)$ contains $SU(3) \times SU(2) \times U(1)$ as a subgroup. We write down the decompositions of a few $SU(5)$ representations under its subgroup $SU(3) \times SU(2) \times U(1)$:

$$\begin{aligned}
\bar{5} &= (\bar{3}, 1, 1/3) + (1, 2, -1/2), \\
10 &= (3, 2, 1/6) + (\bar{3}, 1, -2/3) + (1, 1, 1), \\
24 &= (8, 1, 0) + (1, 3, 0) + (1, 1, 0) + (3, 2, -5/6) + (\bar{3}, 3, 5/6). \qquad (1.61)
\end{aligned}$$

Looking at the above decompositions readily suggests that all the fermions given in Eq. (1.60) can be accommodated in the anomaly free combination of $\bar{5}+10$ representations of $SU(5)$:

$$\psi_{\bar{5}L} = \begin{pmatrix} d_1^c \\ d_2^c \\ d_3^c \\ \nu_e \\ e^- \end{pmatrix}_L , \quad \psi_{10L} = \begin{pmatrix} 0 & u_3^c & -u_2^c & -u^1 & -d^1 \\ -u_3^c & 0 & u_1^c & -u^2 & -d^2 \\ u_2^c & -u_1^c & 0 & -u^3 & -d^3 \\ u^1 & u^2 & u^3 & 0 & -e^c \\ d^1 & d^2 & d^3 & e^c & 0 \end{pmatrix}_L ; \qquad (1.62)$$

while the right handed fermions will belong to the 5 and $\overline{10}$ representations.

The $SU(5)$ group has 24 generators which can be associated with 24 gauge bosons coupled to 24 different currents, out of which 12 currents associated with 12 gauge bosons are identified with the SM currents and gauge bosons associated with $SU(3)_c \times SU(2)_L \times U(1)_Y$, while the rest of the gauge bosons are expected to be very massive making the interactions mediated by them very weak. The 24 gauge bosons of the $SU(5)$ can be put in a matrix form $\mathcal{A}_\mu^m$ with $m = 1, 2, \cdots, 24$ as

$$\begin{pmatrix} G_1^D & G^{12} & G^{13} & X_1^c & Y_1^c \\ G^{21} & G_2^D & G^{23} & X_2^c & Y_2^c \\ G^{31} & G^{32} & G_3^D & X_3^c & Y_3^c \\ X_1 & X_2 & X_3 & G_4^D & W^+ \\ Y_1 & Y_2 & Y_3 & W^- & G_5^D \end{pmatrix} \qquad (1.63)$$

with the diagonal elements given by

$$
\begin{aligned}
G_1^D &= \frac{1}{2}G_3 + \frac{1}{2\sqrt{3}}G_8 - \frac{1}{\sqrt{15}}B \\
G_2^D &= -\frac{1}{2}G_3 + \frac{1}{2\sqrt{3}}G_8 - \frac{1}{\sqrt{15}}B \\
G_3^D &= -\frac{1}{\sqrt{3}}G_8 - \frac{1}{\sqrt{15}}B \\
G_4^D &= \frac{1}{2}W_3 - \frac{3}{2\sqrt{15}}B \\
G_4^D &= -\frac{1}{2}W_3 - \frac{3}{2\sqrt{15}}B,
\end{aligned}
\tag{1.64}
$$

where the four independent diagonal generators of $SU(5)$: G_3, G_8, W_3, and B correspond to the two diagonal generators of $SU(3)_c$, and one diagonal generator of $SU(2)_L$ and $U(1)_Y$ respectively. The gauge bosons

$$
\mathcal{X}^{\mu}_{\alpha i} = \begin{pmatrix} X^{\mu}_{\alpha} \\ Y^{\mu}_{\alpha} \end{pmatrix}, \quad \mathcal{X}^{c\mu}_{\alpha i} = \begin{pmatrix} X^{c\mu}_{\alpha} \\ Y^{c\mu}_{\alpha}, \end{pmatrix} \tag{1.65}
$$

where $\alpha = 1, 2, 3$ and $i = 1, 2$ are the $SU(3)_c$ and $SU(2)_L$ indices respectively, correspond to the raising and lowering operators connecting quarks with the antiquarks or the leptons with the antiquarks (the antileptons with the quarks).

The phenomenology of the $SU(5)$ grand unified theory is determined by the choice of Higgs scalars and the consequent symmetry breaking scheme. A conventional choice for the $SU(5)$ symmetry breaking pattern is given by

$$
SU(5) \xrightarrow{M_U} SU(3)_c \times SU(2)_L \times U(1)_Y \xrightarrow{M_W} SU(3)_c \times U(1)_Q. \tag{1.66}
$$

The first stage is achieved by giving a VEV to a SM singlet component of a Higgs scalar in the adjoint representation $\Sigma\{24\}$

$$
\langle \Sigma \rangle = V \ \mathrm{Diag}[1, 1, 1, -3/2, -3/2]. \tag{1.67}
$$

Since this VEV commutes with the generators of the SM gauge group, the gauge bosons corresponding to the SM remain massless after this stage of symmetry breaking, however, the remaining gauge bosons become superheavy with mass $M_X \sim M_U$. The second stage of symmetry breaking is realized by giving VEV to a Higgs scalar belonging to a 5-plet of $SU(5)$, $H\{5\}$

$$\langle H\rangle = \frac{v}{\sqrt{2}}\begin{pmatrix}0\\0\\0\\0\\1\end{pmatrix}, \tag{1.68}$$

giving masses to the SM fermions and gauge bosons in a similar fashion as the Higgs doublet in the SM. The Yukawa couplings of the left handed fermions with the Higgs scalars are given by

$$\mathcal{L}_{\text{Yuk}} = h^1_{ab}\psi^T_{\bar{5}L}C^{-1}\psi_{10L}H^\dagger + h^2_{ab}\psi^T_{10L}C^{-1}\psi_{10L}H. \tag{1.69}$$

The Hermitian conjugate of the above Lagrangian will contain the right handed particles. After H acquires a VEV, the first term gives masses to the down type quarks and the charged leptons; while the second term gives masses to the up type quarks

$$M_d = h^1_{ab}\langle H\rangle, \quad M_e = h^1_{ab}\langle H\rangle, \quad M_u = h^2_{ab}\langle H\rangle, \tag{1.70}$$

which are then evolved down to the electroweak symmetry breaking scale M_W using the renormalization group equations (RGE). The neutrinos remain massless in this minimal scheme. To explain the neutrino masses one can introduce an $SU(5)$ singlet fermion S with the interactions

$$\mathcal{L}_S = h^S_{ab}\psi_{\bar{5}L}SH + M_S SS + \text{h.c.}\ , \tag{1.71}$$

which can give a tiny seesaw mass to the neutrinos ${h^S_{ab}}^2\langle H\rangle^2/M_S$, after H acquires a VEV. Alternatively, one can introduce a Higgs scalar ξ belonging to the 15-plet of $SU(5)$ with the Yukawa interactions

$$\mathcal{L}_\xi = f^\xi_{ab}\psi^T_{\bar{5}L}C^{-1}\psi_{\bar{5}L}xi^\dagger + \text{h.c.}\ , \tag{1.72}$$

and a term $\mu\xi HH$ in the scalar potential. After the scalar ξ acquires a tiny VEV $\langle\xi\rangle = \mu\langle H\rangle^2/m_\xi^2$, where μ and m_ξ are of the order of M_U, the neutrinos get masses $f^\xi_{ab}\langle\xi\rangle$.

Gauge coupling unification

In a grand unified theory the coupling constants g_3, g_2 and g_1 corresponding to the groups $SU(3)_c$, $SU(2)_L$ and $U(1)_Y$ should get unified at the unification scale, so for the $SU(5)$ unification we should have

$$g_3(M_U) = g_2(M_U) = g_1(M_U) = g_5(M_U). \tag{1.73}$$

The evolution for running coupling constants with energy at one-loop level is governed by the RGEs

$$\mu \frac{\partial g_i}{\partial \mu} = \beta_i(g_i) \equiv \frac{b_i}{16\pi^2} g_i^3, \tag{1.74}$$

which can also be written in the form

$$\frac{1}{\alpha_i(\mu_2)} = \frac{1}{\alpha_i(\mu_1)} - \frac{b_i}{2\pi} \ln\left(\frac{\mu_2}{\mu_1}\right), \tag{1.75}$$

where $\alpha_i = g_i^2/4\pi$ and the one-loop beta-coefficients b_i are given by

$$b_i = -\frac{11}{3}\mathcal{C}_2(G) + \frac{2}{3}\sum_{R_f} T(R_f) \prod_{j\neq i} d_j(R_f) + \frac{1}{3}\sum_{R_s} T(R_s) \prod_{j\neq i} d_j(R_s) \tag{1.76}$$

Here, $\mathcal{C}_2(G)$ is the quadratic Casimir invariant corresponding to the adjoint representations,

$$\mathcal{C}_2(G) \equiv \begin{cases} N & \text{if } SU(N), \\ 0 & \text{if } U(1). \end{cases} \tag{1.77}$$

$T(R_f)$ and $T(R_s)$ are the Dynkin indices of the irreducible representation $R_{f,s}$ for a given fermion and scalar, respectively,

$$T(R_{f,s}) \equiv \begin{cases} 1/2 & \text{if } R_{f,s} \text{ is fundamental}, \\ N & \text{if } R_{f,s} \text{ is adjoint}, \\ 0 & \text{if } R_{f,s} \text{ is singlet}. \end{cases} \tag{1.78}$$

and $d(R_{f,s})$ is the dimension of a given representation $R_{f,s}$ under all the gauge groups except the i-th gauge group under consideration. An additional factor of $1/2$ is multiplied in the case of a real Higgs representation.

By fixing the normalization of $\bar{5}$ one can fix the $U(1)_Y$ normalization, $Y_N = \sqrt{3/5}$, taking the normalization condition for the fundamental representation of any $SU(N)$ group as

$$\mathrm{Tr}[T_i T_j] = \frac{1}{2}\delta_{ij}. \tag{1.79}$$

The precision measurements of the Z mass and Z width at LEP and also the jet cross sections and energy-energy correlations give values of $\sin^2\theta_w$ and α_s at the electroweak scale. Using the fine structure constant at the electroweak scale $\alpha_{\text{em}}(M_W) = 1/127.9$, $\sin^2\theta_w(M_W) = 0.2334$, and $\alpha_s(M_W) = 0.118$ one can obtain the values of the three coupling constants at the electroweak scale given by

$$\begin{aligned}\alpha_1^{-1}(M_W) &\equiv \frac{3}{5}\alpha_{\text{em}}^{-1}(M_W)\cos^2\theta_w(M_W) = 58.83\\ \alpha_2^{-1}(M_W) &\equiv \alpha_{\text{em}}^{-1}(M_W)\sin^2\theta_w(M_W) = 29.85\\ \alpha_3^{-1}(M_W) &\equiv \alpha_s^{-1}(M_W) = 8.47.\end{aligned} \tag{1.80}$$

Using these as the boundary conditions we can evolve the three gauge couplings using RGEs to check whether they meet at a point giving the unified gauge coupling constant.

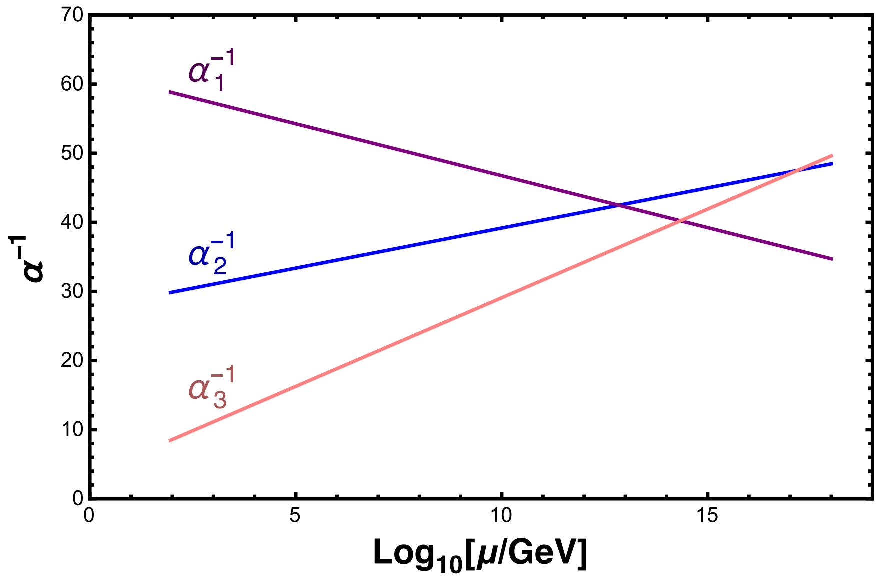

Figure 1.3: The one-loop evolution of the gauge coupling constants in the minimal $SU(5)$ grand unified theory.

The evolution of the three gauge couplings α_1^{-1}, α_2^{-1} and α_3^{-1} with energy in $SU(5)$ unification is shown in Fig. 1.3. Clearly, they do not meet at a point and this result remains valid even when the two loop corrections and errors in the measurement of the coupling constants are included. This rules out the minimal $SU(5)$ grand unified theory. However, by introducing some intermediate symmetry breaking scale or new particles with masses above the electroweak scale it is possible to make the gauge coupling constants meet at a point.

Proton decay

In $SU(5)$ grand unified theory the gauge bosons $\mathcal{X}_\mu$ and $\mathcal{X}^c_\mu$ can mediate proton decay and baryon number violation. The relevant interactions are given by

$$\mathcal{L} = g_5 \bar{d}^c_{\alpha L}\gamma_\mu l_{iL}\mathcal{X}^{c\mu}_{\alpha i} + g_5 \bar{e}^c_L \gamma_\mu Q_{\alpha i L}\mathcal{X}^{c\mu}_{\alpha i} + g_5 \bar{U}^c_{\alpha L}\gamma_\mu Q_{\beta i L}\mathcal{X}^\mu_{\gamma i}\varepsilon_{\alpha\beta\gamma} + \text{h.c.}\,, \quad (1.81)$$

where g_5 is the $SU(5)$ gauge coupling constant, $\varepsilon_{\alpha\beta\gamma}$ is a totally antisymmetric $SU(3)_c$ tensor with $\varepsilon_{123} = 1$. Fig. 1.4 shows a typical diagram for the gauge bosons mediating proton decay $p \to e^+\pi^0$. The amplitude corresponding to this process is given by $\mathcal{A}(p \to e^+\pi^0) \sim \alpha_5/M_X^2$, where $M_X \simeq M_U$. The proton lifetime is then given by $\tau_p = M_X^4/\alpha_5^2 m_p^5$. For the minimal $SU(5)$ theory one obtains [58] 10^{30} years $<$ $\tau_{\rm p} < 10^{31}$ years, which is ruled out by the present experimental limit $\tau_p > 1 \times 10^{34}$years [11]. Note that some extensions such as inclusion of gravity effects or the supersymmetric version may provide a way around this problem. The simplest form of the baryon number violating effective operators is given by $QQQL$ or $QQQL^c$, where Q corresponds to a quark and L represents a lepton. Note that these operators conserve $B-L$. An example of a $B-L$ violating as well as baryon number violating operator is $QQQL\phi$, where ϕ is the usual SM Higgs doulet. In a grand unified theory with larger gauge group such as $SO(10)$ it is possible to have $B-L$ violating neutron-antineutron oscillations [46] or three lepton decay mode of a proton [59].

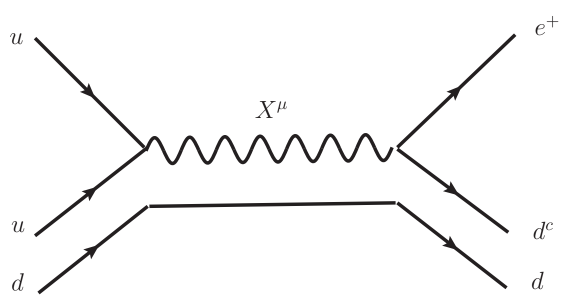

Figure 1.4: An example of gauge boson mediated proton decay $p \to e^+\pi^0$.

Some Remarks on $SO(10)$ and E_6 Grand Unified Theories

The $SO(10)$ grand unified theory has many advantages over the $SU(5)$ grand unified theory. Being a rank-5 group, $SO(10)$ has one extra diagonal generator, which can be identified with $B - L$. In fact, one of the most interesting symmetries as one of the intermediate symmetries can be the left-right symmetric group. The spontaneous breaking of $B - L$ gauge symmetry can have very interesting consequences, for example, new $B - L$ violating processes inducing, e.g., neutron-antineutron oscillations, $B - L$ violating proton decay modes, or neutrinoless double beta decay. Only one 16-plet spinor representation of $SO(10)$ can accommodate all fermions that belong to $\bar{5} + 10$ of $SU(5)$ and the CP conjugate of the right handed neutrino and the gauge interactions of $SO(10)$ also make parity part of a continuous symmetry. For an introductory level discussion on $SO(10)$, see for example Refs. [60, 61] and the references therein.

Another group that we would like to mention before closing this subsection is the exceptional group E_6, which has received considerable attention in the literature thanks to its superstring motivation and a very rich phenomenology. E_6 group is a rank-6 group with 78 generators and is the only exceptional group which can realize a flavor-chiral theory. Moreover it contains $SO(10)$ as one of its subgroups. The only maximal subgroup of E_6 that can contain the $SU(3)_c$ as an explicit factor is $SU(3)_c \times SU(3) \times SU(3)$, under which the 27-dimensional fundamental representation of E_6 has the decomposition $27 = (3^c, 3, 1) + (\bar{3}^c, 1, \bar{3}) + (1^c, \bar{3}, 3)$. There are several other possibilities of breaking E_6 to the SM gauge group, involving other maximal subgroups of E_6 such as $SO(10) \times U(1)$ or $SU(2) \times SU(6)$. For a detailed discussion regarding the E_6 group, see for example Ref. [62].

1.2.4 Supersymmetry

Supersymmetry is a symmetry that interrelates fermions and bosons, so that an irreducible representation of the supersymmetry algebra called a supermultiplet must contain an equal number of fermionic and bosonic degrees of freedom. Thus a fermion will have a scalar superpartner and a scalar or vector will have a fermionic superpartner. Since the generators of gauge symmetry commute with supersymmetry generators, the superpartners must also have the same quantum numbers e.g., electric charge, isospin, color etc.

Supersymmetry is considered to be one of the most attractive extensions of the SM because of its many virtues. It can naturally address the hierarchy problem discussed in section 1.1.3. To see how this works, consider the one-loop diagram shown in Fig. 1.5. Here, s is a superpartner of any of the SM fermions. The one-loop correction is given by

$$\Delta\mu^2 = -\frac{\lambda_s}{8\pi^2}\left[\Lambda_{\mathrm{UV}}^2 - 2m_s^2\ln(\Lambda_{\mathrm{UV}}/m_s) + \cdots\right], \tag{1.82}$$

where m_s is the mass of the scalar particle. We note that quadratic and logarithmic divergences have appeared again in Eq. (1.82), however, this time with an opposite sign with respect to Eq. (1.30). Thus if $\lambda_s = |\lambda_f|^2$, then indeed the divergences cancel neatly. More restrictions on the theory are required to ensure that this cancellation persists to higher orders. Turning to the other motivations, supersymmetry with a discrete symmetry called R-parity can give a natural dark matter candidate in the form of the lightest supersymmetric particle (LSP), usually the lightest neutralino, which is a mass eigenstate formed by a linear combination of the superpartners of the neutral gauge and Higgs fields. In various supersymmetry breaking scenarios soft masses are generated by breaking supersymmetry at some higher energy scale above the electroweak symmetry breaking scale which gives various soft parameters at that scale. Then it is possible to use the RGEs to evolve these parameters to explain the shape of the Higgs potential required for electroweak symmetry breaking in the SM. A supersymmetric version of grand unified theories can often help in unifying the gauge coupling constants at a single point, while naturally solving the gauge hierarchy problem in grand unified theories, protecting the Higgs scalar against the quadratic divergences by cancelling the divergent diagrams with equivalent diagrams with supersymmetric partners. Supersymmetric models can also provide additional sources of CP-violation compared to the SM which may assist in electroweak baryogenesis or alternatively new matter fields in supersymmetry with $B - L$ violating interactions can lead to new leptogenesis mechanisms.

Supersymmetric Lagrangian and superpotential

A free chiral supersymmetric Lagrangian can be written as

$$\mathcal{L}_{\mathrm{free}} = -\partial^\mu\phi^{*i}\partial_\mu\phi_i + i\psi^{\dagger i}\bar{\sigma}^\mu\partial_\mu\psi_i + F^{*i}F_i, \tag{1.83}$$

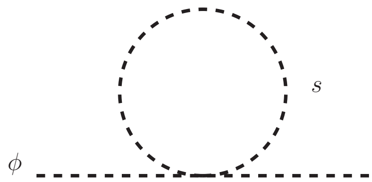

Figure 1.5: One-loop correction to the Higgs squared mass parameter due to a scalar s.

where ϕ_i is a complex scalar field and ψ_i is a left handed two component Weyl fermion. F_i is a nonpropagating auxiliary field (it does not have a kinetic term), which allows the supersymmetry algebra to close off-shell [5] and has equations of motion ($F_i = F_i^* = 0$). In this subsection we closely follow the notations and conventions of Ref. [63]. This Lagrangian is invariant under the infinitesimal supersymmetry transformations

$$\begin{aligned} \delta\phi_i &= \epsilon\psi_i, & \delta\phi^{*i} &= \epsilon^\dagger\psi^{\dagger i}, \\ \delta(\psi_i)_\alpha &= -i(\sigma^\mu\epsilon^\dagger)_\alpha\partial_\mu\phi_i + \epsilon_\alpha F_i, & \delta(\psi^{\dagger i})_{\dot\alpha} &= i(\epsilon\sigma^\mu)_{\dot\alpha}\partial_\mu\phi_{*i} + \epsilon^\dagger_{\dot\alpha}F^{*i}, \\ \delta F_i &= -i\epsilon^\dagger\bar\sigma^\mu\partial_\mu\psi_i, & \delta F^{*i} &= i\partial_\mu\psi^{\dagger i}\bar\sigma^\mu\epsilon \end{aligned} \tag{1.84}$$

where ϵ^α is an infinitesimal anticommuting two component Weyl fermion, parametrizing the supersymmetry transformation.

Now, the most general set of renormalizable interactions involving the chiral supermultiplets must be invariant under the supersymmetry transformations. Wess and Zumino [64] first constructed the interacting supersymmetry preserving Lagrangian given by

$$\mathcal{L}_{\mathrm{WZ}} = -\partial^\mu\phi^{*i}\partial_\mu\phi_i + i\psi^{\dagger i}\bar\sigma^\mu\partial_\mu\psi_i - W^iW_i^* - \frac{1}{2}(W^{ij}\psi_i\psi_j + W_{ij}^*\psi_{\dagger i}\psi_{\dagger j}), \tag{1.85}$$

with

$$W_i = \frac{\partial W}{\partial\phi_i}, \quad W_{ij} = \frac{\partial^2 W}{\partial\phi_i\partial\phi_j}, \tag{1.86}$$

where

$$W = L^i\phi_i + \frac{1}{2}M^{ij}\phi_i\phi_j + \frac{1}{6}y^{ijk}\phi_i\phi_j\phi_k, \tag{1.87}$$

[5] A Weyl spinor has two complex components and so total four degrees of freedom when it is off-shell. However, when it is On-shell the equation of motion imposes two constraints, reducing the number of degrees of freedom to two. On the other hand, a complex scalar field has two degrees of freedom. So on-shell, the number of bosonic and fermionic degrees of freedom match. However, off-shell, the number of bosonic and fermionic degrees of freedom do not match.

is a holomorphic function of the scalar fields ϕ_i treated as complex variables, called the superpotential. L^i are parameters with dimension $[\text{mass}]^2$, M^{ij} is a symmetric matrix with dimension of $[\text{mass}]$ and y^{ijk} is a Yukawa coupling matrix, totally symmetric under interchange of i, j, k. The term $L^i\phi_i$ is often dropped because it is only allowed when ϕ_i is a gauge singlet. Note that the auxiliary fields are eliminated using their equations of motion in the presence of interactions

$$F_i = -W_i^*, \quad F_i^* = -W^i. \tag{1.88}$$

The Lagrangian corresponding to gauge supermultiplets can be written as

$$\mathcal{L}_{\text{gauge}} = -\frac{1}{4}F^a_{\mu\nu}F^{\mu\nu a} + i\lambda^{\dagger a}\bar{\sigma}^\mu D_\mu \lambda^a + \frac{1}{2}D^a D^a, \tag{1.89}$$

where

$$\begin{aligned} F^a_{\mu\nu} &= \partial_\mu A^a_\nu - \partial_\nu A^a_\mu + g f^{abc} A^b_\mu A^c_\nu, && (1.90) \\ D_\mu \lambda^a &= \partial_\mu \lambda^a + g f^{abc} A^b_\mu \lambda^c. && (1.91) \end{aligned}$$

A^a_μ are the massless gauge fields and the two component Weyl fermions λ^a are their superpartners, called gauginos. f^{abc} are totally antisymmetric structure constants corresponding to the relevant gauge groups. D^a are auxiliary fields required to match the bosonic and fermionic degrees of freedom off-shell, similar to the F^i fields in the Wess-Zumino Lagrangian. They can be removed on-shell using their equations of motion. The infinitesimal supersymmetry transformations under which the gauge Lagrangian is invariant are given by

$$\begin{aligned} \delta A^a_\mu &= \frac{1}{\sqrt{2}}(\epsilon^\dagger \bar{\sigma}_\mu \lambda^a + \lambda^{\dagger a}\bar{\sigma}_\mu \epsilon), \\ \delta \lambda^a_\alpha &= \frac{i}{2\sqrt{2}}(\sigma^\mu \bar{\sigma}^\nu \epsilon)_\alpha F^a_{\mu\nu} + \frac{1}{\sqrt{2}}\epsilon_\alpha D^a, \\ \delta D^a &= \frac{i}{\sqrt{2}}(\epsilon^\dagger \bar{\sigma}^\mu D_\mu \lambda^a - D_\mu \lambda^{\dagger a}\bar{\sigma}^\mu \epsilon). && (1.92) \end{aligned}$$

To construct a general supersymmetric Lagrangian with both chiral and gauge supermultiplets, one must take into account the transformation of chiral supermultiplets and auxiliary fields under the gauge groups, and include any other interactions allowed by gauge invariance or interactions involving gauginos and D^a fields such that supersymmetry is preserved. The full Lagrangian containing interacting chiral and gauge supermultiplets is given by

$$\begin{aligned}\mathcal{L}_{\rm int} &= -D^\mu\phi^{*i}D_\mu\phi_i + i\psi^{\dagger i}\bar{\sigma}^\mu D_\mu\psi_i - \frac{1}{2}(M^{ij}\psi_i\psi_j + M^*_{ij}\psi^{\dagger i}\psi^{\dagger j}) \\ &\quad -\frac{1}{2}(y^{ijk}\phi_i\psi_j\psi_k + y^*_{ijk}\phi^{*i}\psi^{\dagger j}\psi^{\dagger k}) - \frac{1}{4}F^a_{\mu\nu}F^{\mu\nu a} + i\lambda^{\dagger a}\bar{\sigma}^\mu D_\mu\lambda^a \\ &\quad -\sqrt{2}g(\phi^*T^a\psi)\lambda^a - \sqrt{2}g\lambda^{\dagger a}(\psi^\dagger T^a\phi) - V(\phi,\phi^*) \end{aligned} \tag{1.93}$$

where

$$V(\phi,\phi^*) = F^{*i}F_i + \frac{1}{2}\sum_a D^aD^a = W^*_iW^i + \sum_a g_a^2(\phi^*T^a\phi)^2 \tag{1.94}$$

is the complete scalar potential after eliminating the auxiliary fields using their equations of motion. The two types of terms in the scalar potential are referred to as F-terms and D-terms, respectively.

From the above discussion, it is clear that in a renormalizable supersymmetric theory once the gauge group, field content, and their transformations are defined, they together with the superpotential readily determine all the interactions. Supersymmetry can be given an elegant geometric interpretation using what is called superspace, a manifold, which in addition to the usual bosonic spacetime coordinates t, x, y, z includes four fermionic coordinates. In this approach, the Lagrangian is defined in terms of integrals over the superspace with fermionic and ordinary bosonic coordinates, which makes the invariance under supersymmetry transformations manifest. However, here we will not develop the superspace formalism, which is a very interesting topic by itself. An interested reader may refer to Refs. [63,65] for details of this formalism. The following working knowledge will suffice to understand most parts of this thesis. Usually, the superpotential is written in terms of superfields as

$$W = L^i\hat{\phi}_i + \frac{1}{2}M^{ij}\hat{\phi}_i\hat{\phi}_j + \frac{1}{6}y^{ijk}\hat{\phi}_i\hat{\phi}_j\hat{\phi}_k, \tag{1.95}$$

where $\hat{\phi}_i$ is a superfield which contains the scalar field ϕ_i, fermionic field ψ_i and the auxiliary field F_i.

Breaking supersymmetry softly

Since the supersymmetric partners of the SM fields have not been observed at LEP, Tevatron or LHC, in a realistic phenomenological model supersymmetry must be broken at some higher scale. In order to naturally maintain the hierarchy between the electroweak and the Planck scale by maintaining the cancellations of the quadratic divergences, one must ensure that dimensionless supersymmetry breaking couplings are absent. In practice, one can introduce extra terms to the Lagrangian, which break supersymmetry softly such that the theory remains free of quadratic divergences in scalar masses [66]

$$\mathcal{L}_{\text{soft}} = -\left(\frac{1}{2}M_a\lambda^a\lambda^a + \frac{1}{6}a^{ijk}\phi_i\phi_j\phi_k + \frac{1}{2}b^{ij}\phi_i\phi_j + t^i\phi_i\right) + \text{c.c.} - (\mathrm{m}^2)^{\mathrm{i}}_{\mathrm{j}}\phi^{*\mathrm{j}}\phi_{\mathrm{i}}. \quad (1.96)$$

The terms (from left to right) corresponds to a gaugino mass term, a massive trilinear scalar coupling term, a massive bilinear scalar coupling term, a tadpole coupling term, and a scalar squared mass term. In particular, the tadpole term requires ϕ_i to be a gauge singlet.

In phenomenology, it is often convenient to consider a particular soft supersymmetry breaking mechanism motivated by a model so that the corresponding parameter space can be constrained. For example, in a spontaneous breaking, one can assume the vacuum to be not invariant under the action of the supersymmetry generators $Q|0\rangle \neq 0$. This can be realized when a VEV is acquired by either a D-term, called Fayet-Iliopoulos supersymmetry breaking [67, 68] or a F-term, called O'Raifeartaigh supersymmetry breaking [69]. In typical phenomenological models such as the Minimal Supersymmetric Standard Model (MSSM), the Next-to-Minimal Supersymmetric Standard Model (NMSSM), the Exceptional Supersymmetric Standard Model (E_6SSM) one does not readily have the right ingredients for implementing a viable supersymmetry breaking and some new scheme needs to be included. An example of such a scheme is hidden sector supersymmetry breaking, where a hidden sector is postulated to have a very small coupling with the visible sector. The typical models of such types include gravity mediation, gauge mediation, and anomaly mediation.

R-parity

In the superpotential it is often possible to write terms that are gauge invariant and holomorphic in chiral superfields, but they violate either baryon number or lepton number. This is rather disturbing, because no such baryon or lepton number violating processes have been observed experimentally. The non-observation of proton decay puts one of the most stringent constraints. While it is possible to impose baryon or lepton number conservation to avoid this, that will kill all possibilities of non-perturbative baryon and lepton number violating processes at high energies, which may be rather important in the early universe, for example, in high scale baryogenesis or Majorana mass generation. Thus, one adds a new symmetry, which eliminates the possibility of B and L violating terms in the renormalizable superpotential. This new symmetry is referred to as R-parity or equivalently the matter parity, with a multiplicatively conserved quantum number defined as

$$P_R = (-1)^{3(B-L)+2s} \quad \text{and} \quad \mathrm{P_M} = (-1)^{3(\mathrm{B-L})} \tag{1.97}$$

where s is the spin of the particle. All the SM particles and the Higgs bosons have $P_R = +1$, while their supersymmetric partners (squarks, sleptons, gauginos and higgsinos) have $P_R = -1$. In the case of matter parity: all the quark and lepton supermultiplets have $P_M = -1$, and the Higgs supermultiplets, the gauge bosons and gauginos have $P_M = +1$. Since the product of $(-1)^{2s}$ for fields involved in any interaction vertex conserving angular momentum is always $(+1)$, the matter parity conservation and R-parity conservation are exactly equivalent. R-parity has some important consequences. The lightest sparticle with $P_R = -1$, often called the lightest supersymmetric particle (LSP), is absolutely stable because its decay into lighter particles will violate R-parity conservation. If it is electrically neutral then it can only have weak interactions and consequently can be an excellent candidate for dark matter. At colliders the sparticles can only be produced in pairs (or in even numbers), which can have important implications for sparticles searches. Current search limits for supersymmetric particles can be found in Ref. [11].

1.3 Cosmological implications of physics beyond the Standard Model

The cosmic frontier of particle physics is driven by the interplay between particle physics and cosmology. In the standard model of cosmology, the universe started from a big-bang and then it continued to expand and cool down to the universe that we observe today. To understand the evolution of the universe at an earlier epoch when the universe was very dense and the average energy per particle was much higher compared to today, an understanding of the particle interactions at that energy scale is required. Extrapolating this logic backwards, the present day astrophysical (cosmological) observations can provide an imprint of information about particle interactions when the universe was much denser and the average energy of the particles were much higher compared to the energy scale reachable at present time colliders such as LHC. Thus the astrophysical observations can provide a unique window to the fundamental interactions of particle physics, far beyond the reach of colliders. One would expect that if the SM is not a complete theory then such observations must have some hints about the physics beyond the SM. In this section we will discuss a few of these issues in cosmology such as the baryon asymmetry of the universe, dark matter and dark energy which points to the existence of new physics beyond the SM of particle physics.

1.3.1 Baryon Asymmetry of the universe and baryogenesis

Cosmological observations (studies of the cosmic microwave background radiation, large scale structure data, the primordial abundances of light elements) indicate that our visible universe is dominated by matter and there is very little antimatter. The baryon asymmetry normalized to number density of photons (n_γ) can be extracted out of these observations, which gives

$$\eta(t = \text{present}) = \frac{n_B - n_{\bar{B}}}{n_\gamma} \sim 10^{-10}. \tag{1.98}$$

The astrophysical observations suggest that at an early epoch before the big-bang nucleosynthesis this asymmetry was generated. Thus it is natural to seek an explanation for this asymmetry from the fundamental particle interactions within or beyond the SM of particle physics. There are three conditions, often called Sakharov's conditions [70], that must be met in order to generate a baryon asymmetry dynamically:

1. baryon number violation,
2. C and CP violation, and
3. departure from thermal equilibrium.

In principle, the SM has all the ingredients to satisfy all three conditions.

1. In the SM baryon number B and lepton number L are violated due to the triangle anomaly, leading to 12-fermion processes (discussed later)involving nine left handed quarks (three of each generation) and three left handed leptons (one from each generation) obeying the selection rule $\Delta(B - L) = 0$. These processes have a highly suppressed amplitude proportional to $e^{-2\pi/\alpha}$ (where α is the fine structure constant) at zero temperature. However, at high temperature this suppression is lifted and these processes can be very fast.

2. The weak interactions in the SM violate C in a maximal way. CP is also violated via the CKM phase δ_{CKM}.

3. The electroweak phase transition can result in the departure from thermal equilibrium if it is sufficiently strongly first order.

However, in practice it turns out that only the first Sakharov condition is fulfilled in a satisfactory manner in the SM. The CP violation coming from the CKM phase is suppressed by a factor T_{EW}^{12} in the denominator, where $T_{\mathrm{EW}} \sim 100$ GeV is the temperature during the electroweak phase transition. Consequently, the CP violation in the SM is too small to explain the observed baryon asymmetry of the universe. Furthermore, the electroweak phase transition is not sufficiently strongly first order for a Higgs mass $m_\phi \sim 125$ GeV.

Thus, to explain the baryon asymmetry of the universe one must go beyond the SM, either by introducing new sources of CP violation and a new kind of out-of-equilibrium situations (such as the out-of-equilibrium decay of some new heavy particles) or modifying the electroweak phase transition itself. Some possible alternatives are GUT baryogenesis, electroweak baryogenesis, Affleck-Dine mechanism, and leptogenesis.

GUT baryogenesis

In the grand unified theories, a natural realization of baryogenesis becomes possible through the out-of-equilibrium decay of the heavy gauge and Higgs bosons [71–78]. As discussed in the section 1.2.3, the heavy bosons in grand unified theories can have baryon number violating decays. Since fermions belong to the chiral representations, C is violated maximally and a CP asymmetry can be generated through complex couplings in the Lagrangian. However, in the simplest GUT models such as $SU(5)$ and $SO(10)$, B and L are violated but $B - L$ is conserved. Consequently, the $B - L$ conserving and $B + L$ violating sphaleron processes, which are in equilibrium untill a temperature $T \lesssim 10^{12}$ GeV will washout any $B + L$ asymmetry created above this scale. Furthermore, the non-observation of proton decay gives stringent limits on the reheat temperature after inflation, which is quite high for the simple inflation models to work.

Electroweak baryogenesis

As the name suggests, in this class of models the departure from thermal equilibrium is provided by the electroweak phase transition [79–85]. If the electroweak phase transition is first order then once the temperature reaches the critical point, the free energies corresponding to true vacuum and false vacuum becomes equal. Both vacua coexist as the bubbles start forming, where inside the bubbles the electroweak symmetry is broken and $B + L$ violating processes, sphaleron transitions are not allowed [6]. Consequently, any baryon number violation along the bubble wall can generate a $B + L$ asymmetry inside the bubbles, which remain unaffected by the sphaleron transitions. Thus, the out-of-equilibrium condition is satisfied. However, as we discussed above the CP violation coming from the CKM phase is too small and the electroweak phase transition is not sufficiently strongly first order for a Higgs scalar with a mass ~ 125 GeV. In fact, in viable models of electroweak baryogenesis the scalar potential is modified such that the nature of electroweak phase transition can be made more strongly first order compared to the SM, and one includes new sources of CP violation.

[6] In Ref. [86] it was pointed out that in the thermal bath of the expanding Universe one can make transitions between the gauge vacua through thermal fluctuations over the barrier (not by tunneling). In fact, At temperatures larger than the height of the barrier, the exponential suppression in the rate provided by the Boltzmann factor disappears. Consequently, $(B + L)$ violating processes can occur at a significant rate and can be in equilibrium in the expanding Universe. The finite temperature transition rate in the electroweak theory is determined by the so called sphaleron configuration [87], which is a saddle point of the field energy of the gauge-Higgs system.

The Affleck-Dine mechanism

In this mechanism the baryon asymmetry is generated via the cosmological evolution of scalar fields carrying baryonic charge [88, 89]. This scenario can be naturally realized in the context of supersymmetric models utilizing supersymmetric flat directions, along which the scalar potential vanishes. The scalar field can be some linear combination of squarks, sleptons and Higgs scalars. Supersymmetry breaking and non-renormalizable operators lift the flat direction, setting the scale for the potential. During inflation, the scalar field gets displaced to a large expectation value, setting the initial conditions for subsequent evolution. After inflation, when the Hubble rate becomes of the order of the curvature of the potential, the field starts oscillating and the non-renormalizable B violating terms in the potential impart baryon number to the scalar field, which subsequently gets transferred to the fermions via decay of the scalar field.

Leptogenesis

Leptogenesis is a mechanism where a lepton asymmetry is generated before the electroweak phase transition, which then gets converted to baryon asymmetry of the universe in the presence of sphaleron induced anomalous $B + L$ violating processes, which converts any primordial L asymmetry, and hence $B - L$ asymmetry, into a baryon asymmetry. A realization of leptogenesis via the decay of out-of-equilibrium heavy neutrinos transforming as singlets under the SM gauge group was proposed in Ref. [90]. The Yukawa couplings provide the CP through interference between tree level and one-loop decay diagrams. The departure from thermal equilibrium occurs when the Yukawa interactions are sufficiently slow [7]. The lepton number violation in

[7] The out of equilibrium condition can be understood as follows. In thermal equilibrium the expectation value of the baryon number can be written as $\langle B \rangle = \mathrm{Tr}[\mathrm{B}e^{-\beta \mathrm{H}}]/\mathrm{Tr}[e^{-\beta \mathrm{H}}]$, where β is the inverse temperature. Since particles and anti particles have opposite baryon number, B is odd under C operation, while it is even under P and T operations. Thus CPT conservation implies a vanishing total baryon number since B is odd and H is even under CPT, unless there is a nonvanishing chemical potential. Assuming a nonvanishing chemical potential implies that the above equation for the expectation value of the baryon number is no longer valid and the baryon number density departs from the equilibrium distribution. This is achieved when the interaction rate is very slow compared to the expansion rate

this scenario comes from the Majorana masses of the heavy neutrinos. The generated lepton asymmetry then gets partially converted to baryon asymmetry in the presence of sphaleron induced anomalous $B + L$ violating interactions before the electroweak phase transition. In what follows, we will discuss the sphaleron processes and few of the most popular scenarios of leptogenesis in some detail.

Anomalous $B+L$ violating processes and relating baryon and lepton asymmetries

In the SM both B and L are accidental symmetries and at the tree level these symmetries are not violated. However, the chiral nature of weak interactions gives rise to equal global anomalies for B and L, giving a vanishing $B - L$ anomaly, but a non-vanishing axial current corresponding to $B + L$, given by [91,92]

$$\partial_\mu j^\mu_{(B+L)} = \frac{2N_f}{8\pi}\left(\alpha_2 W^a_{\mu\nu}\tilde{W}^{a\mu\nu} - \alpha_1 B_{\mu\nu}\tilde{B}^{\mu\nu}\right), \tag{1.99}$$

where $W^a_{\mu\nu}$ and $B_{\mu\nu}$ are the $SU(2)_L$ and $U(1)_Y$ field strength tensors and N_f is the number of fermion generations. The corresponding $B + L$ violation can obtained by integrating the divergence of the $B + L$ current, which is related to the change in the topological charges of the gauge field

$$\Delta(B + L) = \int d^4x \partial^\mu j^{(B+L)}_\mu = 2N_f \Delta N_{\text{cs}}, \tag{1.100}$$

where $N_{\text{cs}} = \pm 1, \pm 2, \cdots$ corresponds to the topological charge of gauge fields, called the Chern-Simons number. Physically speaking, the Chern-Simons number corresponds to infinitely many degenerate ground states separated by potential barrier in the space of the gauge and Higgs field configurations. The probability of tunneling between different neighboring vacua is determined by the instanton configurations. In the SM there are three generations of fermions ($N_f = 3$), leading to $\Delta B = \Delta L = 3N_{\text{cs}}$, thus the vacuum to vacuum transition changes B and L by multiples of 3 units. At the lowest order, one has the $B + L$ violating effective operator

$$\mathcal{O}(B + L) = \prod_{i=123} (q_{Li} q_{Li} q_{Li} l_{Li}), \tag{1.101}$$

which gives rise to 12-fermion sphaleron induced transitions, such as

$$|\text{vac}\rangle \to [u_L u_L d_L e^-_L + c_L c_L s_L \mu^-_L + t_L t_L b_L \tau^-_L]. \tag{1.102}$$

of the universe.

Interactions	μ relations	eliminated μ
$D^\mu \phi^\dagger D_\mu \phi$	$\mu_W = \mu_- + \mu_0$	μ_-
$\bar{q}_L \gamma_\mu q_L W^\mu$	$\mu_{d_L} = \mu_{u_L} + \mu_W$	μ_{d_L}
$\bar{l}_L \gamma_\mu l_L W^\mu$	$\mu_{iL} = \mu_{\nu_{iL}} + \mu_W$	μ_{iL}
$\bar{q}_L u_R \phi^\dagger$	$\mu_{u_R} = \mu_0 + \mu_{u_L}$	μ_{u_R}
$\bar{q}_L d_R \phi$	$\mu_{d_R} = -\mu_0 + \mu_{d_L}$	μ_{d_R}
$\bar{l}_{iL} e_{iR} \phi$	$\mu_{iR} = -\mu_0 + \mu_{iL}$	μ_{iR}

Table 1.2: Relations among chemical potential arising from interactions in chemical equilibrium.

At zero temperature the transition rate is suppressed by $e^{-4\pi/\alpha} = \mathcal{O}(10^{-165})$ [91,92]. However, when the temperature is larger than the barrier height, this Boltzmann suppression disappears and $B+L$ violating transitions can occur at a significant rate [86]. In the symmetric phase, when the temperature is grater than the electroweak phase transition temperature, $T \geq T_{\rm EW}$, the transition rate per unit volume is [93–96]

$$\frac{\Gamma_{B-L}}{V} \sim \alpha^5 \ln \alpha^{-1} T^4, \tag{1.103}$$

where α is the fine-structure constant.

Now to see how the $B-L$ symmetry gets converted to a baryon asymmetry let us follow an analysis of the chemical potential [61,97,98]. In the ultrarelativistic limit, the difference between the number of particles (n_+) and antiparticles (n_-) can be written in terms of the chemical potential (μ) as

$$n_+ - n_- = n_d \frac{gT^3}{6} \frac{\mu}{T} \tag{1.104}$$

where $n_d = 2$ for bosons and $n_d = 1$ for fermions. In Table. 1.2 we summarize the relations among the chemical potential using the relevant interactions of the SM fields. μ_f corresponds to the chemical potential of the SM fermion f, μ_W corresponds to the chemical potential of the gauge boson W and (μ_-, μ_0) corresponds to the chemical potential of the Higgs doublet. The chemical potential of neutrinos always appear as a sum and will be denoted as $\mu_\nu = \sum_i \mu_{iL}$. From Table. 1.2 we note that all chemical potentials can be expressed as a linear combination of four independent chemical potentials $\mu_0, \mu_W, \mu_u \equiv \mu_{uL}$, and μ_ν. The baryon number, lepton number, the electric charge and hypercharge can be written in terms of these four chemical potential as

$$\begin{aligned} B &= 12\mu_u + 6\mu_W, \\ L &= 3\mu + 2\mu_W - \mu_0, \\ Q &= 24\mu_u + (12+2m)\mu_0 - (4+2m)\mu_W, \\ Y &= -(10+m)\mu_W, \end{aligned} \tag{1.105}$$

where m is the number of Higgs doublets. Out of the four chemical potentials, one can further be eliminated using the relation given by the sphaleron processes, $3\mu_u + 2\mu_W + \mu = 0$. At a temperature above the electroweak phase transition, $T > T_{\rm EW}$, both $\langle Q \rangle$ and $\langle Y \rangle$ should vanish; while for $T < T_{\rm EW}$, $\langle Q \rangle$ should vanish, but $\langle Y \rangle$ need not vanish and $\mu_0 = 0$. These conditions together with the relations discussed above allows us to write down the baryon asymmetry in terms of the $B - L$ number density as

$$\begin{aligned} B(T > T_{\rm EW}) &= \frac{24+4m}{66+13m}(B-L), \\ B(T < T_{\rm EW}) &= \frac{32+4m}{98+13m}(B-L). \end{aligned} \tag{1.106}$$

Thus, the primordial $B-L$ asymmetry gets partially converted into a baron asymmetry of the universe after the electroweak phase transition.

Leptogenesis with right handed neutrinos

In section 1.2.1, we have discussed how adding singlet right handed neutrinos N_{Ri} to the SM can generate tiny seesaw masses [16–22] for light neutrinos. Beyond the generation of light neutrino masses, the interaction terms

$$\mathcal{L}_{\rm int} = h_{\alpha i}\bar{l}_{L\alpha}\phi N_{Ri} + M_i\overline{(N_{Ri})^c}N_{Ri}, \tag{1.107}$$

can also provide all the ingredients necessary for realizing leptogenesis. We will work on a basis where the right handed neutrino mass matrix is real and diagonal. Furthermore we assume a hierarchical mass spectrum for the right handed neutrinos $M_3 > M_2 > M_1$. The Majorana mass term gives rise to lepton number violating

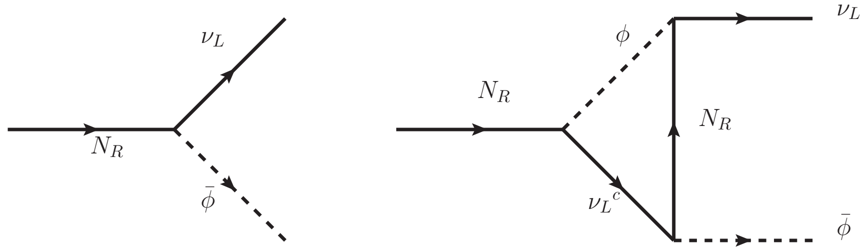

Figure 1.6: Tree level and one-loop vertex diagrams contributing to the vertex type CP violation in models with right handed neutrinos.

decays of the right handed neutrinos

$$\begin{aligned} N_{Ri} &\rightarrow l_{iL} + \bar{\phi}, \\ &\rightarrow {l_{iL}}^c + \phi, \end{aligned} \tag{1.108}$$

which can generate a lepton asymmetry if there is CP violation and the decay is out of equilibrium [90]. This lepton asymmetry (equivalently $B-L$ asymmetry) then gets converted to baryon asymmetry in presence of anomalous $B+L$ violating processes before the electroweak phase transition.

In the original proposal [90] and few subsequent works [99–103], only the CP violation coming from interference of tree level and one-loop vertex diagrams, shown in Fig. 1.6. was considered. This is somewhat analogous to the CP violation in K-physics coming from the penguin diagram. The CP asymmetry parameter corresponding to the vertex type CP violation is given by

$$\varepsilon_v \equiv \frac{\Gamma(N \rightarrow l\phi^\dagger) - \Gamma(N \rightarrow l^c\phi)}{\Gamma(N \rightarrow l\phi^\dagger) + \Gamma(N \rightarrow l^c\phi)} = -\frac{1}{8\pi} \sum_{i=2,3} \frac{\mathrm{Im}\left[\Sigma_\alpha(h^*_{\alpha 1}h_{\alpha i})\Sigma_\beta(h^*_{\beta 1}h_{\beta i})\right]}{\Sigma_\alpha |h_{\alpha 1}|^2} f_v\left(\frac{M_i^2}{M_1^2}\right), \tag{1.109}$$

where the loop function f_v is defined by

$$f_v\,(x) = \sqrt{x}\left[1-(1+x)\ln\left(\frac{1+x}{x}\right)\right]. \tag{1.110}$$

In the limit $M_1 \ll M_2, M_3$ the asymmetry simplifies to

$$\varepsilon_v \simeq -\frac{3}{16\pi}\sum_{i=2,3}\frac{M_1}{M_i}\frac{\mathrm{Im}\left[\Sigma_\alpha(h^*_{\alpha 1}h_{\alpha i})\Sigma_\beta(h^*_{\beta 1}h_{\beta i})\right]}{\Sigma_\alpha |h_{\alpha 1}|^2}. \tag{1.111}$$

It was later pointed out in Refs. [104, 105] and confirmed rigorously in Refs. [106–111], that there is another source of CP violation coming from interference of

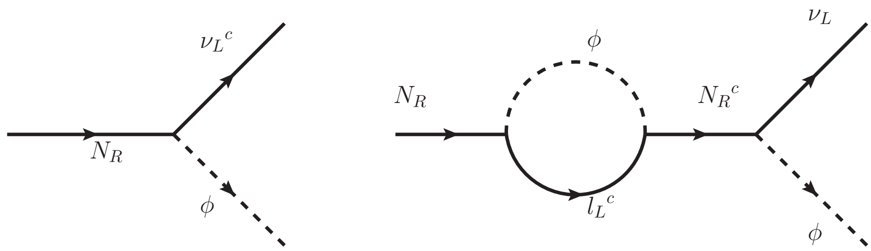

Figure 1.7: Tree level and one-loop self-energy diagrams contributing to the CP violation in models with right handed neutrinos.

tree level diagram with one-loop self-energy diagram shown in Fig. 1.7. This CP violation is similar to the CP violation due to the box diagram, entering the mass matrix in $K-\bar{K}$ mixing in K-physics. If the heavy neutrinos decay in equilibrium, the CP asymmetry coming from the self-energy diagram due to one of the heavy neutrinos may cancel with the asymmetry from the decay of another heavy neutrino to preserve unitarity. However, in out-of-equilibrium decay of heavy neutrinos the number densities of the two heavy neutrinos differ during their decay and consequently, this cancellation is no longer present. This can be understood as the right handed neutrinos oscillating into antineutrinos of different generations, which under the condition $\Gamma[\text{particle} \to \text{antiparticle}] \neq \Gamma[\text{antiparticle} \to \text{particle}]$, can create an asymmetry in right handed neutrinos before they decay. An elementary discussion regarding how the CP violation enters in Majorana mass matrix, which then generates a lepton asymmetry can be found in Ref. [61, 112]. The basic idea is to treat the particles and the antiparticles independently. The CP eigenstates $|N_i\rangle$ and $|N_i^c\rangle$ are no longer physical eigenstates, which evolves with time. Consequently, the physical states, which are admixtures of $|N_i\rangle$ and $|N_i^c\rangle$, can decay into both leptons and antileptons, giving rise to a CP violation. The CP asymmetry parameter coming from the interference of tree level and one-loop self-energy diagram is given by

$$\varepsilon_s \equiv \frac{\Gamma(N \to l\phi^\dagger - N \to l^c\phi)}{\Gamma(N \to l\phi^\dagger + N \to l^c\phi)} = \frac{1}{8\pi}\sum_{i=2,3}\frac{\mathrm{Im}\left[\Sigma_\alpha(h^*_{\alpha 1}h_{\alpha i})\Sigma_\beta(h^*_{\beta 1}h_{\beta i})\right]}{\Sigma_\alpha|h_{\alpha 1}|^2} f_s\left(\frac{M_i^2}{M_1^2}\right), \tag{1.112}$$

where the loop function f_s is defined by

$$f_s\,(x) = \frac{\sqrt{x}}{1-x}. \tag{1.113}$$

When the mass difference between the right handed neutrinos is very large compared to the width, $M_1 - M_2 \gg \frac{1}{2}\Gamma_{N_{1,2}}$, the CP asymmetries coming from vertex and self-energy diagrams are comparable. However, when two right handed neutrinos are nearly degenerate, such that their mass difference is comparable to their width, then CP violation contribution coming from the self-energy diagram becomes very large (orders of magnitude larger than the CP asymmetry generated by the vertex type diagram). This is often referred to as the resonance effect.

To ensure that the lightest right handed neutrino decays out-of-equilibrium so that an asymmetry is generated, the out-of-equilibrium condition given by

$$\frac{h_{\alpha 1}}{16\pi} M_1 < 1.66\sqrt{g_*}\frac{T^2}{m_{\mathrm{Pl}}} \qquad \text{at } T = M_1. \tag{1.114}$$

must be satisfied, where g_* correspond to the effective number of relativistic degrees of freedom. This gives a lower bound $m_{N_1} > 10^8$ GeV [113]. Though this gives us a rough estimate, in an actual calculation of the asymmetry one solves the Boltzmann equation, which takes into account both lepton number violating as well as lepton number conserving processes mediated by heavy neutrinos.The Boltzmann equation governing lepton number asymmetry $n_L \equiv n_l - n_{l^c}$, is given by

$$\frac{dn_L}{dt} + 3Hn_L = (\varepsilon_v + \varepsilon_s)\Gamma_{\psi_1}(n_{\psi_1} - n^{eq}_{\psi_1}) - \frac{n_L}{n_\gamma} n^{eq}_{\psi_1}\Gamma_{\psi_1} - 2n_\gamma n_L \langle \sigma |v| \rangle, \tag{1.115}$$

where Γ_{ψ_1} is the decay rate of the physical state $|\psi_1\rangle$, $n^{eq}_{\psi_1}$ is the equilibrium number density of ψ_1 given by

$$n^{eq}_{\psi_1} = \begin{cases} s{g_*}^{-1} & T \gg m_{\psi_1} \\ \frac{s}{g^*}\left(\frac{m_{\psi_1}}{T}\right)^{3/2} \exp\left(-\frac{m_{\psi_1}}{T}\right) & T \ll m_{\psi_1}, \end{cases} \tag{1.116}$$

where s is the entropy density. The first term on the right hand side of Eq. (1.115) corresponds to the CP violating contribution to the asymmetry and is the only term that generates asymmetry when ψ_1 decays out-of-equilibrium, while the second term corresponds to inverse decay of ψ_1, and the last term corresponds to $2 \leftrightarrow 2$ lepton number violating scattering process such as $l + \phi^\dagger \leftrightarrow l^c + \phi$, with $\langle \sigma |v| \rangle$ being the thermally averaged cross section. The number density of ψ_1 is governed by the Boltzmann equation

$$\frac{dn_{\psi_1}}{dt} + 3Hn_{\psi_1} = -\Gamma_{\psi_1}(n_{\psi_1} - n^{eq}_{\psi_1}). \tag{1.117}$$

One often defines a parameter $K = \Gamma_{\psi_1}(T = m_{\psi_1})/H(T = m_{\psi_1})$, where the Hubble rate $H = 1.66 g_*{}^{1/2}(T^2/M_{\rm Pl})$, which gives a measure of the deviation from thermal equilibrium. For $K \ll 1$ one can find an approximate solution for Eq. (1.115) given by

$$n_L = \frac{s}{g_*}(\varepsilon_v + \varepsilon_s). \tag{1.118}$$

The Yukawa couplings are constrained by the required amount of primordial lepton asymmetry required to generate the correct baryon asymmetry of the universe, while the lightest right handed neutrino mass is constrained from the out-of-equilibrium condition. In the resonant leptogenesis scenario, the CP violation is largely enhanced, making the constrains on Yukawa couplings relaxed. Consequently the scale of leptogenesis can be considerably lower, making it possible to realize a TeV scale leptogenesis, which can be put to test at the LHC.

Leptogenesis with triplet Higgs

In section 1.2.1, we have discussed how small neutrino masses can be generated by adding triplet Higgs scalars ξ_a to the SM [23–26]. The interactions of these triplet Higgs scalar that are relevant for leptogenesis are given by

$$\mathcal{L}_{\rm int} = f_{ij}\xi\psi_{Li} = f^a_{ij}\xi^{++}_a l_i l_j + \mu_a \xi^\dagger_a \phi\phi. \tag{1.119}$$

From these interactions we have the decay modes of the triplet Higgs

$$\xi^{++}_a \to \begin{cases} l^+_i l^+_j \\ \phi^+\phi^+, \end{cases} \tag{1.120}$$

The CP violation is obtained through the interference between the tree level and one-loop self-energy diagrams shown in Fig. 1.8. There are no one-loop vertex diagrams in this case. One needs at least two ξ's. To see how this works, we will follow the mass-matrix formalism [23], in which the diagonal tree-level mass matrix of ξ_a is modified in the presence of interactions to

$$\frac{1}{2}\xi^\dagger \left(M^2_+\right)_{ab}\xi_b + \frac{1}{2}\left(\xi^*_a\right)^\dagger \left(M^2_-\right)_{ab}\xi^*_b, \tag{1.121}$$

where

$$M^2_\pm = \begin{pmatrix} M^2_1 - i\Gamma_{11}M_1 & -i\Gamma^\pm_{12} \\ -i\Gamma^\pm_{21}M_1 & M^2_2 - i\Gamma_{22}M_2 \end{pmatrix}, \tag{1.122}$$

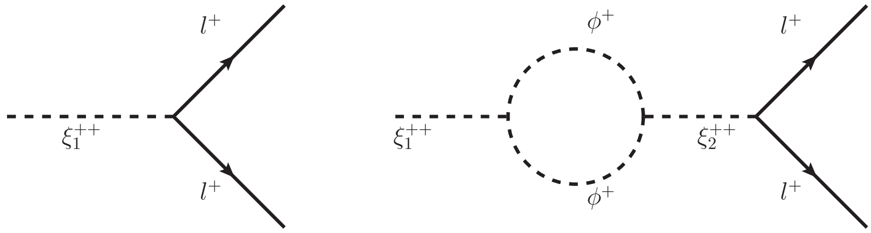

Figure 1.8: Tree level and one-loop self-energy diagrams contributing to the CP violation in a model with triplet Higgs.

with $\Gamma^+_{ab} = \Gamma_{ab}$ and $\Gamma^-_{ab} = \Gamma^*_{ab}$. From the absorptive part of the one-loop diagram for $\xi_a \to \xi_b$ we obtain

$$\Gamma_{ab} M_b = \frac{1}{8\pi}\left(\mu_a \mu_b^* + M_a M_b \sum_{k,l} f_{kl}^{a\,*} f_{kl}^b\right). \tag{1.123}$$

Assuming $\Gamma_a \equiv \Gamma_{aa} \ll M_a$, the eigenvalues of $M^2_\pm$ are given by

$$\lambda_{1,2} = \frac{1}{2}(M_1^2 + M_2^2 \pm \sqrt{S}), \tag{1.124}$$

where $S = (M_1^2 - M_2^2)^2 - 4|\Gamma_{12} M_2|^2$ and $M_1 > M_2$. The physical states, which evolves with time, can be written as linear combinations of the CP eigenstates as

$$\psi^+_{1,2} = a^+_{1,2}\xi_1 + b^+_{1,2}\xi_2\ , \qquad \psi^-_{1,2} = a^-_{1,2}\xi_1^* + b^-_{1,2}\xi_2^*\ , \tag{1.125}$$

where $a_1^\pm = b_2^\pm = 1/\sqrt{1+|C_i^\pm|^2}$, $b_1^\pm = C_1^\pm/\sqrt{1+|C_i^\pm|^2}$, $a_2^\pm = C_2^\pm/\sqrt{1+|C_i^\pm|^2}$ with

$$\begin{aligned} C_1^+ = -C_2^- &= \frac{-2i\Gamma_{12}^* M_2}{M_1^2 - M_2^2 + \sqrt{S}}\ , \\ C_1^- = -C_2^+ &= \frac{-2i\Gamma_{12} M_2}{M_1^2 - M_2^2 + \sqrt{S}}\ . \end{aligned} \tag{1.126}$$

The physical states $\psi^\pm_{1,2}$ evolve with time and decay into lepton and antilepton pairs. Assuming $(M_1^2 - M_2^2)^2 \gg 4|\Gamma_{12} M_2|^2$, the CP asymmetry is given by [23]

$$\varepsilon_i \simeq \frac{1}{8\pi^2 (M_1^2 - M_2^2)^2} \sum_{k,l} \mathrm{Im}\left(\mu_1 \mu_2^* f_{kl}^1 f_{kl}^{2\,*}\right)\left(\frac{M_i}{\Gamma_i}\right). \tag{1.127}$$

For $M_1 > M_2$, when the temperature drops below M_1, ψ_1 decays away to create a lepton asymmetry. However, this asymmetry is washed out by lepton number violating interactions of ψ_2; and the subsequent decay of ψ_2 at a temperature below M_2 sustains.

The generated lepton asymmetry then gets converted to the baryon asymmetry in the presence of the sphaleron induced anomalous $B + L$ violating processes before the electroweak phase transition. The approximate final baryon asymmetry is given by

$$\frac{n_B}{s} \sim \frac{\varepsilon_2}{3g_* K(\ln K)^{0.6}}, \tag{1.128}$$

where $K \equiv \Gamma_2(T = M_2)/H(T = M_2)$ is the parameter measuring the deviation from thermal equilibrium when, $H = 1.66{g_*}^{1/2}(T^2/M_{\rm Pl})$ is the Hubble rate, and g^* corresponds to the number of relativistic degrees of freedom.

In a more rigorous estimation of the baryon asymmetry, in addition to the decays and the inverse decays of triplet scalars, one needs to incorporate the gauge scatterings $\psi\bar{\psi} \leftrightarrow F\bar{F}, \phi\bar{\phi}, G\bar{G}$ (F corresponds to SM fermions and G corresponds to gauge bosons) and $\Delta L = 2$ scattering processes $ll \leftrightarrow \phi^*\phi^*$ and $l\phi \leftrightarrow \bar{l}\phi^*$ into the Boltzmann equation analysis of the asymmetry. Including these washout processes, one finds a lower limit on M_ξ, $M_\xi \gtrsim 10^{11}$ GeV [114]. For a quasi-degenerate spectrum of scalar triplets the resonance effect can enhance the CP asymmetry by a large amount and a successful leptogenesis scenario can be attained for a much smaller value of triplet scalar mass. In Refs. [115, 116], an absolute bound of $M_\xi \gtrsim 1.6\,\text{TeV}$ is obtained for a successful resonant leptogenesis scenario with triplet Higgs.

1.3.2 Dark matter and dark energy

Out of the total mass-energy budget of the universe, the ordinary baryonic matter accounts for only about 4.6% while the rest is accounted for by 24% dark matter and 71.4% dark energy. However, we have yet to find a satisfactory solution about their nature and interactions. Thus, several models beyond the SM of particle physics try to address the issues of dark matter and dark energy.

Evidences from the observations of the Cosmic Microwave Background Radiation (CMBR), the large scale structures and the abundance of light elements during primordial nucleosynthesis suggests that dark matter is primarily non-baryonic, possibly in the form of particles, which can naturally be attributed to models beyond the SM. One of the most popular candidates for dark matter is the weakly interacting massive particles (WIMPs). They can have a mass in the range $\sim$ 100 -1000 GeV and interact weakly. The thermal freeze out of WIMPs in the early universe gives a value of their mass density today, consistent with the observed dark matter relic density. This is often referred to as the WIMP miracle. A popular realization of WIMP comes from supersymmetric models with conserved R-parity in the form of the lightest supersymmetric particle (LSP) [117–122], usually the lightest neutralino, which is a mass eigenstate formed by a linear combination of the superpartners of the neutral gauge and Higgs fields. Axions, heavy sterile neutrinos and "hidden sector" dark matter are among the other popular dark matter candidates. There have also been some interest in the recent literature about some radiative models of neutrino masses, involving Higgs scalars that do not acquire any VEV and can be potential dark matter candidates [33, 123]. Detection and identification of dark matter candidates in direct and indirect detection experiments, and at collider searches will definitely provide a key direction in the study of physics beyond the SM.

One of the interesting approaches, called co-genesis, tries to correlate two of the most important puzzles in cosmology and particle physics: the matter-antimatter asymmetry of the universe and the nature of non-baryonic dark matter. Observations of the cosmic microwave background (CMB) by WMAP [124] and PLANCK [125] suggest comparable values of the baryonic and cold dark matter densities

$$\Omega_b h^2 \sim 0.022, \quad \Omega_{DM} h^2 \sim 0.12. \tag{1.129}$$

This is often referred to as the cosmic coincidence problem. Though, the standard paradigm, in general, adopts unrelated mechanisms to explain the observed baryon asymmetry of the universe and the dark matter relic abundance, several co-genesis mechanisms involving asymmetric dark matter have been proposed in the literature addressing the cosmic coincidence problem [126–141]. In generic co-genesis mechanisms, a matter-antimatter asymmetry in the dark sector determines the dark matter relic abundance and generates the correct baryon asymmetry in the visible sector.

Dark energy is attributed to the accelerated expansion of the universe and remains a challenge to explain. The observed value of the cosmological constant [8] corresponds to a very small mass scale, about 13 orders of magnitude smaller than the electroweak

[8]The cosmological constant is a constant term (remains constant over the entire evolution of the universe) in the Einstein equation.

symmetry breaking scale

$$\frac{|\Lambda|^{1/4}}{\langle\phi\rangle} \sim 10^{-13}. \tag{1.130}$$

Consequently, the cosmological constant induced by the electroweak phase transition is 52 orders of magnitude larger than the observations. In fact, there is also a contribution from the zero-point vacuum fluctuations, which gives a contribution 120 orders of magnitude larger than the observations, if the cutoff is chosen as the reduced Planck scale $m_{\rm Pl} \sim 10^{18}$ GeV. This is often called the cosmological constant problem.

Several models have been considered to solve this problem, which differ by their predictions for the equation of state of the dark energy, $\omega = p/\rho$, where p and ρ are the pressure and the density of dark energy, respectively. A good fit to the observation is obtained for a ω very close to -1, which can be either of dark energy or a cosmological constant.

While the existence of a scalar field called quintessence provides an explanation for the dark energy, a striking proximity of the effective scales of neutrino masses and the dark energy points to a connection between them. This apparent connection is realized in the neutrino dark energy (νDE) models. To this end, several approaches have been proposed in the literature. In some of the scenarios, a direct connection through the formation of neutrino condensate at a late epoch of the early universe using the effective self-interaction has been studied [142–148], while another class of models utilizes the variation of neutrino masses to dynamically obtain the dark energy [149–165].

1.4 Potential hints of new physics from the LHC and flavor physics

The second run of the LHC is already in effect and some preliminary but interesting potential hints of new physics have been reported by the CMS and ATLAS Collaborations at the LHC, as this section is being written. Several potential signals reported at the end of first run are yet to be confirmed or ruled out. On the other hand, several anomalies in the flavor sector, particularly the ones associated with B-decays are growing strong with new measurements at the B-factories. Since one of the key goals of this thesis is to explore physics beyond the SM at a phenomenological level and to study the associated implications, these signals often play a guiding role which motivated several of the studies in this thesis. Thus, without an account of these signals, the introduction of this thesis will remain incomplete. In what follows, we compile a summary of the signals relevant to the studies done in this thesis. An account of the same will be repeated as necessary in the following chapters for an easy and independent reference.

1.4.1 Potential signals of new physics at the LHC

In 2014 the CMS Collaboration at the LHC at CERN announced their results for the right handed gauge boson W_R search at a center of mass energy of $\sqrt{s} = 8$ TeV and 19.7 fb^{-1} of integrated luminosity [166]. They have used the final state $eejj$ to probe $pp \to W_R \to eN_R \to eejj$, with the cuts $p_T > 60\,\mathrm{GeV}, |\eta| < 2.5$ ($p_T > 40\,\mathrm{GeV}, |\eta| < 2.5$) for leading (subleading) electron. The invariant mass m_{eejj} is calculated for all events satisfying $m_{ee} > 200\,\mathrm{GeV}$. In the bin $1.8\,\mathrm{TeV} < m_{eejj} < 2.2\,\mathrm{TeV}$ roughly 14 events have been observed with 4 expected background events, amounting to a 2.8σ local excess, which, however, cannot be explained by W_R decay in Left-Right Symmetric Models (LRSM) with strict left-right symmetry (gauge couplings $g_L = g_R$) [166]. The CMS search for di-leptoquark production, at a center of mass energy of $\sqrt{s} = 8$ TeV and 19.6 fb^{-1} of integrated luminosity has reported a 2.4σ and a 2.6σ local excess in $eejj$ and $e\not{p}_T jj$ channels [9] respectively, and has excluded the first generation scalar leptoquarks with masses less than 1005 (845) GeV for $\beta = 1(0.5)$, where β is the branching fraction of a leptoquark to a charged lepton and a quark [167]. In the $eejj$ channel for a 650 GeV leptoquark signal using the optimization cuts $S_T > 850\,\mathrm{GeV}, m_{ee} > 155\,\mathrm{GeV}$ and $m_{ej}^{\min} > 270\,\mathrm{GeV}$ (where S_T is the scalar sum of the p_T of two leptons and two jets), 36 events have been observed compared with $20.49 \pm 2.4 \pm 2.45$ (syst.) expected events from the Standard Model (SM) backgrounds implying a 2.4σ local excess. While in the $e\not{p}_T jj$ channel using the optimization cuts $S_T > 1040\,\mathrm{GeV}, m_{\not{E}_T} > 145\,\mathrm{GeV}, m_{ej} > 555\,\mathrm{GeV}$ and $m_{T,e\not{p}_T}$

[9] The $e\not{p}_T jj$ channel is often referred to as $e\nu jj$ channel in the literature. Also note that the "ee" in $eejj$ refers to two first generation charged leptons, not necessarily of the same sign.

(where S_T is now the scalar sum of the missing energy $\not{E}_T$ and p_T of the electron and two jets), 18 events have been observed compared with $7.54 \pm 1.20 \pm 1.07$(syst.) expected background events amounting for a 2.6σ local excess.

Using the run one data, the ATLAS and CMS collaborations have also reported a number of diboson and dijet excesses over the SM expectations near the invariant mass region $1.8 - 2.0\,\mathrm{TeV}$. The search for diboson production has been reported by the ATLAS collaboration to show a 3.4σ excess at $\sim 2\,\mathrm{TeV}$ in boosted jets of WZ channel amounting to a global 2.5σ excess over the SM expectation [168]. The method of jet substructure has been used to discriminate the hadronic decays of W and Z bosons from QCD dijets and due to overlaps in the jet masses of the gauge bosons many events can also be interpreted as ZZ or WW resonances, yielding 2.9σ and 2.6σ excesses in two channels respectively. On the other hand, the CMS has reported a 1.4σ excess at $\sim 1.9\,\mathrm{TeV}$ in their search for diboson production without discriminating between the W- and Z-tagged jets [169] and a 1.5σ excess at $\sim 1.8\,\mathrm{TeV}$ in the search for diboson production with a leptonically tagged Z [170]. In the search for dijet resonances the ATLAS and CMS have reported excesses at $1.8\,\mathrm{TeV}$ with 2.2σ and 1σ significance levels respectively [171, 172]. The CMS has also reported a 2.1σ excess in the energy bin 1.8 to $1.9\,\mathrm{TeV}$ in the resonant HW production channel [173].

Very recently, the CMS and ATLAS collaborations have reported a roughly 3σ excess in the diphoton channel at an invariant mass of about 750 GeV in the first 3 fb^{-1} of collected data from Run 2 of the LHC at 13 TeV [174, 175]. The Landau-Yang theorem forbids the possibility of a massive spin one resonance decaying to $\gamma\gamma$. The leading interpretations of the excess within the context of new physics scenarios therefore consist of postulating a fundamental spin zero or spin two particle with mass of about 750 GeV. However no enhancements have been seen in the dijet, $t\bar{t}$, diboson or dilepton channels posing a clear challenge to the possible interpretations of this excess. The absence of a peaked $\gamma\gamma$ angular distribution in the observed events towards the beam direction disfavours [176] the spin two hypothesis and the spin zero resonance interpretation seems more favourable from a theoretical point of view.

1.4.2 Flavor anomalies pointing to new physics beyond the SM

Precision measurements associated with rare decays provide powerful probes for new physics (NP) beyond the Standard Model (SM) in the intensity frontier of modern particle physics. To this end, the study of rare B decays induced by flavor changing neutral current (FCNC) have shown some interesting anomalies hinting towards lepton non-universal NP. In 2012 the BaBar collaboration reported [177, 178] the measurements of the ratio of branching fractions

$$R_{D^{(*)}} = \frac{\mathrm{Br}(\bar{B} \to D^{(*)}\tau\bar{\nu})}{\mathrm{Br}(\bar{B} \to D^{(*)}l\bar{\nu})}, \tag{1.131}$$

$R_D^{\mathrm{BaBar}} = 0.440 \pm 0.058 \pm 0.042$ and $R_{D^*}^{\mathrm{BaBar}} = 0.332 \pm 0.024 \pm 0.018$ showing 2.0σ and 2.7σ enhancements over the SM predictions $R_D^{\mathrm{SM}} = 0.300 \pm 0.010$ and $R_{D^*}^{\mathrm{SM}} = 0.252 \pm 0.005$ respectively. Partially corroborating this result in 2015 the Belle collaboration reported $R_D^{\mathrm{Belle}} = 0.375 \pm 0.064 \pm 0.026$ and $R_{D^*}^{\mathrm{Belle}} = 0.293 \pm 0.038 \pm 0.015$ [179]. Very recently, the LHCb and Belle collaborations have reported $R_{D^*}^{\mathrm{LHCb}} = 0.336 \pm 0.027\ (\mathrm{stat.}) \pm 0.030\ (\mathrm{syst.})$ and $R_{D^*}^{\mathrm{Belle16}} = 0.302 \pm 0.030\ (\mathrm{stat.}) \pm 0.011\ (\mathrm{syst.})$ amounting to $\sim 2.1\sigma$ and $\sim 1.6\sigma$ enhancements, respectively, over the SM predictions [180, 181]. These results are consistent with each other and when combined together show significant enhancements over the SM expectations, hinting towards a large new physics contribution. Interestingly, the LHCb collaboration [182, 183] has recently reported another striking deviation from the SM prediction of the ratio of branching fractions of charged $\bar{B} \to \bar{K}ll$ decays

$$R_K = \frac{\mathrm{Br}(\bar{B} \to \bar{K}\mu^+\mu^-)}{\mathrm{Br}(\bar{B} \to \bar{K}e^+e^-)}. \tag{1.132}$$

The measured value of $R_K^{\mathrm{LHCb}} = 0.745 \pm^{0.090}_{0.074} \pm 0.036$, in the dilepton invariant mass squared bin $1\,\mathrm{GeV}^2 \le q^2 \le 6\,\mathrm{GeV}^2$ corresponds to a 2.6σ deviation from the SM prediction $R_K^{\mathrm{SM}} = 1.0003 \pm 0.0001$ [184].

On the other hand, currently the most precise measurement of the anomalous muon magnetic moment by E821 experiment at BNL has been reported to show a significant deviation from the SM prediction $\Delta a_\mu = a_\mu^{\mathrm{exp}} - a_\mu^{\mathrm{SM}} = (2.8 \pm 0.9) \times 10^{-9}$ amounting to a $\sim 3\sigma$ level deviation [185, 186]. This discrepancy also points to the possible existence of NP beyond the SM.

1.5 Objectives and overview of the chapters

In the next chapter, Chapter 2, we discuss the implications of a right handed charged gauge boson $W_R^\pm$ with mass of around a few TeV on leptogenesis. We point out how the discovery of a TeV scale $W_R^\pm$ will rule out all possibilities of leptogenesis in all classes of the left-right symmetric extensions of the Standard Model due to the unavoidable fast gauge mediated $B - L$ violating interactions. An excess signal of two leptons and two jets that has been reported by CMS in the context of W_R search or a signal of a resonance decaying into a pair of standard model (SM) gauge bosons reported by ATLAS search, if confirmed, can point to such implications.

In chapter 3, we study the framework of left-right symmetric models with additional scalar singlets and vector-like fermions. In this framework, the recent diphoton excess signal at an invariant mass of 750 GeV can be interpreted as due to decay of a singlet scalar. Extending the LRSM framework to include these new vector-like fields, on the other hand, results in interesting phenomenological implications for the LRSM fermion masses and mixing. We also discuss how the introduction of a real bi-triplet scalar, which contains a potential DM candidate, can also allow gauge coupling unification. Furthermore, existence of new vector-like fermions can also have interesting implications for baryogenesis and the dark matter sector.

In chapter 4, we study three effective low energy left-right symmetric subgroups of the superstring inspired E_6 model having a number of additional exotic fields which provides a rich phenomenology. We discuss how these models can explain both the recently detected excess $eejj$ and $e\not{p}_T jj$ signals at CMS, and also accommodate an attractive mechanism of high scale leptogenesis. Working in a R-parity conserving supersymmetric variants, we show that the excess CMS events can be produced via the decay of exotic sleptons in Alternative Left-Right Symmetric Model of E_6, which can also allow leptogenesis at a high scale.

We also discuss a possible explanation of the recent diphoton excess reported by ATLAS and CMS collaborations, at around 750 GeV diphoton invariant mass, within the framework of Alternative Left-Right Symmetric Model. We discuss how gluon-gluon fusion can give the observed production rate of the 750 GeV resonance, through a loop of scalar leptoquarks with masses below a few TeV range. The subsequent decay of this resonance via a loop of scalar leptoquarks and sleptons can give rise to a diphoton final state with the observed cross section of the diphoton signal

In chapter 5, we study low-energy subgroups of E_6 in the context of recent experimental results from the LHCb, BaBar and Belle collaborations on the decays of the B meson: $\bar{B} \to D^{(*)}\tau\bar{\nu}$ and $\bar{B} \to \bar{K}ll$, showing significant deviations from the Standard Model (SM), which hint towards a new physics scenario beyond the SM. First, we discuss how these enhanced decay rates can be explained within the framework of E_6 motivated Alternative Left-Right Symmetric Model, which has been successful in explaining the recent excesses at LHC and has the feature of accommodating high scale leptogenesis. We also study the leptonic decays $D_s^+ \to \tau^+\bar{\nu}$, $B^+ \to \tau^+\bar{\nu}$, $D^+ \to \tau^+\bar{\nu}$ and D^0-$\bar{D}^0$ mixing to constrain the couplings involved in explaining the enhanced B decay rates and we find that ALRSM can explain the current experimental data on $R(D^{(*)})$ quite well while satisfying these constraints.

Next, we discuss a unified explanation for the B-decay anomalies in $R_{D^{(*)}}$ and R_K together with the anomalous muon magnetic moment within the framework of a Left-Right Symmetric Model, which corresponds to one of the low-energy subgroups of E_6 and can naturally accommodate leptoquarks. This explanation is consistent with the constraints from the current measurements of the leptonic decay rates and $D^0 - \bar{D}^0$, $B_s^0 - \bar{B}_s^0$ mixings.

In chapter 6, we study the E_6 motivated $U(1)_N$ extension of the supersymmetric standard model in the context of the recent excess events at CMS and the baryon asymmetry of the universe. In light of the hint, from short-baseline neutrino experiments of the existence of one or more light sterile neutrinos, we also study the neutrino mass matrices, which are dictated by the field quantum number assignments and the discrete symmetries in the variants of this model. We discuss how all the variants can explain the excess events at CMS via the exotic slepton decay. For a standard choice of the discrete symmetry four of the variants have the feature of allowing high scale baryogenesis (leptogenesis), while for one other variant the three body decay induced soft baryogenesis mechanism can be realized, which in turn can induce baryon number violating neutron-antineutron oscillations. Finally, we discuss how the neutrino mass matrix of the $U(1)_N$ model variants can naturally accommodate three active and two sterile neutrinos, giving rise to interesting textures for neutrino masses.

In chapter 7, we study a cogenesis mechanism in which the observed baryon asymmetry of the universe and the dark matter abundance can be produced simultaneously at a low reheating temperature without violating baryon number in the fundamental interactions. In particular, we consider a model where the matter superfields include additional pairs of color triplet and singlet superfields in addition to the Minimal Supersymmetric Standard Model superfields. The modulus dominantly decays into the additional color triplet superfields, which subsequently decay into the fermionic component of a singlet superfield and quarks without violating baryon number. We discuss how the decay of the lightest eigenstate of the scalar component of a color triplet superfield can generate the observed baryon asymmetry in the visible sector and an asymmetric dark matter component with the right abundance, naturally solving the cosmic coincidence problem.

In chapter 8, we present a realization of mass varying neutrino dark energy in two simple extensions of the SM with a dynamical neutrino mass related to a scalar field called the acceleron (which drives the universe to a late time accelerating phase), while satisfying naturalness. In the first scenario the SM is extended to include a TeV scale scalar Higgs triplet and a TeV scale second Higgs doublet, while in the second scenario an extension of the SM with fermion triplet is considered. We also discuss the possible leptogenesis mechanisms for simultaneously generating the observed baryon asymmetry of the universe in both the scenarios and the collider signatures for the TeV scale new fields which make these models testable in the current and next generation of colliders.

Finally, in chapter 9 we present an outlook for future studies.

Chapter 2

Probing Left-Right Symmetric Models at the LHC and implications for leptogenesis

The Left-Right Symmetric Model (LRSM) [19, 21, 41–46] is one of the most popular candidates for extensions of the Standard Model (SM) of particle physics. In LRSM the Standard Model gauge group is extended at higher energies to

$$\mathcal{G}_{LR} \equiv SU(3)_c \times SU(2)_L \times SU(2)_R \times U(1)_{B-L}$$

where $B - L$ is the difference between baryon (B) and lepton (L) numbers. Left-right symmetry breaking predicts the existence of a massive right-handed charged gauge boson ($W_R^\pm$). In this chapter, we argue that if $W_R^\pm$ has a mass of a few TeV and can be detected at the LHC, it will have profound consequences for our understanding of the baryon asymmetry of the Universe. This is a unique situation where by observing $W_R^\pm$ at the LHC, we can make a very strong statement about our origin, that is regarding the baryon asymmetry of the Universe. As discussed earlier, one of the most attractive mechanisms to generate the baryon asymmetry is leptogenesis, in which a lepton asymmetry is created before the electroweak phase transition, which then gets converted to the baryon asymmetry in the presence of $(B + L)$ violating anomalous processes [90]. Detection of a TeV scale $W_R^\pm$ at the LHC would imply violation of $(B - L)$ at a lower energy, which will rule out all scenarios of leptogenesis. In this context we must mention that an excess of 2.8 σ level was observed in the energy bin

$1.8\,\text{TeV} < M_{lljj} < 2.1\,\text{TeV}$ in the two leptons two jets channel at the LHC by the CMS experiment [166], which can be interpreted as due to $W_R^{\pm}$ decay by embedding the conventional LRSM with $g_L \neq g_R$ in $SO(10)$ [187, 188] and with $g_L = g_R$ by taking into account the CP phases and nondegenerate masses of heavy neutrinos [189]. The ATLAS search has also reported a resonance that decays to a pair of SM gauge bosons to show a local excess of 3.4σ (2.5σ global) in the WZ final state at approximately $2\,\text{TeV}$ [168], which can naturally be explained by a W_R in the LRSM framework with a coupling $g_R \sim 0.4$ [190].

In the LRSM the fermion sector transforms under the gauge group $\mathcal{G}_{LR}$ as:

$$\begin{aligned} l_L &: (1, 2, 1, -1), \quad l_R : (1, 1, 2, -1), \\ Q_L &: (3, 2, 1, \frac{1}{3}), \quad Q_R : (3, 1, 2, \frac{1}{3}). \end{aligned} \tag{2.1}$$

In a popular version of the LRSM, the Higgs sector consists of one bidoublet Φ and two triplet $\Delta_{L,R}$ complex scalar fields with the transformations

$$\Phi : (1, 2, 2, 0), \quad \Delta_L : (1, 3, 1, 2), \quad \Delta_R : (1, 1, 3, 2) \tag{2.2}$$

The left-right symmetry is spontaneously broken to reproduce the Standard Model and the smallness of the neutrino masses can be taken care of by the seesaw mechanism [16–22]. The symmetry breaking pattern follows the scheme

$$\begin{aligned} \mathcal{G}_{LR} \quad & \xrightarrow{\langle \Delta_R \rangle} SU(3)_C \times SU(2)_L \times U(1)_Y \equiv \mathcal{G}_{SM} \\ & \xrightarrow{\langle \Phi \rangle} SU(3)_C \times U(1)_{EM} \equiv \mathcal{G}_{EM} \end{aligned} \tag{2.3}$$

In the first stage of symmetry breaking the right-handed triplet Δ_R acquires a Vacuum Expectation Value (VEV) $\langle \Delta_R \rangle = \frac{1}{\sqrt{2}} v_R$ which breaks the $SU(2)_R$ symmetry and gives masses to the $W_R^{\pm}$, Z_R bosons. The electroweak symmetry is broken by the Higgs bidoublet Φ, which gives masses to the charged fermions and the gauge bosons $W_L^{\pm}$ and Z_L. Δ_L gets an induced seesaw VEV which is tiny and can give a Majorana mass to the left-handed neutrinos. The generators of the broken gauge groups are then related to the electric charge by the modified Gell-Mann-Nishijima formula $Q = T_{3L} + T_{3R} + \frac{B-L}{2}$.

In a variant of the LRSM one considers only doublet Higgs scalars to break all the symmetries. This scenario is more popular than the LRSM scenario with triplet Higgs scalars in all superstring inspired models. Here the Higgs sector consists of doublet scalars

$$\Phi : (1,2,2,0), \quad H_L : (1,2,1,1), \quad H_R : (1,1,2,1), \tag{2.4}$$

and there is one additional singlet fermion field S_R (1,1,1,0) in addition to the fermions mentioned in Eq. (2.1). The Higgs doublet H_R acquires a VEV and breaks the left-right symmetry and results in mixing of S with right-handed neutrinos, giving rise to one light Majorana neutrino, and one heavy pseudo-Dirac neutrino or two Majorana neutrinos.

In the conventional LRSM, the left-right symmetry is broken at a fairly high scale, $M_R > 10^{10}\,\mathrm{GeV}$. First, the gauge coupling unification requires this scale to be high, and second, thermal leptogenesis in this scenario gives a comparable bound. One often introduces a parity odd scalar and gives a large VEV to this field. This is called D-parity breaking, which may then allow $g_L \neq g_R$ even before the left-right symmetry breaking, and hence, this allows gauge coupling unification with TeV scale M_R. This is true for both triplet and doublet models of LRSM. Embedding the LRSM in an $SO(10)$ GUT framework, the violation of D-parity [191] at a high scale can explain the CMS TeV scale W_R signal for $g_R \approx 0.6 g_L$ [187, 188].

2.1 Falsifying leptogenesis with a TeV-scale $W_R^\pm$ at the LHC

For a TeV scale $W_R^\pm$, all leptogenesis models may be classified into two groups:

- A lepton asymmetry is generated at a very high scale either in the context of D-parity breaking LRSM or through some other interactions, both thermal and nonthermal.

- A lepton asymmetry is generated at the TeV scale with resonant enhancement, when the left-right symmetry breaking phase transition is taking place.

These discussions are valid for the LRSM with both triplet as well as doublet Higgs scalars. We use the reference of the two variants of the LRSM mentioned above to study the lepton number violating washout processes and demonstrate that all these possible scenarios of leptogenesis are falsifiable for a TeV scale W_R. In models with high-scale leptogenesis with $T > 10^9$ GeV, the low energy $B-L$ breaking is associated with giving mass to the $W_R^{\pm}$, which allows gauge interactions that wash out all the baryon asymmetry before the electroweak phase transition is over. On the other hand, the same lepton number violating gauge interactions will slow down the generation of the lepton asymmetry for resonant leptogenesis at the TeV scale, so that generation of the required baryon asymmetry of the universe is not possible for TeV scale $W_R^{\pm}$.

The most stringent constraints on the $W_R^{\pm}$ mass for successful high-scale leptogenesis for a hierarchical neutrino mass spectrum ($M_{N_{3R}} \gg M_{N_{2R}} \gg M_{N_{1R}} = m_{N_R}$) come from the $SU(2)_R$ interactions [192]. To have successful leptogenesis in the case $M_{N_R} > M_{W_R}$, the out-of-equilibrium condition for the scattering process $e_R^- + W_R^+ \to N_R \to e_R^+ + W_R^-$ gives

$$M_{N_R} \gtrsim 10^{16}\,\text{GeV} \tag{2.5}$$

with $m_{W_R}/m_{N_R} \gtrsim 0.1$. Now for the case $M_{W_R} > M_{N_R}$ leptogenesis can happen either at $T \simeq M_{N_R}$ or at $T > M_{W_R}$ but at less than the $B-L$ breaking scale. Considering the out-of equilibrium condition for the scattering process $e_R^{\pm} e_R^{\pm} \to W_R^{\pm} W_R^{\pm}$ through N_R exchange one obtains the constraint

$$M_{W_R} \gtrsim 3 \times 10^6\,\text{GeV}(M_{N_R}/10^2\,\text{GeV})^{2/3}. \tag{2.6}$$

Thus observing a W_R signal with a mass in the TeV range for hierarchical neutrino masses rules out the high-scale leptogenesis scenario. In Refs. [193, 194], the constraints obtained from the observation of lepton number violating processes and neutrinoless double beta decay were studied to rule out typical scenarios of high-scale thermal leptogenesis, particularly leptogenesis models with right-handed neutrinos with mass greater than the mass scale observed at the LHC by the CMS experiment. The possibility of generating the required lepton asymmetry with a considerably low value of the W_R mass has been discussed in the context of the resonant leptogenesis scenario [104–111]. In the LRSM, it has been pointed out that successful low-scale leptogenesis with a quasidegenerate right-handed neutrino mass spectrum, requires an absolute lower bound of 18 TeV on the W_R mass [195]. Recently, it was reported that just the right amount of lepton asymmetry can be produced even for a substantially lower value of the W_R mass ($M_{W_R} > 3\,\text{TeV}$) [196] by considering relatively large Yukawa couplings, which has been updated to $13.1\,\text{TeV}$ after a more careful analysis in Ref. [197]. In Refs. [195, 196], the lepton number violating gauge scattering processes such as $N_R e_R \to \bar{u}_R d_R$, $N_R \bar{u}_R \to e_R d_R$, $N_R d_R \to e_R u_R$ and $N_R N_R \to e_R \bar{e}_R$ have been analyzed in detail. However, lepton number violating scattering processes with external W_R have been ignored on the account of the fact that for a heavy W_R, there will be a relative suppression of $e^{-m_{W_R}/m_{N_R}}$ in comparison to the processes with no external W_R. Now if the W_R mass is a few TeV's as suggested by the excess signal at the LHC reported by the CMS experiment then one has to take the latter processes seriously.

In Ref. [198], we pointed out that the lepton number violating washout processes ($e_R^{\pm} e_R^{\pm} \to W_R^{\pm} W_R^{\pm}$ and $e_R^{\pm} W_R^{\mp} \to e_R^{\mp} W_R^{\pm}$) can be mediated by doubly charged Higgs scalars in the conventional LRSM. Following that, in Ref. [197] only this channel was considered, and for a parity-asymmetric type-I seesaw model with relatively small M_{N_R} it was found to have a small contribution, as expected for a large M_{W_R}/M_{N_R}. However the other gauge scattering processes in that scenario are strong enough to give a lower bound of $13.1\,\text{TeV}$ on the W_R mass. In this chapter, we discuss the above lepton number violating scattering processes mediated by both Δ_R^{++} and N_R in a much more general context, where we have also taken into account the interference of these channels [199]. The former channel has one gauge vertex and one Yukawa vertex, while for the latter channel both the vertices are gauge vertices, thus are highly unsuppressed compared to the processes involving Yukawa vertices. We find that the lepton number violating scattering process $e_R^{\pm} W_R^{\mp} \to e_R^{\mp} W_R^{\pm}$ mediated via both N_R and Δ_R^{++} can stay in equilibrium till the electroweak phase transition for a TeV scale W_R and wash out the lepton asymmetry [1]. Thus if one incorporates the above washout process in the Boltzmann equation for lepton number asymmetry, the mentioned lower limit on M_{W_R} for successful TeV-scale resonant leptogenesis will further go up. In

[1] Note that the other scattering process is doubly phase space suppressed at a temperature below the W_R mass and hence we will not consider it for leptogenesis at $T \lesssim M_{W_R}$.

the latter variant of LRSM mentioned above the doubly charged Higgs is not there, however, the lepton number violating scattering processes mediated via N_R are still present and will wash out the lepton asymmetry.

In the LRSM, the charged current interaction involving the right-handed neutrino and the right-handed gauge boson is given by

$$\mathcal{L}_N = \frac{1}{2\sqrt{2}} g_R J_{R\mu} W_R^{-\mu} + h.c. \tag{2.7}$$

where $J_{R\mu} = \bar{e}_R \gamma_\mu (1+\gamma_5) N_R$. The Lagrangian for the right-handed Higgs triplet is given by

$$\mathcal{L}_{\Delta_R} \supset \left(D_{R\mu}\vec{\Delta}_R\right)^\dagger \left(D_R^\mu \vec{\Delta}_R\right), \tag{2.8}$$

where $\vec{\Delta}_R = \left(\Delta_R^{++}, \Delta_R^{+}, \Delta_R^{0}\right)$ in the spherical basis and the covariant derivative is defined as $D_{R\mu} = \partial_\mu - i g_R \left(T_R^j A_{R\mu}^j\right) - i g' B_\mu$. The $A_{R\mu}^j$ and B_μ are gauge fields associated with $SU(2)_R$ and $U(1)_{B-L}$ groups with the gauge couplings given by g_R and g', respectively. After spontaneous breaking of the left-right symmetry by giving VEV to the neutral Higgs field Δ_R^0 i.e. $\langle \Delta_R^0 \rangle = \frac{1}{\sqrt{2}} v_R$, the interaction between the doubly charged Higgs and the gauge boson W_R will be given by [200]

$$\mathcal{L}_{\Delta_R} \supset \left(-\frac{v_R}{\sqrt{2}}\right) g_R^2 W_{\mu R}^{-} W_R^{-\mu} \Delta_R^{++} + h.c. \tag{2.9}$$

The Yukawa interaction between the lepton doublet $\psi_{eR} = (N_R, e_R)^T$ and the Higgs triplet $\vec{\Delta}_R$ will be given by

$$\mathcal{L}_Y = h_{ee}^R \overline{(\psi_{eR})^c} \left(i\tau_2 \vec{\tau}.\vec{\Delta}_R\right) \psi_{eR} + h.c., \tag{2.10}$$

where τ's are the Pauli matrices. By giving a VEV to the neutral Higgs triplet field, the Yukawa coupling can be expressed as $h_{ee}^R = \frac{M_{N_R}}{2v_R}$ where M_{N_R} corresponds to mass of the Majorana neutrino (N_R).

The Feynman diagrams of the lepton number violating scattering processes induced by the above interactions are shown in Fig. 2.1. Utilizing the interactions in Eqs. (2.7)-(2.10), the differential scattering cross section for the $e_R^\mp(p) W_R^\pm(k) \to e_R^\pm(p') W_R^\mp(k')$ process is given by [200]

$$\frac{d\sigma_{e_R W_R}^{e_R W_R}}{dt} = \frac{1}{384\pi M_{W_R}^4 \left(s - M_{W_R}^2\right)^2} \Lambda_{e_R W_R}^{e_R W_R}(s,t,u), \tag{2.11}$$

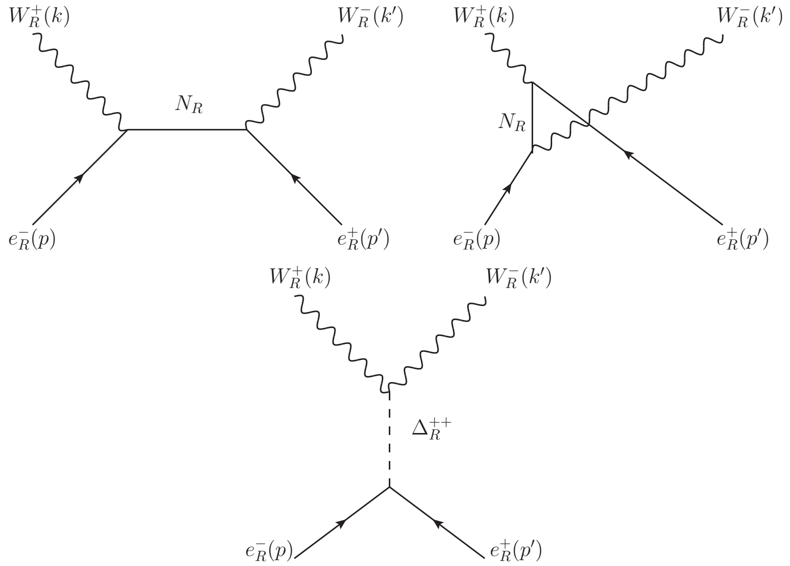

Figure 2.1: Feynman diagrams for $e_R^- W_R^+ \to e_R^+ W_R^-$ scattering mediated by N_R and Δ_R^{++} fields. The Feynman diagrams for $e_R^- e_R^- \to W_R^- W_R^-$ are the same as above with appropriate change in direction of the external lines.

where

$$\Lambda_{e_R W_R}^{e_R W_R}(s,t,u) = \Lambda_{e_R W_R}^{e_R W_R}(s,t,u)\big|_{N_R} + \Lambda_{e_R W_R}^{e_R W_R}(s,t,u)\big|_{\Delta_R^{++}} \tag{2.12}$$

and

$$\begin{aligned}\Lambda_{e_R W_R}^{e_R W_R}(s,t,u)\big|_{N_R} &= g_R^4 \left\{ -t \left| M_{N_R} \left(\frac{s}{s - M_{N_R}^2} + \frac{u}{u - M_{N_R}^2} \right) \right|^2 \right. \\ &-4M_{W_R}^2 \left(su - M_{W_R}^4 \right) (s-u)^2 \left| \frac{M_{N_R}}{\left(s - M_{N_R}^2\right)\left(u - M_{N_R}^2\right)} \right|^2 \\ &\left. -4M_{W_R}^4 t \left(\left| \frac{m_{N_R}}{\left(s - M_{N_R}^2\right)} \right|^2 + \left| \frac{M_{N_R}}{\left(u - M_{N_R}^2\right)} \right|^2 \right) \right\},\end{aligned} \tag{2.13}$$

$$\begin{aligned}\Lambda_{e_R W_R}^{e_R W_R}(s,t,u)\big|_{\Delta_R^{++}} &= 4g_R^4(-t) \left\{ \frac{(s+u)^2 + 8M_{W_R}^4}{\left(t - M_{\Delta_R}^2\right)^2} |M_{N_R}|^2 \right. \\ &+ \frac{(s+u)}{t - M_{\Delta_R}^2} |M_{N_R}|^2 \left(\frac{s}{s - M_{N_R}^2} + \frac{u}{u - M_{N_R}^2} \right) \\ &\left. + \frac{4M_{W_R}^4}{t - M_{\Delta_R}^2} |M_{N_R}|^2 \left(\frac{1}{s - M_{N_R}^2} + \frac{1}{u - M_{N_R}^2} \right) \right\},\end{aligned} \tag{2.14}$$

where we have neglected any mixing between W_L and W_R. Note that on the right-hand side of Eq. (2.14) the first term represents the Higgs scalar exchange itself while the last two terms correspond to the interference between the Higgs scalar exchange and the N_R exchange mechanisms. The relation between Mandelstam variables $s = (p+k)^2$, $t = (p-p')^2$ and $u = (p-k')^2$ and scattering angle θ is given by

$$\begin{pmatrix} st \\ su - M_{W_R}^4 \end{pmatrix} = -\frac{1}{2}\left(s - M_{W_R}^2\right)^2 (1 \mp \cos\theta) . \tag{2.15}$$

The differential scattering cross section for the $e_R^{\pm}(p)e_R^{\pm}(p') \rightarrow W_R^{\pm}(k)W_R^{\pm}(k')$ process is given by [200]

$$\frac{d\sigma_{W_R W_R}^{e_R e_R}}{dt} = \frac{1}{512\pi M_{W_R}^4 s^2}\Lambda_{W_R W_R}^{e_R e_R}(s,t,u), \tag{2.16}$$

where

$$\Lambda_{W_R W_R}^{e_R e_R}(s,t,u) = \Lambda_{W_R W_R}^{e_R e_R}(s,t,u)\Big|_{N_R} + \Lambda_{W_R W_R}^{e_R e_R}(s,t,u)\Big|_{\Delta_R^{++}} . \tag{2.17}$$

The expressions of $\Lambda_{W_R W_R}^{e_R e_R}(s,t,u)$ in this case are obtained by interchanging $s \leftrightarrow t$ in $\Lambda_{e_R W_R}^{e_R W_R}(s,t,u)$: $\Lambda_{W_R W_R}^{e_R e_R}(t,s,u)$= -$\Lambda_{e_R W_R}^{e_R W_R}(s,t,u)$. In this case, the Mandelstem variables $t = (p-k)^2$ and $u = (p-k')^2$ are related to $s = (p+p')^2$ and scattering angle θ by

$$\begin{pmatrix} t \\ u \end{pmatrix} = -\frac{s}{2}\left(1 - \frac{2M_{W_R}^2}{s}\right)\left\{1 \mp \sqrt{1 - \left(\frac{2M_{W_R}^2}{s - 2M_{W_R}^2}\right)^2}\cos\theta\right\} . \tag{2.18}$$

2.1.1 Wash out of lepton asymmetry for $T > M_{W_R}$

During the period $v_R > T > M_{W_R}$, both the lepton number violating processes are very fast without any suppression. To get an idea of the effectiveness of these scattering processes in wiping out the lepton asymmetry, we estimate the parameter

$$K \equiv \frac{n\langle\sigma|v|\rangle}{H}, \tag{2.19}$$

for both the processes during $v_R > T > M_{W_R}$, where n is the number density of relativistic species and is given by $n = 2 \times \dfrac{3\zeta(3)}{4\pi^2}T^3$, H is the Hubble rate given by $H \simeq 1.7 g_*^{1/2} T^2/M_{\rm Pl}$, where $g_* \sim 100$ corresponds to the number of relativistic degrees of freedom, and $\langle\sigma|v|\rangle$ is the thermally averaged cross section. In order to obtain a rough estimate of v_R, let us draw an analogy with the Standard Model, where we have $\langle\phi\rangle = \frac{v_L}{\sqrt{2}}$ where $v_L = 246\,\text{GeV}$, and $M_{W_L} \sim 80\,\text{GeV}$. Now in the LRSM scenario, where we have $\langle\Delta_R^0\rangle = \frac{v_R}{\sqrt{2}}$ breaking the left-right symmetry and $M_{W_R} = g_R v_R$. Then taking $g_R \sim g_L$, we have $\frac{\langle\phi\rangle}{M_{W_L}} = \frac{\langle\Delta_R^0\rangle}{M_{W_R}} \approx 3$.

Using the differential cross-section given in Eqs. (2.11) and (2.16), we plot the behavior of K as a function of temperature in the range $3M_{W_R} > T > M_{W_R}$ for $M_{W_R} = 2.1\,\text{TeV}$ (in the mass range of CMS excess) in Fig. 2.2. The high value of K

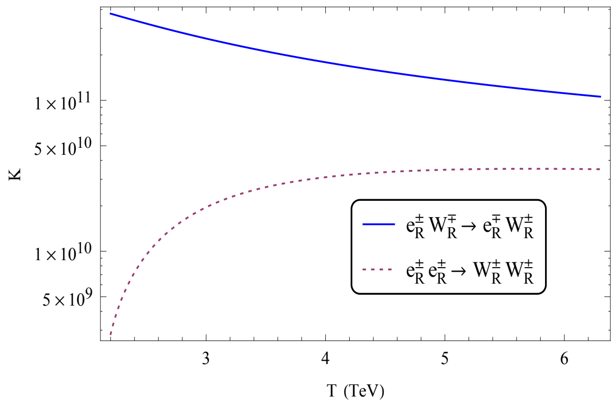

Figure 2.2: Plot showing K as a function of temperature (T) with $M_{W_R} = 2.1\,\text{TeV}$ for the scattering processes $e_R^\pm W_R^\mp \to e_R^\mp W_R^\pm$ and $e_R^\pm e_R^\pm \to W_R^\pm W_R^\pm$ (including both Δ_R^{++} and N_R mediated diagrams) for $v_R > T > M_{W_R}$.

in Fig. 2.2 for both the processes implies that these scattering processes are very fast in washing out lepton asymmetry for $T \gtrsim M_{W_R}$. In the variant of LRSM with doublet Higgs scalars the scattering processes cannot be mediated via a doubly charged Higgs scalar. However, these lepton number violating scattering processes can still be mediated via heavy neutrinos, which washes out the lepton asymmetry in this scenario for $T \gtrsim M_{W_R}$.

2.1.2 Wash out of asymmetry for $T < M_{W_R}$

For $T < M_{W_R}$, the process $e_R^\pm W_R^\mp \to e_R^\mp W_R^\pm$ is more important. Below we will estimate a lower bound on T until which the latter process stays in equilibrium below $T = M_{W_R}$. The cross section of this process as a function of temperature T can be obtained from Eq. (2.11). The scattering rate is given by [2] $\Gamma = \bar{n}\langle\sigma v_{\rm rel}\rangle$. At a temperature $T < M_{W_R}$ the number density $\bar{n} = g\left(\frac{TM_{W_R}}{2\pi}\right)^{3/2}\exp\left(-\frac{M_{W_R}}{T}\right)$ accounts for the Boltzmann suppression of the scattering rate. The condition for the scattering process to be in thermal equilibrium is $\Gamma > H$. Using $M_{N_R} \lesssim M_{W_R}$ and $v_{\rm rel} = 1$ we plot the temperature until which the scattering process $e_R^{\pm}W_R^{\mp} \to e_R^{\mp}W_R^{\pm}$

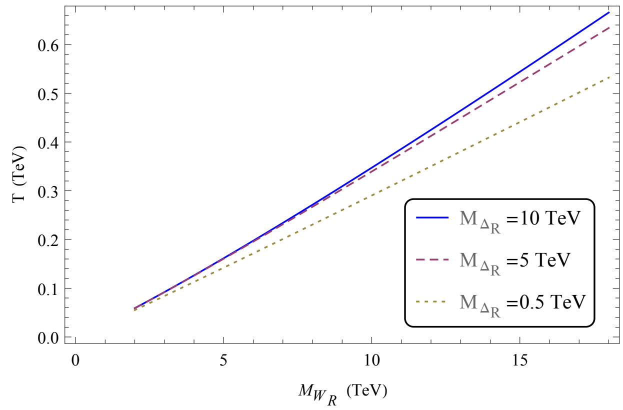

Figure 2.3: Plots showing the out-of-equilibrium temperature (T) of the scattering process $e_R^{\pm}W_R^{\mp} \to e_R^{\mp}W_R^{\pm}$ (mediated via Δ_R^{++} and N_R fields) as a function of M_{W_R} for three different values of M_{Δ_R} and $M_{N_R} \sim M_{W_R}$.

stays in equilibrium as a function of the M_{W_R} in Fig. 2.3 for three different values of M_{Δ_R}. We have chosen the lowest value of M_{Δ_R} to be $500\,\mathrm{GeV}$ in accordance with the recent search limits on the doubly charged Higgs boson mass [11]. The plot clearly shows that unless M_{W_R} is significantly larger than the TeV scale, the scattering process $e_R^{\pm}W_R^{\mp} \to e_R^{\mp}W_R^{\pm}$ will stay in equilibrium until a temperature close to the electroweak phase transition and will continue to wash out the lepton asymmetry until that temperature. In the LRSM scenario with doublet Higgs scalars, the lepton number violating scattering processes mediated only via heavy neutrinos will continue to wash out the asymmetry till the electroweak phase transition, pushing up the lower limit on the W_R mass for a successful leptogenesis scenario far beyond the W_R signal range reported by the CMS experiment, ruling out the possibility of generating the observed baryon asymmetry from TeV scale resonant leptogenesis as well.

[2]We have ignored any finite temperature effects to simplify the analysis.

2.2 Summary of the chapter

To summarize, for the high-scale leptogenesis scenario ($T \gtrsim M_{W_R}$), in both the variants of the LRSM the lepton number violating scattering processes ($e_R^\pm e_R^\pm \to W_R^\pm W_R^\pm$ and $e_R^\pm W_R^\mp \to e_R^\mp W_R^\pm$) are very efficient in wiping out the lepton asymmetry, while for a TeV scale resonant leptogenesis scenario the latter process will stay in equilibrium until the electroweak phase transition, washing out the lepton asymmetry for $T < M_{W_R}$. Hence we rule out the possibility of successful leptogenesis for $W_R^\pm$ with mass in the TeV range

- in all possible high-scale leptogenesis scenarios for the LRSM variants with (i) triplet Higgs and (ii) doublet Higgs, and
- in TeV scale resonant leptogenesis scenarios for LRSM variants with (i) triplet Higgs and (ii) doublet Higgs.

Complementing the above results, we have also explored the low-energy subgroups of the superstring motivated E_6 model. In one of the supersymmetric low-energy subgroups of E_6 (known as the Alternative Left-Right Symmetric Model) one can allow for high-scale leptogenesis, and explain the excess signal at the LHC reported by the CMS experiment from resonant slepton decay. However, the excess signal cannot be explained by right-handed gauge boson decay while allowing leptogenesis, in both supersymmetric and non-supersymmetric low-energy subgroups of the superstring motivated E_6 model [201]. Thus, if the two leptons and two jets excess at the LHC reported by the CMS experiment is indeed due to $W_R^\pm$ decay, then one needs to resort to a post-electroweak phase transition mechanism to explain the baryon asymmetry of the Universe. In this context, the experiments to observe the neutron-antineutron oscillation [202, 203] or $(B - L)$ violating proton decay [59] will play a crucial role in confirming such possibilities.

Chapter 3

Left-Right Symmetric Model in light of the diphoton excess, unification and baryogenesis

The CMS and ATLAS collaborations had recently reported a roughly 3σ excess in the diphoton channel at an invariant mass of about 750 GeV in the first 3 fb^{-1} of collected data from Run 2 of the LHC at 13 TeV [174, 175]. The Landau-Yang theorem forbids the possibility of a massive spin one resonance decaying to $\gamma\gamma$. The leading interpretations of the excess within the context of new physics scenarios therefore consist of postulating a fundamental spin zero or spin two particle with mass of about 750 GeV. However no enhancements have been seen in the dijet, $t\bar{t}$, diboson or dilepton channels posing a clear challenge to the possible interpretations of this excess. The absence of a peaked $\gamma\gamma$ angular distribution in the observed events towards the beam direction disfavors [176] the spin two hypothesis and the spin zero resonance interpretation seems more favorable from a theoretical point of view.

A large number of interpretations of the diphoton signal in terms of physics beyond the Standard Model have been proposed in the literature. For a partial list see Ref. [204] and the references therein. One of the possibilities that has been largely explored in the literature is a scalar or pseudo-scalar resonance produced through gluon-gluon fusion and decaying to $\gamma\gamma$ via loop diagrams with circulating fermions or bosons. A new resonance coupling with the Standard Model (SM) t quark or $W^{\pm}$ can give rise to such loop diagrams, however, they will be highly suppressed at the large $\gamma\gamma$ invariant masses and the dominant decay channel would have to be $t\bar{t}$ or W^+W^-. Hence the observation of the $\gamma\gamma$ resonance at 750 GeV (much greater than the electroweak symmetry breaking scale) can potentially hint towards the existence of vector-like fermions around that mass scale. Given that both the ATLAS and CMS collaborations have suggested signal events consistent with each other at a tempting 3σ statistical significance level, hinting towards a new physics scenario, it is important to explore possible model frameworks that can naturally accommodate such vector-like fermions.

From a theoretical standpoint, a framework that can explain the diphoton excess while being consistent with other searches for new physics is particularly intriguing. To this end, one must mention the results reported by the CMS Collaboration in the first run of LHC for the right-handed gauge boson W_R search at $\sqrt{s} = 8$ TeV and 19.7fb^{-1} of integrated luminosity [166]. As discussed earlier, a 2.8σ local excess was reported in the $eejj$ channel in the energy range 1.8 TeV $< m_{eejj} < 2.2$ TeV, hinting at a right handed gauge counterpart of the SM $SU(2)_L$ broken around the TeV scale. The Left-Right Symmetric Model (LRSM) framework with $g_R \neq g_L$ can explain such signal with the possibility of being embedded into a ultraviolet complete higher gauge group [187, 188, 205, 206]. It is thus an interesting exercise to explore the possibility of naturally accommodating the $\gamma\gamma$ excess also in such a framework.

In this chapter, we discuss the possibility of extending the standard LRSM framework with vector-like fermions and singlet scalars which can explain the diphoton signal [207]. Adding such new vector-like fermionic fields, on the other hand, results in interesting phenomenological implications for the LRSM fermion masses and mixing. Moreover, existence of such vector-like fermions can have interesting implications for baryogenesis and the potential dark matter sector. In gauged flavor groups with left-right symmetry [208] or quark-lepton symmetric models [209], vector-like fermions are naturally accommodated while LRSMs originating from D-brane or heterotic string compactifications also often include vector-like fermions [210, 211]. We first discuss a minimal LRSM that hosts such vector-like fermions and which can explain the diphoton signal. Then we also discuss the possible fermion masses and mixing phenomenology and the implications of these vector-like particles in baryogenesis and the dark matter sector.

3.1 Left-Right Symmetric Model framework with vector-like fermions

The left-right symmetric extension of the SM has the basic gauge group given by

$$\mathcal{G}_{L,R} \equiv SU(3)_C \times SU(2)_L \times SU(2)_R \times U(1)_{B-L}, \tag{3.1}$$

where $B-L$ is the difference between baryon and lepton number. The electric charge is related to the third component of isospin in the $SU(2)_{L,R}$ gauge groups and the $B-L$ charge as

$$Q = T_{3L} + T_{3R} + 1/2(B-L). \tag{3.2}$$

The quarks and leptons transform under the LRSM gauge group as

$$q_L = \begin{pmatrix} u_L \\ d_L \end{pmatrix} \equiv [2, 1, \frac{1}{3}, 3], \;\; q_R = \begin{pmatrix} u_R \\ d_R \end{pmatrix} \equiv [1, 2, \frac{1}{3}, 3] \,,$$
$$\ell_L = \begin{pmatrix} \nu_L \\ e_L \end{pmatrix} \equiv [2, 1, -1, 1], \ell_R = \begin{pmatrix} \nu_R \\ e_R \end{pmatrix} \equiv [1, 2, -1, 1],$$

where the gauge group representations are written in the form $[SU(2)_L, SU(2)_R, B-L, SU(3)_C]$.

Originally the left-right symmetric extension of the SM [19, 21, 41–46] was introduced to give a natural explanation for parity violation seen in radioactive beta decay and to consistently address the light neutrino masses via the seesaw mechanism [16–22]. The right handed neutrinos form doublets with the right handed charged fermions under the $SU(2)_R$ gauge group. If $SU(2)_R$ breaks at around the TeV scale, LRSMs offer a rich interplay between high energy collider signals and low energy processes such as neutrinoless double beta decay and lepton flavor violation [212]. The principal prediction of this scenario is a TeV scale right-handed gauge boson W_R. The CMS and ATLAS collaborations had reported several excesses around 2 TeV in Run 1 of the LHC, pointing towards such a possibility. From the first results of Run 2, no dijet and diboson excesses have been reported (more data is required to exclude the diboson excesses reported in Run 1), the $eejj$ channel signal hinting at a 2 TeV W_R

is still not excluded. Thus, in light of the diphoton excess it is important to revisit the LRSM framework to explore the possibility of accommodating such a signal and the possible implications.

As will be discussed in section 3.2, the 750 GeV diphoton excess can be explained through the resonant production and decay of a scalar or pseudoscalar particle. To this end, we discuss a simple left-right symmetric model with a scalar singlet S and vector-like fermions added to the minimal particle content of left-right symmetric models [1].

We extend the standard LRSM framework to include isosinglet vector-like copies of LRSM fermions. This kind of a vector-like fermion spectrum is very naturally embedded in gauged flavour groups with left-right symmetry [208] or quark-lepton symmetric models [209]. The field content of this model and the relevant transformations under the LRSM gauge group are shown in Tab. 3.1. The fields U, D, E and N correspond to the vector-like fermions.

Field	$SU(2)_L$	$SU(2)_R$	$B-L$	$SU(3)_C$
q_L	2	1	1/3	3
q_R	1	2	1/3	3
ℓ_L	2	1	-1	1
ℓ_R	1	2	-1	1
$U_{L,R}$	1	1	4/3	3
$D_{L,R}$	1	1	-2/3	3
$E_{L,R}$	1	1	-2	1
$N_{L,R}$	1	1	0	1
H_L	2	1	1	1
H_R	1	2	1	1
S	1	1	0	1

Table 3.1: LRSM representations of extended field content.

[1] We assume the resonance to be a new singlet scalar and it can easily be generalized to the pseudoscalar case.

The relevant Yukawa part of the Lagrangian is given by

$$\begin{aligned}\mathcal{L} = &-\sum_X(\lambda_{SXX}S\overline{X}X + M_X\overline{X}X) - (\lambda_U^L\tilde{H}_L\overline{q}_LU_R + \lambda_U^R\tilde{H}_R\overline{q}_RU_L \\ &+\ \lambda_D^LH_L\overline{q}_LD_R + \lambda_D^RH_R\overline{q}_RD_L +\ \lambda_E^LH_L\overline{\ell}_LE_R + \lambda_E^RH_R\overline{\ell}_RE_L \\ &+\ \lambda_N^L\tilde{H}_L\overline{\ell}_LN_R + \lambda_N^R\tilde{H}_R\overline{\ell}_RN_L + \text{h.c.}),\end{aligned} \tag{3.3}$$

where the summation is over $X = U, D, E, N$ and we suppress flavour and colour indices on the fields and couplings. $\tilde{H}_{L,R}$ denotes $\tau_2 H^*_{L,R}$, where τ_2 is the usual second Pauli matrix.

The vacuum expectation values (VEVs) of the Higgs doublets $H_R(1, 2, -1)$ and $H_L(2, 1, -1)$ break the LRSM gauge group to the SM gauge group and the SM gauge group to $U(1)_{\text{EM}}$ respectively, with an ambiguity regarding parity breaking, which can either be broken at the TeV scale or at a much higher scale M_P. In the latter case, the Yukawa couplings can be different for right-type and left-type Yukawa terms because of the renormalization group running below M_P, $\lambda_X^R \neq \lambda_X^L$. Hence, we distinguish the left and right handed couplings explicitly with the subscripts L and R. We use the VEV normalizations $\langle H_L\rangle = (0, v_L)^T$ and $\langle H_R\rangle = (0, v_R)^T$ with $v_L = 175$ GeV and v_R constrained by searches for the heavy right-handed W_R boson at colliders and at low energies, $v_R \gtrsim 1 - 3$ TeV (depending on the right-handed gauge coupling). Due to the absence of a bidoublet Higgs scalar, normal Dirac mass terms for the SM fermions are absent and the charged fermion mass matrices assume a seesaw structure. However, if one does not want to depend on a "universal" seesaw structure, a Higgs bidoublet Φ can be introduced along with $H_{L,R}$.

After symmetry breaking, the mass matrices for the fermions are given by

$$\begin{aligned}M_{uU} &= \begin{pmatrix} 0 & \lambda_U^Lv_L \\ \lambda_U^Rv_R & M_U\end{pmatrix},\ M_{dD} = \begin{pmatrix} 0 & \lambda_D^Lv_L \\ \lambda_D^Rv_R & M_D\end{pmatrix}, \\ M_{eE} &= \begin{pmatrix} 0 & \lambda_E^Lv_L \\ \lambda_E^Rv_R & M_E\end{pmatrix},\ M_{\nu N} = \begin{pmatrix} 0 & \lambda_N^Lv_L \\ \lambda_N^Rv_R & M_N\end{pmatrix},\end{aligned} \tag{3.4}$$

The mass eigenstates can be found by rotating the mass matrices via left and right orthogonal transformations $O^{L,R}$ (we assume all parameters to be real). For example, the up quark diagonalization yields $O_U^{LT} \cdot M_{uU} \cdot O_U^R = \text{diag}(\hat{m}_u, \hat{M}_U)$. Up to leading order in $\lambda_U^L v_L$, the resulting up-quark masses are

$$\hat{M}_U \approx \sqrt{M_U^2 + (\lambda_U^R v_R)^2}, \quad \hat{m}_u \approx \frac{(\lambda_U^L v_L)(\lambda_U^R v_R)}{\hat{M}_U}, \tag{3.5}$$

and the mixing angles $\theta_U^{L,R}$ parametrizing $O_U^{L,R}$,

$$\tan(2\theta_U^L) \approx \frac{2(\lambda_U^L v_L)M_U}{M_U^2 + (\lambda_U^R v_R)^2}, \tan(2\theta_U^R) \approx \frac{2(\lambda_U^R v_R)M_U}{M_U^2 - (\lambda_U^R v_R)^2}. \tag{3.6}$$

The other fermion masses and mixings are given analogously. For an order of magnitude estimate one may approximate the phenomenologically interesting regime with the limit $\lambda_U^R v_R \to M_U$ in which case the mixing angles approach $\theta_U^L \to \hat{m}_u/\hat{M}_U$ and $\theta_U^R \to \pi/4$. This means that θ_U^L is negligible for all fermions but for the top quark and its vector partner [213]. We have neglected the flavor structure of the Yukawa couplings $\lambda_X^{L,R}$ and λ_{SXX} which will determine the observed quark and leptonic mixing. The hierarchy of SM fermion masses can be generated by either a hierarchy in the Yukawa couplings or in the masses of the of the vector like fermions.

As described above, the light neutrino masses are of Dirac-type as well, analogously given by

$$\hat{m}_\nu = \frac{\lambda_N^L \lambda_N^R v_L v_R}{M_N}, \tag{3.7}$$

It is natural to assume that $M_N \gg v_R$, as the vector like N is a singlet under the model gauge group. In this case, the scenario predicts naturally light Dirac neutrinos [208].

3.2 Diphoton signal from a scalar resonance

One may attempt to interpret the diphoton excess as the resonant production of the singlet scalar S with mass $M_S = 750$ GeV. Considering the possible production mechanisms for the resonance at 750 GeV it is interesting to note that the CMS and ATLAS did not report a signal in the $\sim 20\text{fb}^{-1}$ data at 8 TeV in Run 1. One possible interpretation of this can be that the resonance at 750 GeV is produced through a mechanism with a steeper energy dependence. Excluding the possibility of an associated production of this resonance, the most favourable mechanism is gluon-gluon fusion which we will consider as the dominant production mechanism. Subsequently, the scalar with mass 750 GeV decays to two photons via a loop [207] [2]. The cross section can be expressed as

$$\sigma(pp \to \gamma\gamma) = \frac{C_{gg}}{M_S s}\Gamma_{gg}\text{Br}_{\gamma\gamma}, \tag{3.8}$$

with the proton centre of mass energy $\sqrt{s}$ and the parton distribution integral $C_{gg} = 174$ at $\sqrt{s} = 8$ TeV and $C_{gg} = 2137$ at $\sqrt{s} = 13$ TeV [216]. One can obtain a best fit guess of the cross section by reconstructing the likelihood, assumed to be Gaussian, from the 95% C.L. expected and observed limits in an experimental search. For the diphoton excess, we use a best fit cross section value of 7 fb found by combining the 95% CL ranges from ATLAS and CMS at 13 TeV and 8 TeV for a resonance mass of 750 GeV [216].

Apart from the necessary decay modes of the scalar S i.e, $S \to gg$ and $S \to \gamma\gamma$, S may also decay to other particles; due to the necessary SM invariance and the fact that $M_S > m_Z$, $S \to \gamma\gamma$ necessitates the decays $S \to \gamma Z$ and ZZ which are suppressed by $2\tan^2\theta_W \approx 0.6$ and $\tan^4\theta_W \approx 0.1$ relative to $\Gamma(S \to \gamma\gamma)$ [216]. Furthermore, S in this model may also decay to SM fermions due to mixing with the heavy vector-like fermions. As described above, the mixing is only sizable for the top and its vector partner. The total width is thereby given by $\Gamma_S \approx \Gamma_{gg} + 1.7 \times \Gamma_{\gamma\gamma} + \Gamma_{t\bar{t}}$.

Production of a scalar resonance in gluon fusion via a loop of vector-like quarks and subsequent decay of scalar resonance to $\gamma\gamma$ via a loop of vector-like quarks and leptons. There are contributions to $\Gamma(S \to \gamma\gamma)$ from quark-like vector fermion $\psi_Q = U, D$ and lepton-like vector fermion $\psi_L = E$ propagating inside the loop. Apart from quark-like vector fermion contributing to the production of scalar through gluon fusion, there could be another top-quark mediated diagram via mixing with SM Higgs boson.

In the LRSM framework discussed in section 3.1, the vector-like degrees of freedom contribute to the loop leading to $S \to gg$ and $S \to \gamma\gamma$. The partial decay widths

[2] One can find similar interpretations of the diphoton excess in [213–215] in models with a singlet scalar accompanied by vector-like fermions.

are given by [217]

$$\Gamma_{\gamma\gamma} = \frac{\alpha^2 M_S^3}{256\pi^3}\left|\sum_X \frac{N_X^C Q_X^2 \lambda'_{SXX}}{M_X}\mathcal{A}\left(\frac{m_S^2}{4M_X^2}\right)\right|^2,$$

$$\Gamma_{gg} = K\frac{\alpha_s^2 M_S^3}{128\pi^3}\left|\sum_X^C \frac{\lambda'_{SXX}}{M_X}\mathcal{A}\left(\frac{m_S^2}{4M_X^2}\right)\right|^2. \tag{3.9}$$

Here, the sums in $\Gamma_{\gamma\gamma}$ and Γ_{gg} are over all and coloured fermion species and flavours, respectively. N_X^C is the number of color degrees of freedom of a species, i.e 1 for leptonic vector-like fermions and 3 for quark-like fermions. Similarly, Q_X is the electric charge of the species. The effective coupling of S to a fermion species is $\lambda'_{SXX} = \lambda_{SXX}(O_X^R)_{1X}(O_X^L)_{1X}$, i.e. the coupling λ_{SXX} dressed with the corresponding left and right mixing matrix element. We take the value of the parameters $\alpha \approx 1/127$, $\alpha_s \approx 0.1$ and $K \approx 1.7$ [217]. $A(x)$ is a loop function defined by

$$A(x) = \frac{2}{x^2}[x + (x-1)f(x)], \tag{3.10}$$

with

$$f(x) = \begin{cases} \arcsin^2\sqrt{x} & x \le 1 \\ -\frac{1}{4}\left[\ln\left(\frac{1+\sqrt{1-x}}{1-\sqrt{1-x}}\right) - i\pi\right]^2 & x > 1. \end{cases} \tag{3.11}$$

In addition, the decay of S to a pair of fermions (here only relevant for the top) is given by

$$\Gamma_{f\bar{f}} = \frac{N_f^C \lambda'^2_{Xff} M_S}{16\pi}\left(1 - \frac{4M_f^2}{M_S^2}\right)^{2/3}. \tag{3.12}$$

In order to arrive at an estimate for the diphoton production cross section, we assume that the vector fermion masses and couplings to S are degenerate (M_X, λ_{SXX}), except for the the top partner (M_T, λ_{STT}). In the limit of large vector fermion masses $M_X \gtrsim M_S/2$, we arrive at the approximation for the partial widths,

$$\frac{\Gamma_{gg}}{M_S} \approx 1.3\times 10^{-4}\left(\frac{\lambda_{SXX}\cdot \text{TeV}}{M_X}\right)^2,$$

$$\frac{\Gamma_{\gamma\gamma}}{M_S} \approx 3.4\times 10^{-7}\left(\frac{\lambda_{SXX}\text{TeV}}{M_X}\right)^2,$$

$$\frac{\Gamma_{t\bar{t}}}{M_S} \approx 1.3\times 10^{-3}\left(\frac{\lambda_{TXX}\text{TeV}}{M_T}\right)^2. \tag{3.13}$$

As discussed in [216] in a model-independent fashion, the diphoton excess can be explained for $10^{-6} \lesssim \Gamma_{gg}/M_S \lesssim 2 \times 10^{-3}$ (the upper limit is due to the limit from dijet searches) and $\Gamma_{\gamma\gamma}/M_S \approx 10^{-6}$, as long as gg and $\gamma\gamma$ are the only decay modes of S. In order to achieve this, the top partner T needs to have a significantly weaker coupling or heavier mass than the rest of the vector fermions. Assuming the decay width to $t\bar{t}$ contributes negligibly to the total width, the diphoton cross section is given by

$$\sigma(pp \to \gamma\gamma) \approx 1.7 \text{ fb} \cdot \left(\frac{\lambda_{SXX} \cdot \text{TeV}}{M_X}\right)^2, \tag{3.14}$$

The experimentally suggested cross section $\sigma(pp \to \gamma\gamma) \approx 7$ fb can be achieved with $M_X/\lambda_{SXX} \approx 0.5$ TeV (and $\Gamma_{gg}/M_S \approx 5 \times 10^{-4}$ satisfying the dijet limit). In such a scenario, the total width of S is of the order $\Gamma_S \approx 0.5$ GeV, i.e. much smaller than the 45 GeV suggested by ATLAS if interpreted as a single particle resonance. $\Gamma_{\gamma\gamma}/\Gamma_{gg}$ can also be independently boosted by introducing a hierarchy with leptonic partners lighter than the quark partners. While certainly marginal and requiring a specific structure among the vector fermions, this demonstrates that the diphoton excess, apart from the broad width seen by ATLAS, can be accommodated in this model.

3.3 Gauge coupling unification

In the previous section, we have discussed how the inclusion of new vector-like fermions in LRSM can aptly explain the diphoton excess traced around 750 GeV at the LHC. Interestingly this framework can also be embedded in a non-SUSY grand unified theory like $SO(10)$ having left-right symmetry as its only intermediate symmetry breaking step with the breaking chain given as follows

$$SO(10) \xrightarrow{\langle\Sigma\rangle} \mathcal{G}_{2213P} \xrightarrow{\langle H_R\rangle} \mathcal{G}_{213} \xrightarrow{\langle H_L\rangle} \mathcal{G}_{13}. \tag{3.15}$$

The $SO(10)$ group breaks down to left-right symmetric group $\mathcal{G}_{2213P} \equiv SU(2)_L \times SU(2)_R \times U(1)_{B-L} \times SU(3)_c \times \mathcal{P}$ via a non-zero VEV of $\Sigma \subset 210_H$. Here, $\mathcal{P}$ is defined as the discrete left-right symmetry, a generalized parity symmetry or charge-conjugation symmetry. The vital step is to break the left-right gauge symmetry and this is attained with the help of the right-handed Higgs doublet H_R. Finally, the SM gauge group is spontaneously broken by its left-handed counterpart H_L. As described above we add another scalar singlet S in order to explain the diphoton signal though it is not contributing to the renormalization group (RG) evolution of the gauge couplings.

In addition to the particle content described in Tab. 3.1, we include a bi-triplet $\eta \equiv (3,3,0,1)$ under $\mathcal{G}_{2213P}$ to achieve successful gauge unification. This can be confirmed by using the relevant RG equation for the gauge couplings g_i,

$$\mu\frac{\partial g_i}{\partial \mu} = \frac{b_i}{16\pi^2} g_i^3, \tag{3.16}$$

where the one-loop beta-coefficients b_i are given by

$$\begin{aligned} b_i = -\frac{11}{3}\mathcal{C}_2(G) + \frac{2}{3}\sum_{R_f} T(R_f)\prod_{j\neq i} d_j(R_f) \\ +\frac{1}{3}\sum_{R_s} T(R_s)\prod_{j\neq i} d_j(R_s). \end{aligned} \tag{3.17}$$

Here, $\mathcal{C}_2(G)$ is the quadratic Casimir operator for gauge bosons in their adjoint representation,

$$\mathcal{C}_2(G) \equiv \begin{cases} N & \text{if } SU(N), \\ 0 & \text{if } U(1). \end{cases} \tag{3.18}$$

$T(R_f)$ and $T(R_s)$ are the traces of the irreducible representation $R_{f,s}$ for a given fermion and scalar, respectively,

$$T(R_{f,s}) \equiv \begin{cases} 1/2 & \text{if } R_{f,s} \text{ is fundamental}, \\ N & \text{if } R_{f,s} \text{ is adjoint}, \\ 0 & \text{if } R_{f,s} \text{ is singlet}. \end{cases} \tag{3.19}$$

and $d(R_{f,s})$ is the dimension of a given representation $R_{f,s}$ under all $SU(N)$ gauge groups except the i-th gauge group under consideration. An additional factor of $1/2$ should be multiplied in the case of a real Higgs representation. Using the above particle content, the beta-coefficients at one loop are found to be $b_{2L} = -19/6$, $b_Y = 41/10$, $b_{3C} = -7$ from the SM to the LR breaking scale and $b_{2L} = b_{2R} = -13/6$, $b_{BL} = 59/6$, $b_{3C} = -17/3$ from the LR breaking scale to the GUT scale. The two loop contributions give a very marginal deviation from one loop contributions. The resulting running of the gauge couplings at one loop and two loop orders are shown in Fig. 3.1 with the

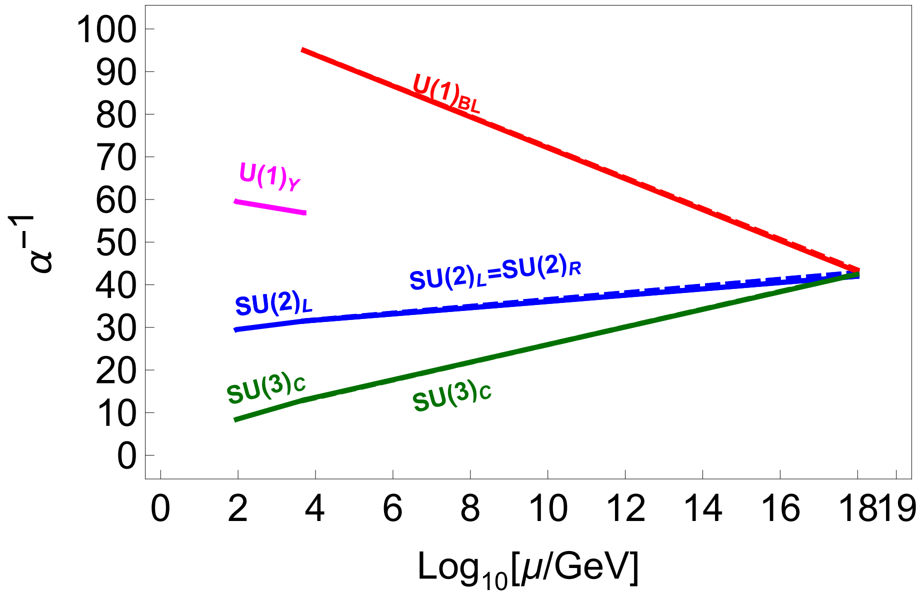

Figure 3.1: Gauge coupling running in the considered model accommodating the diphoton excess, demonstrating successful gauge unification at the scale $M_{\rm GUT} = 10^{17.75}$ GeV with an intermediate left-right symmetry breaking scale at 10 TeV. The dashed lines correspond to one loop RGE of gauge couplings while the two loop effects are displayed in solid lines.

breaking scales

$$M_{\rm GUT} = 10^{17.75}\ \text{GeV}, \quad M_{\rm LR} = 10\ \text{TeV}. \tag{3.20}$$

3.4 Implications for baryogenesis and dark matter

The vector-like fermions added to the spectrum of the LRSM framework can have very profound implications for a baryogenesis mechanism such as leptogenesis, and the dark matter sector. While the proposal of high scale leptogenesis via singlet heavy Majorana neutrinos (or a heavy Higgs triplet) decay added to the SM is beyond the reach of the present and near future collider experiments, the LRSM scenario provides a window of opportunity for low TeV scale leptogenesis testable at the LHC. However, the observation of a 2 TeV W_R boson at the LHC, through confirmation of the 2.8σ signal of two leptons and two jets reported by the CMS collaboration, would rule out the possibility of high scale as well as TeV scale resonant leptogenesis with the standard LRSM fields due to the unavoidable fast gauge mediated $B - L$ violating interactions [192–199].

On the other hand, the new vector-like fermions added to the LRSM to accommodate the diphoton excess can open up a whole new world of possibilities. A particularly interesting possibility is the realization of baryogenesis and dark matter annihilation through a vector-like portal first explored in [139]. As an example, let us consider the following additional terms in the Lagrangian,

$$\begin{aligned}\mathcal{L} \supset &- (\lambda_{XU} X \overline{u_R} U_L + \text{h.c.}) - m_X^2 X^\dagger X - \lambda_X (X^\dagger X)^2 \\ &- \lambda_{HX} H^\dagger H X^\dagger X, \end{aligned} \tag{3.21}$$

where X is an inert doublet (a singlet complex) dark matter scalar field in the LR(SM) case. X is charged under some exotic global $U(1)_\eta$ symmetry, under which only the vector-like quarks and dark matter fields transform non-trivially. Thus, the introduction of vector-like quarks can connect the dark matter to the usual LR(SM) quarks, which can be readily used to make a connection between the baryon asymmetry and dark matter, as pointed out in [139]. In the rest of this section, we will sketch the simpler case of the extended SM which can be expanded to the LRSM case by replacing the singlets with appropriate doublet representations. However, in the case of the LRSM some subtleties are present and we will comment on them towards the end of this section. On the other hand, this idea can easily be generalized to accommodate a down-type quark portal or charged lepton portal (corresponding to a leptogenesis scenario of baryogenesis).

The basic idea behind the vector-like portal is to generate an asymmetry in the vector-like sector through baryogenesis, which then subsequently gets transferred to the SM baryons and the dark matter sector through the renormalizable couplings in Eq. (3.21). In addition to the scalar field X one can introduce a scalar field Y with the couplings

$$\begin{aligned}\mathcal{L} \supset &- (\lambda_{\nu Y} Y \nu_R \nu_R + \text{h.c.}) - m_Y^2 Y^\dagger Y - \lambda_Y (Y^\dagger Y)^2 \\ &- \lambda_{XY} X^\dagger X Y^\dagger Y, \end{aligned} \tag{3.22}$$

which allows the annihilation of a pair of X into Y fields. The latter can subsequently decay into two singlet right handed neutrinos ensuring the asymmetric nature of the dark matter X relic density for a large enough annihilation cross section. Now turning to the question of how to generate the primordial asymmetry in the vector-like sector which defines the final dark matter asymmetry and baryon asymmetry, let us further add two types of heavy diquarks with the couplings

$$\mathcal{L} \supset \lambda_{\Delta U_L}\Delta_u U_L U_L + \lambda_{\Delta U_R}\Delta_u U_R U_R + \lambda_{\Delta d}\Delta_d d_R d_R \\ + \lambda_\chi \Delta_u \Delta_d \Delta_d \chi + \text{h.c.}, \tag{3.23}$$

where $\Delta_u : (\bar{6}, 1, -4/3)$, $\Delta_d : (\bar{6}, 1, 2/3)$ and the field χ breaks the local $U(1)_\chi$ symmetry under which X and U have non-trivial charges denoted by $q_\chi(U)$ and $q_\chi(X)$. For the SM fields this charge is simply $B - L$, which right away gives $q_\chi(\Delta_d) = -2/3$. The rest of the charges are determined in terms of the free charge $q_\chi(U)$,

$$q_\chi(\Delta_u) = -2q_\chi(U), q_\chi(\chi) = 2q_\chi(U) + 4/3, \\ q_\chi(X) = 1/3 - q_\chi(U). \tag{3.24}$$

In order to forbid the dangerous proton decay induced by the operators $\mathcal{O} = X^2, S^2, X^2S^2, X^4, S^4$ [218], one needs to satisfy the condition

$$q_\chi(\mathcal{O}) \neq n(2q_\chi(U) + 4/3), \text{ where n} = 0, \pm 1, \pm 2, \cdots . \tag{3.25}$$

From Eq. (3.23) it follows that after χ acquires a VEV to break the $U(1)_\chi$ symmetry, Δ_u has the decay modes

$$\Delta_u \to \Delta_d^* \Delta_d^*, \quad \Delta_u \to \bar{U}\bar{U}, \tag{3.26}$$

and a CP asymmetry (between the above modes and their conjugate modes) can be obtained by interference of the tree level diagrams with one loop self energy diagrams with two generations of Δ_u. Finally, the asymmetry generated in the vector-like quarks gets transferred to the dark matter asymmetry and baryon asymmetry via the λ_{XU} term in Eq. (3.21). This mechanism gives a ratio between the dark matter relic density and the baryon asymmetry given by

$$\frac{\Omega_{DM}/m_X}{\Omega_B/M_p} = \frac{79}{28}, \tag{3.27}$$

in this model for dark matter mass $m_X \sim 2$ GeV (where X is a gauge singlet complex dark matter scalar field) [3]. A typical prediction of this model is neutron-antineutron

[3]The relation between the dark matter relic density and the baryon asymmetry follows from the baryon asymmetry given by Eq. (1.106) and the dark matter asymmetry $\Delta n_X = \Delta\eta$. This gives $\frac{\Omega_{DM}/m_X}{\Omega_B/M_p} = \frac{79}{28}|\Delta\chi/\Delta(B-L)|$. Now from Eq. (3.26) we note that $\Delta\chi/\Delta(B-L) = -1$. This leads to the relation given in Eq. (3.27).

oscillations induced by the up-type and two down-type diquarks through the mixing of vector-like up-type quarks with the usual up quarks. However, such oscillations will be suppressed by the mixing.

One can similarly construct a leptogenesis model involving vector-like charged leptons. In case of the LRSM a generalization of the above scheme is straightforward; however, the lepton number violating gauge scattering processes involving a low scale W_R can rapidly wash out any primordial asymmetry generated above the mass scale of W_R. In fact, some of these gauge processes can continue to significantly reduce the rate of generation of lepton asymmetry below the mass scale of W_R, thus the vector-like quark portals seem to be more promising option for leptogenesis. Other alternatives include mechanisms like neutron-antineutron oscillation or some alternative LRSM scheme such as the Alternative Left-Right Symmetric Model [219] where the dangerous gauge scatterings can be avoided by means of special gauge quantum number assignments of a heavy neutrino [201]. Also note that, in general, one can utilize the singlet neutral vector-like lepton as a dark matter candidate by ensuring the stability against decay into usual LRSM fermions. Finally, the real bi-triplet scalar field η introduced to achieve successful gauge unification can also be a potential dark matter candidate.

Attempts have been made in the literature to address the broadness of the resonance using an invisible component of the scalar width. This in turn gives a large monojet signal which have been constrained from Run-1 monojet searches at ATLAS [220] and CMS [221], see for example Ref. [222]. However, the monojet search data seems to disfavor the required rates to explain the broadness of the resonance. In our model, S can couple to $XX^\dagger$ and $YY^\dagger$ etc. leading to decay of S into them, which produces missing energy final state. This mode can be constrained from monojet searches as long as $M_{X,Y} < M_S/2$. Even without the scalar S being directly coupled to X's, its decay can produce a pair of jets and X's via the λ_{XU} coupling term, which can again be constrained using dijet searches at ATLAS and CMS. In the discussion above we assume that these constrains are respected if $M_{X,Y} < M_S/2$. While for the case $M_{X,Y} > M_S/2$, the monojet and the dijet constraints are no longer applicable since in this case S will decay via a loop of $X(Y)$'s.

3.5 Summary of the chapter

We have discussed a unified framework to explain the recent diphoton excess reported by ATLAS and CMS around 750 GeV. The addition of vector-like fermions and a singlet scalar S to LRSM but without a scalar bidoublet explains the fermion masses and mixing via a universal seesaw mechanism. The diphoton signal with $\sigma(pp \rightarrow S \rightarrow \gamma\gamma) \approx 4 - 12$ fb can be explained in this model with TeV scale vector fermions. The broad width suggested by the ATLAS excess cannot be understood, though. We have discussed how this model can be embedded within an SO(10) GUT framework by introducing a real bi-triplet scalar. This additional scalar, which contains a potential DM candidate, allows the gauge couplings to unify at the scale $10^{17.7}$ GeV. We have also discussed further possibilities in this class of LRSM models with vector-like fermions for mechanisms of baryogenesis and DM.

Chapter 4

Left-Right Symmetric low-energy subgroups of E_6 in light of LHC and baryogenesis

As discussed earlier the CMS Collaboration at the LHC at CERN announced their results for the right-handed gauge boson W_R search at a center of mass energy of $\sqrt{s} = 8\text{TeV}$ and 19.7fb^{-1} of integrated luminosity [166]. They have used the final state $eejj$ to probe $pp \to W_R \to eN_R \to eejj$, with the cuts $p_T > 60\,\text{GeV}, |\eta| < 2.5$ ($p_T > 40\,\text{GeV}, |\eta| < 2.5$) for leading (subleading) electron. The invariant mass m_{eejj} is calculated for all events satisfying $m_{ee} > 200\,\text{GeV}$. In the bin $1.8\,\text{TeV} < m_{eejj} < 2.2\,\text{TeV}$ roughly 14 events have been observed with 4 expected background events, amounting to a 2.8σ local excess, which, however, can not be explained by W_R decay in Left-Right Symmetric Models (LRSM) with strict left-right symmetry (gauge couplings $g_L = g_R$) [166]. The CMS search for di-leptoquark production, at a center of mass energy of $\sqrt{s} = 8\text{TeV}$ and 19.6fb^{-1} of integrated luminosity has reported a 2.4σ and a 2.6σ local excess in $eejj$ and $e\not{p}_T jj$ channels [167] [1] respectively, and has excluded the first generation scalar leptoquarks with masses less than 1005 (845) GeV for $\beta = 1(0.5)$, where β is the branching fraction of a leptoquark to a charged lepton and a quark . In the $eejj$ channel for a $650\,\text{GeV}$ leptoquark signal using the optimization cuts $S_T > 850\,\text{GeV}, m_{ee} > 155\,\text{GeV}$ and $m_{ej}^{\text{min}} > 270\,\text{GeV}$ (where S_T

[1]The $e\not{p}_T jj$ channel is often referred to as $e\nu jj$ channel in the literature. Also note that the "ee" in $eejj$ refers to two first generation charged leptons, not necessarily of the same sign.

is the scalar sum of the p_T of two leptons and two jets), 36 events have been observed compared with $20.49 \pm 2.4 \pm 2.45(\text{syst.})$ expected events from the SM backgrounds implying a 2.4σ local excess. While in the $e\not{p}_T jj$ channel using the optimization cuts $S_T > 1040\,\text{GeV}, m_{\not{E}_T} > 145\,\text{GeV}, m_{ej} > 555\,\text{GeV}$ and $m_{T,e\not{p}_T}$ (where S_T is now the scalar sum of the missing energy $\not{E}_T$ and p_T of the electron and two jets), 18 events have been observed compared with $7.54 \pm 1.20 \pm 1.07(\text{syst.})$ expected background events amounting for a 2.6σ local excess [167].

Attempts have been made to explain the above CMS excesses in the context of different models. The excesses have been explained in the context of W_R decay by embedding the conventional LRSM ($g_L \neq g_R$) in the $SO(10)$ gauge group in Refs. [187, 188, 223]. The $eejj$ excess has been discussed in the context of W_R and Z' gauge boson production and decay in Ref. [224]. The excesses have also been interpreted as due to pair production of vector-like leptons in Refs. [225]. In Refs. [226–228], the excess of $eejj$ events has been shown to occur in R-parity violating processes via the resonant production of a slepton. In Refs. [229, 230], a different scenario is proposed by connecting leptoquarks to dark matter which fits the data for the recent excess seen by CMS. The feasibility of probing lepton number violation through the production of same sign leptons pairs in a dilepton +2 jets channel was first explored in Ref. [231].

The conventional LRSM (even embedded in higher gauge groups) are inconsistent with the canonical mechanism of leptogenesis in the predicted range of the mass of W_R ($\sim 2\,\text{TeV}$) at CMS [192]. In these models, leptogenesis can generate the lepton asymmetry in two possible ways: (i) decay of right-handed Majorana neutrinos which do not conserve lepton number [90] and (ii) decay of very heavy Higgs triplet scalars with couplings that break lepton number [23]. Since the right-handed neutrinos interact with the $SU(2)_R$ gauge bosons, the W_R interactions with the right-handed neutrino N can wash out any existing primordial $B - L$ asymmetry, and hence also baryon and lepton asymmetry in the presence of anomalous $(B + L)$ violating interactions before the electroweak phase transition. Successful primordial leptogenesis involving N decay for $m_{W_R} > m_N$ then requires $m_{W_R} \gtrsim 2 \times 10^5\,\text{GeV}(m_N/10^2\,\text{GeV})^{3/4}$ if leptogenesis occurs at $T = m_N$ and $m_{W_R} \gtrsim 3 \times 10^6\,\text{GeV}(m_N/10^2\,\text{GeV})^{2/3}$ if it occurs at $T > m_{W_R}$. Note that the $m_N > m_{W_R}$ option is excluded in supersymmetric theories with gravitinos [192]. Thus, the observed $1.8\,\text{TeV} < m_{W_R} < 2.2\,\text{TeV}$ range at CMS implies that the decay of right-handed neutrinos cannot generate the required amount of lepton and baryon asymmetry of the universe in the conventional LRSM. Such models would then require some other mechanism to generate the baryon asymmetry of the universe. With regards to the interpretation of the excess events as due to leptoquarks, it is difficult to accommodate any scenario that allows a light leptoquark in any simple extension of the standard model.

In this chapter, we discuss some simple left-right symmetric extensions of the SM, which can explain the excess CMS events and simultaneously explain the baryon asymmetry of the universe via leptogenesis [198,201]. To this end we explore whether models based on heterotic superstring theory have all the necessary ingredients embedded in their effective low-energy theories. The heterotic superstring theory with $E_8 \times E_8'$ gauge group after compactification on a Calabi-Yau manifold leads to the breaking of $E_8 \to SU(3) \times E_6$ [232,233]. The flux breaking of E_6 results in different effective subgroups of rank-5 and rank-6 at low-energy, some of which include new right-handed gauge bosons in their spectrum. In addition to this, these low-energy subgroups provide the existence of new exotic (s)particles. We will systematically study the possible decay modes of right-handed gauge bosons in the three effective low-energy subgroups of the superstring inspired E_6 model, to see that it is not possible to explain the excess of both $eejj$ and $e\not{p}_T jj$ events from the the right-handed gauge boson decay and accommodate leptogenesis simultaneously in any of the effective low-energy subgroups of E_6. We then discuss a different scenario in which both the excess signals can be produced from the decay of an exotic slepton in two of the effective low-energy subgroups of the superstring inspired E_6 model. The added advantage of this scenario is that unlike R-parity violating slepton decay in Refs. [226–228], the production as well as decay of the exotic slepton in this scenario involves only R-parity conserving interactions. Interestingly, one of the two effective low-energy subgroups (generally known as the Alternative Left-right Symmetric Model (ALRSM)) also explains high-scale leptogenesis. Therefore, we argue that the ALRSM is the most suitable choice for explaining both the excess of events at CMS and the generation of the baryon asymmetry via leptogenesis [201].

4.1 Left-right symmetric low-energy subgroups of E_6

Within the context of heterotic superstring theory in ten dimensions, it was shown in Ref. [234–236] that there is gauge and gravitational anomaly cancellation if the underlying gauge group is $E_8 \times E_8'$ or $SO(32)$. The $E_8 \times E_8'$ leads to chiral fermions, whereas $SO(32)$ does not lead to the same. Therefore, $E_8 \times E_8'$ is considered to be more attractive from the phenomenological point of view. By integrating out the massive modes, the low-energy limit of the superstring theory (massless modes of the string) leads to ten-dimensional supergravity with an $E_8 \times E_8'$ gauge sector. To make connection with the four-dimensional world, the extra six dimensions must be compactified on a particular kind of manifold. Though there exists several compactification scenarios, the compactification on a Calabi-Yau manifold (with $SU(3)$ holonomy) [233] results in the breaking of $E_8 \to SU(3) \times E_6$ and also produces $\mathcal{N} = 1$ supersymmetry [232]. The remaining E_8' couples to the usual matter representations of the E_6 only by gravitational interactions and provides the role of the hidden sector needed to break supersymmetry.

One of the maximal subgroups of E_6 is given by $SU(3)_C \times SU(3)_L \times SU(3)_R$. The fundamental 27 representation of E_6 under this subgroup decomposes as

$$27 = (3, 3, 1) + (3^*, 1, 3^*) + (1, 3^*, 3) \tag{4.1}$$

where (u, d, h) : $(3, 3, 1)$, (h^c, d^c, u^c) : $(3^*, 1, 3^*)$ and the leptons are assigned to $(1, 3^*, 3)$. Here h denotes an exotic $-\dfrac{1}{3}$ charge quark. Other than h and its charge conjugate, a right-handed neutrino N^c and two lepton isodoublets (ν_E, E) and (E^c, N_E^c) are among the new particles. Although these exotic particles have not been observed so far, they promise rich phenomenology and their detection may also become an indirect indication for the superstring inspired models.

The particles of the first family are assigned as

$$\begin{pmatrix} u \\ d \\ h \end{pmatrix} + \begin{pmatrix} u^c & d^c & h^c \end{pmatrix} + \begin{pmatrix} E^c & \nu & \nu_E \\ N_E^c & e & E \\ e^c & N^c & n \end{pmatrix}, \tag{4.2}$$

where $SU(3)_L$ operates vertically and $SU(3)_{(R)}$ operates horizontally [2]. When the $SU(3)_{(L,R)}$ further breaks to $SU(2)_{(L,R)} \times U(1)_{(L,R)}$, there are three choices corresponding to T, U, V isospins of $SU(3)$, which corresponds to the three different embedding of the residual $SU(2)$ on $SU(3)$ and the different isospins T, U, V would be the generators of $SU(2)$. These three choices give three kinds of heavy W_R's (compared to their left-handed counterparts) and the exotic fermions belong to the different $SU(2)$ representations.

4.1.1 Conventional Left-Right Symmetric Model like case

We first consider the usual left-right symmetric extension of the standard model and include the exotic particles. In that case, for the standard model particles the sum of the generators Y_L and Y_R can be identified with the generator $(B-L)$, where B is the baryon number and L is the lepton number. We shall extend this identification to the exotic particles as well, because that will help us understand the B and L violation in this scenario.

The right-handed up and down quarks, or their CP conjugate states $(d^c, u^c)_L$ belong to the $SU(2)_R$ doublet as in the LRSM. The charge equation

$$\begin{aligned} Q &= T_{3L} + \frac{1}{2}Y_L + T_{3R} + \frac{1}{2}Y_R \\ &= T_{3L} + T_{3R} + \frac{(B-L)}{2} \end{aligned} \tag{4.3}$$

holds for all the SM particles and we want the new fermions that belong to the fundamental representation of E_6 to have a gauge invariant Yukawa interactions with the SM particles. Thus this relation may be extended as a definition to make all Yukawa and gauge interactions conserve $B-L$. So under the subgroup $G = SU(3)_c \times SU(2)_L \times$

[2]For example $\begin{pmatrix} u \\ d \\ h \end{pmatrix}$ is a $SU(3)_L$ triplet, whereas $\begin{pmatrix} u^c & d^c & h^c \end{pmatrix}$ is a $SU(3)_{(R)}$ triplet.

$SU(2)_R \times U(1)_{B-L}$ the fields transform as

$$\begin{aligned}
(u,d)_L &: (3,2,1,\frac{1}{6}) \\
(d^c,u^c)_L &: (\bar{3},1,2,-\frac{1}{6}) \\
(\nu_e,e)_L &: (1,2,1,-\frac{1}{2}) \\
(e^c,N^c)_L &: (1,1,2,\frac{1}{2}) \\
h_L &: (3,1,1,-\frac{1}{3}) \\
h_L^c &: (\bar{3},1,1,\frac{1}{3}) \\
\begin{pmatrix} \nu_E & E^c \\ E & N_E^c \end{pmatrix}_L &: (1,2,2,0) \\
n_L &: (1,1,1,0).
\end{aligned} \tag{4.4}$$

The presence of $SU(2)_R$ tells us that the right-handed charged currents must be incorporated in weak decays. If the Dirac neutrino is formed by combining ν_e and N^c, then the mass of the $W_R^\pm$ is constrained from polarized μ^+ decay [237]. Furthermore there is a charged current mixing matrix for the known quarks in the right-handed sector. Assuming this to be similar to Kobayashi- Maskawa matrix one can constraint the $W_R^\pm$ mass from the $K_L - K_S$ mass difference [238–240]. In Ref. [241] it was shown that the mixing matrix for the right-handed quark sector is calculable and that the difference between left and right mixing angles turns out to be very small. Also the rare decays and neutron electric dipole moment can give further constraints on the W_R mass [240, 242].

This case can produce the $eejj$ signal in the decays of W_R, and can explain the observed events for $g_L \neq g_R$ [187]. However, this scenario is not very interesting for us as it cannot explain the canonical mechanism of leptogensis.

4.1.2 Alternative Left-Right Symmetric Model

Another choice for the $SU(2)_R$ doublet is (h^c, u^c) [219] with the charge equation $Q = T_{3L} + \frac{1}{2}Y_L + T'_{3R} + \frac{1}{2}Y'_R$, where

$$T'_{3R} = \frac{1}{2}T_{3R} + \frac{3}{2}Y_R, \quad Y'_R = \frac{1}{2}T_{3R} - \frac{1}{2}Y_R, \tag{4.5}$$

and we have $T'_{3R}+Y'_R = T_{3R}+Y_R$. Thus it follows that for interactions involving only the standard model particles and left-handed gauge bosons, one cannot distinguish this model from the case discussed in previous subsection. In this scenario, the fields transform under the subgroup $G = SU(3)_c \times SU(2)_L \times SU(2)_{R'} \times U(1)_{Y'}$ as

$$\begin{aligned}
(u,d)_L &: (3,2,1,\frac{1}{6}) \\
(h^c,u^c)_L &: (\bar{3},1,2,-\frac{1}{6}) \\
(\nu_E,E)_L &: (1,2,1,-\frac{1}{2}) \\
(e^c,n)_L &: (1,1,2,\frac{1}{2}) \\
h_L &: (3,1,1,-\frac{1}{3}) \\
d^c_L &: (\bar{3},1,1,\frac{1}{3}) \\
\begin{pmatrix} \nu_e & E^c \\ e & N^c_E \end{pmatrix}_L &: (1,2,2,0) \\
N^c_L &: (1,1,1,0),
\end{aligned} \tag{4.6}$$

where $Y' = Y_L + Y'_R$. This model is often referred to as the Alternative Left-Right Symmetric Model (ALRSM) in the literature [219]. Note that, in this case N^c has a trivial transformation under G and thus can allow high-scale leptogenesis. However, the assignment of quantum numbers for N^c is not unique and that can result in some interesting consequences.

With the above assignments, the superpotential governing interactions of Standard Model and exotic particles is given as

$$\begin{aligned}
W &= \lambda_1 \left(uu^cN^c_E - du^cE^c - uh^ce + dh^c\nu_e\right) + \lambda_2 \left(ud^cE - dd^c\nu_E\right) \\
&+ \lambda_3 \left(hu^ce^c - hh^cn\right) + \lambda_4 hd^cN^c_L + \lambda_5 \left(ee^c\nu_E + EE^cn - Ee^c\nu_e - \nu_E N^c_E n\right) \\
&+ \lambda_6 \left(\nu_e N^c_L N^c_E - eE^cN^c_L\right).
\end{aligned} \tag{4.7}$$

The superpotential given in Eq. (4.7) leads to the following assignments of R, B and L for the exotic fermions which also guarantees proton stability. For leptoquark h we have $R = -1, B = \frac{1}{3}, L = 1$; ν_E, E and n carry $R = -1, B = L = 0$. There are two possible assignments for N^c determining whether a massive ν_e is possible or not. For the assignment $R = -1$ and $B = L = 0$ for N^c (which demands $\lambda_4 = \lambda_6 = 0$

in Eq. (4.7) for a R-parity conserving scenario), one has an exactly massless ν_e, but from the perspective of leptogenesis the more interesting choice is the case where N^c is assigned $R = +1$, $B = 0$, $L = -1$, so that it gives a tiny mass to ν_e via the seesaw mechanism. Thus we consider the latter scenario in the following discussions.

In this case, the right-handed charged current couples e to n, but with n being presumably heavier ($m_n \gtrsim \mathcal{O}(\text{ TeV})$), there is no constraint on the mass of $W^{\pm}_{R'}$ from polarized μ^+ decay in contrast to the conventional LRSM like case. Also since $W^{\pm}_{R'}$ does not couple to d and s quarks there is no constraint on the mass of $W^{\pm}_{R'}$ from the $K_L - K_S$ mass difference either. Thus this model allows a much lighter $W^{\pm}_{R}$ than the conventional LRSM like case. However this model can give rise to $D^0 - \bar{D}^0$ mixing through the $W_{R'}$ coupling of the c and u quarks to h [243]. The relevant diagrams are shown in Fig. 4.1. This mixing can constrain the $SU(2)_{R'}$ breaking scale in this model. It is interesting to note that in contrast to the conventional LRSM like case, where all

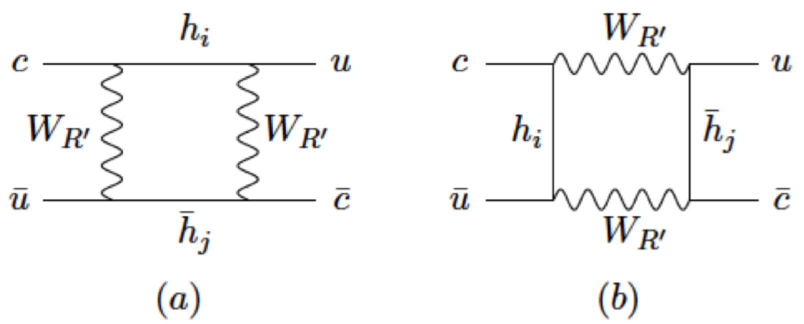

Figure 4.1: Box diagrams in the ALRSM contributing to $D^0 - \bar{D}^0$ mixing.

the gauge bosons have $B = 0$ and $L = 0$, in this case $W^{-}_{R'}$ has leptonic charge $L = 1$. The coupling of the $W_{R'}$ to the fermions is given by

$$\mathcal{L} = \frac{1}{\sqrt{2}} g_R W^{\mu}_{R'} (\bar{h}^c \gamma_\mu u^c_L + \bar{E}^c \gamma_\mu \nu_L + \bar{e}^c \gamma_\mu n_L + \bar{N}^c_E \gamma_\mu e_L) + \text{h.c.} \tag{4.8}$$

So $W_{R'}$ is coupled to the leptoquark h^c_L and the n field, compared to the coupling with the d^c_L and N^c in the conventional LRSM.

Let us discuss the possible production channels of $W_{R'}$. The quantum numbers of $W_{R'}$ imply that the production of $W_{R'}$ from the usual $u\bar{d}$ scattering in hadronic colliders cannot take place. The process that can yield a large cross section for $W_{R'}$ production is the associated production of $W_{R'}$ and leptoquark via the process $g+u \to h+W^{+}_{R'}$ [244],

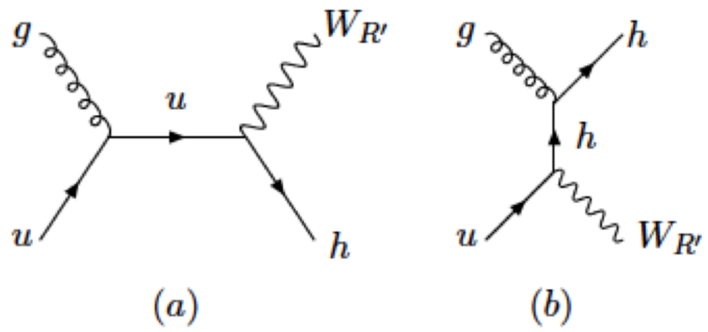

Figure 4.2: s- and t-channel Feynman diagrams for the process: $g + u \to h + W_{R'}$.

which proceeds through the diagrams shown in Fig. 4.2. The differential cross section of this process is given by

$$\frac{d\hat{\sigma}}{dt} = \frac{1}{16\pi\hat{s}^2}|\bar{\mathcal{M}}_{R'}|^2, \tag{4.9}$$

with the spin and color averaged partonic amplitude given by [245]

$$\begin{aligned} |\bar{\mathcal{M}}_{R'}|^2 \quad = \quad & \frac{4\pi G_F M_{W_{R'}}^2}{3\sqrt{2}}\,\alpha_s\Bigg[-\left(\frac{t'}{\hat{s}}+\frac{\hat{s}}{t'}\right)\left(2+\frac{M_h^2}{M_{W_{R'}}^2}\right)-2\frac{M_h^2}{M_{W_{R'}}^2} \\ & +2\left(2M_{W_{R'}}^2-M_h^2-\frac{M_h^4}{M_{W_{R'}}^2}\right)\left(\frac{1}{\hat{s}}+\frac{1}{t'}\right)+\frac{2}{\hat{s}t'} \\ & \times\left(-\frac{M_h^6}{M_{W_{R'}}^2}+3M_h^2M_{W_{R'}}^2-2M_{W_{R'}}^4\right)+2\frac{M_h^2}{t'^2}\left(2M_{W_{R'}}^2-M_h^2-\frac{M_h^4}{M_{W_{R'}}^2}\right)\Bigg], \end{aligned} \tag{4.10}$$

where $\hat{s}$, t are the Mandelstam variables, $t' = t - M_h^2$, and M_h ($M_{W_{R'}}$) is the mass of h ($W_{R'}$). The partonic cross section of the process can be obtained by integrating the differential cross section over t' between the limits

$$t'_{1,2} = -\frac{1}{2}\left(\hat{s}+M_h^2-M_{W_{R'}}^2\right) \pm \frac{1}{2}\left[\left(\hat{s}-M_h^2-M_{W_{R'}}^2\right)^2-4M_h^2M_{W_{R'}}^2\right]^{1/2}. \tag{4.11}$$

The total hadronic cross section is obtained by convoluting the partonic cross section with the parton distribution functions

$$\sigma \sim \int_0^1 dx_1dx_2[u^p(x_1)g^p(x_2)+g^p(x_1)u^p(x_2)]\hat{\sigma}(x_1x_2s), \tag{4.12}$$

where s is the squared hadronic center of mass energy, $\hat{s} = x_1x_2s$, and u^p, g^p are the parton distribution functions relative to the proton. A quantitative benchmark for the same is given in Refs. [244] and [245]. To give a quantitative estimate, for $M_h \sim 1\,\mathrm{TeV}$

and $M_{W_{R'}} \sim 2.1\,\text{TeV}$ the cross section at the LHC for the process $pp \to W^+_{R'}h$ is about $\sigma \sim 0.2$ pb at $\sqrt{s} = 14\,\text{TeV}$ and is about $\sigma \sim 0.02$ pb at $\sqrt{s} = 8\,\text{TeV}$, where we have used the parton distribution functions given in Ref. [246] for the numerical estimations. Note however that the production cross section of $\sigma(W^+_{R'}h)$ is always substantially larger compared to $\sigma(W^-_{R'}\bar{h})(\sim 10^{-3}$ pb at $\sqrt{s} = 14\,\text{TeV}$ and $\sim 5 \times 10^{-4}$ pb at $\sqrt{s} = 8\,\text{TeV}$, for $M_h \sim 1\,\text{TeV}$ and $W^-_{R'} \sim 2.1\,\text{TeV})$. This is due to the fact that u distribution function in a proton beam is larger than the $\bar{u}$ distribution function.

The two-body decay modes of the $W_{R'}$ can be obtained from Eq. (4.8). An inspection of all the further decays of the exotic particles coming from $W_{R'}$ decay imply that the $W_{R'}$ decay can not give rise to the $ee + 2j$ signal even in the presence of supersymmetry. However, there is a possibility to produce the $e\not{p}_T jj$ signal from the decay modes of $W_{R'}$ if n is considered as the Lightest Supersymmetric Particle (LSP). The relevant decay modes of $W_{R'}$ producing $e\not{p}_T jj$ are given as:

$$\begin{aligned}
(i) \quad W_{R'} &\to h^c\bar{u}^c \to \tilde{h}^*\bar{n}\bar{u}^c \to \boxed{u^c e^c \bar{n}\bar{u}^c} \\
&\to \tilde{e}^*\bar{u}\bar{u}^c \to \boxed{\bar{e}\tilde{\gamma}\bar{u}\bar{u}^c} \\
&\to W_{R'}u^c\bar{u}^c \to \boxed{e^c\bar{n}u^c\bar{u}^c} \\
\\
(iv) \quad W_{R'} &\to N^c_E\bar{e} \to \nu_E\bar{n}\bar{e} \to \boxed{dd^c\bar{n}\bar{e}}\,. \qquad (4.13)
\end{aligned}$$

Thus, in this scenario, which has an attractive feature of allowing high-scale leptogenesis, a signal like two electrons and two jets can not correspond to the decay of $W_{R'}$ whereas there are many channels which can produce a signal like an electron, missing energy and two jets via the decay of $W_{R'}$ as given above. In the next section we will see that both $eejj$ and $e\not{p}_T jj$ signals can be explained in this case by considering R-parity conserving resonant production and decay of an exotic slepton.

4.1.3 Neutral Left-Right Symmetric Model

A third way of choosing the $SU(2)_R$ doublet is (h^c, d^c) [247] and the charge equation is given by

$$Q = T_{3L} + \frac{1}{2}Y_L + \frac{1}{2}Y_N\,,$$

where the $SU(2)$ corresponding to the mentioned doublet does not contribute to the electric charge equation and we will denote it as $SU(2)_N$. For this reason we will often call this model as the "Neutral" Left-Right Symmetric Model (NLRSM) in later chapters. When this $SU(2)_N$ is broken, the gauge bosons $W_N^{\pm}$ and Z_N acquire masses. Note that the $\pm$ in the superscript of W_N refers to the $SU(2)_N$ charge. Under the subgroup $G = SU(3)_c \times SU(2)_L \times SU(2)_N \times U(1)_Y$ the fields transform as

$$\begin{aligned}
(u, d)_L &: (3, 2, 1, \frac{1}{6}) \\
(h^c, d^c)_L &: (\bar{3}, 1, 2, \frac{1}{3}) \\
(E^c, N_E^c)_L &: (1, 2, 1, \frac{1}{2}) \\
(N^c, n)_L &: (1, 1, 2, 0) \\
h_L &: (3, 1, 1, -\frac{1}{3}) \\
u_L^c &: (\bar{3}, 1, 1, -\frac{2}{3}) \\
\begin{pmatrix} \nu_e & \nu_E \\ e & E \end{pmatrix}_L &: (1, 2, 2, -\frac{1}{2}) \\
e_L^c &: (1, 1, 1, 1).
\end{aligned} \tag{4.14}$$

The superpotential governing interactions of SM and exotic particles is given as:

$$\begin{aligned}
W = {} & \lambda_1 \left(\nu_e N_L^c N_E^c + e E^c N_L^c + \nu_E N_E^c n + E E^c n\right) + \\
& \lambda_2 \left(d^c N_L^c h + h h^c n\right) + \lambda_3 u^c e^c h + \lambda_4 \left(u u^c N_E^c + u^c d E^c\right) + \\
& \lambda_5 \left(\nu_e e^c E + e e^c \nu_E\right) + \lambda_6 \left(u d^c E + d d^c \nu_E + u h^c e + d h^c \nu_e\right)
\end{aligned} \tag{4.15}$$

Note that in this case as well, the superpotential ensures that h is a leptoquark ($B = \frac{1}{3}, L = 1$) while ν_E, E and n carry $B = L = 0$ as in Case 2. N^c has the assignment $B = 0, L = -1$. W_N has negative R-parity, nonzero leptonic charge $L = -1$ and zero baryonic charge.

W_N and Z_N can induce $K^0 - \bar{K}^0$ mixing. Consider a scenario where there is mixing between the six quarks (three generations) forming $SU(2)_N$ doublets

$$\begin{pmatrix} \bar{h}_1 \\ \bar{d} \end{pmatrix} \quad \begin{pmatrix} \bar{h}_2 \\ \bar{s} \end{pmatrix} \quad \begin{pmatrix} \bar{h}_3 \\ \bar{b} \end{pmatrix} \tag{4.16}$$

Then the tree level Flavor Changing Neutral Current (FCNC) processes as shown in

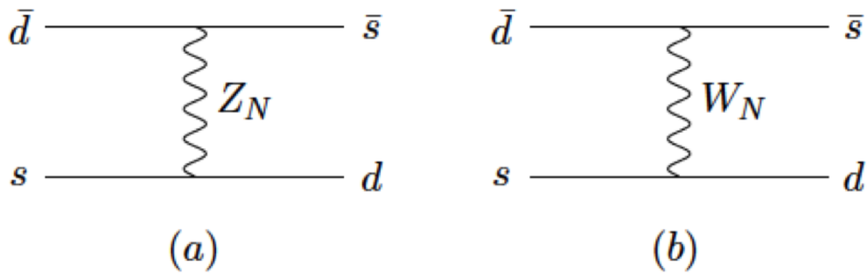

Figure 4.3: Tree level flavor changing neutral-current processes due to mixing of the six quarks, d, s, b and exotic quarks: h_i $(i = 1, 2, 3)$.

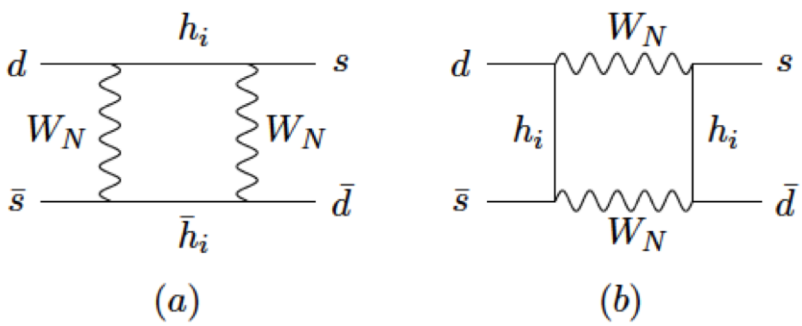

Figure 4.4: Box diagrams leading to $\bar{d}s - \bar{s}d$ mixing if only exotic $h_i(i = 1, 2, 3)$ mix.

Fig. 4.3 will be present and one can get a bound for the W_N from the $K_L - K_S$ mass difference [247]. Even if $\bar{d}$ and $\bar{s}$ do not mix with the exotic $\bar{h}_i$, there may still be a tree level contribution to the kaon mixing. If we assign opposite T_{3N} to $\bar{d}_L$ and $\bar{s}_L$ and if they mix then the diagrams shown in Fig. 4.3 are still possible [247]. On the other hand if only the exotic $\bar{h}_i$ mix and the $\bar{d}_L$ and $\bar{s}_L$ are assigned the same T_{3N}, then one gets the box diagrams shown in Fig. 4.4 [247]. Similarly, considering $SU(2)_N$ doublets in the leptonic sector,

$$\begin{pmatrix} E \\ e \end{pmatrix} \begin{pmatrix} M \\ \mu \end{pmatrix} \begin{pmatrix} T \\ \tau \end{pmatrix}, \tag{4.17}$$

even in the absence of mixing between the ordinary and exotic fermions the process $\mu \to e\gamma$ can take place if the exotic fermions mix among themselves [247] as shown in Fig. 4.5. The coupling of the W_N to the fermions is given by

$$\mathcal{L} = \frac{1}{\sqrt{2}} g_R W_N^\mu (\bar{h}\gamma_\mu d_R + \bar{e}\gamma_\mu E_L + \bar{\nu}\gamma_\mu(\nu_E)_L + \bar{N}^c\gamma_\mu n_L) + \text{h.c.} \tag{4.18}$$

On similar grounds, as in the ALRSM case, the W_N cannot be produced via the usual

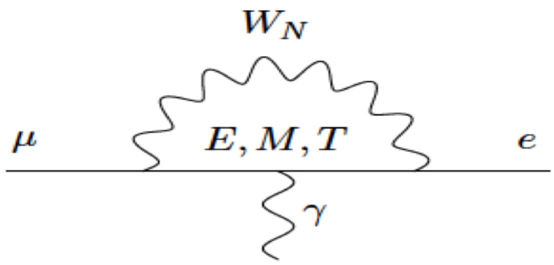

Figure 4.5: Loop diagrams involving exotic fermions and W_N leading to $\mu \to e\gamma$.

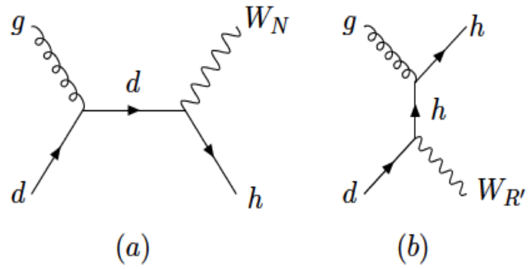

Figure 4.6: s- and t-channel Feynman diagrams for the process: $g + d \to h + W_N$.

Drell-Yan mechanism or via the decay of the heavy Z_N. The process that can yield a large cross section for W_N production [248] is $g + d \to h + W_N$ which consists of the diagrams shown in Fig. 4.6.

The invariant amplitude squared averaged over partonic spin and color is given by [245, 248]

$$\begin{aligned} |\bar{\mathcal{M}}_N|^2 &= \frac{4\pi G_F M_{W_N}^2}{3\sqrt{2}}\,\alpha_s\left[-\left(\frac{t'}{s}+\frac{s}{t'}\right)\left(2+\frac{M_h^2}{M_{W_N}^2}\right)-2\frac{M_h^2}{M_{W_N}^2}\right. \\ &+ 2\left(2M_{W_N}^2-M_h^2-\frac{M_h^4}{M_{W_N}^2}\right)\left(\frac{1}{s}+\frac{1}{t'}\right) \\ &+ \left.\frac{2}{st'}\left(-\frac{M_h^6}{M_{W_N}^2}+3M_h^2M_{W_N}^2-2M_{W_N}^4\right)\right], \end{aligned} \tag{4.19}$$

where $t' = t - M_h^2$, and M_h (M_{W_N}) is the mass of h (W_N). The partonic cross section of the process can be obtained by integrating over t' between the limits

$$t'_{1,2} = -\frac{1}{2}\left(\hat{s}+M_h^2-M_{W_N}^2\right) \pm \frac{1}{2}\left[\left(\hat{s}-M_h^2-M_{W_N}^2\right)^2-4M_h^2M_{W_N}^2\right]^{1/2}. \tag{4.20}$$

A comparison of Eq. (4.19) with Eq. (4.10) reveals that the production cross sections for W_N and $W_{R'}$ are similar, particularly if $M_h \sim M_W$. A detailed account of the above W_N production cross section is given in Refs. [245, 248], both of which find the cross section to be substantially large. To give a quantitative order of magnitude estimate, for $M_h = 1\,\text{TeV}$ and $M_{W_N} \sim 2.1\,\text{TeV}$ the cross section at the LHC for the process $pp \to W_N^+ h$ is about $\sigma \sim 0.05$ pb at $\sqrt{s} = 14\,\text{TeV}$ and $\sigma \sim 0.005$ pb at $\sqrt{s} = 8\,\text{TeV}$. In this case also the production cross sections $\sigma(W_N^+) > \sigma(W_N^-)$, due to the fact that d-quark distribution function in a proton beam is larger than the $\bar{d}$-quark distribution function.

Pair production of W_N can take place via the process $e^+e^- \to W_N^+ W_N^-$ [248]. The relevant diagrams are shown in Fig. 4.7. This process is particularly sensitive to the underlying gauge structure and cancellations between the given amplitudes. Thus it can serve as a probe for the non-abelian $SU(2)_N$ gauge theory. Under the approximation that $M_{Z_N} \sim M_{W_N}$, the differential cross section for this process is given by [248]

$$\frac{d\sigma}{dz} = \frac{G_F^2 M_{W_N}^4}{8\pi s}\beta\left(F_1 + \frac{1}{8}F_2\frac{s^2}{(s-M_{Z_N}^2)^2 + M_{Z_N}^2\Gamma_{Z_N}^2} - \frac{1}{2}F_3\frac{s(s-M_{Z_N}^2)}{(s-M_{Z_N}^2)^2 + M_{Z_N}^2\Gamma_{Z_N}^2}\right), \tag{4.21}$$

where $\beta \equiv (1 - 4M_{W_N}^2/s)^{1/2}$ and the F_i's are given by

$$\begin{aligned} F_1 &\equiv r^2[2y + \frac{1}{2}(1-z^2)\beta^2\{(y/x)^2 + \frac{1}{4}y^2\}], \\ F_2 &\equiv \beta^2[16y + (1-z^2)(y^2 - 4y + 12)], \\ F_3 &\equiv r[16(1+X^{-1}) + \gamma y\beta^2 + \frac{1}{2}\beta^2(1-z^2)(y^2 - 2y - 4y/x)], \end{aligned} \tag{4.22}$$

with

$$y \equiv s/M_{Z_N}^2, \quad x \equiv t/M_{Z_N}^2, \quad r \equiv \frac{t}{t - M_{Z_N}^2}, \tag{4.23}$$

and $t = M_{Z_N}^2 - \frac{1}{2}s(1-\beta z)$. In Ref. [248] the total cross section for the process $e^+e^- \to W_N^+ W_N^-$ is estimated as a function of M_{W_N} and M_E for $\sqrt{s} = 1\,\text{TeV}$. To have a quantitative order of magnitude estimate, for $\sqrt{s} = 1\,\text{TeV}$, $M_E \sim 1.0\,\text{TeV}$ and $M_{W_N} \sim 350\,\text{GeV}$ the total cross section for the process $e^+e^- \to W_N^+ W_N^-$ is about 1 pb. For $M_{W_N} \lesssim 270\,\text{GeV}$, the production cross section increases substantially with increasing M_E, while for $M_{W_N} \gtrsim 370\,\text{GeV}$ the production cross section decreases with increasing M_E. An inspection of all the further decays of the exotic particles coming from the two-body decay modes of W_N listed above tells us that a $ee{+}2j$ signal cannot be obtained from the decay of W_N even in the presence of supersymmetry.

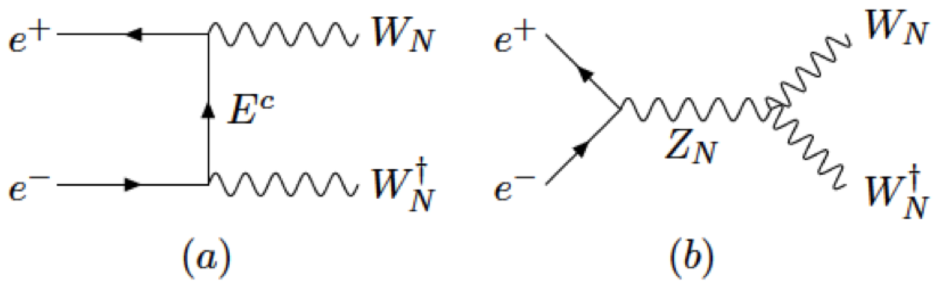

Figure 4.7: s- and t-channel Feynman diagrams for the process: $e^+e^- \to W_N^+ W_N^-$.

However, there is a possibility to produce the $e\not{p}_T jj$ signal from the decay modes of W_N if n is considered as Lightest Supersymmetric Particle (LSP). The relevant decay modes of W_N producing $e\not{p}_T jj$ are given as

$$
\begin{aligned}
(i) \quad W_N &\to h^c \bar{d}^c \to \tilde{h}^* \bar{n} \bar{d}^c \to \boxed{u^c e^c \bar{n} \bar{d}^c} \\
&\to \tilde{e}^* \bar{u} \bar{d}^c \to \boxed{\bar{e} \tilde{\gamma} \bar{u} \bar{d}^c} \\
(ii) \quad W_N &\to e \bar{E}_L \to e \tilde{\bar{E}}^c n \to \boxed{e \bar{u}^c \bar{d} n}
\end{aligned} \tag{4.24}
$$

Thus, similar to the ALRSM case, a signal like two electrons and two jets can not correspond to the decay of W_N whereas there are some channels which can produce a signal like an electron, missing energy and two jets via the decay of W_N as given above. However, in this case also both $eejj$ and $e\not{p}_T jj$ signals can be interpreted in this case also by considering R-parity conserving resonant production and decay of an exotic slepton.

4.2 Exotic sparticle(s) production leading to an $eejj(e\not{p}_T jj)$ signal

In this Section we show that two of the effective low-energy subgroups (discussed in sections 4.1.2 and 4.1.3) of the E_6 group can produce both $eejj$ and $e\not{p}_T jj$ signals from the decay of scalar superpartner(s) of the exotic particle(s). Both events can be produced naturally in the above schemes by considering (i) resonant production of the exotic slepton $\tilde{E}$ (ii) pair production of scalar leptoquarks $\tilde{h}$. Interestingly, as

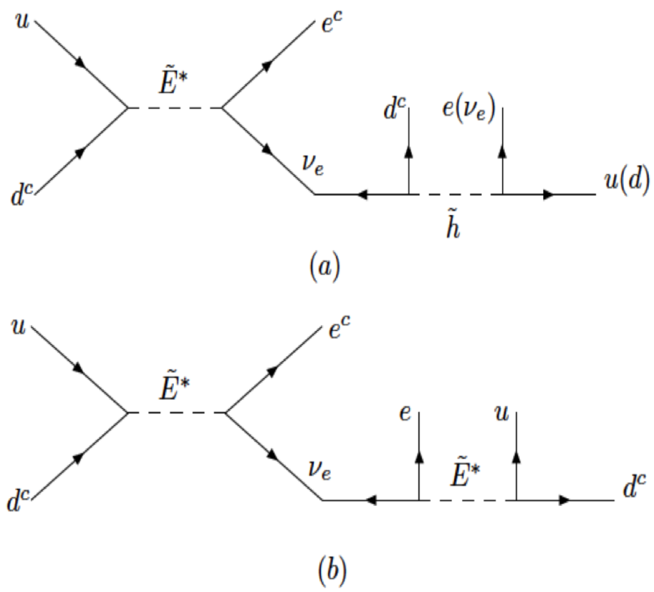

Figure 4.8: R-parity conserving Feynman diagrams for a single exotic particle $\tilde{E}$ production leading to both $eejj$ and $e\not{p}_T jj$ signals.

compared to the resonant production of sleptons as discussed in Ref. [228], the exotic slepton $\tilde{E}$ can be resonantly produced in pp collisions without violating R-parity. The exotic slepton then subsequently decays to a charged lepton and neutrino, followed by R-parity conserving interactions of the neutrino producing an excess of events in both $eejj$ and $e\not{p}_T jj$ channels. The R-parity conserving processes leading to both $eejj$ and $e\not{p}_T jj$ signals are given in Fig. 4.8(a) and the one giving only $eejj$ signal is given in Fig. 4.8(b). The cross section of the $eejj$ process as given in Fig. 4.8(a) and Fig. 4.8(b) can be expressed as:

$$\sigma\,(pp \to eejj) = \sigma(pp \to \tilde{E}_L) \times BR(\tilde{E}_L \to eejj) \tag{4.25}$$

whereas the cross section of the $e\not{p}_T jj$ processes as given in Fig. 4.8(b) can be expressed as

$$\sigma\left(pp \to e\not{p}_T jj\right) = \sigma(pp \to \tilde{E}_L) \times BR(\tilde{E}_L \to e\not{p}_T jj). \tag{4.26}$$

In Case 2, the resonant production of the slepton as well as decay modes of the same are given by the following terms in the superpotential

$$W_2 = -\lambda_1\,(uh^c e - dh^c \nu_e) + \lambda_2 u d^c E - \lambda_5 E e^c \nu_e, \tag{4.27}$$

while in Case 3, the relevant interaction terms are given by

$$W_3 = \lambda_5' \left(\nu_e e^c E + e e^c \nu_E\right) + \lambda_6' \left(u d^c E + u h^c e + d h^c \nu_e\right).$$

The parton cross section of a single slepton production in Case 2 is given by [249]

$$\hat{\sigma} = \frac{\pi}{12\hat{s}} \left|\lambda_2\right|^2 \delta(1 - \frac{m_{\tilde{E}}^2}{\hat{s}}) \tag{4.28}$$

where $\hat{s}$ is the partonic centre of mass energy, and $m_{\tilde{E}}$ is the mass of the resonant slepton. Including effects from parton distribution functions, the total cross section to a good approximation is given by [249]

$$\sigma\left(pp \to eejj\right) \propto \frac{\left|\lambda_2\right|^2}{m_{\tilde{E}}^3} \times \beta_1 \tag{4.29}$$

and

$$\sigma\left(pp \to e\not{p}_T jj\right) \propto \frac{\left|\lambda_2\right|^2}{m_{\tilde{E}}^3} \times \beta_2 \tag{4.30}$$

where β_1 is the branching fraction for the decay of the exotic slepton to $eejj$ and β_2 is the branching fraction to $e\not{p}_T jj$. Similarly, in Case 3, the cross sections in the $eejj$ and $e\not{p}_T jj$ channels depend on $\frac{\left|\lambda_6\right|^2}{m_{\tilde{E}}^3} \times \beta_1$ and $\frac{\left|\lambda_6\right|^2}{m_{\tilde{E}}^3} \times \beta_2$ respectively. By choosing $\beta_{1,2}$ as well as couplings $\lambda_2(\lambda_6')$ as free parameters, the cross section can be calculated as a function of the exotic slepton mass. Stringent bounds can also be obtained on the value of the mass of the exotic slepton by comparing the theoretically calculated cross section with the data collected by CMS at a centre of mass energy $\sqrt{s} = 8$ TeV. Thus, we propose that the alternative schemes of E_6 might explain the excess $eejj$ and $e\not{p}_T jj$ signals at CMS naturally via resonant exotic slepton decay.

4.3 Explaining the diphoton excess in Alternative Left-Right Symmetric Model

The CMS and ATLAS collaborations have recently announced the search results based on the first 3 fb^{-1} of collected data from Run 2 of the LHC at $\sqrt{s} = 13$ TeV [174, 175]. The ATLAS collaboration has reported a 3.9 σ local (2.3 σ global) excess in the diphoton channel at the diphoton invariant mass of around $750\,\mathrm{GeV}$ with 3.2fb^{-1} integrated luminosity. This excess corresponds to about 14 events appearing in at least two energy bins, suggesting a large width $\sim 45\,\mathrm{GeV}$ [175]. The CMS collaboration has partially endorsed this result with an integrated luminosity of $2.6\mathrm{fb}^{-1}$. They have reported about 10 excess events in the $\gamma\gamma$ channel peaked at $760\,\mathrm{GeV}$ amounting to a 2.6σ local ($< 1.2\sigma$ global) excess [174].

A new resonance coupling with the Standard Model (SM) t quark or $W^{\pm}$ can give rise to loop diagrams with $\gamma\gamma$ final state. However, such diagrams are highly suppressed at the large $\gamma\gamma$ invariant masses and the dominant decay channels are $t\bar{t}$ or $W^{+}W^{-}$. Thus, the observation of the $\gamma\gamma$ resonance at 750 GeV (much larger than the electroweak symmetry breaking scale) presumably hints towards new physics around that mass scale. Several new physics interpretations of the diphoton signal have been proposed in the literature explaining the excess events.

In light of the fact that the two collaborations have suggested signal events consistent with each other at a 3σ statistical significance level, hinting towards a new physics scenario, it is important to explore the possible model framework that can naturally accommodate the diphoton signal. In this section, we argue that the E_6 motivated Alternative Left-Right Symmetric Model (ALRSM) provides a very attractive framework to address the diphoton excess [250].

Interestingly, the gluon-gluon fusion can give the observed production rate of the $750\,\mathrm{GeV}$ resonance, $\tilde{n}$ in our model, through a loop of scalar leptoquarks ($\tilde{h}^{(c)}$). Subsequently, $\tilde{n}$ decays into gg and $\gamma\gamma$ final states via loops of $\tilde{h}^{(c)}$ and $\tilde{E}^{(c)}$. Note that, considering only scalar leptoquarks in the decay loop of $\tilde{n}$ yields a diphoton branching ratio suppressed by a factor of $10^{-3} - 10^{-4}$, and it is the contribution from $\tilde{E}^{(c)}$ loop which enhances the diphoton branching ratio significantly to give the observed cross section of the diphoton signal. The fermionic components of h, h^c and E, E^c can also enter the loops and contribute to the production cross section and $\gamma\gamma$ branching fraction. This will improve the parameter space freedom of the trilinear scalar couplings and scalar component masses, however, a significant contribution from the fermionic states require quite large Yukawa couplings inconsistent with perturbativity (for example see Ref. [251]). In the present case, we assume the Yukawa couplings to be small such that the $\sigma(pp \to \gamma\gamma)$ contribution coming from the fermionic component is small compared to the contribution coming from the scalar components running in the loop.

This helps us evade the dangerous perturbativity constraints on Yukawa couplings and reduces the effective number of free parameters, giving us a better handle on the scalar parameter space. The relavant terms in the superpotential are given by

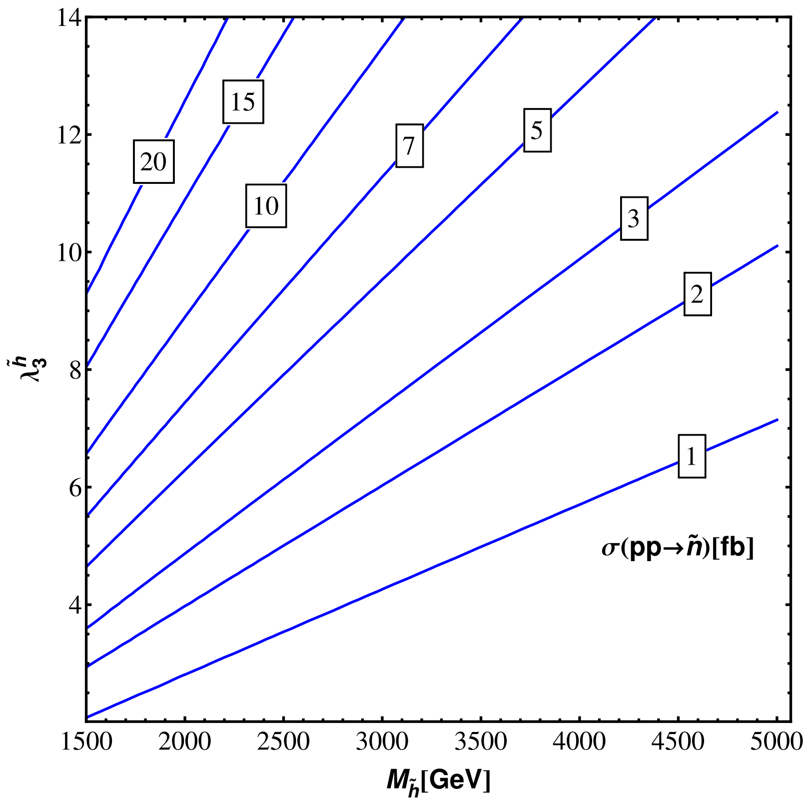

Figure 4.9: $pp \to \tilde{n}$ production cross section in gluon fusion at $\sqrt{s} = 13\,\mathrm{TeV}$ as function of scalar leptoquark mass and $\lambda_3^{\tilde{h}}$. The numbers in the boxes are the production cross sections corresponding to the contours.

$$W_1 = -\lambda_3 h h^c n + \lambda_5 E E^c n, \tag{4.31}$$

where we have dropped the generation indices for simplicity. The production cross section can be conveniently parametrized in terms of the corresponding production cross section of the SM Higgs H with its mass replaced by the $\tilde{n}$ mass $M_H = M_{\tilde{n}}$ [252]. This eliminates the factors due to higher order QCD corrections to give

$$\frac{\sigma(pp \to \tilde{n})}{\sigma(pp \to H)} = \left(\frac{\lambda_3^{\tilde{h}\tilde{n}} \cos\theta_{\tilde{h}} \sin\theta_{\tilde{h}} v}{8 M_{\tilde{h}}} \right)^2 \left| \frac{A_0(x_{\tilde{h}})}{A_{1/2}(x_t)} \right|^2, \tag{4.32}$$

where the dimensionful coupling corresponding to the λ_3 trilinear scalar term in Eq. (4.31) is parametrized as $\lambda_3^s = \lambda_3^{\tilde{h}\tilde{n}} M_{\tilde{n}}$, θ is the left-right mixing angle of the scalar leptoquark sector corresponding to $\tilde{h}-\tilde{h}^c$, v is the vacuum expectation value $\langle H\rangle = v$, $x_{\tilde{h}} = m_{\tilde{n}}^2/4M_{\tilde{h}}^2$ and $x_t = m_{\tilde{n}}^2/4M_t^2$ where M_t is the top mass. The loop functions are given by

$$\begin{aligned} A_0(x) &= \frac{3(f(x)-x)}{x^2}, \\ A_{1/2}(x) &= \frac{3}{2x^2}\left[x+(x-1)f(x)\right], \end{aligned} \tag{4.33}$$

with $f(x)$ given by

$$f(x) = \begin{cases} \arcsin^2(\sqrt{x}) & x \leq 1 \\ -\frac{1}{4}\left[\ln\left(\frac{1+\sqrt{1-x}}{1-\sqrt{1-x}}\right) - i\pi\right]^2 & x \geq 1. \end{cases} \tag{4.34}$$

$\sigma(pp \to H)$ at $\sqrt{s} = 13\,\mathrm{TeV}$ can be obtained by boosting the $\sqrt{s} = 8\,\mathrm{TeV}$ cross section $\sigma = 0.157\mathrm{pb}$ (for $M_H = 750\,\mathrm{GeV}$) by a factor 4.7 corresponding to increased gluon luminosity [253]. The $pp \to \tilde{n}$ production cross section in gluon fusion as function of scalar leptoquark mass and $\lambda_3^{\tilde{h}} = \lambda_3^{\tilde{h}\tilde{n}}(M_{\tilde{n}}/M_{\tilde{h}})$ is shown in Fig. 4.9. Note that, we take the maximum value of $\lambda_3^{\tilde{h}}$ as 14 corresponding to the rough upper limit from perturbativity [254, 255] and $\theta_{\tilde{h}} = \pi/4$ corresponding to maximal mixing between left and right handed scalar leptoquarks. Now, for $2M_{\tilde{h}(\tilde{E})} > M_{\tilde{n}}$, $\tilde{n}$ can not decay to two on shell $\tilde{h}(\tilde{E})$, giving appreciable branching ratios for $\gamma\gamma$ and gg final states. The partial widths for the $\gamma\gamma$ final state are given by

$$\Gamma_{\gamma\gamma}^X = \frac{\alpha^2 M_{\tilde{n}}^3}{256\pi^3}\frac{\left|\lambda_y^{\tilde{X}\tilde{n}}\cos\theta_X\sin\theta_X M_{\tilde{n}}\right|^2}{M_X^4}\left|A_0(x_X)\right|^2, \tag{4.35}$$

where $X(y)$ can be $\tilde{h}(3)$ and $\tilde{E}(5)$, A_0 corresponds to the loop function defined in Eq. (4.33) and $x_X = m_{\tilde{n}}^2/4M_X^2$. The corresponding decay width for the gg final state can be obtained by

$$\Gamma_{gg} = \Gamma_{\gamma\gamma}^{\tilde{h}}\frac{2K_{gg}\alpha_s^2}{9Q_{\tilde{h}}^4\alpha^2}, \tag{4.36}$$

where $K_{gg} \sim 2$ arises from higher order QCD corrections, $\alpha_s(M_{\tilde{n}}) \approx 0.092$, $Q_{\tilde{h}} = -1/3$. Considering $\tilde{h}$ as the only field running in the decay loop yields a branching fraction $\sim 10^{-3} - 10^{-4}$ for the $\gamma\gamma$ final state. Thus, the contribution coming from $\tilde{E}$ running in the final decay loop plays an essential role in controlling the branching ratio to the $\gamma\gamma$ final state. The branching fraction as a function of slepton mass

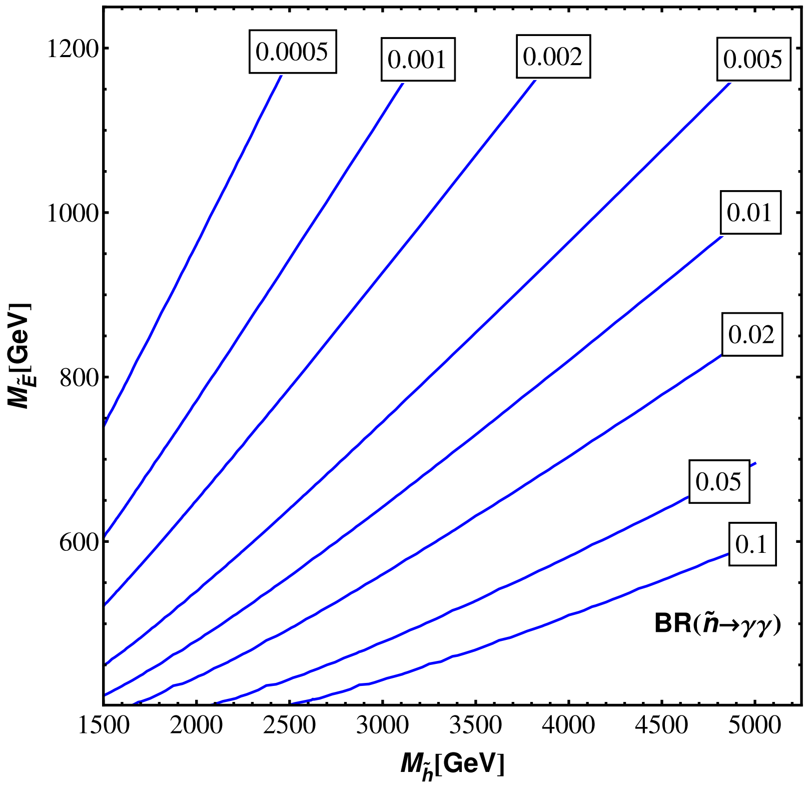

Figure 4.10: The branching fraction as a function of slepton mass $M_{\tilde{E}}$ and scalar leptoquark mass $M_{\tilde{h}}$ with $\lambda_3^{\tilde{h}} = \lambda_5^{\tilde{E}} = 14$. The numbers in the boxes are the branching fractions corresponding to the contours.

$M_{\tilde{E}}$ and scalar leptoquark mass $M_{\tilde{h}}$ is shown in Fig. 4.10. In Fig. 4.11, the production cross section times branching ratio $\sigma(pp \to \tilde{n}) \times \mathrm{BR}(\tilde{n} \to \gamma\gamma)$ is presented for $\lambda_3^{\tilde{h}} = \lambda_3^{\tilde{E}} = 14$ corresponding to the rough upper limits allowed by perturbativity for the lowest masses of scalar leptoquark ($\tilde{h}$) and slepton ($\tilde{E}$) respectively (${M_{\tilde{h}}}^{\min} \sim 2M_{\tilde{n}}$ and ${M_{\tilde{E}}}^{\min} \sim M_{\tilde{n}}/2$)[3] [254, 255], $\theta_{\tilde{h}} = \theta_{\tilde{E}} = \pi/4$ corresponding to maximal mixing between the left and right handed scalar leptoquarks and sleptons. The pink band corresponds to $\sigma(pp \to \tilde{n}) \times \mathrm{BR}(\tilde{n} \to \gamma\gamma) = 2 - 8$ fb, corresponding to 95% CL upper limit on the allowed cross section at $13\,\mathrm{TeV}$, consistent with cross section exclusion at 95% CL by the absence of a signal in the CMS run 1 data [216]. We find that the slepton mass $M_{\tilde{E}} \lesssim 400\,\mathrm{GeV}$ is favored by the fit, while scalar leptoquark mass $M_{\tilde{h}} \lesssim 2500\,\mathrm{GeV}$ is preferred by the diphoton excess. Note that for different generations of $\tilde{n}$ with a mass difference $\mathcal{O}(10)\,\mathrm{GeV}$ one can address the wider peak hinted by ATLAS, given that the present statistics can not resolve these different masses.

[3]Note that, here we have used the parametrizations $\lambda_3^{\tilde{h}} = \lambda_3^{\tilde{h}\tilde{n}}\left(M_{\tilde{n}}/M_{\tilde{h}}\right)$ and $\lambda_5^{\tilde{E}} = \lambda_5^{\tilde{E}\tilde{n}}\left(M_{\tilde{n}}/M_{\tilde{E}}\right)$.

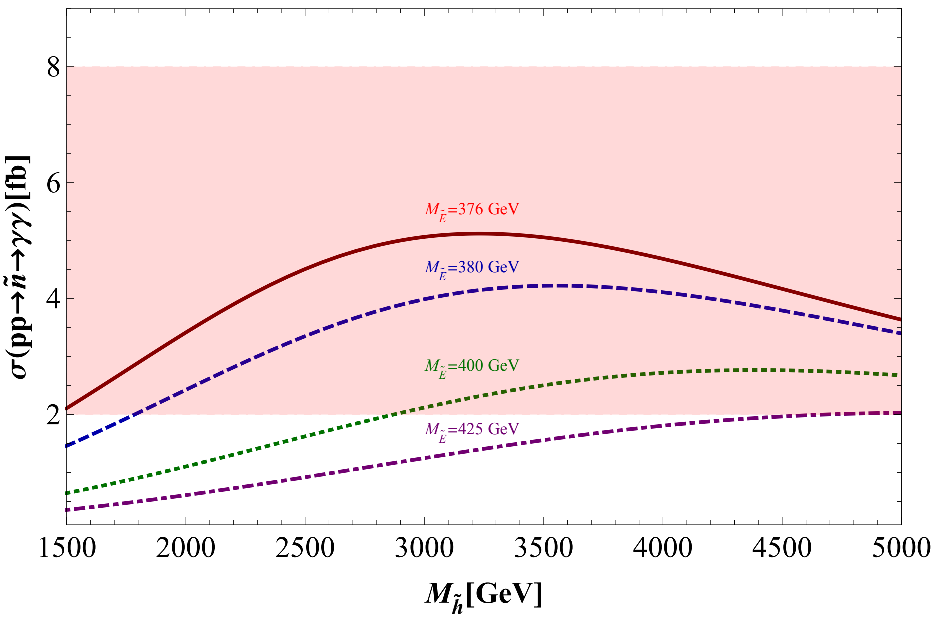

Figure 4.11: The production cross section times branching ratio $\sigma(pp \to \tilde{n}) \times \mathrm{BR}(\tilde{\mathrm{n}} \to \gamma\gamma)$ as a function of scalar leptoquark mass $M_{\tilde{h}}$ (for three different values of slepton mass $M_{\tilde{E}}$) with $\lambda_3^{\tilde{h}} = \lambda_3^{\tilde{E}} = 14$, $\theta_{\tilde{h}} = \theta_{\tilde{E}} = \pi/4$. The pink band corresponds to the observed value of $\sigma(pp \to \tilde{n}) \times \mathrm{BR}(\tilde{\mathrm{n}} \to \gamma\gamma) = 2 - 8$ fb, corresponding to 95% CL upper limit on the allowed cross section at 13 TeV.

4.4 Leptogenesis in supersymmetric low energy E_6-subgroups

In the conventional LRSM scenario for successful high-scale leptogenesis, constraints on the W_R mass mentioned in the introduction follow from the out-of-equilibrium condition of the scattering processes involving the $SU(2)_R$ gauge interactions [192]. In the case $M_N > M_{W_R}$ the condition that the process

$$e_R^- + W_R^+ \to N_R \to e_R^+ + W_R^- \tag{4.37}$$

goes out of equilibrium gives

$$M_N \gtrsim 10^{16}\,\mathrm{GeV} \tag{4.38}$$

with $m_{W_R}/m_N \gtrsim 0.1$. For the case $M_{W_R} > M_N$ leptogenesis can occur either at $T \simeq M_N$ or at $T > M_{W_R}$ below the $B-L$ breaking scale. For $T \simeq M_N$, the out-of-equilibrium condition of the scattering processes which maintain the equilibrium number density for N_R leads to

$$M_{W_R} \gtrsim 2 \times 10^5 \,\mathrm{GeV}(M_N/10^2 \,\mathrm{GeV})^{3/4}. \tag{4.39}$$

For leptogenesis at $T > M_{W_R}$ the condition that the scattering process

$$W_R^\pm + W_R^\pm \to e_R^\pm + e_R^\pm \tag{4.40}$$

through N_R exchange goes out of equilibrium gives

$$M_{W_R} \gtrsim 3 \times 10^6 \,\mathrm{GeV}(M_N/10^2 \,\mathrm{GeV})^{2/3}. \tag{4.41}$$

Consequently, observing a W_R signal in the range $1.8 \,\mathrm{TeV} < M_{W_R} < 2.2 \,\mathrm{TeV}$ implies that it is not possible to generate the required baryon asymmetry of the universe from high-scale leptogenesis for a hierarchical neutrino mass spectrum ($M_{N_{3R}} \gg M_{N_{2R}} \gg M_{N_{1R}} = m_N$) in the usual LRSM scenario (even if it is embedded in a higher gauge group).

The E_6 group allows the possibility of explaining leptogenesis in two of its effective low-energy subgroups [256]. One of them is $G_1 = SU(3)_C \times SU(2)_L \times U(1)_Y \times U(1)_N$ [257], which we will discuss in detail in the next chapter, and the other is $G_2 = SU(3)_C \times SU(2)_L \times SU(2)_{R'} \times U(1)_{Y'}$, which is the case discussed in section 4.1.2. With the assignment given in Eqs. (4.4), (4.6) and (4.14), amongst the five neutral fermions, only ν_e and N^c carry nonzero $B - L$ in all subgroups. Therefore, leptogenesis can be addressed via the decay of the Majorana neutrino N^c in all three cases. Now to generate the $B - L$ asymmetry from the heavy neutrinos, one needs to satisfy the conditions: (i) violation of $B - L$ from the Majorana mass of N (ii) CP violation from complex couplings and (iii) the out-of-equilibrium condition for the decay of the physical heavy Majorana neutrino N given by

$$\Gamma_N < H(T = m_N) = \sqrt{\frac{4\pi^3 g_*}{45}} \frac{T^2}{M_{Pl}}, \tag{4.42}$$

where Γ_N is the decay width, $H(T)$ is the Hubble expansion rate, g_* is the number of relativistic degrees of freedom at temperature T and M_{Pl} is the Planck mass. This translates into the condition that the mass of N must be many orders of magnitude greater than the $\,\mathrm{TeV}$ scale and consequently N^c cannot transform nontrivially under the low-energy subgroup G. From the assignments of Eq. (4.4) and Eq. (4.14), it follows that N^c transforms as a doublet under both $SU(2)_R$ and $SU(2)_N$. This implies that if $SU(2)_R$ gets broken at the TeV scale, a successful leptogenesis scenario can not be obtained in Case 1 (similar to the conventional left-right model) and Case 3. In Case 2, since N^c transforms trivially under the low-energy subgroup G, the out-of-equilibrium decay of heavy neutrinos can give rise to high-scale leptogenesis [4]. In this case, the Majorana neutrino N_k^c decays to $B - L = -1$ final states $\nu_{e_i}\tilde{N}^c_{E_j}, \tilde{\nu}_{e_i}N^c_{E_j}, e_i\tilde{E}^c_j, \tilde{e}_i, E^c_j$ and $d_i\tilde{h}_j, \tilde{d^c}_i\tilde{h}_j$ and to their conjugate states, via the interaction terms involving λ_4 and λ_6 in Eq. (4.7). One-loop diagrams, such as the two shown in Fig. 4.12 for a given final state, can interfere with the tree level N_k decays to provide the required CP violation for particular values of couplings λ_4^{ijk} and λ_6^{ijk} . An

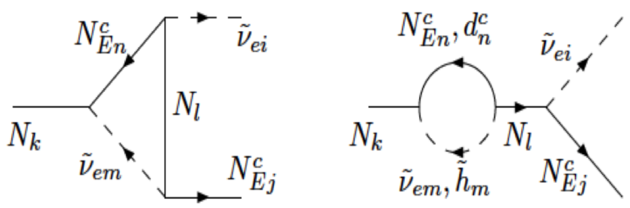

Figure 4.12: Loop diagrams for N_k decay.

order of magnitude estimate of the upper bound on the couplings λ_4^{ijk} and λ_6^{ijk} can be obtained from the out-of-equilibrium condition given by Eq. (4.42). Considering the total decay width of N_k given by

$$\Gamma_{N_k} = \frac{1}{4\pi}\sum_{i,j}(|\lambda_4^{ijk}|^2 + 2|\lambda_6^{ijk}|^2)m_{N_k} \tag{4.43}$$

and taking $g_* \sim 100$ at $T \sim m_{N_k}$, the condition given by Eq. (4.42) gives

$$\sum_{i,j}(|\lambda_4^{ijk}|^2 + 2|\lambda_6^{ijk}|^2) \lesssim 2\times 10^{-17}\,\mathrm{GeV}^{-1}m_{N_k}. \tag{4.44}$$

So for $m_{N_k} \sim 10^{15}\,\mathrm{GeV}$, $\lambda_4^{ijk}, \lambda_6^{ijk} \lesssim 10^{-1}$. In fact $\lambda_{4,6}^{ijk} \sim 10^{-3}$ can give the observed baryon-to-entropy ratio $n_B/s \sim 10^{-10}$ for maximal CP violation [256]. Therefore,

[4]Note that Ref. [114] considers a scenario in which the lepton asymmetry is generated via Higgs triplet decays while the wash out processes involving gauge interactions are in effect. In this scheme, the leptogenesis can work in the strong wash out regime. However in our case where lepton asymmetry gets generated at a high scale, the wash out processes involving gauge interactions (effective at a lower energy scale) must go out of equilibrium so that the lepton asymmetry does not get wiped out.

the ALRSM case has the attractive feature that it can explain both the excess $eejj$ and $e\not{p}_T jj$ signals, and also high-scale leptogenesis.

4.5 Summary of the chapter

We have discussed the effective low-energy theories of the superstring inspired E_6 group that is broken to its maximal subgroup by flux breaking at a very high scale. Our aim was to look for extensions of the standard model that can explain the excess $eejj$ and $e\not{p}_T jj$ events that have been observed by CMS at the LHC at the center of mass energy $\sqrt{s} = 8$ TeV, and simultaneously explain the baryon asymmetry of the universe via leptogenesis.

The decay of the right-handed gauge boson is able to produce $eejj$ events in one of the effective low-energy subgroups given by $G = SU(3)_c \times SU(2)_L \times SU(2)_R \times U(1)_{B-L}$. The right-handed gauge boson decay in the other two effective low-energy subgroups of E_6: $G = SU(3)_c \times SU(2)_L \times SU(2)_{R'} \times U(1)_{Y'}$ (the case discussed in section 4.1.2) and $G = SU(3)_c \times SU(2)_L \times SU(2)_N \times U(1)_Y$ (the case discussed in section 4.1.3), can produce the $e\not{p}_T jj$ signal if the exotic particle n is considered to be the LSP. However, neither of these subgroups is able to produce both excess signals simultaneously from the decay of right-handed gauge bosons. On the other hand, both signals can be produced simultaneously in these two effective low-energy subgroups of E_6 via the R-parity conserving resonant production of an exotic slepton, followed by its decay via R-parity conserving interactions.

We have also discussed the possibility of explaining the diphoton signal in ALRSM. We found that gluon-gluon fusion can give the observed production rate of the $750\,\mathrm{GeV}$ resonance, $\tilde{n}$, through a loop of scalar leptoquarks ($\tilde{h}^{(c)}$) with a mass below a few TeV range. $\tilde{n}$ can subsequently decay into gg and $\gamma\gamma$ final states via loops of $\tilde{h}^{(c)}$ and $\tilde{E}^{(c)}$. Considering only scalar leptoquarks in the decay loop of $\tilde{n}$ yields a suppressed diphoton branching ratio; however, the contribution from the $\tilde{E}^{(c)}$ loop can enhance the diphoton branching ratio significantly to explain the observed cross section of the diphoton signal.

Since the effective low-energy subgroup of E_6 discussed in section 4.1.1 allows breaking of $U(1)_{B-L}$ at a scale lower than the $SU(2)_R$ breaking scale, it is not consistent with leptogenesis at a high scale. The other two subgroups allow breaking of $SU(2)_R$ at a low scale which is independent of the $B-L$ breaking scale. However, since in the subgroup discussed in 4.1.3, the right-handed neutrino transforms nontrivially under the low energy group, it can not give rise to high scale leptogenesis. In ALRSM, the the right-handed neutrino transforms trivially under the low energy group, allowing leptogenesis at a high scale. Therefore, we conclude that the $G = SU(3)_c \times SU(2)_L \times SU(2)_{R'} \times U(1)_{Y'}$ subgroup, also referred to as the Alternative Left-Right Symmetric Model, can explain both the excess $eejj$ and $e\not{p}_T jj$ signals and also satisfy the constraints for successful leptogenesis.

Chapter 5

Explaining the B-decay anomalies in the left-right symmetric low energy subgroups of E_6

In the intensity frontier of modern particle physics, precision measurements associated with rare decays can provide powerful probes for new physics (NP) beyond the SM. To this end, one must mention the recent measurements of rare B decays induced by flavor changing neutral current (FCNC), which have shown some interesting anomalies hinting towards lepton non-universal NP as well as deviations in the charged current induced processes. In 2012 the BaBar collaboration reported [177] the measurements of the ratio of branching fractions

$$R_{D^{(*)}} = \frac{\mathrm{Br}(\bar{B} \to D^{(*)}\tau\bar{\nu})}{\mathrm{Br}(\bar{B} \to D^{(*)}l\bar{\nu})}, \tag{5.1}$$

where $l = e, \mu$, $R_D^{\mathrm{BaBar}} = 0.440 \pm 0.058 \pm 0.042$ and $R_{D^*}^{\mathrm{BaBar}} = 0.332 \pm 0.024 \pm 0.018$ showing 2.0σ and 2.7σ enhancements over the SM predictions $R_D^{\mathrm{SM}} = 0.300 \pm 0.010$ and $R_{D^*}^{\mathrm{SM}} = 0.252 \pm 0.005$ respectively. Corroborating this result, in 2015, the Belle collaboration reported $R_D^{\mathrm{Belle}} = 0.375 \pm 0.064 \pm 0.026$ and $R_{D^*}^{\mathrm{Belle}} = 0.293 \pm 0.038 \pm 0.015$ [179]. More recently, the LHCb and Belle collaborations have reported $R_{D^*}^{\mathrm{LHCb}} = 0.336 \pm 0.027(\mathrm{stat.}) \pm 0.030(\mathrm{syst.})$ and $R_{D^*}^{\mathrm{Belle16}} = 0.302 \pm 0.030(\mathrm{stat.}) \pm 0.011(\mathrm{syst.})$ amounting to $\sim 2.1\sigma$ and $\sim 1.6\sigma$, respectively, enhancements over the SM predictions [180, 181]. These results, when combined together, show significant enhancements over the SM predictions, hinting towards an NP contribution. Interestingly, the

LHCb collaboration [182] has also reported another tantalizing deviation from the SM expectation of the ratio of branching fractions of charged $\bar{B} \to \bar{K}ll$ decays

$$R_K = \frac{\mathrm{Br}(\bar{B} \to \bar{K}\mu^+\mu^-)}{\mathrm{Br}(\bar{B} \to \bar{K}e^+e^-)}. \tag{5.2}$$

The measured value, $R_K^{\mathrm{LHCb}} = 0.745 \pm^{0.090}_{0.074} \pm 0.036$, in the dilepton invariant mass squared bin $1\,\mathrm{GeV}^2 \leq q^2 \leq 6\,\mathrm{GeV}^2$, amounts to a 2.6σ deviation from the SM prediction $R_K^{\mathrm{SM}} = 1.0003 \pm 0.0001$ [184].

The measurement of the anomalous muon magnetic moment also points to the possible existence of NP beyond the SM. The current measurement of the anomalous muon magnetic moment by the E821 experiment at BNL has been reported to show a significant deviation from the SM prediction $\Delta a_\mu = a_\mu^{\mathrm{exp}} - a_\mu^{\mathrm{SM}} = (2.8 \pm 0.9) \times 10^{-9}$ corresponding to a 3σ level deviation [185].

5.1 Explaining $\overline{B} \to D^{(*)}\tau\overline{\nu}$ excesses in Alternative Left-Right Symmetric Model

A number of NP scenarios explaining the semileptonic $b \to c$ transition have been proposed in the literature to explain these excesses [258–283]. NP scenarios explaining the $b \to c$ decay together with other direct or indirect collider searches for NP are particularly intriguing. To this end, we once again recall the results for the right-handed gauge boson W_R search and the di-leptoquark production search by the CMS Collaboration at the LHC. Interestingly, in some of these NP scenarios attempts were made to explain the discrepancies in the decays of B meson in an unified framework [228] or separately [277]. In chapter 4, we have already discussed how the excess signals at the LHC can be explained in the E_6 motivated Alternative Left-Right Symmetric Model (ALRSM) [198, 199, 219], which can also accommodate high scale leptogenesis.

In this section we study the flavor structure of ALRSM in detail to explore if this framework can explain the discrepancy of the $R_{D^{(*)}}$ data with the SM expectations [284]. To this end, a careful analysis of the constraints coming from the rare decays and the mixing of mesons can play a crucial role in determining the viability of ALRSM as a NP scenario. Therefore, we also discuss the leptonic decays $D_s^+ \to \tau^+\bar{\nu}$, $B^+ \to \tau^+\bar{\nu}$,

$D^+ \to \tau^+\bar{\nu}$ and $D^0 - \bar{D}^0$ mixing, which can constrain the semileptonic $b \to c$ transition in ALRSM.

5.1.1 The effective Hamiltonian for $\overline{B} \to D^{(*)}\tau\overline{\nu}$ decay

In presence of NP contributions, the SM effective Hamiltonian for the quark level transition $b \to cl\bar{\nu}_l$ can be augmented with a general set of effective operators in the form [266]

$$\mathcal{H}_{\text{eff}} = \frac{4G_F}{\sqrt{2}} V_{cb} \sum_{l=e,\mu,\tau} [(1+C^l_{V_L})O^l_{V_L} + C^l_{V_R}O^l_{V_R} + C^l_{S_L}O^l_{S_L} + C^l_{S_R}O^l_{S_R} + C^l_{T_L}O^l_{T_L}], \quad (5.3)$$

where G_F corresponds to the Fermi constant, V_{cb} corresponds to the relevant CKM matrix element and C^l_i (with $i = V_{L/R}, S_{L/R}, T_L$) corresponds to the Wilson coefficients associated with the effective vector, scalar and tensor NP interaction operators respectively. These new effective operators, generated by NP contributions at some energy scale higher than the electroweak scale, are defined as

$$\begin{aligned}
O^l_{V_L} &= (\bar{c}_L\gamma^\mu b_L)(\bar{l}_L\gamma_\mu\nu_{lL}), \\
O^l_{V_R} &= (\bar{c}_R\gamma^\mu b_R)(\bar{l}_L\gamma_\mu\nu_{lL}), \\
O^l_{S_L} &= (\bar{c}_R b_L)(\bar{l}_R\nu_{lL}), \\
O^l_{S_R} &= (\bar{c}_L b_R)(\bar{l}_R\nu_{lL}), \\
O^l_{T_L} &= (\bar{c}_R\sigma^{\mu\nu} b_L)(\bar{l}_R\sigma_{\mu\nu}\nu_{lL}),
\end{aligned} \quad (5.4)$$

where $\sigma^{\mu\nu} = (i/2)[\gamma^\mu, \gamma^\nu]$. The SM effective Hamiltonian can be recovered by setting $C^l_i = 0$. Note that we treat the neutrinos to be strictly left-handed and therefore, we neglect the tiny contributions coming from the right-handed neutrinos in $\mathcal{H}_{\text{eff}}$.

The numerical analysis of the transition $B \to D^{(*)}\tau\nu$, depends on the hadronic form factors which parametrize the vector, scalar and tensor current matrix elements. The $B \to D^{(*)}\tau\nu$ matrix elements corresponding to the effective operators depend on the momentum transfer between B and $D^{(*)}$ ($q^\mu = p^\mu_B - k^\mu$) and a relevant parametrization can be found in Refs. [266, 285]. However, we follow the parametrization of the form factors given in Refs. [261, 271, 286], which are more suitable for including the results of the heavy quark effective theory (HQET). For a more detailed account of the details of the form factors we refer the reader to the original work [284].

5.1.2 Analysis of the operators mediating $\overline{B} \to D^{(*)}\tau\overline{\nu}$ in ALRSM

In chapter 4, we have already discussed ALRSM in detail. Here we repeat the superpotential governing the interactions of the superfields in ALRSM for easy reference:

$$
\begin{aligned}
W &= \lambda_1 \left(uu^c N_E^c - du^c E^c - uh^c e + dh^c \nu_e\right) + \lambda_2 \left(ud^c E - dd^c \nu_E\right) \\
&+ \lambda_3 \left(hu^c e^c - hh^c n\right) + \lambda_4 hd^c N_L^c + \lambda_5 \left(ee^c \nu_E + EE^c n - Ee^c \nu_e - \nu_E N_E^c n\right) \\
&+ \lambda_6 \left(\nu_e N_L^c N_E^c - eE^c N_L^c\right). \qquad (5.5)
\end{aligned}
$$

We recall the following assignments of R-parity, baryon number (B) and lepton number (L) for the exotic fermions ensuring proton stability. The leptoquark h has the assignments $R = -1, B = \frac{1}{3}, L = 1$. The leptons ν_E, E, and n have the assignments $R = -1, B = L = 0$. For N^c we have two possible assignments. If N^c is assigned $R = -1$ and $B = L = 0$ (demanding $\lambda_4 = \lambda_6 = 0$ in Eq. (5.5)), then ν_e is exactly massless. Alternatively, if N^c is assigned $R = +1$, $B = 0$, $L = -1$, then ν_e can acquire a tiny mass via the seesaw mechanism.

In ALRSM there are two possible diagrams shown in Fig. 5.1, which can induce new operators contributing to the decay $\bar{B} \to D^{(*)}\tau\bar{\nu}$. The effective Lagrangian corresponding to these diagrams can be written as

$$
\mathcal{L}_{\text{eff}} = -\sum_{j,k=1}^{3} V_{2k} \left[\frac{\lambda^5_{33j}\lambda^{2*}_{3kj}}{m^2_{\tilde{E}^j}} \bar{c}_L b_R \; \bar{\tau}_R \nu_L + \frac{\lambda^1_{33j}\lambda^{1*}_{3kj}}{m^2_{\tilde{h}^{j*}}} \bar{c}_L (\tau^c)_R \; (\bar{\nu}^c)_R b_L\right], \qquad (5.6)
$$

where the superscripts correspond to the superpotential indices and the subscripts correspond to the generation indices. The mass of slepton $\tilde{E}^j$ (scalar leptoquark $\tilde{h}^{j*}$) is denoted by $m_{\tilde{E}}(m_{\tilde{h}})$ and V_{ij} is the ij-th element of the CKM matrix. The second term in the right hand side of Eq. (5.6) can be Fiertz transformed to obtain

$$
\bar{c}_L (\tau^c)_R \; (\bar{\nu}^c)_R b_L = \frac{1}{2} \bar{c}_L \gamma^\mu b_L \; \bar{\tau}_L \gamma_\mu \nu_L. \qquad (5.7)
$$

The Wilson coefficients, defined in Eq. (5.4), are given by

$$
\begin{aligned}
C^\tau_{S_L} &= \frac{1}{2\sqrt{2} G_F V_{cb}} \sum_{j,k=1}^{3} V_{2k} \frac{\lambda^5_{33j}\lambda^{2*}_{3kj}}{m^2_{\tilde{E}^j}}, \\
C^\tau_{V_L} &= \frac{1}{2\sqrt{2} G_F V_{cb}} \sum_{j,k=1}^{3} V_{2k} \frac{\lambda^1_{33j}\lambda^{1*}_{3kj}}{2\, m^2_{\tilde{h}^{j*}}}, \qquad (5.8)
\end{aligned}
$$

where we assume that the neutrinos of tau flavor give the dominant contribution.

In what follows, we further assume that, in addition to the SM contribution only one of the NP operators in Eq. (5.4) contributes dominantly. This simplifies the determination of the limits on the dominant Wilson coefficient from the experimental data on $R_{D^{(*)}}$.

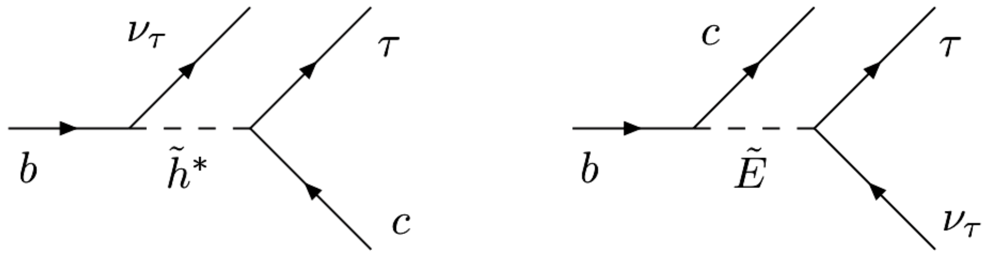

Figure 5.1: Feynman diagrams for the decays $\bar{B} \to D^{(*)}\tau\bar{\nu}$ induced by the exchange of scalar leptoquark ($\tilde{h}^*$) and slepton ($\tilde{E}$).

First, let us consider the case where $C^{\tau}_{S_L}$ gives the dominant contribution. This case is similar to 2HDM of type-II or type-III with minimal flavor violation, and can not explain both R_D and R_{D^*} data simultaneously [267, 276]. This can be seen from Fig. 5.2. However, when $C^{\tau}_{V_L}$ gives the dominant contribution, we find an allowed region which can explain both R_D and R_{D^*} data as can be seen from Fig. 5.3, which shows that $\left|C^{\tau}_{V_L}\right| > 0.08$ can explain the current experimental data. Note that the Wilson coefficients are computed at the electroweak scale by matching the NP theory with the effective theory, followed by the running of the Wilson coefficients down to the scale $\mathcal{O}(m_b)$, governed by the RGEs. The Wilson coefficient $C^{\tau}_{S_L}$ has a non-trivial running, while $C^{\tau}_{V_L}$ does not run under the RGEs. Since we are interested in the case where $C^{\tau}_{V_L}$ contribution is dominant, RG running can be neglected. Furthermore, since the theoretical uncertainties are sufficiently small compared to the experimental accuracy, we will only consider the central values of the theoretical predictions in our analysis.

5.1.3 Constraints from B, D decays and $D^0 - \overline{D}^0$ oscillations

Constraints from $B \to \tau\nu$

The decay $B^+ \to \tau^+\nu$ can occur in the SM via s-channel annihilation to a W boson. In ALRSM, the exchange of the scalar leptoquark $\tilde{h}^{j*}$ can induce the additional diagrams

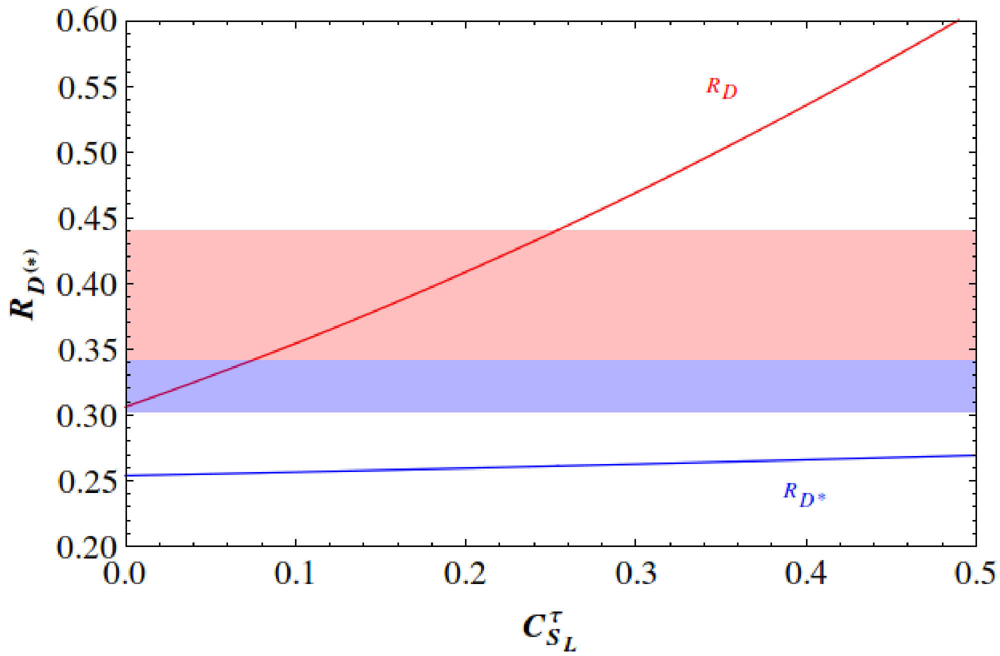

Figure 5.2: A plot showing the dependence of the observables $R_{D^{(*)}}$ on $C^{\tau}_{S_L}$: red (blue) curve corresponds to R_D (R_{D^*}) corresponding to $C^{\tau}_{S_L}$, and the horizontal red (blue) band corresponds to the experimentally allowed 1σ range. No common region exists for $C^{\tau}_{S_L}$ which can simultaneously explain both R_D and R_{D^*} data.

shown in Fig. 5.4. When the scalar leptoquark mass is much heavier compared to the mass scale of the B meson, we can integrate out the heavy leptoquark degrees of freedom to generate the effective four-fermion interaction $\sim \bar{q}_L(\tau^c)_R\ (\bar{\nu}^c)_R b_L$. The relevant effective Hamiltonian is given by

$$\mathcal{H}^{\text{NP}}_{\text{eff}}(b\bar{q} \to \tau\bar{\nu}) = \frac{4G_F}{\sqrt{2}} V_{qb}\, C^{qb}_{V_L}(\bar{q}_L\gamma^{\mu}b_L)(\bar{\tau}_L\gamma_{\mu}\nu_L), \tag{5.9}$$

where V_{qb} is the relevant CKM matrix element. The Wilson coefficient $C^{ub}_{V_L}$ can be expressed in terms of the couplings λ's as

$$C^{ub}_{V_L} \;=\; \frac{1}{2\sqrt{2}G_F V_{ub}} \sum_{j,k=1}^{3} V_{1k} \frac{\lambda^{1}_{33j}\lambda^{1*}_{3kj}}{2\, m^2_{\tilde{h}^{j*}}}. \tag{5.10}$$

For simplicity, we will neglect the subleading $\mathcal{O}(\lambda)$ terms and retain only the leading CKM element V_{11} in further analysis. The decay $B \to \tau\nu$ is the only experimentally measured purely leptonic mode of charged $B^{\pm}$ and the current experimental value for the branching ratio of $B \to \tau\nu$ is $(1.14 \pm 0.27) \times 10^{-4}$ [11]. The SM decay rate is modified in presence of NP effects as

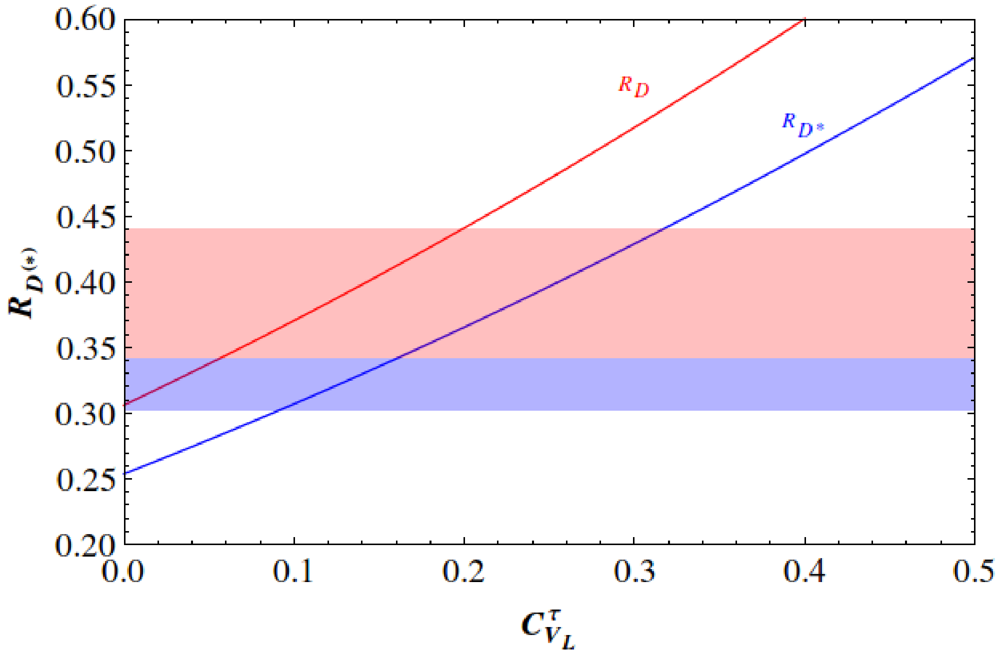

Figure 5.3: A plot showing the dependence of the observables $R_{D^{(*)}}$ on $C^{\tau}_{V_L}$: red (blue) curve corresponds to R_D (R_{D^*}) corresponding to $C^{\tau}_{V_L}$, and the horizontal red (blue) band corresponds to the experimentally allowed 1σ range. $C^{\tau}_{V_L}$ can simultaneously explain both R_D and R_{D^*} data.

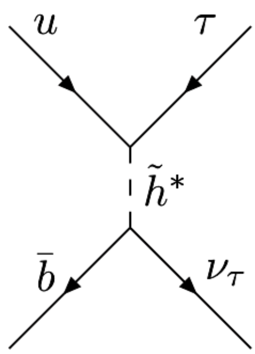

Figure 5.4: Feynman diagram for the decay $B \to \tau\nu$ induced by the exchange of the scalar leptoquark $\tilde{h}^{j*}$.

$$\frac{d\Gamma}{dq^2}(B \to \tau\nu) = \frac{G_F^2|V_{ub}|^2}{8\pi} m_B f_B^2 m_\tau^2 \times \left(1 - \frac{m_\tau^2}{m_B^2}\right)^2 |1 + C^{ub}_{V_L}|^2, \quad (5.11)$$

where m_B is the mass of $B^{\pm}$. The decay constant f_B parametrizes the matrix element of the corresponding current as

$$\langle 0|\bar{b}_L\gamma^\mu q_L|B_q(p_B)\rangle = p_B^\mu f_B, \quad (5.12)$$

where p_B is the four-momentum of the $B^{\pm}$ meson.

For the CKM matrix elements, the lifetimes, particle masses and decay constants f_B, f_{D_s}, f_{D^+} we use the current PDG values [11]. For simplicity, we assume the couplings to be real in the rest of this chapter. The relevant constraints on the product of the couplings $\lambda_{33j}\lambda_{31j}$ can be numerically expressed as

$$\lambda_{33j}\lambda_{31j} \leq 0.04 \left(\frac{m_{\tilde{h}^{j*}}}{1000 \text{ GeV}}\right)^2. \tag{5.13}$$

Constraints from $D_s^+ \to \tau\nu$ and $D^+ \to \tau\nu$

The measured branching ratios of the purely leptonic decays $D_s^+ \to \tau\nu$ and $D^+ \to \tau\nu$ can give constraints on the couplings $(\lambda_{32j})^2$ and $\lambda_{32j}\lambda_{31j}$, respectively, in ALRSM. The Feynman diagrams inducing the decays $D_s^+ \to \tau\nu$ and $D^+ \to \tau\nu$ in ALRSM are shown in Fig. 5.5. Integrating out the heavy degrees of freedom we obtain the following non-standard effective Hamiltonian

$$\mathcal{H}_{\text{eff}}^{\text{NP}}(c\bar{q} \to \tau\bar{\nu}) = \frac{4G_F}{\sqrt{2}} V_{cq}\, C_{V_L}^{cq} (\bar{q}_L \gamma^\mu c_L)(\bar{\nu}_L \gamma_\mu \tau_L) \tag{5.14}$$

where $q = s, d$ for D_s^+ and D^+, respectively. The Wilson coefficient $C_{V_L}^{cq}$ parameterizing the NP effects in ALRSM is given by

$$C_{V_L}^{cq} \;=\; \frac{1}{2\sqrt{2}G_F V_{cq}} \sum_{j,k=1}^{3} V_{kq} \frac{\lambda_{32j}^1 \lambda_{3kj}^{1*}}{2\, m_{\tilde{h}^{j*}}^2}. \tag{5.15}$$

We keep only the leading term V_{cs} for D_s^+ decay and V_{ud} for D^+ decay, respectively

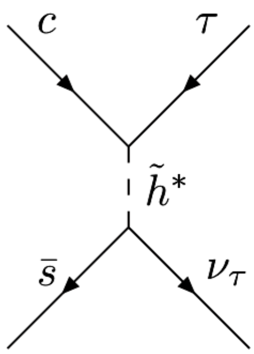

Figure 5.5: Feynman diagram for the decay $D_s^+ \to \tau\nu$ induced by scalar leptoquarks. The diagram for the decay $D^+ \to \tau\nu$ can be obtained by replacing the s quark by a d quark.

and neglect the next leading order Cabibbo suppressed $\mathcal{O}(\lambda)$ terms. In ALRSM the scalar leptoquark induced contribution modifies the SM decay rate as [287, 288]

$$\frac{d\Gamma}{dq^2}(D_q^+ \to \tau\nu) = \frac{G_F^2|V_{cq}|^2}{8\pi} m_{D_q} f_{D_q}^2 m_\tau^2 \times \left(1 - \frac{m_\tau^2}{m_{D_q}^2}\right)^2 |1 + C_{V_L}^{cq}|^2, \quad (5.16)$$

where m_{D_q} is the mass of charm mesons D_s^+ and D^+ for $q = s, d$, respectively; V_{cq} is the corresponding CKM element; and f_{D_q} is the decay constant.

Now, assuming that only one combination of the product of scalar leptoquark couplings is nonzero at a time, we obtain upper bounds on $(\lambda_{32j}^1)^2$ and $\lambda_{32j}^1\lambda_{31j}^{1*}$, given by

$$\begin{aligned} \lambda_{32j}^2 &\leq 0.85 \left(\frac{m_{\tilde{h}^{j*}}}{1000 \text{ GeV}}\right)^2, \\ \lambda_{32j}\lambda_{31j} &\leq 3.12 \left(\frac{m_{\tilde{h}^{j*}}}{1000 \text{ GeV}}\right)^2. \end{aligned} \quad (5.17)$$

Constraints from $D^0 - \bar{D}^0$ mixing

The $D^0 - \bar{D}^0$ mixing is described by a $\Delta C = 2$ effective Hamiltonian which induces off-diagonal terms in the mass matrix for neutral D meson pair and is often parametrized in terms of the experimental observables

$$x_D \equiv \frac{\Delta M_D}{\Gamma_D} \quad \text{and} \quad y_D \equiv \frac{\Delta\Gamma_D}{2\Gamma_D}. \quad (5.18)$$

Here ΔM_D and $\Delta\Gamma_D$ corresponds to the mass and width splittings between the mass eigenstates of the $D^0 - \bar{D}^0$ systems respectively and Γ_D is the average width. The observables x_D and y_D can be expressed in terms of the mixing matrix as

$$\begin{aligned} x_D &= \frac{1}{2M_D\Gamma_D}\text{Re}\left[2\langle\bar{D}^0|H^{|\Delta C|=2}|D^0\rangle + \langle\bar{D}^0|i\int d^4x\, T\{\mathcal{H}_w^{|\Delta C|=1}(x)\mathcal{H}_w^{|\Delta C|=1}(0)\}|D^0\rangle\right], \\ y_D &= \frac{1}{2M_D\Gamma_D}\text{Im}\langle\bar{D}^0|i\int d^4x\, T\{\mathcal{H}_w^{|\Delta C|=1}(x)\mathcal{H}_w^{|\Delta C|=1}(0)\}|D^0\rangle, \end{aligned} \quad (5.19)$$

where T denotes the time ordered product and $\mathcal{H}_w^{|\Delta C|=1}(x)$ is the Hamiltonian describing the $|\Delta C| = 1$ transitions. The current measured values of x_D and y_D reported by the HFAG Collaboration are [289]

$$\begin{aligned} x_D &= 0.49^{+0.14}_{-0.15} \times 10^{-2}, \\ y_D &= (0.61 \pm 0.08) \times 10^{-2}, \end{aligned} \quad (5.20)$$

For a review of $D^0 - \bar{D}^0$ mixing in the context of several NP models see, for example,

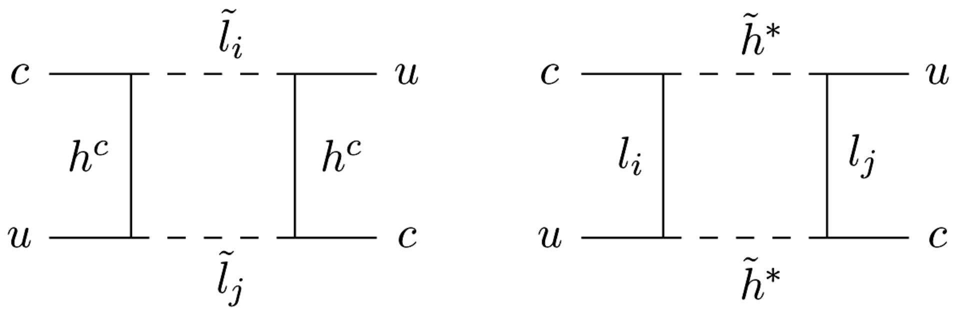

Figure 5.6: Feynman diagrams inducing $D^0 - \bar{D}^0$ mixing in ALRSM.

Ref. [290]. The Feynman diagrams contributing to $D^0 - \bar{D}^0$ mixing in the ALRSM are shown in Fig. 5.6. The constraints obtained from $D^0 - \bar{D}^0$ mixing are tighter than those obtained from the measured branching ratio (BR) of the decay process $D^+ \to \tau\nu$. These diagrams are quite similar to the diagrams in the case of R-parity violating SUSY models [290, 291]. The effective Hamiltonian is given by

$$\mathcal{H}_{\text{eff}} = \frac{1}{128\pi^2}(\lambda_{32j}\lambda_{31j})^2 \left(\frac{1}{m_{\tilde{\tau}}^2} + \frac{1}{m_{\tilde{h}^{j*}}^2}\right)(\bar{c}_L\gamma^\mu u_L)(\bar{c}_L\gamma_\mu u_L). \tag{5.21}$$

Taking $m_{\tilde{h}^{j*}} \simeq m_{\tilde{\tau}}$, we obtain the constraints on the couplings, given by [290, 291]

$$\lambda_{32j}\lambda_{31j} \leq 0.17\sqrt{x_D^{\text{expt}}}\left(\frac{m_{\tilde{h}^{j*}}}{1000\text{ GeV}}\right). \tag{5.22}$$

5.1.4 λ_{33j}-λ_{32j} parameter space explaining both R_{D^*} and R_D data

In Fig. 5.7, we plot the parameter space of the couplings λ_{33j} and λ_{32j} (for $m_{\tilde{h}^j*} = 1000\,\text{GeV}$) that can explain both R_D and R_{D^*} data. We use the decay $D_s^+ \to \tau^+\bar{\nu}$, to constrain the upper limit of the coupling λ_{32j}, the $D^0 - \bar{D}^0$ mixing to constrain the upper limit of the product of couplings $\lambda_{32j}\lambda_{31j}$, and the decay $B^+ \to \tau^+\bar{\nu}$ to constrain the upper limit of $\lambda_{33j}\lambda_{31j}$. Note that, the latter two constraints have λ_{31j} as a common free parameter. The blue shaded rectangles in Fig. 5.7 correspond to the allowed regions of the λ_{33j}-λ_{32j} parameter space from the above constraints for different values of λ_{31j} marked on top of the corresponding allowed upper boundary shown in dashed lines. The deep blue band corresponds to the allowed parameter space of λ_{33j}-λ_{32j} explaining the $R(D)$ data and the orange band corresponds to the allowed parameter space of λ_{33j}-λ_{32j} explaining both R_D and R_{D^*} data simultaneously.

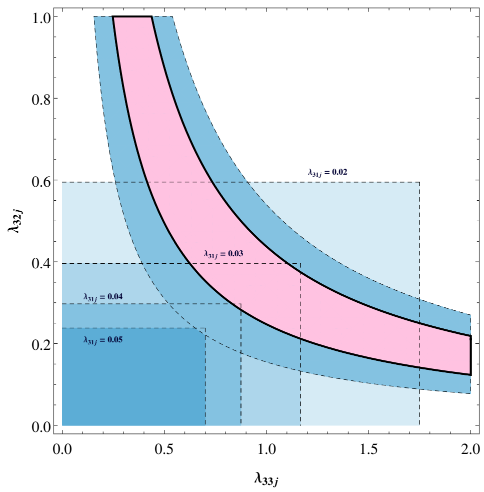

Figure 5.7: The parameter space of λ_{33j}-λ_{32j} explaining the experimental data on $\mathcal{R}(D^{(*)})$ for $m_{\tilde{h}^{j*}} = 1000\,\mathrm{GeV}$. The deep blue band corresponds to the allowed parameter space from R_D data, and the orange band shows the allowed parameter space explaining both R_{D^*} and R_D data simultaneously. The light blue shaded rectangles correspond to λ_{33j}-λ_{32j} parameter space for different values of λ_{31j} (marked on top of the allowed upper boundary shown in dashed lines) allowed by the current measurement of the decay rates of $B \to \tau\nu$, $D_s \to \tau\nu$, $D^+ \to \tau\nu$, and $D - \bar{D}$ mixing.

Note that the list of constraints used in this parameter space analysis is far from exhaustive and many other leptonic and semileptonic decay modes can also give independent constrains. For example, the decay process $\tau^+ \to \pi^+\nu$ can give a constraint on λ_{31j}, which we find to be consistent with the values used for the parameter space analysis here. Another example would be the semileptonic decay $t \to b\tau\nu$, which can give a constraint on λ_{33j} which is again consistent with the values used in the above parameter space analysis. Interestingly, the effective NP operators in ALRSM, which explain the R_{D^*} and R_D data, can also induce processes like $b \to s\nu\bar{\nu}$ [292, 293], which can be probed at future experiments.

5.2 Explaining $R_{D^{(*)}}$, R_K and $(g-2)_\mu$ anomalies in the Neutral Left-Right Symmetric Model

In this section, we discuss possible explanation of $R_{D^{(*)}}$, R_K and $(g-2)_\mu$ anomalies within the framework of one of the low energy subgroups of E_6 discussed in section

4.1.3 [294]. In this subgroup the residual $SU(2)_R$ does not contribute to the electric charge [247] and hence we will call this model the "Neutral" Left-Right Symmetric Model (NLRSM). In NLRSM it is possible to enhance both $\bar{B} \to D\tau\bar{\nu}$ and $\bar{B} \to D^{(*)}\tau\bar{\nu}$ via the exchange of scalar leptoquarks in a similar manner as ALRSM. The R_K anomaly can also be explained in NLRSM through one loop diagrams induced by scalar leptoquarks. Furthermore, NLRSM has the feature of explaining the anomalous muon magnetic moment without utilizing a nonzero right handed coupling of leptoquarks.

We have already discussed NLRSM in detail in section 4.1.3. Here we rewrite the superpotential for easy reference [1]

$$
\begin{aligned}
W \quad &= \quad \lambda^1 \left(\nu_e N_L^c N_E^c + eE^c N_L^c + \nu_E N_E^c n + EE^c n\right) \\
&+ \quad \lambda^2 \left(d^c N_L^c h + hh^c n\right) + \lambda^3 u^c e^c h + \lambda^4 \left(uu^c N_E^c + u^c dE^c\right) \\
&+ \quad \lambda^5 \left(\nu_e e^c E + ee^c \nu_E\right) + \lambda^6 \left(ud^c E + dd^c \nu_E + uh^c e + dh^c \nu_e\right). \qquad (5.23)
\end{aligned}
$$

We recall that the leptoquark h has the baryon and lepton number assignments $B = 1/3$ and $L = 1$, while the exotic fields ν_E, E and n have the baryon and lepton number assignments $B = L = 0$ and N^c has $B = 0, L = -1$. We also recall that the gauge couplings of W_N and Z_N to the fermions can also induce FCNC processes like $B^0 - \bar{B}^0, K^0 - \bar{K}^0$ mixings and lepton flavor violating (LFV) decays such as $h \to \tau\mu$, $\mu \to e\gamma$. In what follows we assume that the dominant FCNC and LFV contributions come from scalar leptoquark induced processes. Note that, the Alternative Left-Right Symmetric Model [219] and variants of $U(1)_N$ model [257] have leptoquark couplings somewhat similar to this model, and the following analysis can be adopted for those cases in a straightforward manner.

5.2.1 Explaining $R_{D^{(*)}}$ anomalies in NLRSM

Similar to the ALRSM case, in NLRSM also the scalar leptoquark ($\tilde{h}^*$) and slepton ($\tilde{E}$) can mediate the semileptonic decays $\bar{B} \to D^{(*)}\tau\bar{\nu}$ at the tree level. The effective

[1] Note that we have made the superpotential coupling indices as superscripts for convenience.

Lagrangian in NLRSM is given by

$$\mathcal{L}_{\text{eff}} = \sum_{i,k=1}^{3} V_{2i} \left[\frac{\lambda^5_{33k}\lambda^{6*}_{i3k}}{m^2_{\tilde{E}^k}} \bar{c}_L b_R \, \bar{\tau}_R \nu_L + \frac{\lambda^6_{33k}\lambda^{6*}_{i3k}}{m^2_{\tilde{h}^{k*}}} \bar{c}_L (\tau^c)_R \, (\bar{\nu}^c)_R b_L \right], \qquad (5.24)$$

where the generation indices are explicitly written as subscripts. Here $m_{\tilde{h}}$ and $m_{\tilde{E}}$ are the masses of scalar leptoquark $\tilde{h}^{k*}$ and slepton $\tilde{E}^k$, respectively, and V_{ij} is the ij-th element of the CKM matrix. The Wilson coefficients are given by

$$\begin{aligned} C^\tau_{S_L} &= -\frac{1}{2\sqrt{2}G_F V_{cb}} \sum_{i,k=1}^{3} V_{2i} \frac{\lambda^5_{33k}\lambda^{6*}_{i3k}}{m^2_{\tilde{E}^k}} \,, \\ C^\tau_{V_L} &= -\frac{1}{2\sqrt{2}G_F V_{cb}} \sum_{i,k=1}^{3} V_{2i} \frac{\lambda^6_{33k}\lambda^{6*}_{i3k}}{2\, m^2_{\tilde{h}^{k*}}}. \end{aligned} \qquad (5.25)$$

Closely following the ALRSM case discussed in the previous section, the leptonic decay modes $B \to \tau\nu$, $D_s^+ \to \tau\nu$, $D^+ \to \tau\nu$ and $D^0 - \bar{D}^0$ mixing can be used to derive constraints on the couplings. Assuming the couplings to be real, we can use the decay process $B \to \tau\nu$ to obtain constraint on the product of couplings $\lambda^6_{33k}\lambda^{6*}_{13k}$

$$-0.04 \left(\frac{m_{\tilde{h}^{k*}}}{1000\text{ GeV}}\right)^2 \le \lambda^6_{33k}\lambda^6_{13k} \le 0.03 \left(\frac{m_{\tilde{h}^{k*}}}{1000\text{ GeV}}\right)^2. \qquad (5.26)$$

From the decay $D_s^+ \to \tau\nu$ we obtain the constraint

$$(\lambda^6_{23k})^2 \le 1.9 \left(\frac{m_{\tilde{h}^{k*}}}{1000\text{ GeV}}\right)^2. \qquad (5.27)$$

The $D^0 - \bar{D}^0$ mixing gives the constraint on the product of couplings $\lambda^6_{23k}\lambda^6_{13k}$

$$-0.012 \left(\frac{m_{\tilde{h}^{k*}}}{1000\text{ GeV}}\right) \le \lambda^6_{23k}\lambda^6_{13k} \le 0.012 \left(\frac{m_{\tilde{h}^{k*}}}{1000\text{ GeV}}\right). \qquad (5.28)$$

Fig. 5.8 shows the parameter space of the couplings λ^6_{33k} and λ^6_{23k} (for $m_{\tilde{h}^k *} = 750\,\text{GeV}$) compatible with both R_D and R_{D^*} data. The shaded (light gray) rectangles with dashed boundaries correspond to the allowed λ^6_{33k}-λ^6_{23k} parameter space from the decays $B \to \tau\nu$, $D_s^+ \to \tau\nu$ and $D^0 - \bar{D}^0$ mixing for different values of λ^6_{13k}. The (deep) blue bands shows the $(1\sigma)2\sigma$ allowed band compatible with the R_D data and the (deep) pink bands shows the allowed band compatible with both R_D and R_{D^*} data simultaneously.

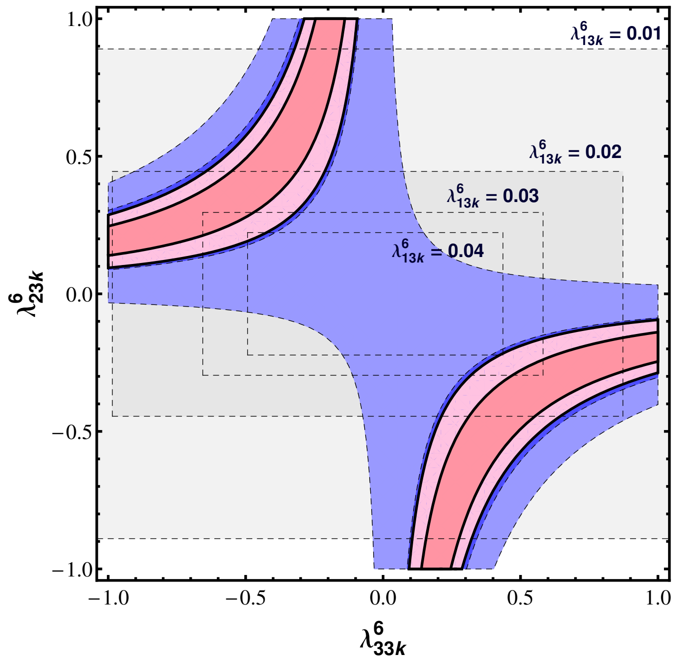

Figure 5.8: $\lambda^6_{33k} - \lambda^6_{23k}$ parameter space compatible with $R_{D^{(*)}}$ data and constraints from $B \to \tau\nu$, $D_s^+ \to \tau\nu$ and $D^0 - \bar{D}^0$ mixing.

5.2.2 Explaining R_K anomaly and constraints from $B_s^0 - \overline{B}_s^0$ mixing

The lepton non-universality in the ratio R_K has been discussed in Refs. [295, 296] in a model independent way. A good fit to the experimental data is obtained when [295, 296]

$$\begin{aligned} -1.5 \lesssim C^{\mu}_{LL} \lesssim -0.7\,, \\ -1.9 \lesssim C^{\mu}_{LL} - C^{\mu}_{LR} \lesssim 0. \end{aligned} \tag{5.29}$$

In Ref. [297] it was first pointed out that one-loop box diagrams, induced by scalar leptoquarks can explain the R_K data. In NLRSM, the transition $b \to s\ell\ell$ can occur at the one-loop level via the exchange of scalar and fermionic leptoquarks [2] as shown in Fig. 5.9. The γ- and Z-penguin diagrams give a vanishing contribution.

In the limit $m^2_{\tilde{h},h} \gg m^2_{W,t}$, the contribution to C^{μ}_{LL} from box diagrams induced by

[2] Note that the charginos and neutralinos can also induce new contributions. However, they give a subdominant contribution compared to the leptoquarks.

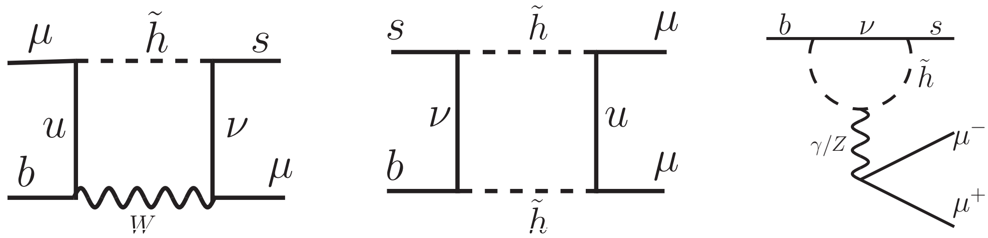

Figure 5.9: Representative diagrams for $b \to s\ell\ell$ transition.

the scalar and fermionic leptoquark is given by

$$\begin{aligned} C_{LL}^{\mu} &= \frac{\lambda^6_{32k}\lambda^{6*}_{32k}}{8\pi\alpha_e}\left(\frac{m_t}{m_{\tilde{h}_j}}\right)^2 - \frac{\lambda^6_{3jk}\lambda^{6*}_{2jl}\lambda^6_{i2k}\lambda^{6*}_{i2l}}{32\sqrt{2}\,G_F\,V_{tb}V^*_{ts}\pi\alpha_e m^2_{\tilde{h}}} \\ &- \frac{\lambda^6_{3jk}\lambda^{6*}_{2jl}\lambda^6_{i2k}\lambda^{6*}_{i2l}}{32\sqrt{2}\,G_F\,V_{tb}V^*_{ts}\pi\alpha_e m^2_{\tilde{h}}}\, g\left(\frac{m^2_{\tilde{u}_i}}{m^2_{\tilde{h}}}, 1, \frac{m^2_{\tilde{\nu}_j}}{m^2_{\tilde{h}}}\right), \end{aligned} \tag{5.30}$$

where the loop function $g(x,y,z)$ is defined as

$$g(x,y,z) = \frac{x^2 \log x}{(x-1)(x-y)(x-z)} + (\text{cycl. perm.}).$$

We note that C^{μ}_{LL} depends on the product of couplings $\lambda^6_{3jk}\lambda^{6*}_{2jk}$, and $\lambda^{6*}_{i2k}\lambda^6_{i2l}$. The latter can be constrained from the measurement of the decay rate for $Z \to \mu\bar{\mu}$. For a TeV scale leptoquark, the couplings can be as large as $\sim \mathcal{O}(1)$ [297]. The product of couplings $\lambda^6_{3jk}\lambda^{6*}_{2jk}$ also appears in $B_s - \bar{B}_s$ mixing amplitude. Thus the experimental measurement of $B_s - \bar{B}_s$ mixing amplitude can be used to obtain constraints on $\lambda^6_{3jk}\lambda^{6*}_{2jk}$. The constraints on $\lambda^6_{3jk}\lambda^{6*}_{2jk}$ from $B_s - \bar{B}_s$ mixing (using the latest UTfit Collaboration values) in NLRSM turns out to be consistent with the value required to explain the R_K data [294]. In NLRSM, the leptoquark induced new contribution to $C_{7\gamma}$ also turns out to be too small to have any interesting effects.

5.2.3 Explaining anomalous muon magnetic moment

In the SM the muon anomalous magnetic moment suffers from a chiral suppression due to a small muon mass, $a_\mu \sim m^2_\mu/m^2_W$. In NLRSM, leptoquark can induce a new contribution to the anomalous magnetic moment of the muon. However, such a contribution is not sufficient to explain the experimental deviation. A nonzero right handed coupling of the leptoquark can be utilized to enhance the leptoquark contribution significantly [297]. In NLRSM, one can explain the experimental data through a dominant contribution from λ^5 terms in Eq. (5.23), without invoking a nonzero right handed coupling of the leptoquark. The new contribution to the muon anomalous magnetic moment coming from the λ^5_{ijk} terms in Eq. (5.23) is given by

$$\begin{aligned}\delta a_\mu(\lambda^5) \quad = \quad & \frac{m_\mu^2}{16\pi^2}\Big[|\lambda_{i2k}|^2 F(e_k, \tilde{\nu}_{Ei}) - |\lambda_{i2k}|^2 F(\tilde{e}_k, \nu_{Ei}) \\ & +|\lambda_{ij2}|^2 F(e_j, \tilde{\nu}_{Ei}) - |\lambda_{ij2}|^2 F(\tilde{e}_j, \nu_{Ei}) \\ & +|\lambda_{ij2}|^2 F(E_j, \tilde{\nu}_{ei}) - |\lambda_{ij2}|^2 F(\tilde{E}_j, \nu_{ei})\Big] , \end{aligned} \tag{5.31}$$

where $F(a, b)$ is given by

$$F(a,b) = \int_0^1 dx \frac{x^2 - x^3}{m_\mu^2 x^2 + (m_a^2 - m_\mu^2)x + m_b^2(1-x)}. \tag{5.32}$$

The current experimental data can be explained with less than order unity values of the couplings for a hierarchy between charged and neutral sleptons, for example taking $m_{\tilde{E},\tilde{e}} \sim 700$ GeV and $m_{\tilde{\nu}_E,\tilde{\nu}_e} \sim 250$ GeV.

5.3 Summary of the chapter

In conclusion, we have discussed the low energy subgroups of E_6 in the context of current flavor anomalies. The current experimental data for both R_D and R_{D^*} can be simultaneously explained in ALRSM and NLRSM, while satisfying the constraints from the leptonic decays $D_s^+ \to \tau^+\bar{\nu}$, $B^+ \to \tau^+\bar{\nu}$, $D^+ \to \tau^+\bar{\nu}$ and $D^0 - \bar{D}^0$ mixing. We have also discussed how the B-decay anomalies in $R_{D^{(*)}}$ and R_K data can be addressed together with the anomalous muon magnetic moment in NLRSM.

Chapter 6

Addressing the LHC excesses, baryogenesis and neutrino masses in E_6 motivated $U(1)_N$ model

One of the simplest and well motivated extensions of the Standard Model (SM) gauge group $SU(3)_c \times SU(2)_L \times U(1)_Y$ is the $U(1)_N$ extension of the supersymmetric SM motivated by the superstring theory inspired E_6 model. This model, realizing the implementation of supersymmetry and the extension of the SM gauge group to a larger symmetry group, offers an attractive possibility of TeV-scale physics beyond the SM, testable at the LHC. On the other hand, small neutrino masses explaining the solar and atmospheric neutrino oscillations data and a mechanism for generating the observed baryon asymmetry of the universe can be naturally accommodated in this model.

The presence of new exotic fields in addition to the SM fields and new interactions involving the new gauge boson Z' provides a framework to explore the associated rich phenomenology which can be tested at the LHC. To this end, we must mention the CMS excesses in the searches for the right-handed gauge boson W_R at a center of mass energy of $\sqrt{s} = 8\,\mathrm{TeV}$ and $19.7\mathrm{fb}^{-1}$ of integrated luminosity [166] and di-leptoquark production at a center of mass energy of $\sqrt{s} = 8\,\mathrm{TeV}$ and $19.6\mathrm{fb}^{-1}$ of integrated luminosity [167].

In this chapter, we discuss the E_6 motivated $U(1)_N$ extension of the supersymmetric SM gauge group to explain the excess CMS events, neutrino masses, and the baryon asymmetry of the universe via baryogenesis (leptogenesis) [257]. To this end, we impose discrete symmetries to the above gauge group which ensures proton stability, forbids the tree level flavor changing neutral current (FCNC) processes and dictates the form of the neutrino mass matrix in the variants of the $U(1)_N$ model. We find that all the variants can explain the excess CMS events via the exotic slepton decay, while for a standard choice of the discrete symmetry some of them have the feature of allowing high scale baryogenesis (via leptogenesis) via the decay of a heavy Majorana baryon (lepton) and some are not consistent with such mechanisms. We have pointed out the possibility of the three body decay induced soft baryogenesis mechanism which can induce baryon number violating neutron-antineutron ($n - \bar{n}$) oscillations [46] in one such variant. On the other hand, we have also explored a new discrete symmetry for these variants which has the feature of ensuring proton stability and forbidding tree level FCNC processes while allowing for the possibilities of high scale leptogenesis through the decay of a heavy Majorana lepton. We also comment on the more recent ATLAS and CMS diboson and dijet excesses in the context of $U(1)_N$ model and other alternatives that can address these excesses. In light of the hints from short-baseline neutrino experiments [298–306] for the existence of one or more light sterile neutrinos which can interact only via mixing with the active neutrinos, we have explored the neutrino mass matrix of the $U(1)_N$ model variants which naturally contain three active and two sterile neutrinos [307, 308]. These neutrinos acquire masses through their mixing with extra neutral fermions giving rise to interesting textures for neutrino masses governed by the field assignments and the imposed discrete symmetries.

6.1 $U(1)_N$ extension of supersymmetric Standard Model

In the heterotic superstring theory with $E_8 \times E_8'$ gauge group the compactification on a Calabi-Yau manifold leads to the breaking of E_8 to $SU(3) \times E_6$ [232, 233]. The flux breaking of E_6 can result in different low-energy effective subgroups of rank-5 and rank-6. One such possibility is realized in the $U(1)_N$ model. The rank-6 group E_6 can be broken down to low-energy gauge groups of rank-5 or rank-6 with one or two additional $U(1)$ in addition to the SM gauge group. For example E_6 contains the subgroup $SO(10) \times U(1)_\psi$ while $SO(10)$ contains the subgroup $SU(5) \times U(1)_\chi$. In fact some mechanisms can break the E_6 group directly into the rank-6 gauge scheme

$$E_6 \to SU(3)_C \times SU(2)_L \times U(1)_Y \times U(1)_\psi \times U(1)_\chi. \tag{6.1}$$

These rank - 6 schemes can further be reduced to rank - 5 gauge group with only one additional $U(1)$ which is a linear combination of $U(1)_\psi$ and $U(1)_\chi$

$$Q_\alpha = Q_\psi \cos\alpha + Q_\chi \sin\alpha, \tag{6.2}$$

where

$$Q_\psi = \sqrt{\frac{3}{2}}(Y_L - Y_R), \;\; Q_\chi = \sqrt{\frac{1}{10}}(5T_{3R} - 3Y). \tag{6.3}$$

For a particular choice of $\tan\alpha = \sqrt{\frac{1}{15}}$ the right-handed counterpart of the neutrino superfield (N^c) can transform trivially under the gauge group and the corresponding $U(1)$ gauge extension to the SM is denoted as $U(1)_N$. The trivial transformation of N^c can allow a large Majorana mass of N^c in the $U(1)_N$ model thus providing an attractive possibility of baryogenesis (via leptogenesis).

Let us consider one of the maximal subgroups of E_6 given by $SU(3)_C \times SU(3)_L \times SU(3)_R$. The fundamental 27 representation of E_6 under this subgroup is given by

$$27 = (3, 3, 1) + (3^*, 1, 3^*) + (1, 3^*, 3) \tag{6.4}$$

The matter superfields of the first family are assigned as:

$$\begin{pmatrix} u \\ d \\ h \end{pmatrix} + \begin{pmatrix} u^c & d^c & h^c \end{pmatrix} + \begin{pmatrix} E^c & \nu & \nu_E \\ N_E^c & e & E \\ e^c & N^c & n \end{pmatrix}, \tag{6.5}$$

where $SU(3)_L$ operates vertically and $SU(3)_R$ operates horizontally. Now if the $SU(3)_L$ gets broken to $SU(2)_L \times U(1)_{Y_L}$ and the $SU(3)_R$ gets broken to $U(1)_{T_{3R}} \times U(1)_{Y_R}$ via the flux mechanism then the resulting gauge symmetry is given by $SU(3)_C \times SU(2)_L \times U(1)_Y \times U(1)_N$, where the $U(1)_N$ charge assignment is given by

$$Q_N = \sqrt{\frac{1}{40}}(6Y_L + T_{3R} - 9Y_R), \tag{6.6}$$

and the electric charge is given by

$$Q = T_{3L} + Y, \;\; Y = Y_L + T_{3R} + Y_R. \tag{6.7}$$

	$SU(3)_c$	$SU(2)_L$	Y_L	T_{3R}	Y_R	$U(1)_Y$	$U(1)_N$
Q	3	2	$\frac{1}{6}$	0	0	$\frac{1}{6}$	$\frac{1}{\sqrt{40}}$
u^c	3^*	1	0	$-\frac{1}{2}$	$-\frac{1}{6}$	$-\frac{2}{3}$	$\frac{1}{\sqrt{40}}$
d^c	3^*	1	0	$\frac{1}{2}$	$-\frac{1}{6}$	$\frac{1}{3}$	$\frac{2}{\sqrt{40}}$
L	1	2	$-\frac{1}{6}$	0	$-\frac{1}{3}$	$-\frac{1}{2}$	$\frac{2}{\sqrt{40}}$
e^c	1	1	$\frac{1}{3}$	$\frac{1}{2}$	$\frac{1}{6}$	1	$\frac{1}{\sqrt{40}}$
h	3	1	$-\frac{1}{3}$	0	0	$-\frac{1}{3}$	$-\frac{2}{\sqrt{40}}$
h^c	3^*	1	0	0	$\frac{1}{3}$	$\frac{1}{3}$	$-\frac{3}{\sqrt{40}}$
X	1	2	$-\frac{1}{6}$	$-\frac{1}{2}$	$\frac{1}{6}$	$-\frac{1}{2}$	$-\frac{3}{\sqrt{40}}$
X^c	1	2	$-\frac{1}{6}$	$\frac{1}{2}$	$\frac{1}{6}$	$\frac{1}{2}$	$-\frac{2}{\sqrt{40}}$
n	1	1	$\frac{1}{3}$	0	$-\frac{1}{3}$	0	$\frac{5}{\sqrt{40}}$
N^c	1	1	$\frac{1}{3}$	$-\frac{1}{2}$	$\frac{1}{6}$	0	0

Table 6.1: Transformations of the various superfields of the 27 representation under $SU(3)_C \times SU(2)_L \times U(1)_Y \times U(1)_N$.

The transformations of the various superfields of the fundamental 27 representation of E_6 under $SU(3)_C \times SU(2)_L \times U(1)_Y \times U(1)_N$ and the corresponding assignments of Y_L, T_{3R} and Y_R are listed in Table 6.1, where $Q = (u, d)$, $L = (\nu_e, e)$, $X = (\nu_E, E)$ and $X^c = (E^c, N_E^c)$.

6.2 Discrete symmetries and variants of $U(1)_N$ model

The presence of the extra particles in this model can have interesting phenomenological consequences. However, they can also cause serious problems regarding fast proton decay, tree level flavor changing neutral current (FCNC) and neutrino masses. Considering the decomposition of $27 \times 27 \times 27$ there are eleven possible superpotential terms.

The most general superpotential can be written as

$$\begin{aligned} W &= W_0 + W_1 + W_2, \\ W_0 &= \lambda_1 Q u^c X^c + \lambda_2 Q d^c X + \lambda_3 L e^c X + \\ & \quad \lambda_4 S h h^c + \lambda_5 S X X^c + \lambda_6 L N^c X^c + \lambda_7 d^c N^c h, \\ W_1 &= \lambda_8 Q Q h + \lambda_9 u^c d^c h^c, \\ W_2 &= \lambda_{10} Q L h^c + \lambda_{11} u^c e^c h. \end{aligned} \tag{6.8}$$

The first five terms of W_0 give masses to the usual SM particles and the new heavy particles h, h^c, X and X^c. The last term of W_0 i.e. LN^cX^c can generate a non zero Dirac neutrino mass and in some scenarios it is desirable to have the coupling λ_6 very small or vanishing, so that the three neutrinos pick up small masses. Now the remaining five terms corresponding to W_1 and W_2 cannot all be there together as that would induce rapid proton decay. Imposition of a discrete symmetry can forbid such terms and give a sufficiently long lived proton [309]. We will impose a $Z_2^B \times Z_2^H$ discrete symmetry, where the first $Z_2^B = (-1)^{3B}$ prevents rapid proton decay and the second discrete symmetry Z^H distinguishes between the Higgs and matter supermultiplets and suppress the tree level FCNC processes.

Under $Z_2^B = (-1)^{3B}$ we have

$$Q, u^c, d^c \ : \ -1; \qquad L, e^c, X, X^c, S \ : \ +1, \tag{6.9}$$

now depending on the assignments of h, h^c and N^c one can have different variants of the model. Such different possibilities are listed in Table 6.2.

In the models where h, h^c are even under Z_2^B the superfields $h(B = -2/3)$ and $h^c(B = 2/3)$ are diquarks while for the rest $h(B = 1/3, L = 1)$ and $h^c(B = -1/3, L = -1)$ are leptoquarks. N^c with the assignment $Z_2^B = -1$ are baryons and the assignment $Z_2^B = +1$ are leptons. In addition to the trilinear terms listed in Table 6.2 there can be bilinear terms such as LX^c and N^cN^c. The former can give rise to nonzero neutrino mass and the latter can give heavy Majorana baryon (lepton) N^c mass. Model 1 is similar to model 5 of Ref. [310] and model A of Ref. [311]. Model 2 is same as model B of Ref. [311]. Model 8 is quite different from the ones that have been discussed in connection with leptogenesis in the literature (e.g. [256]). Here the

Model	h, h^c	N^c	Allowed trilinear terms
1	+1	-1	W_0 ($\lambda_6 = 0$), W_1
2	+1	-1 for $N^c_{1,2}$, +1 for N^c_3	W_0 ($\lambda_6 = 0$ for $N^c_{1,2}$, $\lambda_7 = 0$ for N^c_3), W_1
3	-1	+1	W_0, W_2
4	-1	+1 for $N^c_{1,2}$, -1 for N^c_3	W_0 ($\lambda_6 = \lambda_7 = 0$ for N^c_3), W_2
5	+1	+1 for $N^c_{1,2}$, -1 for N^c_3	W_0 ($\lambda_6 = 0$ for N^c_3, $\lambda_7 = 0$ for $N^c_{1,2}$), W_1
6	+1	+1	W_0 ($\lambda_7 = 0$), W_1
7	-1	-1	W_0 ($\lambda_6 = \lambda_7 = 0$), W_2
8	-1	-1 for $N^c_{1,2}$, +1 for N^c_3	W_0 ($\lambda_6 = \lambda_7 = 0$ for $N^c_{1,2}$), W_2

Table 6.2: Possible transformations of h, h^c and N^c under Z_2^B and the allowed superpotential terms.

matter superfields X, X^c carry non zero $B - L$ quantum numbers and the tree level FCNC processes are forbidden.

6.2.1 Model 1

In this model we take the second discrete symmetry Z_2^H to be $Z_2^L = (-1)^L$ following Ref. [311] and it is imposed as follows

$$\begin{aligned} L, e^c, X_{1,2}, X^c_{1,2}, S_{1,2} &\quad : \quad -1 \\ Q, u^c, d^c, N^c, h, h^c, S_3, X_3, X^c_3 &\quad : \quad +1. \end{aligned} \tag{6.10}$$

The neutral Higgs superfields S_3, X_3 and X_3^c have zero lepton numbers and can pick up vacuum expectation values (VEVs) while the presence of the bilinear terms $LX_{1,2}^c$ imply that $X_{1,2}^c$ have $L = -1$ and $X_{1,2}$ have $L = 1$. In this model N^c is a baryon with $B = 1$ and it acquires a Majorana mass from the bilinear term mN^cN^c. The complete superpotential of model 1 is given by

$$\begin{aligned} W &= \lambda_1^{ij} Q_j u_i^c X_3^c + \lambda_2^{ij} Q_j d_i^c X_3 + \lambda_3 L_j e_i^c X_3 + \lambda_4^{ij} S_3 h_i h_j^c \\ &+ \lambda_5^{3ab} S_3 X_a X_b^c + \lambda_5^{a3b} S_a X_3 X_b^c + \lambda_5^{ab3} S_a X_b X_3^c \\ &+ \lambda_5^{333} S_3 X_3 X_3^c + \lambda_7^{ijk} d_i^c h_j N_k^c + \mu^{ia} L_i X_a^c \\ &+ m_N^{ij} N_i^c N_j^c + W_1, \end{aligned} \tag{6.11}$$

where i, j, k are flavor indices which run over all 3 flavors and $a, b = 1, 2$ [1]. The form of the superpotential clearly shows that the up-type quarks couple to X_3^c only while the down-type quarks and the charged leptons couple to X_3 only, resulting in the suppression of the FCNC processes at the tree level.

6.2.2 Model 2

Here the second discrete symmetry Z_2^L is imposed as follows

$$\begin{aligned} L, e^c, X_{1,2}, X_{1,2}^c, S_{1,2}, N_3^c &: \quad -1 \\ Q, u^c, d^c, N_{1,2}^c, h, h^c, S_3, X_3, X_3^c &: \quad +1. \end{aligned} \tag{6.12}$$

In this model $N_{1,2}^c$ are baryons with $B = 1$ but N_3^c is a lepton and can give mass to one of the neutrinos via the term $LN_3^cX_3^c$. The complete superpotential of model 2 is given by

$$\begin{aligned} W &= \lambda_1^{ij} Q_j u_i^c X_3^c + \lambda_2^{ij} Q_j d_i^c X_3 + \lambda_3 L_j e_i^c X_3 + \lambda_4^{ij} S_3 h_i h_j^c \\ &+ \lambda_5^{3ab} S_3 X_a X_b^c + \lambda_5^{a3b} S_a X_3 X_b^c + \lambda_5^{ab3} S_a X_b X_3^c \\ &+ \lambda_5^{333} S_3 X_3 X_3^c + \lambda_6^{i} L_i N_3^c X_3^c + \lambda_7^{ija} d_i^c h_j N_a^c + \mu^{ia} L_i X_a^c \\ &+ m_N^{ab} N_a^c N_b^c + m_N^{33} N_3^c N_3^c + W_1. \end{aligned} \tag{6.13}$$

[1] We will use this notation hereafter in this chapter. The indices i, j, k run over 1,2,3, while the indices a, b run over 1,2.

6.2.3 Model 3

The second discrete symmetry $Z_2^H = Z_2^L = (-1)^L$ is imposed as follows

$$\begin{aligned} L, e^c, X_{1,2}, X^c_{1,2}, S_{1,2}, N^c, h, h^c &\quad : \quad -1 \\ Q, u^c, d^c, S_3, X_3, X^c_3 &\quad : \quad +1. \end{aligned} \tag{6.14}$$

In this model all the N^cs are leptons. The complete superpotential of model 4 is given by

$$\begin{aligned} W &= \lambda_1^{ij} Q_j u_i^c X_3^c + \lambda_2^{ij} Q_j d_i^c X_3 + \lambda_3 L_j e_i^c X_3 + \lambda_4^{ij} S_3 h_i h_j^c \\ &+ \lambda_5^{3ab} S_3 X_a X_b^c + \lambda_5^{a3b} S_a X_3 X_b^c + \lambda_5^{ab3} S_a X_b X_3^c \\ &+ \lambda_5^{333} S_3 X_3 X_3^c + \lambda_6^{ij3} L_i N_j^c X_3^c + \lambda_7^{ijk} d_i^c h_j N_k^c \\ &+ \mu^{ia} L_i X_a^c + m_N^{ij} N_i^c N_j^c + W_2. \end{aligned} \tag{6.15}$$

6.2.4 Model 4

Here the second discrete symmetry Z_2^H is again chosen to be $(-1)^L$ and it is imposed as follows

$$\begin{aligned} L, e^c, X_{1,2}, X^c_{1,2}, S_{1,2}, N^c_{1,2}, h, h^c &\quad : \quad -1 \\ Q, u^c, d^c, N^c_3, S_3, X_3, X^c_3 &\quad : \quad +1. \end{aligned} \tag{6.16}$$

$N^c_{1,2}$ are leptons while N^c_3 is a baryon. The complete superpotential of model 2 is given by

$$\begin{aligned} W &= \lambda_1^{ij} Q_j u_i^c X_3^c + \lambda_2^{ij} Q_j d_i^c X_3 + \lambda_3 L_j e_i^c X_3 + \lambda_4^{ij} S_3 h_i h_j^c \\ &+ \lambda_5^{3ab} S_3 X_a X_b^c + \lambda_5^{a3b} S_a X_3 X_b^c + \lambda_5^{ab3} S_a X_b X_3^c \\ &+ \lambda_5^{333} S_3 X_3 X_3^c + \lambda_6^{ia3} L_i N_a^c X_3^c + \lambda_7^{ija} d_i^c h_j N_a^c \\ &+ \mu^{ia} L_i X_a^c + m_N^{ab} N_a^c N_b^c + m_N^{33} N_3^c N_3^c + W_2. \end{aligned} \tag{6.17}$$

6.2.5 Model 5 and 6

In model 5 if we choose the second discrete symmetry Z_2^H to be $Z_2^L = (-1)^L$ and it is imposed as follows

$$\begin{aligned} L, e^c, X_{1,2}, X_{1,2}^c, S_{1,2}, N_{1,2}^c &\quad : \quad -1 \\ Q, u^c, d^c, N_3^c, h, h^c, S_3, X_3, X_3^c &\quad : \quad +1, \end{aligned} \tag{6.18}$$

which forbids the terms $\lambda_6 L_i N_a^c X_b^c$ (λ_7 is already vanishing for $N_{1,2}^c$ from the imposition of the first discrete symmetry Z_2^B) and thus the possibility of high scale baryogenesis (via leptogenesis) through the decay of Majorana N^c gets ruled out. However there can be soft baryogenesis through three body decays which can induce $n - \bar{n}$ oscillations. We will elaborate on this in Section 6.5. With the above choice of the second discrete symmetry given in Eq. (6.18) the complete superpotential for model 5 is given by

$$\begin{aligned} W &= \lambda_1^{ij} Q_j u_i^c X_3^c + \lambda_2^{ij} Q_j d_i^c X_3 + \lambda_3 L_j e_i^c X_3 + \lambda_4^{ij} S_3 h_i h_j^c \\ &+ \lambda_5^{3ab} S_3 X_a X_b^c + \lambda_5^{a3b} S_a X_3 X_b^c + \lambda_5^{ab3} S_a X_b X_3^c \\ &+ \lambda_5^{333} S_3 X_3 X_3^c + \lambda_6^{ia} L_i N_a^c X_3^c + \lambda_7^{ij3} d_i^c h_j N_3^c + \mu^{ia} L_i X_a^c \\ &+ m_N^{ab} N_a^c N_b^c + m_N^{33} N_3^c N_3^c + W_1. \end{aligned} \tag{6.19}$$

We find that in this model it is possible to allow high scale leptogenesis through the decay of Majorana N^c by a clever choice of the second discrete symmetry such that it can distinguish between the matter and Higgs superfields and also suppress the unwanted FCNC processes at the tree level. One such choice can be Z_2^E which is associated with most of the exotic states. We define the transformation properties of the various superfields under $Z_2^H = Z_2^E$ as follows

$$\begin{aligned} X_{1,2}, X_{1,2}^c, S_{1,2}, N^c &\quad : \quad -1 \\ L, e^c, Q, u^c, d^c, h, h^c, S_3, X_3, X_3^c &\quad : \quad +1, \end{aligned} \tag{6.20}$$

Thus for this choice also X_3, X_3^c and S_3 are the Higgs superfields that acquire VEVs. Since up-type quarks couple to X_3^c only and down-type quarks and charged SM leptons couple to only X_3 the FCNC processes at the tree level are suppressed. The complete superpotential of model 5 with the assignments in Eq. (6.20) reduces to

$$\begin{aligned} W' &= \lambda_1^{ij} Q_j u_i^c X_3^c + \lambda_2^{ij} Q_j d_i^c X_3 + \lambda_3 L_j e_i^c X_3 + \lambda_4^{ij} S_3 h_i h_j^c \\ &+ \lambda_5^{3ab} S_3 X_a X_b^c + \lambda_5^{a3b} S_a X_3 X_b^c + \lambda_5^{ab3} S_a X_b X_3^c \\ &+ \lambda_5^{333} S_3 X_3 X_3^c + \lambda_6^{iab} L_i N_a^c X_b^c \\ &+ m_N^{ab} N_a^c N_b^c + m_N^{33} N_3^c N_3^c + W_1. \end{aligned} \tag{6.21}$$

In model 6 also, the similar assignments for the superfields as given in Eq. (6.20) holds good and the complete superpotential is similar to Eq. (6.21) except the λ_6 term which now reads $\lambda_6^{ija} L_i N_j^c X_a^c$.

6.2.6 Model 7 and 8

Taking the second discrete symmetry to be $Z_2^H = (-1)^L$ the superfields have the assigments

$$\begin{aligned} L, e^c, X_{1,2}, X_{1,2}^c, S_{1,2}, h, h^c &: -1 \\ Q, u^c, d^c, N^c, S_3, X_3, X_3^c &: +1. \end{aligned} \tag{6.22}$$

In this model all the N^cs are baryons. The complete superpotential of model 7 is given by

$$\begin{aligned} W &= \lambda_1^{ij} Q_j u_i^c X_3^c + \lambda_2^{ij} Q_j d_i^c X_3 + \lambda_3 L_j e_i^c X_3 + \lambda_4^{ij} S_3 h_i h_j^c \\ &+ \lambda_5^{3ab} S_3 X_a X_b^c + \lambda_5^{a3b} S_a X_3 X_b^c + \lambda_5^{ab3} S_a X_b X_3^c \\ &+ \lambda_5^{333} S_3 X_3 X_3^c + \mu^{ia} L_i X_a^c + m_N^{ij} N_i^c N_j^c + W_2. \end{aligned} \tag{6.23}$$

Note that the λ_6 and λ_7 terms which are essential for baryogenesis through N^c decay (as discussed in Section 6.5) are forbidden by the Z_2^B symmetry irrespective of what Z_2^H one chooses. For model 8 also one can write down the superfield transformations and the superpotential. In this case the mass term for N^c is given by $m_N^{ab} N_a^c N_b^c + m_N^{33} N_3^c N_3^c$ and the terms $\lambda_6^{i33} L_i N_3^c X_3^c$, $\lambda_7^{ij3} d_i^c h_j N_3^c$ are present in addition to the terms given in Eq. (6.23).

6.3 Explaining the CMS $eejj$ (and $e\not{p}_T jj$) excess(es)

An inspection of Table 6.2 and the corresponding allowed superpotential terms reveals that all the models listed there contain the terms $\lambda_2 Q_i d_j^c X_3$ and $\lambda_3 L_i e_j^c X_3$ in the superpotential ($\tilde{N}_E^c$ and $\tilde{\nu}_E$ acquires VEVs and $SU(2) \times U(1)_Y$ gets broken to $U(1)_{\rm EM}$) and can give rise to an $eejj$ signal from the exotic slepton $\tilde{E}$ decay. $\tilde{E}$ can be resonantly produced in pp collisions, and then subsequently it decays to a charged lepton and neutrino, followed by interactions of the neutrino producing an $eejj$ signal. The process leading to $eejj$ signal is given in Fig. 6.1.

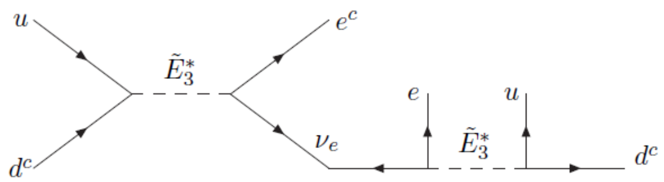

Figure 6.1: Feynman diagram for a single exotic particle $\tilde{E}$ production leading to $eejj$ signal.

The models where h and h^c are leptoquarks (Models 3, 4, 7 and 8 in Table 6.2) can produce both $eejj$ and $e\not{p}_T jj$ signals from the decay of scalar superpartner(s) of the exotic particle(s). Both events can be produced in the above scenarios via (i) resonant production of the exotic slepton $\tilde{E}$ (ii) and pair production of scalar leptoquarks $\tilde{h}$. The processes involving exotic slepton decay leading to both $eejj$ and $e\not{p}_T jj$ signals are given in Fig. 6.2. The superpotential terms involved in these processes are $\lambda_{10} Q L h^c$ and $\lambda_{11} u^c e^c h$ in addition the two terms responsible for the first signal. The partonic

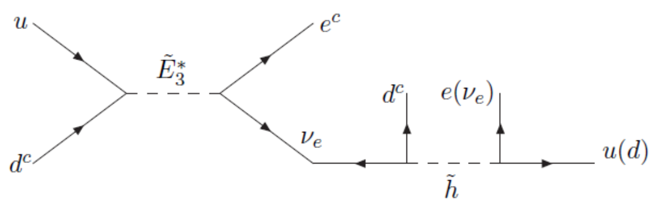

Figure 6.2: Feynman diagram for exotic slepton $\tilde{E}$ production leading to both $eejj$ and $e\not{p}_T jj$ signal

cross section of slepton production is given by [249]

$$\hat{\sigma} = \frac{\pi}{12\hat{s}} |\lambda_2|^2 \, \delta(1 - \frac{m^2_{\tilde{E}}}{\hat{s}}), \tag{6.24}$$

where $\hat{s}$ is the partonic center of mass energy, and $m_{\tilde{E}}$ is the mass of the resonant slepton. The total cross section is approximated to be [249]

$$\sigma\,(pp \to eejj) \propto \frac{|\lambda_2|^2}{m^3_{\tilde{E}}} \times \beta_1 \tag{6.25}$$

and

$$\sigma\left(pp \to e\not{p}_T jj\right) \propto \frac{|\lambda_2|^2}{m^3_{\tilde{E}}} \times \beta_2, \tag{6.26}$$

where β_1 is the branching fraction for the decay of $\tilde{E}$ to $eejj$ and β_2 is the branching fraction for the decay to $e\not{p}_T jj$. Choosing $\beta_{1,2}$ and the coupling λ_2 the cross section for the processes can be calculated as a function of the exotic slepton mass. Bounds for the value of the mass of the exotic slepton can be obtained by matching the theoretically calculated excess events with the ones observed at the LHC at a center of mass energy $\sqrt{s} = 8\,\text{TeV}$. Thus, the $U(1)_N$ models can explain the excess $eejj$ (and $e\not{p}_T jj$) signal(s) at the LHC via resonant exotic slepton decay.

6.4 ATLAS and CMS diboson and dijet excesses

More recently, the ATLAS and CMS collaborations have also reported a number of diboson and dijet excesses over the SM expectations near the invariant mass region $1.8-2.0\,\text{TeV}$. The search for diboson production has been reported by the ATLAS collaboration to show a 3.4σ excess at $\sim 2\,\text{TeV}$ in boosted jets of WZ channel amounting to a global 2.5σ excess over the SM expectation [168]. The method of jet substructure has been used to discriminate the hadronic decays of W and Z bosons from QCD dijets and due to overlaps in the jet masses of the gauge bosons many events can also be interpreted as ZZ or WW resonances, yielding 2.9σ and 2.6σ excesses in two channels respectively. On the other hand, the CMS collaboration has reported a 1.4σ excess at $\sim 1.9\,\text{TeV}$ in their search for diboson production without discriminating between the W- and Z-tagged jets [169] and a 1.5σ excess at $\sim 1.8\,\text{TeV}$ in the search for diboson production with a leptonically tagged Z [170]. In the search for dijet resonances the

ATLAS and CMS collaborations have reported excesses at $1.8\,\mathrm{TeV}$ with 2.2σ and 1σ significance levels respectively [171, 172]. The CMS has also reported a 2.1σ excess in the energy bin 1.8 to $1.9\,\mathrm{TeV}$ in the resonant HW production channel [173].

Several phenomenological explanations have been proposed addressing these excesses [190, 312–333]. In the framework of simple extensions of the SM, a heavy W' with mass $\sim 2\,\mathrm{TeV}$ produced via $q\bar{q}$ annihilation can explain the excess in the WZ channel via its mixing with the SM W for a mixing angle greater than 10^{-2}. A heavy Z' can mix with the SM Z and then decay into W^+W^- to explain the excess in the W^+W^- channel. Assuming that the SM Z_1 boson mixes with Z_2 via a mixing angle ϕ_z to give the mass eigenstates Z and Z'

$$\begin{pmatrix} Z_1 \\ Z_2 \end{pmatrix} = \begin{pmatrix} \cos\phi_z & -\sin\phi_z \\ \sin\phi_z & \cos\phi_z \end{pmatrix} \begin{pmatrix} Z \\ Z' \end{pmatrix}, \tag{6.27}$$

the relevant vertex for the Z' can be written as

$$\begin{aligned} \mathcal{V}_{Z'WW}: \quad & g\cos\theta_w \sin\phi_z \left[(p_{Z'} - p_{W^+})^\beta g^{\mu\alpha}\right. \\ & \left. +(p_{W^+} - p_{W^-})^\mu g^{\alpha\beta} + (p_{W^-} - p_{Z'})^\alpha g^{\mu\beta}\right] \\ & \times\varepsilon_\mu(p_{Z'})\varepsilon_\alpha(p_{W^+})\varepsilon_\beta(p_{W^-}), \end{aligned} \tag{6.28}$$

where $\cos\phi_z \simeq 1$ is assumed. The partial decay width of Z' into W^+W^- is given by [313]

$$\begin{aligned} \Gamma_{Z'W^+W^-} = \quad & \sin^2\phi_z \left(\frac{g^2\cos^2\theta_w}{192\pi}\frac{M_{Z'}^5}{M_W^4}\right)\left(1 - \frac{M_W^2}{M_{Z'}^2}\right)^{3/2} \\ & \left(1 + 20\frac{M_W^2}{M_{Z'}^2} + 12\frac{M_W^4}{M_{Z'}^4}\right). \end{aligned} \tag{6.29}$$

For Z', the 7 - 8 events around the 2 TeV peak give the benchmark $\sigma(Z') \times B(Z' \to W^+W^-) \simeq 5 - 6$ fb. However, the semileptonic channel of the W^+W^- decay puts an upper limit on $\sigma(Z') \times B(Z' \to W^+W^-) \simeq 3$ fb at 95% confidence level [170]. Ignoring this slight inconsistency one can obtain a range of values for g' and $\sin\phi_z$ which can explain the excess. It turns out that to explain the excess one must have $\sin\phi_z \gtrsim 10^{-3}$ [313]. However from electroweak precision data $\sin\phi_z$ corresponding to Z_N in our model is constrained as $\sin\phi_z \leq 7 \times 10^{-4}$ [334]. Thus, all the excess events cannot be addressed via the Z_N decay. For a leptophobic Z' the mixing angle can be relaxed to 8×10^{-3}, which is close to the required value to explain the diboson anomaly [313].

It is also interesting to note that the ATLAS diboson excess can also be explained with a $2\,\mathrm{TeV}$ sgoldstino scalar assuming that the SUSY breaking scale is in the few TeV range as pointed out in Ref. [333]. Our model being a supersymmetric one can also entertain such a possibility. Lastly, since the $U(1)_N$ model is a low energy subgroup of the superstring motivated E_6 group, it is also possible to rely on additional anomalous $U(1)$ fields coming from a stringy construct. For example in the context of D-brane compactifications it was shown in Ref. [332] that under the assumption of a low string scale, the dibosn and dijet excesses can be addressed by an anomalous $U(1)$ field with very small couplings to the leptons.

6.5 Baryogenesis (via leptogenesis) in $U(1)_N$ models

Some of the variants of low-energy $U(1)_N$ subgroup of E_6 model allow for the possibility of explaining baryogenesis (via leptogenesis) from the decay of the heavy Majorana particle N^c. In order to generate the baryon asymmetry of the universe from N^c decay the conditions that must be satisfied are (i) violation of $B - L$ from Majorana mass of N^c, (ii) complex couplings must give rise to sufficient CP violation and (iii) the out-of-equilibrium condition given by

$$\Gamma_N < H(T = m_N) = \sqrt{\frac{4\pi^3 g_*}{45}}\frac{T^2}{M_{Pl}}, \tag{6.30}$$

must be satisfied, where Γ_N is the decay width of Majorana N^c, $H(T)$ is the Hubble rate, g_* is the effective number of relativistic degrees of freedom at temperature T and M_{Pl} is the Planck mass. This implies that N^c cannot transform nontrivially under the low-energy subgroup $G = SU(3)_C \times SU(2)_L \times U(1)_Y \times U(1)_N$, which is readily satisfied in some variants of $U(1)_N$ model (see Table 6.1). Thus the out-of-equilibrium decay of heavy N^c can give rise to high-scale baryogenesis (leptogenesis).

Models 1 and 2 have distinctive features of allowing direct baryogenesis via decay of heavy Majorana baryon N^c [311]. In both schemes, $N^c_{k(a)}$ decays to $B - L = B = -1$ final states $d^c_i \tilde{h}_j, \tilde{d^c}_i h_j$ and to their conjugate states with $B - L = B = 1$, via the interaction term λ_7^{ijk} (λ_7^{ija}) in Eq. (6.11 (6.13)). In both cases, CP violation comes from the complex Yukawa coupling λ_7^{ijk} (λ_7^{ija}) given in eqs. (6.11) and (6.13). The asymmetry is generated from interference between tree level decays and one-loop vertex and self-energy diagrams. The one-loop vertex and self-energy diagrams are shown in Fig. 6.3.

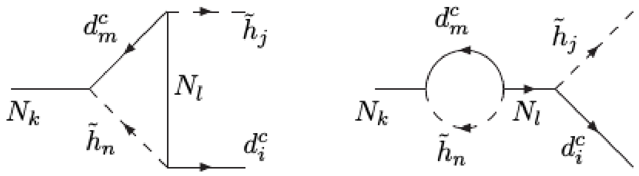

Figure 6.3: One-loop diagrams for N_k decay which interferes with the tree level decay to provide CP violation.

The asymmetry is given by

$$\epsilon^k = \frac{1}{24\pi} \frac{\sum_{i,j,l,m,n} \mathrm{Im}\left[\lambda_7^{ijk}\lambda_7^{inl*}\lambda_7^{mjl*}\lambda_7^{mnk}\right]}{\sum_{i,j}\lambda_7^{ijk*}\lambda_7^{ijk}} \times \left[\mathcal{F}_V\left(\frac{M^2_{N_l}}{M^2_{N_k}}\right) + 3\mathcal{F}_S\left(\frac{M^2_{N_l}}{M^2_{N_k}}\right)\right], \tag{6.31}$$

where

$$\mathcal{F}_V = \frac{2\sqrt{x}}{x-1}, \mathcal{F}_S = \sqrt{x}\,\ln\left(1+\frac{1}{x}\right). \tag{6.32}$$

$\mathcal{F}_V$ corresponds to the one-loop function for the vertex diagram and $\mathcal{F}_S$ corresponds to the one-loop function for the self-energy diagram. The baryon to entropy ratio generated by decays of N_k is given by $n_B/s \sim \epsilon\ n_\gamma/s \sim (\epsilon/g_*)(45/\pi^4)$, where n_γ is number density of photons per comoving volume and g_* corresponds to the number of relativistic degrees of freedom. By considering $\lambda^7_{ijk} \sim 10^{-3}$ in model 1, one can generate $n_B/s \sim 10^{-10}$ for maximal CP violation. Similarly, one needs $\lambda_7^{ija} \sim 10^{-3}$ to satisfy required bound on n_B/s in model 2.

In models 3 and 4, $N^c_{1,2}$ (N^c) are Majorana leptons and hence a $B-L$ asymmetry is created via the decay of heavy N^c which then gets converted to the baryon asymmetry of the Universe in the presence of the $B+L$ violating anomalous processes before the electroweak phase transition. In these two cases, $N^c_{k(a)}$ decays to the final states $d^c_i\tilde{h}_j, \tilde{d^c}_i h_j$ with $B-L = -1$ and to their conjugate states with $B-L = 1$, via the interaction term λ_7^{ija} (λ_7^{ijk}) in Eq. (6.17 (6.15)). The one-loop diagrams that can interfere with the tree level $N_a(N_k)$ decays to provide the required CP violation are again the diagrams given in Fig. 6.3. However in these scenarios a $B-L$ asymmetry is created from the decay of Majorana N^c in contrast to the B asymmetry created in models 1 and 2. Again utilizing the general expression for calculating asymmetry parameter as given in (6.31), one needs $\lambda_7^{ija}(\lambda_7^{ijk}) \sim 10^{-3}$ in order to satisfy $n_B/s \sim 10^{-10}$ bound in both models 3 and 4.

For models 5 and 6, we have discussed two possible choices for the second discrete symmetries in section 6.2. In model 5, $N^c_{1,2}$ are leptons and N^c_3 is a baryon while in model 6 all the N^c's are leptons. For the first choice of second discrete symmetry $Z_2^H = Z_2^L$ the form of the superpotential (Eq. 6.19 for model 5) clearly shows that one cannot generate the baryon asymmetry of the Universe from high scale leptogenesis via the decay of heavy Majorana N^c in these models. However, the term $\lambda_7^{ij3} d_i^c h_j N_3^c$ can give rise to baryogenesis at TeV scale or below if one consider soft supersymmetry (SUSY) breaking terms in model 5. The relevant soft SUSY terms in the Lagrangian is given by

$$\mathcal{L} \sim m^2_{\tilde{h}_i} \tilde{h}_i^\dagger \tilde{h}_i + m^2_{\tilde{Q}_l} \tilde{Q}_l^\dagger \tilde{Q}_l + A^{ilm} \tilde{h}_i \tilde{Q}_l \tilde{Q}_m + \dots \quad , \tag{6.33}$$

where i corresponds to the different generations of leptoquarks and $Q_{l(m)} = (u_l, d_l)$, $l, m = 1, 2, 3$, corresponds to three generations of superpartners of the Standard Model quarks. The Feynman diagrams for the tree level process and the one-loop process interfering with it to provide the CP violation are shown in Fig. 6.4. The asymmetry

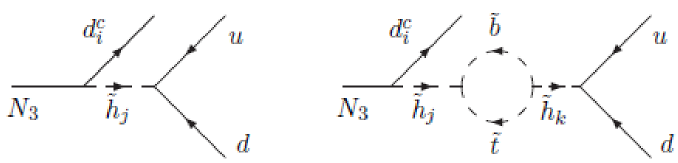

Figure 6.4: The tree level and one-loop diagrams for N_3 decay giving rise to baryogenesis in model 5.

parameter in this case is given by [335]

$$\begin{aligned}\epsilon &= A_{N_3}\sum_{i,j,k}\Bigg[\mathrm{Im}\left[\lambda_7^{ij3*}\lambda_7^{ik3}\mathcal{A}^{j33*}\mathcal{A}^{k33}\right]\left(\frac{|\lambda_8^{j11}|^2}{m^2_{\tilde{h}_j}}-\frac{|\lambda_8^{k11}|^2}{m^2_{\tilde{h}_k}}\right)\\ &\quad+\mathrm{Im}\left[\lambda_7^{ij3*}\lambda_7^{ik3}\lambda_8^{j11}\lambda_8^{k11*}\right]\left(\frac{|\mathcal{A}^{j33}|^2}{m^2_{\tilde{h}_1}}-\frac{|\mathcal{A}^{k33}|^2}{m^2_{\tilde{h}_1}}\right)\\ &\quad+\mathrm{Im}\left[\mathcal{A}^{j33}\mathcal{A}^{k33*}\lambda_8^{j11}\lambda_8^{k11*}\right]\left(\frac{|\lambda_7^{ij3}|^2}{m^2_{\tilde{h}_j}}-\frac{|\lambda_7^{ik3}|^2}{m^2_{\tilde{h}_k}}\right)\Bigg]\end{aligned} \tag{6.34}$$

where $A_{N_3}=\dfrac{1}{\Gamma_{N_3}}\dfrac{1}{(2\pi)^3}\dfrac{1}{12}\dfrac{\pi}{4\pi^2}\dfrac{M^5_{N_3}}{m^2_{\tilde{h}_j}m^2_{\tilde{h}_k}}$ and Γ_{N_3} is the total decay width of N_3. Thus, by considering the soft SUSY breaking terms (given in Eq. (6.33)) of TeV scale, one can generate required amount of baryon asymmetry for particular values of Yukawa couplings.

This can also induce neutron-antinutron (n-$\bar{n}$) oscillation violating baryon number by two units ($\Delta B = 2$) [46]. The effective six-quark interaction inducing n-$\bar{n}$ oscillation is shown in Fig. 6.5. In fact, models 1 and 2 can also induce n-$\bar{n}$ oscillation in a

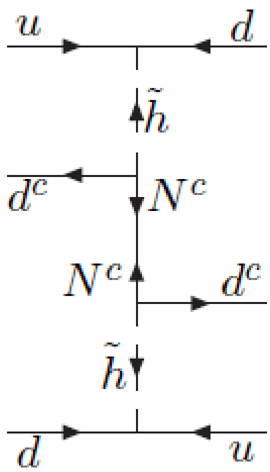

Figure 6.5: n-$\bar{n}$ oscillation induced by effective six-quark interaction.

similar fashion. However in model 6 all the N^cs are leptons and hence in this model a scheme for baryogenesis similar to above is not possible.

Now if we choose the second discrete symmetry to be $Z_2^H = Z_2^E$ in models 5 and 6 (see Eq. (6.20)) then it is possible to allow high scale leptogenesis via the decay of heavy Majorana N^c. In these two models $N^c_{a(j)}$ decays to the final states

$\nu_{e_i}\tilde{N}^c_{E_b}, \tilde{\nu}_{e_i}N^c_{E_b}, e_i\tilde{E}^c_b, \tilde{e}_iE^c_b$ with $B-L=-1$ and to their conjugate states with $B-L=1$, via the interaction term λ_7^{iab} (λ_7^{ijb}) in Eq. (6.21). Here we take advantage of the fact that Z_2^E symmetry forbids bilinear term like LX^c and consequently X^c need not to carry any lepton number, it can simply have the assignment $B=L=0$. The one-loop diagrams for $N_a(N_j)$ decays that can interfere with the tree level decay diagrams to provide the required CP violation are given in Fig. 6.6.

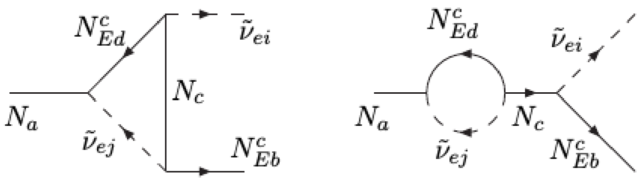

Figure 6.6: One-loop diagrams for N_a decay which interferes with the tree level decay to provide CP violation.

For models 7 and 8 the imposition of the Z_2^B symmetry implies vanishing λ_6 and λ_7 for two or more generations of N^c. Thus in these models, no matter what kind of Z_2^H we choose, sufficient CP violation cannot be produced and consequently the possibility of baryogenesis (leptogenesis) from the decay of heavy Majorana N^c is ruled out. Thus one needs to resort to some other mechanism to generate the baryon asymmetry of the universe.

6.6 Neutrino masses

In all the variants of $U(1)_N$ model that we have considered in Section 6.2, the scalar component of S_3 acquires a VEV to break the $U(1)_N$. The fermionic component of S_3 pairs up with the gauge fermion to form a massive Dirac particle. However the fields $S_{1,2}$ still remains massless and can give rise to an interesting neutrino mass matrix structure.

In model 1, the field $N^c_{1,2,3}$ are baryons and hence they do not entertain the possibility of canonical seesaw mechanism of generating mass for neutrinos. However, the bilinear terms $\mu^{ia}L_iX^c_a$ can give rise to four nonzero masses for $\nu_{e,\mu,\tau}$ and $S_{1,2}$ as noted in Ref. [311]. The 9×9 mass matrix for the neutral fermionic fields of this model

$\nu_{e,\mu,\tau}, S_{1,2}, \nu_{E_{1,2}}$ and $N^c_{E_{1,2}}$ is given by

$$\mathcal{M}^1 = \begin{pmatrix} 0 & 0 & 0 & \mu^{ia} \\ 0 & 0 & \lambda_5^{ab3} v_2 & \lambda_5^{a3b} v_1 \\ 0 & \lambda_5^{ba3} v_2 & 0 & M_a \delta_{ab} \\ (\mu^T)^{ai} & \lambda_5^{b3a} v_1 & M_a \delta_{ab} & 0 \end{pmatrix}, \tag{6.35}$$

where v_1 and v_2 are the VEVs acquired by $\tilde{\nu}_{E_3}$ and $\tilde{N}^c_{E_3}$ respectively, and $M_{1,2}$ corresponds to the mass eigenvalues of the neutral fields $X_{1,2}$ and $X^c_{1,2}$. We will further assume that the field $\nu_{E_{1,2}}$ pairs up with the charge conjugate states to obtain a heavy Dirac mass. Thus in Eq. 6.35, four of the nine fields are very heavy with masses M_1, M_1, M_2 and M_2 to a good approximation. This becomes apparent once we diagonalize $\mathcal{M}^1$ in M_a by a rotation about the 3-4 axis to get $\mathcal{M}'^1$ given by

$$\begin{pmatrix} 0 & 0 & \mu^{ia}/\sqrt{2} & \mu^{ia}/\sqrt{2} \\ 0 & 0 & (\lambda_5^{ab3} v_2 + \lambda_5^{a3b} v_1)/\sqrt{2} & (-\lambda_5^{ab3} v_2 + \lambda_5^{a3b} v_1)/\sqrt{2} \\ (\mu^T)^{ai}/\sqrt{2} & (\lambda_5^{ba3} v_2 + \lambda_5^{b3a} v_1)/\sqrt{2} & M_a \delta_{ab} & 0 \\ (\mu^T)^{ai}/\sqrt{2} & (-\lambda_5^{ba3} v_2 + \lambda_5^{b3a} v_1)/\sqrt{2} & 0 & -M_a \delta_{ab} \end{pmatrix}. \tag{6.36}$$

Then we readily obtain the 5×5 reduced mass matrix for the three neutrinos and $S_{1,2}$ given by

$$\mathcal{M}^1_\nu = \begin{pmatrix} 0 & \mu^{ic} \lambda_5^{cb3} v_2 M_c^{-1} \\ \lambda_5^{ac3} \mu^{cj} v_2 M_c^{-1} & (\lambda_5^{ac3} \lambda_5^{c3b} + \lambda_5^{a3c} \lambda_5^{cb3}) v_1 v_2 M_c^{-1} \end{pmatrix}, \tag{6.37}$$

where the repeated dummy indices are summed over. Note that one neutrino remains massless in this model, two of the active neutrinos acquire small masses and the remaining eigenvalues correspond to sterile neutrino states. From Eq. 6.37 it follows that the bilinear terms $\mu L X_c$ and the sterile neutrinos are essential for the nonzero active neutrino masses in this model. The fields $N^c_{1,2,3}$, which are responsible for creating the baryon asymmetry of the Universe do not enter the neutrino mass matrix anywhere and hence the neutrino masses in this model do not have any direct connection with the baryon asymmetry. To have the active neutrino masses of the order $10^{-4}\,\mathrm{eV}$ one can choose the sterile neutrino mass of the order $1\,\mathrm{eV}$ and the off-diagonal entries in Eq. (6.37) to be of the order $10^{-2}\,\mathrm{eV}$. In this model the oscillations between the three active neutrinos and two sterile neutrinos is natural, and this allows the possibility of accommodating the LSND results [298]. The mixing between $S_{1,2}$ and the heavy neutral leptons ν_E, N_E^c can give rise to the decays $E_{1,2} \to W^- S_{1,2}$, $E_{1,2}^c \to W^+ S_{1,2}$, $\nu_{E_{1,2}} \to Z S_{1,2}$ and $N_{1,2}^c \to Z S_{1,2}$; which will compete with the decays arising from the Yukawa couplings $E_{1,2} \to H^- S_{1,2}$, $E_{1,2}^c \to H^+ S_{1,2}$, $\nu_{E_{1,2}} \to H^0 S_{1,2}$ and $N_{1,2}^c \to H^0 S_{1,2}$, where $H^+(H^0)$ are physical admixture of $\tilde{E}_3(\tilde{\nu}_{E_3})$ and $\tilde{E}_3^c(\tilde{N}_{E_3}^c)$.

In model 2, N_3^c is a lepton and hence the term $\lambda_6^{i33} L_i N_3^c X_3^c$ in the superpotential given in Eq. (6.13) can give rise to a seesaw mass for one active neutrino, while the other two active neutrinos can acquire masses from Eq. (6.37) as before. Thus in this model all three neutrinos can be massive instead of two in model 1. Note that this model can allow the neutrino mass texture where one of the active neutrinos can have mass much larger compared to the other two, which can naturally give atmospheric neutrino oscillations with a Δm^2 orders of magnitude higher than Δm^2 for solar neutrino oscillations.

In the case of model 3 all three N^c fields are leptons and the 12×12 mass matrix for the neutral fermions spanning $\nu_{e,\mu,\tau}$, $S_{1,2}$, $N_{1,2,3}^c$, $\nu_{E_{1,2}}$ and $N_{E_{1,2}}^c$ is given by

$$\mathcal{M}^3 = \begin{pmatrix} 0 & 0 & \lambda_6^{ij3} v_2 & 0 & \mu^{ia} \\ 0 & 0 & 0 & \lambda_5^{ab3} v_2 & \lambda_5^{a3b} v_1 \\ \lambda_6^{ji3} v_2 & 0 & M_{N_i} \delta_{ij} & 0 & 0 \\ 0 & \lambda_5^{ba3} v_2 & 0 & 0 & M_a \delta_{ab} \\ (\mu^T)^{ai} & \lambda_5^{b3a} v_1 & 0 & M_a \delta_{ab} & 0 \end{pmatrix}. \tag{6.38}$$

This gives the reduced 5×5 matrix for three active and two sterile neutrinos as follows

$$\mathcal{M}_\nu^3 = \begin{pmatrix} \lambda_6^{ik3} \lambda_6^{kj3} v_2^2 M_{N_k}^{-1} & \mu^{ic} \lambda_5^{cb3} v_2 M_c^{-1} \\ \lambda_5^{ac3} \mu^{cj} v_2 M_c^{-1} & (\lambda_5^{ac3} \lambda_5^{c3b} + \lambda_5^{a3c} \lambda_5^{cb3}) v_1 v_2 M_c^{-1} \end{pmatrix}. \tag{6.39}$$

This clearly shows that in this model active neutrinos can acquire seesaw masses even in the absence of the bilinear term $\mu L X^c$ and the sterile neutrinos. As we have discussed in section 6.5, the out-of-equilibrium decay of N^c creates the lepton asymmetry in this model, thus, M_N can be constrained from the requirement of successful leptogenesis. However one still has some room left to play with λ_5, μ and M_a, which can give rise to interesting neutrino mass textures. In model 4, the fields $N_{1,2}^c$ are leptons while

N_3^c is a baryon and hence the 11×11 mass matrix spanning $\nu_{e,\mu,\tau}$, $S_{1,2}$, $N_{1,2}^c$, $\nu_{E_{1,2}}$ and $N_{E_{1,2}}^c$ will reduce to a 5×5 matrix similar to Eq. (6.39), except the $(1,1)$ entry which is now given by $\lambda_6^{ic3}\lambda_6^{cj3}v_2^2 M_{N_c}^{-1}$. Thus it follows that two of the active neutrinos can acquire masses even without the bilinear term $\mu L X^c$ and the sterile neutrinos.

For models 5 and 6 we have discussed two possible choices for the second discrete symmetry Z_2^H in section 6.2. In the former model $N_{1,2}^c$ are leptons and N_3^c is a baryon while in the latter model all $N_{1,2,3}^c$ are leptons. In model 5, for the first choice i.e. $Z_2^B = Z_2^L$ the 11×11 mass matrix for the neutral fermions spanning $\nu_{e,\mu,\tau}$, $S_{1,2}$, $N_{1,2}^c$, $\nu_{E_{1,2}}$ is given by

$$\mathcal{M}^5 = \begin{pmatrix} 0 & 0 & \lambda_6^{id3}v_2 & 0 & \mu^{ia} \\ 0 & 0 & 0 & \lambda_5^{ab3}v_2 & \lambda_5^{a3b}v_1 \\ \lambda_6^{di3}v_2 & 0 & M_{N_d}\delta_{dg} & 0 & 0 \\ 0 & \lambda_5^{ba3}v_2 & 0 & 0 & M_a\delta_{ab} \\ (\mu^T)^{ai} & \lambda_5^{b3a}v_1 & 0 & M_a\delta_{ab} & 0 \end{pmatrix}, \tag{6.40}$$

which can be reduced to 5×5 matrix for 3 active and 2 sterile neutrinos

$$\mathcal{M}_\nu^3 = \begin{pmatrix} \lambda_6^{ic3}\lambda_6^{cj3}v_2^2 M_{N_c}^{-1} & \mu^{ic}\lambda_5^{cb3}v_2 M_c^{-1} \\ \lambda_5^{ac3}(\mu^T)^{cj}v_2 M_c^{-1} & (\lambda_5^{ac3}\lambda_5^{c3b} + \lambda_5^{a3c}\lambda_5^{cb3})v_1 v_2 M_c^{-1} \end{pmatrix}, \tag{6.41}$$

which is similar to the form in model 4 and hence similar conclusions follow. Model 6 gives a reduced mass matrix similar to model 3 given in Eq. (6.39).

For the second choice in model 5, i.e. $Z_2^B = Z_2^E$ the 11×11 mass matrix for the neutral fermions is given by

$$\mathcal{M}^5 = \begin{pmatrix} 0 & 0 & 0 & 0 & 0 \\ 0 & 0 & 0 & \lambda_5^{ab3}v_2 & \lambda_5^{a3b}v_1 \\ 0 & 0 & M_{N_d}\delta_{dg} & 0 & 0 \\ 0 & \lambda_5^{ba3}v_2 & 0 & 0 & M_a\delta_{ab} \\ 0 & \lambda_5^{b3a}v_1 & 0 & M_a\delta_{ab} & 0 \end{pmatrix}, \tag{6.42}$$

which clearly shows that the active neutrinos are massless in this case while the sterile neutrinos acquire masses $(\lambda_5^{ac3}\lambda_5^{c3b} + \lambda_5^{a3c}\lambda_5^{cb3})v_1 v_2 M_c^{-1}$. The masslessness of the active neutrinos is a consequence of the exotic discrete Z_2^E symmetry which forbids the mixing among the exotic and nonexotic neutral fermion fields defined in Eq. (6.20). The situation is similar for $Z_2^B = Z_2^E$ in model 6 also.

The analysis of mass matrix for models 7 and 8 are exactly similar to that for model 1 and 2 respectively with similar conclusions.

6.7 Summary of the chapter

We have discussed the variants of effective low-energy $U(1)_N$ model motivated by the superstring inspired E_6 group in the presence of discrete symmetries ensuring proton stability and forbidding tree level flavor changing neutral current processes. Our aim was to explore the eight possible variants to explain the excess $eejj$ and $e\not{p}_T jj$ events that have been observed by CMS at the LHC and to simultaneously explain the baryon asymmetry of the universe via baryogenesis (leptogenesis). We have also studied the neutrino mass matrices governed by the field assignments and the discrete symmetries in these variants.

To summarize the results, all the variants can produce an $eejj$ excess signal via exotic slepton decay, while, the models where h and h^c are leptoquarks (models 3, 4, 7 and 8) both $eejj$ and $e\not{p}_T jj$ signals can be produced simultaneously, while the constraints coming from the electroweak precision data on the mixing angle between Z_N and the SM Z makes it difficult to address the recent diboson and dijet excesses reported by ATLAS and CMS in the framework of $U(1)_N$ model. For the choice $Z_2^H = Z_2^L = (-1)^L$ as a second discrete symmetry, two of the variants (model 1 and 2) offers the possibility of direct baryogenesis at high scale via the decay of heavy Majorana baryon, while two other (models 3 and 4) can accommodate high-scale leptogenesis via the heavy neutrino decay. For the above choice of the second discrete symmetry none of the other variants are consistent with high-scale baryogenesis (leptogenesis), however, model 5 allows for the possibility of baryogenesis at the TeV scale or below by considering soft supersymmetry breaking terms and this mechanism can induce baryon number violating $n-\bar{n}$ oscillations. On the other hand we have also pointed out a new choice for the second discrete symmetry which has the feature of ensuring proton stability and forbidding tree level FCNC processes, while allowing for the possibility of high scale leptogenesis for models 5 and 6. Studying the neutrino mass matrices for the $U(1)_N$ model variants we also found that these variants can naturally give three active and two sterile neutrinos and accommodate the LSND results. These neutrinos acquire masses through their mixing with extra neutral fermions and can give rise to interesting neutrino mass textures where the results for the atmospheric and solar neutrino oscillations can be naturally explained.

Chapter 7

Correlating the baryon asymmetry of the universe with the dark matter abundance

In cosmology some of the important puzzles are related to the origin of baryon asymmetry of the universe and the nature of dark matter. The comparable values of dark matter density and baryon density [125] $\Omega_{DM} h_0^2 \sim 5\ \Omega_B h_0^2$, points to the possibility that they might have a common origin. However, the standard paradigm adopts completely different mechanisms to explain observable baryon asymmetry of the universe and dark matter abundance. The baryon asymmetry is generated from an initially baryon-antibaryon symmetric universe by considering baryon number (B), C and CP violating processes that went out of equilibrium in the early universe, while the dark matter density is often produced by considering weakly interacting massive particles (WIMPs) (with mass around $\mathcal{O}(100)$ GeV) with the relic density being determined by the freeze out condition. The fact that they have a comparable abundance is often referred to as the "cosmic coincidence" puzzle. Recently, the CDMS collaboration has reported an excess in the dark matter events [336] which sets an upper limit of $\mathcal{O}(10^{-41})\ \mathrm{cm}^2$ on the value of spin-independent (SI) dark matter-nucleon cross section for dark matter mass around $10\,\mathrm{GeV}$ at 3.1σ significance level. The excess reported by the CoGeNT collaboration [337] also hints at a light dark matter mass, almost in the same region of parameter space. The data taken by the XENON100 experiment [338] also gives a very stringent constraint on SI dark matter-nucleon cross section which points towards a dark matter mass around $\mathcal{O}(\text{ GeV})$. The light dark matter is often also motivated due to the possibility of explaining 3.5 KeV X-ray line by radiative decay of $\mathcal{O}(\text{ GeV})$ neutral dark matter particle [339]. However, for an $\mathcal{O}(\text{ GeV})$ mass the thermal WIMPs give an over-abundance of dark matter particles for an annihilation cross-section less than 10^{-26} cm^2, and thus the alternative schemes where an $\mathcal{O}(\text{ GeV})$ mass dark matter can be accommodated have gained significant attention. To this end, the cogenesis scenarios are particularly interesting because they have an attractive feature of explaining the observed baryon asymmetry of the universe together with an asymmetric dark matter component which can naturally satisfy the criterion for $\mathcal{O}(\text{ GeV})$ mass dark matter. Furthermore, the apparent coincidence of the baryon and dark matter densities can also be addressed in such a framework using the underlying connection between the baryogenesis scenarios and dark matter production. There exist several different mechanisms in the literature [126–141], which address simultaneous generation of baryon (or lepton) asymmetry and the asymmetric dark matter abundance. The cogenesis of both without violating B or $B-L$ is discussed in Refs. [126, 131, 137, 140, 141].

7.1 Cogenesis of baryon asymmetry and dark matter from moduli decay

In the $\mathcal{N}=1$ supergravity limit of string theory, the moduli appear while compactification of the extra dimensions takes place [233]. Let us consider a scenario where the moduli come to dominate the energy density of the universe and then they decay into radiation reheating the universe at a late time. Their decay can have significant implications for the cosmological history of the universe [340]. The entropy released due to the late decay of the lightest modulus dilutes the existing baryon asymmetry of the universe as well as the relic dark matter abundance produced at high scale. However, the correct amount of dark matter can be produced non-thermally from the decay of the modulus into the lightest supersymmetric particle. Non-thermal realizations of dark matter is discussed in Refs. [341–344] in the context of the Minimal Supersymmetric Standard Model (MSSM) and string-motivated models. Given that the decay of the heavy modulus leads to a very low reheating temperature, it renders electroweak baryogenesis and leptogenesis ineffective. However, it is possible to accommodate direct baryogenesis and the correct dark matter abundance by considering late-decaying moduli in the presence of additional color triplet superfields along with the MSSM superfields [345–347], or by means of some other mechanism [348, 349]. The coincidence problem has also been addressed by considering Affleck-Dine (AD) baryogenesis in the presence of the moduli in Refs. [350, 351].

The presence of the gravitationally coupled moduli fields can have significant impact on the standard cosmology. During inflation i.e. when the Hubble expansion rate $H_{\rm inf} \gg m_\Phi$, the modulus (Φ) gets significantly displaced from the minimum of its potential [89]. Thus, if one takes into consideration the presence of modulus and high scale inflation, it is a rather generic consequence to expect the modulus to be displaced from the low-energy minimum by an amount $|\Delta\Phi| = |\langle\Phi\rangle_{\rm inf} - \langle\Phi\rangle_0| \approx M_P$. Since the energy density of these oscillations dilutes in the same way as non-relativistic matter, they will come to dominate the expansion of the universe. This will continue until the modulus decays at a time $t \sim \Gamma_\Phi^{-1}$, transferring the remaining oscillation energy into radiation, hence reheating the universe at a late time. The reheating temperature after the modulus decay is given by [340],

$$T_R = \frac{1}{{g_*}^{1/4}}\sqrt{\Gamma_\Phi M_P}, \tag{7.1}$$

where g_* is the total number of relativistic degrees of freedom and $\Gamma_\Phi \sim m_\Phi^3/M_P^2$ is the decay width of the modulus. The number density of any particle X produced from the decay of the modulus is given by

$$Y_X = Y_\Phi {\rm Br}_X = \frac{3T_R}{4M_\Phi}{\rm Br}_X \tag{7.2}$$

It has been a challenging task to obtain a realistic low energy spectrum in the string compactifications. The foremost step while constructing a realistic model in the string compactifications is the issue of moduli stabilization. A realistic model should be able to realize the de-Sitter minima and also avoid the Cosmological Moduli Problem (CMP) [352]. The Large Volume Scenario (LVS) has been considered as an ideal framework to build a consistent MSSM-(like) chiral model in which the soft terms are calculated explicitly. In such a scenario the soft supersymmetry breaking scale $m_{\text{soft}} \sim \mathcal{O}(\text{ TeV})$ constrains the value of the Calabi-Yau manifold volume $\mathcal{V} \sim \mathcal{O}(1) \times 10^7$ in string length units. The choice of $\mathcal{V} \sim 10^7$ also provides 60 e-folds of inflation, generating the right amount of density perturbations in this model [353]. For the lightest modulus mass $m_\phi \sim M_P/\mathcal{V}^{3/2} \sim \mathcal{O}(1) \times 10^7\,\text{GeV}$ and taking $\mathcal{V} \sim 10^7$ and $g_* \sim \mathcal{O}(100)$, the reheating temperature is $T_R \sim 10\,\text{GeV}$.

In this section, we discuss a model for moduli induced cogenesis which simultaneously generates the baryon asymmetry of the universe and an asymmetric dark matter (ADM) component with a dark matter mass around $5\,\text{GeV}$ [141]. In this model, the particle content includes two additional iso-singlet color triplet superfields χ and $\bar{\chi}$ with hypercharges $-4/3$ and $4/3$ respectively and two singlet superfields $\mathcal{N}$ and $\bar{\mathcal{N}}$ in addition to the Minimal Supersymmetric Standard Model (MSSM) superfields[1]. In this model, the mass of color triplet superfields being larger than the mass of singlet superfields, the modulus decays dominantly into a pair of color triplet superfields (χ and $\bar{\chi}$). The terms analogous to the Giudice-Masiero term [354] in the Kähler potential dictate the decay width of the modulus into the colored and singlet superfields. In $\mathcal{N} = 1$ supergravity, the effective supersymmetric mass terms as well as the soft SUSY breaking terms depend on the coupling strength of the hidden sector field (modulus) to the visible sector fields [355]. Interestingly, the effective masses of the additional colored (singlet) superfields are also governed by the same Giudice-Masiero like term(s) considered in the Kähler potential. Therefore, the coefficient of the interaction term responsible for the decay of the modulus into a pair of colored(singlet) superfields i.e. the coefficient of the new Giudice-Masiero like term(s) ($z_{\chi(\mathcal{N})}$) can be constrained based on the given masses of the superfields. For a Calabi-Yau manifold volume $\mathcal{V} \sim 10^7$, to obtain $\hat{M}_\chi \sim \mathcal{O}(\text{ TeV})$ and $\hat{M}_\mathcal{N} \sim \mathcal{O}(\text{ TeV})$ one needs $z_\chi \sim 1$ and $z_\mathcal{N} \sim 0.005$, respectively. Thus one obtains $\dfrac{\Gamma_{\Phi\to\mathcal{N}\bar{\mathcal{N}}}}{\Gamma_{\Phi\to\chi\bar{\chi}}} = \dfrac{z_\mathcal{N}^2}{z_\chi^2} \sim 10^{-5}$, which ensures that the modulus will dominantly decay into a pair of color triplet superfield $(\chi, \bar{\chi})$ as compared to a pair of singlet superfields $(\mathcal{N}, \bar{\mathcal{N}})$ [141]. Now the scalar component of color triplet superfields further decay into quarks and additional singlet fermions ($\mathcal{N}$ and $\bar{\mathcal{N}}$) and

[1] Though the particle content is quite similar to the model considered in Ref. [347], the cogenesis mechanism producing the observed baryon asymmetry and the dark matter abundance discussed in this work is completely different.

the baryon number of the color triplet superfield ($\pm 2/3$) gets distributed between a quark and an additional singlet fermion. By imposing a discrete $\mathcal{Z}_2$ symmetry, under which the colored field χ and singlet fermion $\mathcal{N}$ are kept odd, while all SM and MSSM fields are even, we ensure that the singlet fermion will not further decay into the Standard Model (SM) particles and therefore can be considered as a dark matter candidate [2]. The decay process $\tilde{\chi} \to \mathcal{N}\bar{u}$ is baryon number conserving at tree level as well as at one-loop level, however, it is CP asymmetric at one-loop level due to the presence of soft SUSY breaking terms. Consequently, an asymmetry is generated in both the visible and the dark matter sector. The symmetric component of dark matter gets annihilated for a dark matter mass $\mathcal{O}(\,\mathrm{GeV})$, and the required order of baryon asymmetry and dark matter relic abundance can be successfully generated in this mechanism for certain values of Yukawa couplings.

The details of the phenomenological model based on Large Volume Scenario (LVS) dictating the modulus decay is beyond the scope of this thesis and we refer the readers to the original work [141] for an account of the same. Here we will only give the superpotential for an easy reference. Including the additional color triplet superfields $(\chi, \bar{\chi})$ and singlet superfields $(\mathcal{N}, \bar{\mathcal{N}})$, the matter superpotential is given by [3]

$$\begin{aligned} W_{\mathrm{matter}} &= \mu(\Phi) H_u H_d + \frac{1}{6} Y_{ijk}\,(\Phi)\, C^i C^j C^k \\ &+ M_\chi(\Phi)\chi\bar{\chi} + M_N\,(\Phi)\,\mathcal{N}\bar{\mathcal{N}} + \kappa_i(\Phi)\mathcal{N}\bar{\chi}u_i^c + \cdots\ . \end{aligned} \tag{7.3}$$

where C^i, $i = 1, 2, 3$ correspond to the three generations of MSSM superfields. In what follows, we will focus on the cogenesis mechanism itself.

7.1.1 Cogenesis mechanism

In this section, we discuss the cogenesis mechanism in which both the baryon asymmetry as well as the dark matter abundance are produced via the baryon number con-

[2] Note that the scalar and fermionic components of the superfield $\mathcal{N}$ (and similarly for $\bar{\mathcal{N}}$) have R-parity assignments -1 and 1, respectively. This means that the fermionic components of $\mathcal{N}$ and $\bar{\mathcal{N}}$ are not protected by R-parity alone (for example it can decay into quarks through a coupling like $\chi d_i d_j$). Consequently, to make the fermionic components stable dark matter candidates we had to invoke an additional Z_2 symmetry on $\mathcal{N}$ as well as the colored field χ.

[3] Note that the couplings like $\chi d_i d_j$ in the superpotential are forbidden due to the $\mathcal{Z}_2$ symmetry.

serving decay of a color triplet superfield χ. We consider the mass of the scalar and fermionic component of $(\mathcal{N}, \bar{\mathcal{N}})$ to be of the order of GeV, while the masses of the scalar and fermionic components of $(\chi, \bar{\chi})$ to be of the order of TeV. It follows from the results for the decay of the modulus into different species (discussed in [141]) that the modulus can dominantly decay into pairs of Higgses, axions associated with the imaginary part of the volume modulus, or color triplets. We are interested in a scenario where the baryon asymmetry can be produced at a low temperature through the decay of χ and in the process, one ends up with an asymmetric component of dark matter with a mass $\mathcal{O}(\text{ GeV})$ giving the correct relic density [4].

Baryon asymmetry and asymmetric dark matter

In this subsection, we describe a mechanism of baryogenesis where the fundamental interactions conserve baryon number, and baryogenesis happens by generating a certain amount of asymmetry in both the visible and the dark sector. We show that the decay products of the lightest eigenstate of the color triplet $\tilde{\chi}_-(\tilde{\bar{\chi}}_-)$ can simultaneously explain the observed baryon asymmetry and give rise to an asymmetric dark matter component, if $\mathcal{N}$ is light (mass $\mathcal{O}(\text{ GeV})$). The ratio of the asymmetric dark matter to the baryon density fractions is given by

$$\frac{\Omega_{\text{ADM}}}{\Omega_{\text{B}}} = \frac{\mathcal{Y}_{\text{ADM}}}{\mathcal{Y}_{\text{B}}} \frac{m_{\text{ADM}}}{m_B}, \tag{7.4}$$

where $\mathcal{Y}_{\text{ADM}}$ and $\mathcal{Y}_{\text{B}}$ are the asymmetric dark matter and the baryon abundances, respectively. The cosmic coincidence $\Omega_{\text{ADM}}/\Omega_{\text{B}} \sim 5$ is satisfied if $\mathcal{Y}_{\text{ADM}} \sim \mathcal{Y}_{\text{B}} \sim 10^{-10}$ for a dark matter mass $M_{\mathcal{N}}$ around 5 GeV. We have already mentioned that the modulus decays dominantly into pair of χ and $\bar{\chi}$ superfields. A cartoon showing the decay of the modulus into color triplet superfields which further decay into a singlet and a quark is given in Figure 7.1. Using the interaction term given in equation (7.3), it follows that the lightest mass eigenstate of $\chi(\bar{\chi})$ decays into quarks and fermionic component of the singlet superfield $\mathcal{N}(\bar{\mathcal{N}})$. The χ and $\bar{\chi}$ have baryon number assignments $B = +2/3$ and $B = -2/3$ respectively, while $\mathcal{N}$ and $\bar{\mathcal{N}}$ have baryon numbers $B = +1$ and

[4] Though the Higgs can further decay into the SM particles, it is not very relevant for explaining baryogenesis and the dark matter abundance in our scenario. Similar conclusions follow for closed (open) string axions.

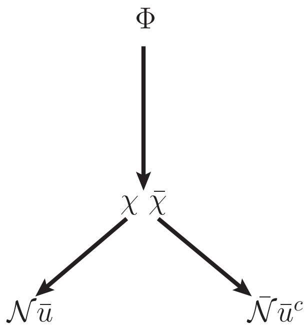

Figure 7.1: A cartoon showing decay of the modulus into color triplet and singlet superfields.

$B = -1$ respectively. Therefore, the interaction of χ with $\mathcal{N}$ and $\bar{u}$ conserves baryon number. The scalar and fermionic components of χ and $\bar{\chi}$ have R-parity assignments +1 and -1 respectively, while the scalar and fermionic components of $\mathcal{N}$ and $\bar{\mathcal{N}}$ have R-parity assignments -1 and +1 respectively. It follows that the decay process also conserves R-parity. Further, we impose a discrete $\mathcal{Z}_2$ symmetry under which additional color and singlet fields are kept odd, while all SM and MSSM fields are even. The symmetry ensures that the fermionic component of $\mathcal{N}(\bar{\mathcal{N}})$ will further not decay into the SM particles. Consequently, the fermionic component of $\mathcal{N}$ superfield produced during the decay of $\tilde{\chi}_-$ can be considered as a stable asymmetric dark matter particle. Thus, it follows that the decay of a scalar component of χ generates an equal and opposite amount of baryon asymmetry in the visible sector and the dark sector i.e.

$$\mathcal{Y}_B + \mathcal{Y}_{DM} = 0 \Rightarrow \mathcal{Y}_{DM} = -\mathcal{Y}_B. \tag{7.5}$$

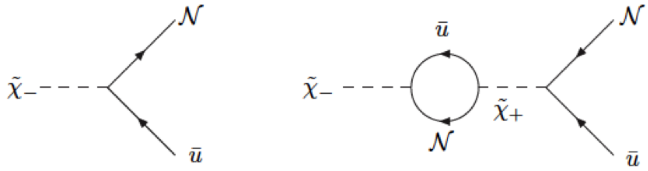

Figure 7.2: Feynman diagrams contributing to the baryon asymmetry and the dark matter asymmetry via a baryon number conserved interaction vertex.

Let us first calculate the baryon asymmetry generated in the visible sector. We begin by considering a single generation of singlet superfield $\mathcal{N}$. The CP violation arises due to the soft SUSY breaking terms. The degeneracy between the two states belonging to the supermultiplet of the same generation can be removed by including the SUSY breaking effects and the CP violation occurs due to the interference between the two states of a single generation [356,357], as compared to conventional baryogenesis mechanism where at least two generations are required for CP violation. The SUSY breaking Lagrangian involving χ and $\bar{\chi}$ superfields is given by

$$\begin{aligned}\mathcal{L}_{\text{soft}} &= m_{ij}^2 \tilde{\chi}_i{}^\dagger \tilde{\chi}_j + m_{ij}^2 \tilde{\bar{\chi}}_i^\dagger \tilde{\bar{\chi}}_j + B_{\chi ij} \hat{M}_{\chi ij} \tilde{\chi}_i \tilde{\bar{\chi}}_j \\ &+ A_{ijk} \kappa_{ijk} \tilde{\chi}_i \tilde{\mathcal{N}}_j \tilde{u}_k^* + h.c. \,,\end{aligned} \tag{7.6}$$

where indices i, j, k correspond to the different generations of the particles. The evolution of the system governing $\chi - \chi^\dagger$ mixing is given by [356,357]

$$\langle \tilde{\chi} | \mathcal{H} | \tilde{\chi}^\dagger \rangle = M_{\chi(12)} - \frac{i}{2} \Gamma_{\chi(12)}. \tag{7.7}$$

This induces a mass difference $\Delta m_{\tilde{\chi}}$ and a decay width difference $\Delta \Gamma_\chi$ between two mass states given by

$$|\tilde{\chi}_\pm\rangle = p|\tilde{\chi}\rangle \pm q|\tilde{\chi}^\dagger\rangle, \quad R = |q/p|. \tag{7.8}$$

The tree level and the one-loop diagrams responsible for generating CP violation are shown in Figure 7.2. The interaction Lagrangian in the mass basis $(\tilde{\chi}_+, \tilde{\chi}_-)$ is given by

$$-\mathcal{L}_{\text{int}} = \frac{\kappa}{\sqrt{2}} \tilde{\chi}_+ \mathcal{N} \bar{u} + \frac{\kappa}{\sqrt{2}} \tilde{\chi}_- \mathcal{N} \bar{u} + h.c. \,. \tag{7.9}$$

After the modulus decay produces an equal densities of $\tilde{\chi}$ and $\tilde{\chi}^\dagger$ (say at $t = 0$), the time evolution of the states are given by

$$\begin{aligned}\tilde{\chi}(t) &= f_+(t) \tilde{\chi}(0) + \frac{q}{p} f_-(t) \tilde{\chi}^\dagger(0), \\ \tilde{\chi}^\dagger(t) &= \frac{q}{p} f_-(t) \tilde{\chi}(0) + f_+(t) \tilde{\chi}^\dagger(0),\end{aligned} \tag{7.10}$$

where

$$\begin{aligned}f_+(t) &= e^{-i m_{\tilde{\chi}} t} e^{-\Gamma_{\tilde{\chi}} t/2} \cos(\Delta m_{\tilde{\chi}} t/2), \\ f_-(t) &= e^{-i m_{\tilde{\chi}} t} e^{-\Gamma_{\tilde{\chi}} t/2} \sin(\Delta m_{\tilde{\chi}} t/2).\end{aligned} \tag{7.11}$$

Here, $\Gamma_{\tilde{\chi}}$ corresponds to total decay width of $\tilde{\chi}$. The excess of $\mathcal{N}, \bar{u}$ over the CP conjugate states $\mathcal{N}^c, \bar{u}^c$ is given by

$$\epsilon_\chi = \frac{\int_0^\infty dt\,(A-B)}{\int_0^\infty dt\,(A+B)}, \tag{7.12}$$

where

$$\begin{aligned} A &= \Gamma\left(\tilde{\chi}(t) \to \mathcal{N}\bar{u}\right) + \Gamma(\tilde{\chi}(t)^\dagger \to \mathcal{N}\bar{u}), \\ B &= \Gamma\left(\tilde{\chi}(t) \to \bar{\mathcal{N}}\bar{u}^c\right) + \Gamma(\tilde{\chi}(t)^\dagger \to \bar{\mathcal{N}}\bar{u}^c). \end{aligned} \tag{7.13}$$

The decay width for the decay modes of $\tilde{\chi}(t)$ and $\tilde{\chi}(t)^\dagger$ is given by[5]

$$\begin{aligned} &\Gamma(\tilde{\chi}(t) \to \mathcal{N}\bar{u}) = \Gamma(\tilde{\chi}(t)^\dagger \to \bar{\mathcal{N}}\bar{u}_i^c) = X_1|M_{u\mathcal{N}}|^2 f_+(t), \\ &\Gamma(\tilde{\chi}(t)^\dagger \to \mathcal{N}\bar{u}) = X_1|M_{u\mathcal{N}}|^2 R^{-2} f_-(t), \\ &\Gamma(\tilde{\chi}(t) \to \bar{\mathcal{N}}\bar{u}^c) = X_1|M_{u\mathcal{N}}|^2 R^{+2} f_-(t), \end{aligned} \tag{7.14}$$

where X_1 is the normalization factor and $M_{u\mathcal{N}}$ is the amplitude of the decay mode considered. Incorporating these expressions into equation (7.12), the asymmetry parameter is given by [356, 357]

$$\epsilon_\chi = \frac{1}{2}\left(\left|\frac{q}{p}\right|^2 - \left|\frac{p}{q}\right|^2\right) \frac{\int_0^\infty dt\,|f_-|^2}{\int_0^\infty dt\left(|f_+|^2 + |f_-|^2\right)}, \tag{7.15}$$

with

$$\left|\frac{q}{p}\right|^2 - \left|\frac{q}{p}\right|^2 \sim \mathrm{Im}\frac{\Gamma_{\chi(12)}}{M_{\chi(12)}} = \frac{\Gamma_\chi\,\mathrm{Im}A}{B_\chi M_\chi}, \tag{7.16}$$

and

$$\frac{\int_0^\infty dt\,|f_-|^2}{\int_0^\infty dt\left(|f_+|^2 + |f_-|^2\right)} = \frac{(\Delta M_\chi)^2}{2(\Gamma_\chi^2 + (\Delta M_\chi)^2)}. \tag{7.17}$$

The decay width for χ_- decaying into $\mathcal{N}\bar{u}$ is given by $\Gamma_\chi = \frac{\kappa\kappa^\dagger}{4\pi}\hat{M}_\chi$. The asymmetry is given by

$$\epsilon_B = \frac{\Gamma_\chi}{\Gamma_\chi^2 + B_\chi^2}\frac{B_\chi\,\mathrm{Im}A}{2\hat{M}_\chi}. \tag{7.18}$$

Now, $B_\chi \hat{M}_\chi = \hat{M}_\chi \sim \mathcal{O}(\,\mathrm{TeV})$, and $\kappa \lesssim 1$, implying $\Gamma_\chi < B_\chi$. In the small κ limit, the above equation reduces to

$$\epsilon_B = \frac{\kappa\,\mathrm{Im}\mathcal{A}}{8\pi}\frac{\hat{M}_\chi}{B_\chi \hat{M}_\chi}, \tag{7.19}$$

[5] Since we are working with a single generation, the direct CP violation [358] can be neglected. Therefore, the amplitude of the decay process $(\tilde{\chi}(t) \to \mathcal{N}u^c)$ and its CP conjugate state are the same.

where $\mathcal{A} = \kappa\, A$. The baryon asymmetry generated from the modulus decay is given by

$$Y_B = \frac{n_B - n_{\bar{B}}}{n_\gamma} = Y_{\tilde{\chi}}\epsilon_B. \tag{7.20}$$

Since the Yukawa couplings do not depend on the compactification volume in this model, we choose $\kappa \sim 10^{-2}$. For $\mathcal{A} \sim \mathcal{O}(\,\mathrm{TeV})$, we get $\epsilon_B = 10^{-3}$.

The value of $Y_{\tilde{\chi}}$ is given by

$$Y_{\tilde{\chi}} = Y_\Phi \mathrm{Br}_\chi = \frac{3T_R}{4M_\Phi}\mathrm{Br}_\chi, \tag{7.21}$$

where T_R is the reheating temperature after the modulus decay and M_Φ is the mass of the modulus field Φ. For $\mathrm{Br}_\chi = 1, T_R \sim 10\,\mathrm{GeV}$ and $M_\Phi \sim 5\times 10^7\,\mathrm{GeV}$, we get $Y_{\tilde{\chi}} \sim 10^{-7}$. Finally, from equation (7.20) the baryon asymmetry is given by $\mathcal{Y}_B \sim 10^{-3-7} = 10^{-10}$, which is the observed baryon asymmetry of the universe. From equation (7.5), the asymmetry in the dark matter sector is given by $\mathcal{Y}_{\mathrm{DM}} \equiv \mathcal{Y}_{\mathcal{N}} \sim 10^{-10}$.

7.1.2 Annihilation of the symmetric dark matter component

In additional to an asymmetric DM component, a symmetric non-zero DM density can also be produced either directly via the modulus decay (with a very small branching ratio) or via χ decay. The fractional asymmetry [359, 360] in case of asymmetric DM is defined by

$$r = \frac{n(\mathcal{N})}{n(\bar{\mathcal{N}})} \tag{7.22}$$

where $r = 0$ and $r = 1$ correspond to complete asymmetric and symmetric DM abundance respectively. In order to ensure that the symmetric component is not out-of-equilibrium initially and starts to get depleted, the annihilation cross section of the symmetric component should be higher than the freeze out cross section corresponding to the number density of DM produced after modulus decay. On the other hand, the asymmetry generation mechanism presented in the previous section dynamically produces an asymmetry between particles and antiparticles in both visible and the dark sectors during decay of χ. In order to ensure make overall dark matter abundance asymmetric, one also needs to ensure that the symmetric component of dark matter produced during decay of χ gets depleted efficiently. Solving the Boltzmann equation yields the late time dark matter asymmetry [359, 360] given by

$$r_\infty = \exp\left[-2\left(\frac{\sigma_0}{\sigma_{\rm WIMP}}\right)\left(\frac{1-r_\infty}{1+r_\infty}\right)\right] \to \exp\left[-2\frac{\sigma_0}{\sigma_{\rm WIMP}}\right] \tag{7.23}$$

where σ_0 corresponding to DM annihilation is related to thermally-averaged cross-section by

$$\langle\sigma_0 v\rangle = \sigma_0\left(\frac{T}{M_{\mathcal{N}}}\right)^n, \tag{7.24}$$

with n = 0 and 1 for s-wave and p-wave annihilation respectively. Thus, Eq. (7.23) right away tells that r_∞ depends exponentially on the annihilation cross section and complete annihilation of the symmetric part of DM in ADM models requires an annihilation cross-section

$$\sigma_0 \geq \text{few} \times \sigma_{\rm WIMP}. \tag{7.25}$$

In our model, the annihilation of $\mathcal{N}$ and $\mathcal{N}^c$ can be mediated through the electroweak neutral Z boson. The thermally averaged annihilation cross section for $\mathcal{N}\mathcal{N}^c \to Z \to f\bar{f}$ is given by

$$\langle\sigma\,|v|\rangle_{\rm annihilation} = \sigma_0 \sim \frac{1}{4\pi}\frac{g'^2 g^2 M_{\mathcal{N}}^2}{M_Z^4}, \tag{7.26}$$

where g' corresponds to the gauge coupling of neutral Z boson to the pair of singlet superfields $(\mathcal{N}, \bar{\mathcal{N}})$, g corresponds to the gauge coupling of Z boson to a pair of fermions, M_Z is the mass of Z boson and the annihilation is presumed to be s-wave.

Now, the freeze-out cross-section can be roughly estimated by the rule of thumb given by

$$\Gamma = n\langle\sigma\,|v|\rangle = H, \tag{7.27}$$

similar to the case of WIMP dark matter. However, in this case the reference temperature is the reheating temperature after the decay of the modulus. The Hubble expansion rate is given by $H = 1.67\sqrt{g_*}\frac{T_R^2}{M_P}$. The density of the symmetric component of $\mathcal{N}$ is given by $n = {\rm Br}_{\mathcal{N}}\frac{3T_R}{4m_\Phi} \times s$, where s is the entropy density. Using $s = \frac{2\pi^2}{45}g_* T_R^3$, the freeze-out cross-section is given by

$$\langle\sigma\,|v|\rangle_{\rm freeze\ out} = \frac{50}{\pi^2\sqrt{g_*}}\frac{m_\Phi}{{\rm Br}_{\mathcal{N}}\, T_R^2 M_P}. \tag{7.28}$$

Using $T_R = g_*^{-1/4}\sqrt{\Gamma_\Phi M_P}$, $\Gamma_\Phi \sim \frac{1}{24\pi}\frac{m_\Phi^3}{M_P^2}$, $m_\Phi = \mathcal{O}(1)\times 10^7$ GeV and ${\rm Br}_{\mathcal{N}} \sim 10^{-5}$, we get

$$\langle\sigma\,|v|\rangle_{\rm freeze\ out} \sim 10^{-9}\,{\rm GeV}^{-2} \sim 10^{-26}{\rm cm}^3{\rm s}^{-1}, \tag{7.29}$$

On the other hand, the thermally averaged cross-section for thermal WIMP with mass $\leq$ few GeV is $\langle\sigma\,|v|\rangle_{\rm WIMP} \sim (4.5-5)\times 10^{-26}{\rm cm}^3{\rm s}^{-1}$. In Eq. (7.26), taking $g \sim 0.74, g' \sim 0.8$ and $M_{\mathcal{N}} = 5\,{\rm GeV}$, we find

$$\langle\sigma\,|v|\rangle_{\rm annihilation} = \sigma_0 \sim \langle\sigma_0 v\rangle \sim 10^{-8}\,{\rm GeV}^{-2} \sim 10^{-25}{\rm cm}^3{\rm s}^{-1}. \tag{7.30}$$

Thus it follows that $\langle\sigma\,|v|\rangle_{\rm annihilation} > \sigma\,|v|\rangle_{\rm freeze-out}$ and consequently the symmetric component of the abundance of singlet fermion $\mathcal{N}$ is not out-of-equilibrium and starts to get depleted. On the other hand, $\langle\sigma_0 v\rangle > \langle\sigma\,|v|\rangle_{\rm WIMP}$ ensures that the symmetric component of the initial dark matter abundance, produced during modulus decay and asymmetry generation from decay of χ, gets annihilated rapidly and does not contribute to final the dark matter relic abundance in our scenario. Thus, we conclude that all the symmetric DM density gets annihilated away and the required DM abundance is produced due to an overall asymmetric DM density only.

7.2 Summary of the chapter

We have discussed a cogenesis mechanism unifying the generation of both baryon asymmetry of the universe and dark matter abundance in a model, where both baryon asymmetry and non-thermal dark matter abundance can be generated simultaneously from the decay of a pair of color triplets produced after reheating. We discussed a case where the modulus dominantly decays into a pair of color triplets, and the lightest eigenstate of the scalar component of the color triplet further decays into a singlet fermion and an up type quark. Imposition of a discrete $\mathcal{Z}_2$ symmetry ensures that the singlet fermion does not further decay into the SM particles and therefore it can be considered as a stable dark matter candidate. The CP asymmetry is generated via the interference of tree level and one loop diagrams for the decay of the color triplets in the presence of soft SUSY breaking terms. We have also discussed the possibility of obtaining the observed baryon asymmetry of the universe and the asymmetric dark matter abundance by considering dark matter mass around 5 GeV, and the cosmic coincidence is natural in this scenario.

Chapter 8

Neutrino dark energy and leptogenesis with TeV scale triplets

Evidence from the astrophysical observations suggests that out of the total mass-energy budget of the universe, the baryonic and dark matter together account for only about 30% while the remaining 70%, referred to as dark energy, is attributable to the entity that causes the accelerated expansion of the universe which remains a challenge to explain. While the existence of a scalar field provides an explanation, the striking proximity of the effective scales of neutrino masses and the dark energy points to a connection between them, realized in the neutrino dark energy (νDE) models. To this end, several approaches have been proposed in the literature [142–165]. In some of the scenarios, a direct connection through the formation of a neutrino condensate at a late epoch of the early universe using the effective self-interaction has been studied [142–148]. Another class of models utilizes the variation of neutrino masses to dynamically obtain the dark energy [149–165]. In this section, we will focus on this latter approach [165].

The atmospheric, solar, and reactor neutrino oscillation experiments have confirmed the existence of nonzero masses of neutrinos. An attractive explanation of neutrino masses employs the seesaw mechanism [16–22], giving rise to naturally small masses for neutrinos. In addition, the baryon asymmetry of the universe can be generated through leptogenesis [90] in the framework of the seesaw scenario. In the original νDE models, the Standard Model (SM) is extended to accommodate singlet right-handed neutrinos (N_i, $i = 1, 2, 3$) giving Majorana masses to light neutrinos. The Majorana mass of the right-handed neutrinos are made to vary with a scalar field, called the acceleron (which drives the universe to a late time accelerating phase), connecting the light neutrino masses with the scale of dark energy [150]. However, for a sufficiently flat potential one requires the Majorana masses of the right-handed neutrinos to be in the eV range, in contradiction to the expected scenario of a very heavy M_{N_i} triggering the canonical seesaw mechanism. One requires a flat potential for the acceleron to have $\omega \sim -1$ in the equation of state $p(t) = \omega\rho(t)$, where p and ρ are the pressure and energy density, respectively. As discussed later the acceleron field can be associated with a varying light neutrino mass and hereafter we will describe the scalar potential in terms of the varying light neutrino mass rather than the acceleron. From the cutoff insensitive correction to the scalar potential $\delta V_0 \sim \bar{m}^4 \log(\bar{m}/\mu)/32\pi^2$, where μ is the renormalization scale, we note that μ needs to be of the order of $\bar{m}$ today for a small correction. Using this, one can get a rough estimation for the mass of the variable mass particle. If we want a variable mass particle to give dark energy with an equation of state parameter $\omega \sim -1$ then we require [150] $|\delta V_0'(\bar{m})\bar{m}/V| < 1$, which gives $\bar{m}^4 \lesssim (10^{-2}\ \mathrm{eV})^4$. Here we use $V \sim \rho_{DE} \simeq 0.7\rho_c \sim 10^{-11}\ \mathrm{eV}^4$, where ρ_c is the critical density. Note that a value of the neutrino mass can also be obtained by equating the acceleron potential energy density today, which depends on the neutrino mass, to the dark energy density. However, given the mild dependence of the potential on the neutrino mass, we prefer the above estimation to that. Now for a particle with a variable mass $\bar{m}$, at the one-loop level the quadratically divergent contribution to the potential is given by $\delta V \sim \bar{m}^2\Lambda^2/16\pi^2$, where Λ is the cutoff scale of the theory, which can be identified with the heavy neutrino mass scale in type-I seesaw. One might assume that this short distance physics is such that this contribution is small, however, this is conventionally thought to be unnatural. Now to obtain a bound on Λ we use the condition $\delta V \sim \bar{m}^2\Lambda^2/16\pi^2 < V$, which requires a sub-$\mathrm{eV}$ Λ for $\bar{m} \sim 10^{-2}\ \mathrm{eV}$. Note that we have done a very rough estimation above and typically this bound is relaxed to $\Lambda \sim \mathrm{eV}$ [150] and this is naturally realized in the models that we discuss later. In Ref. [158], it was pointed out that the above problem can be avoided if the SM is extended to include triplet Higgs scalars. However, in such a scheme the coefficient of the trilinear scalar coupling with mass dimension varies with the acceleron field and this predicts the mass scale of the triplet Higgs scalars to be close to the electroweak symmetry breaking scale (of order $100\,\mathrm{GeV}$), which has not been observed at the LHC so far.

In this chapter, we discuss two ways to get around the above constraint, while simultaneously explaining the observed baryon asymmetry of the universe. One way is to add some additional scalar field to push the additional scalar field masses to TeV scale, readily testable at the current run of LHC. Another way is to add fermion triplets instead of scalar triplets and utilize the type III seesaw scheme.

First we discuss a realization of mass varying neutrinos in an extension of the usual triplet Higgs model which includes a second Higgs doublet (η) in addition to the SM Higgs doublet (Φ) and Higgs triplet (ξ), but no right-handed neutrinos [23, 361]. In this scenario both additional Higgs fields are of the TeV scale and the smallness of neutrino mass comes from the lepton number breaking scalar sector. This model has highly predictive collider signatures and thus it can be right away put to test in the current run of LHC. Next we discuss a model of νDE utilizing an extension of the SM with fermion triplet $(\Sigma^+, \Sigma^0, \Sigma^-)_R$, where the neutrino mass is dynamical and related to the acceleron field. This model can naturally give the correct energy scale associated with the neutrino mass and it provides a rich TeV scale phenomenology, testable at the LHC. We also point out possible leptogenesis mechanisms for simultaneously generating the observed baryon asymmetry of the universe in both models.

8.1 Neutrino masses and the dark energy connection

By extending the SM to include a heavy Higgs triplet (ξ^{++}, ξ^{+}, ξ^{0}) with trilinear couplings to both the lepton doublet $L_i = (\nu_i, l_i)$ and the Higgs doublet $\Phi = (\phi^+, \phi^0)$, one can realize the unique dimension-five effective operator [12]

$$\mathcal{L}_{\text{eff}} = \frac{f_{ij}}{\Lambda} L_i L_j \Phi\Phi, \tag{8.1}$$

obtained by integrating out the heavy degrees of freedom (with mass much larger than the ordinary SM particles) associated to a characteristic heavy mass scale Λ. Thus the neutrinos, massless in the minimal SM, acquire small Majorana masses. The relevant interaction terms are given by

$$\mathcal{L}_{\rm int} = f_{ij}\left[\nu_i\nu_j\xi^0 + \frac{1}{\sqrt{2}}(\nu_i l_i + l_j\nu_j)\xi^+ + l_i l_j\xi^{++}\right] + \text{h.c.}\,, \tag{8.2}$$

and the general Higgs potential is given by

$$\begin{aligned} V &= m^2\Phi^\dagger\Phi + M^2\xi^\dagger\xi + \frac{1}{2}\lambda_1(\Phi^\dagger\Phi)^2 + \frac{1}{2}\lambda_2(\xi^\dagger\xi)^2 + \lambda_3(\Phi^\dagger\Phi)(\xi^\dagger\xi) \\ &+ \mu(\bar{\xi}^0\phi^0\phi^0 + \sqrt{2}\xi^-\phi^+\phi^0 + \xi^{--}\phi^+\phi^+) + \text{h.c.} \quad . \end{aligned} \tag{8.3}$$

The above interaction terms give [23]

$$(M_\nu)_{ij} = \frac{2f_{ij}\mu\langle\phi^0\rangle^2}{m^2_{\xi^0}}. \tag{8.4}$$

Thus it follows that if μ is a function of the acceleron field $\mathcal{A}$ i.e. $\mu = \mu(\mathcal{A})$, then the mass varying neutrinos can be realized for m_ξ of the order of the electroweak scale. However, if the νDE is indeed realized through the Higgs triplet, then at least ξ^{++} should have been observable at the LHC. Thus it is worth exploring if such a Higgs triplet can be schemed to have a mass of TeV scale in light of the current run of LHC.

8.1.1 Model A

In the presence of the additional Higgs doublet η in the above scheme, the neutrino masses come from the Higgs triplet ξ (with lepton number assignment $L = -2$) and its interaction with η (carrying lepton number $L = -1$) [361]. The most general lepton number conserving scalar potential is given by

$$\begin{aligned} V &= m_1^2\Phi^\dagger\Phi + m_2^2\eta^\dagger\eta + m_3^2\text{Tr}[\Delta^\dagger\Delta] \\ &+ \frac{1}{2}\lambda_1(\Phi^\dagger\Phi)^2 + \frac{1}{2}\lambda_2(\eta^\dagger\eta)^2 + \frac{1}{2}\lambda_3(\text{Tr}[\Delta^\dagger\Delta])^2 \\ &+ \frac{1}{2}\lambda_4(\text{Tr}[\Delta^\dagger\Delta^\dagger])(\text{Tr}[\Delta\Delta]) + \lambda_5(\Phi^\dagger\Phi)(\eta^\dagger\eta) \\ &+ \lambda_6(\Phi^\dagger\Phi)(\text{Tr}[\Delta^\dagger\Delta]) + \lambda_7(\eta^\dagger\eta)(\text{Tr}[\Delta^\dagger\Delta]) \\ &+ \lambda_8(\Phi^\dagger\eta)(\eta^\dagger\Phi) + \lambda_9(\Phi^\dagger\Delta^\dagger\Delta\Phi) + \lambda_{10}(\eta^\dagger\Delta^\dagger\Delta\eta) \\ &+ \mu(\eta^\dagger\Delta\tilde{\eta}) + \text{h.c.}\,, \end{aligned} \tag{8.5}$$

where

$$\Delta = \begin{pmatrix} \xi^+/\sqrt{2} & \xi^{++} \\ \xi^0 & -\xi^+/\sqrt{2} \end{pmatrix}, \tag{8.6}$$

$\tilde{\eta} = (\bar{\eta}^0, -\eta^-)$ and μ has the dimension of mass. The lepton number is softly broken by the terms

$$V_{\rm soft} = \mu_1^2 \Phi^\dagger \eta + \mu_2 \left(\Phi^\dagger \Delta \tilde{\eta}\right) + \mu_3 \left(\Phi^\dagger \Delta \tilde{\Phi}\right) + {\rm h.c.}\ , \tag{8.7}$$

where $\tilde{\Phi} = (\bar{\phi}^0, -\phi^-)$. Next we define vacuum expectation values (VEVs) of the scalar fields to be $\langle \phi^0 \rangle = v_1$, $\langle \eta^0 \rangle = v_2$ and $\langle \xi^0 \rangle = v_3$. Now minimization of the potential with respect to the various Higgs fields give the consistency conditions and the relations between the different VEVs, which can be solved assuming $m_1^2 < 0$, but $m_2^2 > 0$ and $m_3^2 > 0$ to obtain

$$\begin{aligned} v_1^2 &\simeq -m_1^2/\lambda_1, \\ v_2 &\simeq -\mu_1^2 v_1/[m_2^2 + (\lambda_5 + \lambda_8) v_1^2], \\ v_3 &\simeq -\left(\mu v_2^2 + \mu_2 v_1 v_2 + \mu_3 v_1^2\right)/(m_3^2 + \lambda_6 v_1^2). \end{aligned} \tag{8.8}$$

Thus taking m_2, m_3 and μ to be $M \sim$ TeV we have

$$v_2 \sim \mu_1^2 v_1/M^2, \qquad v_3 \sim v_2^2/M. \tag{8.9}$$

Consequently, $u \ll v_2 \ll v_1$ and

$$v_3 \sim \mu_1^2 v_1^2/M^5. \tag{8.10}$$

For $v_1 \sim 10^2\,$GeV and $\mu_1 \sim 1\,$GeV we have $v_2 \sim 0.1\,$MeV and $v_3 \sim 10^{-2}\,$eV, which gives the correct order of magnitude for neutrino mass $(m_\nu)_{ij} = 2 f_{ij} v_3$. Thus we have a natural realization of the required small neutrino masses with TeV scale additional Higgs fields, which does not need any large extra space dimensions constraining m_ξ below the cutoff energy scale. Moreover, this model is much more flexible compared to the scenario with only Higgs triplet in the sense that there is no strict constraint on m_ξ to be of the order of electroweak scale. Now the realization of νDE model through mass varying neutrinos is straightforward. The idea is to make μ_1 a function of the acceleron field $\mathcal{A}$, i.e. $\mu_1 = \mu_1(\mathcal{A})$. We will come back to the realization of νDE once we give the account of the other model below.

8.1.2 Model B

The extension of the fermion (lepton) sector of the SM can be realized in two ways. The basic idea is that the new lepton multiplet gains a large mass and then it mixes with the ordinary lepton doublet triggering the seesaw mechanism. The new lepton multiplet can only be a singlet or a triplet of $SU(2)_L$. The idea of the triplet lepton representation to utilize the seesaw structure in neutrino mass matrix was first proposed in Ref. [27], referred to as type III seesaw, which have been generalized in the context of unified theories in Ref. [52]. The simplest way to utilize type III seesaw is to add the $SU(2)_L$ triplet with zero hypercharge,

$$\Sigma = \begin{pmatrix} \Sigma^0/\sqrt{2} & \Sigma^+ \\ \Sigma^- & -\Sigma^0/\sqrt{2} \end{pmatrix}, \tag{8.11}$$

to the SM, with the interaction terms

$$\begin{aligned} \mathcal{L}_{\rm int} = & - \frac{1}{2}\mathrm{Tr}\left[\bar{\Sigma}\mathrm{M}_\Sigma\Sigma^c + \bar{\Sigma}^c\mathrm{M}_\Sigma^*\Sigma\right] - \tilde{\Phi}^\dagger\bar{\Sigma}\sqrt{2}\mathrm{Y}_\Sigma\mathrm{L} \\ & - \bar{L}\sqrt{2}Y_\Sigma^\dagger\Sigma\tilde{\Phi}. \end{aligned} \tag{8.12}$$

The terms related to the neutrino mass matrix can be identified readily to obtain the mass matrix as

$$\mathcal{L}_{\nu,\rm mass} = \begin{pmatrix} \nu & \Sigma^0 \end{pmatrix} \begin{pmatrix} 0 & Y_\Sigma v/2\sqrt{2} \\ Y_\Sigma^T v/2\sqrt{2} & M_\Sigma/2 \end{pmatrix} \begin{pmatrix} \nu \\ \Sigma^0 \end{pmatrix}. \tag{8.13}$$

This gives the non-zero neutrino masses

$$M_\nu = -\frac{v^2}{2} Y_\Sigma^T M_\Sigma^{-1} Y_\Sigma. \tag{8.14}$$

Now the neutrino masses can be connected to the dark energy by simply taking $M_\Sigma = M_\Sigma(\mathcal{A})$; however, such a scenario is constrained from the flatness of the potential as discussed earlier. This scheme can be generalized right away by accommodating the right-handed neutrinos $N_i^c, i = 1, 2, 3$ in the scenario. The most general neutrino mass matrix in such a scenario can be written as

$$\mathcal{L}_{\nu,\rm mass} = \begin{pmatrix} \nu & N^c & \Sigma^0 \end{pmatrix} \begin{pmatrix} 0 & M_N & F_1 u \\ M_N^T & 0 & F_2\Omega \\ F_1^T u & F_2^T\Omega & M_\Sigma \end{pmatrix} \begin{pmatrix} \nu \\ N^c \\ \Sigma^0 \end{pmatrix}, \tag{8.15}$$

where the off-diagonal terms in the third column and row correspond to the mass terms $F_{1ij}\nu_i\Sigma^0 u$ and $F_{2ij}N_i^c\Sigma^0\Omega$ with u and Ω being the VEVs of the corresponding Higgs fields. The realization of the nonrenormalizable term, giving rise to type III seesaw,

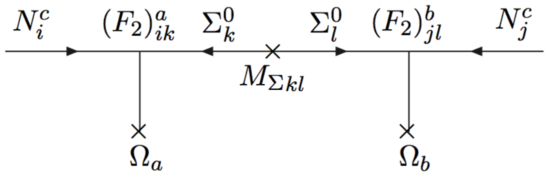

Figure 8.1: Diagram realizing the effective nonrenormalizable operator generating right handed neutrino mass $M_R = (F_2\Omega)M_\Sigma^{-1}(F_2^T\Omega)$.

by integrating out heavy fields, is shown in Fig. 8.1. The neutrino mass in the above scenario has two kinds of contributions, given by

$$M_\nu = -M_N(F_2\Omega M_\Sigma^{-1}F_2^T\Omega)^{-1}M_N^T - (M_N + M_N^T)\frac{u}{\Omega}, \tag{8.16}$$

where the first term corresponds to a "double seesaw" contribution and the second term corresponds to the type III seesaw contribution. The relative contributions of the two kinds of terms to M_ν is model dependent. We will consider the case $M_N \sim 1\,\text{eV}$. Now taking $u \sim v \sim 10^2\,\text{GeV}$, $\Omega \sim 10^4\,\text{GeV}$ and considering the phenomenologically interesting case $M_\Sigma \sim 10^3\,\text{GeV}$ with verifiable implications at the current run of LHC, it follows that for $F_2 \gtrsim 10^{-6}$ the dominant contribution to M_ν in Eq. (8.16) comes from the second term associated with the type III seesaw contribution and for the above set of values we obtain $M_\nu \sim 10^{-2}\,\text{eV}$ as desired. The mass varying neutrinos can be realized by taking $M_N = M_N(\mathcal{A})$.

8.1.3 Realization of neutrino dark energy

Having given the details of the two models realizing mass varying neutrinos with desired small masses, we are now ready to discuss the realization of νDE where the neutrino mass (assumed to be a function of the canonically normalized acceleron field $\mathcal{A}$) $M_\nu(\mathcal{A})$ is a dynamical quantity and $\partial M_\nu/\partial\mathcal{A} \neq 0$ [150]. We will describe the scalar potential associated with the acceleron in terms of the varying neutrino mass. In the nonrelativistic limit, the energy density consists of the thermal neutrino (and antineutrino) background ($M_\nu n_\nu$) and the scalar potential $V_0(M_\nu)$. The effective potential can be written as

$$V(M_\nu) = M_\nu n_\nu + V_0(M_\nu). \tag{8.17}$$

The neutrino background (driving M_ν to small values) gets diluted as the universe expands and the source term decreases as a result, while we assume that V_0 is minimized for a large M_ν. Thus the two terms act in the opposite directions with a minimum at some intermediate M_ν with a non-zero V_0. The minimum of the effective potential is given by

$$V'(M_\nu) = n_\nu + V_0'(M_\nu) = 0. \tag{8.18}$$

We consider a scenario where the field sits at the minimum of the potential and it varies with time as n_ν gets diluted. Now at any instant of time assuming the simple equation of state

$$p(t) = \omega \rho(t), \tag{8.19}$$

and taking $\rho(t) \simeq V(t)$, we use the equation

$$\dot{\rho} + 3H(1+\omega)\rho = 0, \tag{8.20}$$

to obtain

$$\begin{aligned}
\omega + 1 \simeq -\frac{\partial \log V}{3\partial \log a} \quad &= -\frac{a}{3V}\left(M_\nu \frac{\partial n_\nu}{\partial a} + n_\nu \frac{\partial M_\nu}{\partial a} + V_0'(M_\nu)\frac{\partial M_\nu}{\partial a}\right) \\
&= \frac{M_\nu n_\nu}{V} \equiv \frac{\Omega_\nu}{\Omega_\nu + \Omega_{\mathcal{A}}} \\
&= -\frac{M_\nu V_0'(M_\nu)}{V},
\end{aligned} \tag{8.21}$$

where we have used Eq. (8.18) and $\Omega_\nu = M_\nu n_\nu/\rho_c$ is the neutrino energy density and $\Omega_{\mathcal{A}} = \rho_A/\rho_c$ corresponds to the contribution of $V_0(M_\nu)$ to the energy density, with ρ_c is the critical density and a is the cosmic scale factor. Since the observed value of $\omega \simeq -1$, Eqn. (8.21) implies that the energy density in the thermal neutrino background must be much less compared to the total dark energy density. This in turn suggests that the potential $V_0(M_\nu)$ should be a flat potential. For the case where $d\omega/dn_\nu$ is small, the relation

$$M_\nu \propto n_\nu^\omega \tag{8.22}$$

holds. The above considerations are independent from any specific model of neutrino mass [150] and we will use them to draw out the phenomenological consequences specific to the two models of interest.

As we have discussed above in model A, $\mu_1 = \mu_1(\mathcal{A})$ makes the effective mass of the neutrinos to vary. While in model B, $M_N = M_N(\mathcal{A})$ does the same. Now for the self interactions of the acceleron field $\mathcal{A}$ we take as an example flat effective potential of the form

$$V_0 = \lambda^4 \log(1 + |\bar{\mathcal{M}}/\mathcal{M}(\mathcal{A})|), \tag{8.23}$$

where $\bar{\mathcal{M}}$ is a constant. In model A, $\mathcal{M}(\mathcal{A}) = \mu_1(\mathcal{A})$ and in model B, $\mathcal{M}(\mathcal{A}) = M_N(\mathcal{A})$. Hence Eqn. (8.17) takes the form

$$V(x) = a_1 x + a_2 \log\left(1 + \frac{a_3}{x}\right), \tag{8.24}$$

where $x = M_\nu \propto |\mu(\mathcal{A})|$ and a_1, a_2, a_3, and x are all positive. Now assuming $a_3/x \gg 1$ it follows that $x_{\min} \propto a_2/a_1$ implying

$$M_\nu \propto n_\nu^{-1}, \tag{8.25}$$

which gives the desired $\omega \simeq -1$. Thus, the two models under consideration can naturally explain the νDE for TeV scale ξ, η masses in model A and TeV scale mass of the new fermion triplet Σ in model B. The TeV scale mass of these particles makes these models particularly interesting in the context of collider phenomenology at the LHC. We will come back to the implications and signatures of these two models for colliders such as the LHC, once we address the issue of leptogenesis in these two models.

8.2 Leptogenesis

In model A, the SM is extended to include scalar triplets and an additional Higgs doublet η, providing an attractive possibility of realizing a successful leptogenesis scenario. We start with the conventional formalism of scalar triplet leptogenesis in a hierarchical case. $SU(2)_L \times U(1)_Y$ is the valid gauge group at an energy scale far above the electroweak symmetry breaking. Thus it follows that if we analyze one of the three components of the triplet scalar field then the results will hold for the other two. From Eqs. (8.2), (8.5) and (8.7) we can read off the decay modes of ξ^{++} as

$$\xi_a^{++} \to \begin{cases} l_i^+ l_j^+ & (L=-2), \\ \phi^+\phi^+ & (L=-2), \\ \eta^+\eta^+ & (L=-0). \end{cases}, \tag{8.26}$$

where $a = 1, 2, 3$ is the generation index. The coexistence of the above decay modes implies nonconservation of lepton number, however, the lepton asymmetry generated by ξ^{++} gets compensated by the decays of ξ^{--}, unless CP is also violated and the decays take place out-of-equilibrium. We follow the mass matrix formalism [23, 104], where the tree level mass matrix for the triplets are assumed to be real and diagonal. Hence CP is conserved at tree level; however, CP conservation occurs at one-loop level due to interference between the tree and one-loop diagrams shown in Fig. 8.2. Note that at least two ξ's are required for CP nonconservation to occur. Following the

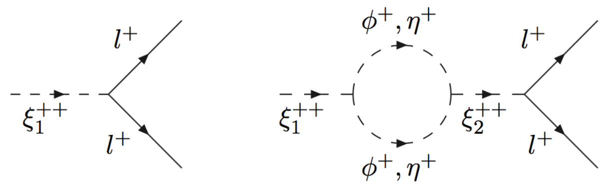

Figure 8.2: The tree level (left) and one-loop (right) decay diagrams for $\xi^{++} \to l^+ l^+$. A lepton asymmetry is generated by the CP violation occurring due to the interference between them.

mass-matrix formalism of Ref. [104], the diagonal tree-level mass matrix of ξ_a in Eq. (8.5) is modified in the presence of interactions to

$$\frac{1}{2}\xi^\dagger \left(M_+^2\right)_{ab} \xi_b + \frac{1}{2}\left(\xi_a^*\right)^\dagger \left(M_-^2\right)_{ab} \xi_b^*, \tag{8.27}$$

where

$$M_\pm^2 = \begin{pmatrix} M_1^2 - i\Gamma_{11}M_1 & -i\Gamma_{12}^\pm \\ -i\Gamma_{21}^\pm M_1 & M_2^2 - i\Gamma_{22}M_2 \end{pmatrix}, \tag{8.28}$$

with $\Gamma_{ab}^+ = \Gamma_{ab}$ and $\Gamma_{ab}^- = \Gamma_{ab}^*$. From the absorptive part of the one-loop diagram for $\xi_a \to \xi_b$ we have

$$\Gamma_{ab}M_b = \frac{1}{8\pi}\left(\mu_a\mu_b^* + \mu_{3a}\mu_{3b}^* + M_aM_b\sum_{k,l} f_{akl}^* f_{bkl}\right). \tag{8.29}$$

Now for $\Gamma_a \equiv \Gamma_{aa} \ll M_a$, the eigenvalues of $M_\pm^2$ are given by

$$\lambda_{1,2} = \frac{1}{2}(M_1^2 + M_2^2 \pm \sqrt{S}), \tag{8.30}$$

where $S = (M_1^2 - M_2^2)^2 - 4|\Gamma_{12}M_2|^2$ and $M_1 > M_2$. The physical states are given by

$$\psi_{1,2}^+ = a_{1,2}^+\xi_1 + b_{1,2}^+\xi_2 \,, \qquad \psi_{1,2}^- = a_{1,2}^-\xi_1^* + b_{1,2}^-\xi_2^* \,, \tag{8.31}$$

where $a_1^\pm = b_2^\pm = 1/\sqrt{1+|C_i^\pm|^2}$, $b_1^\pm = C_1^\pm/\sqrt{1+|C_i^\pm|^2}$, $a_2^\pm = C_2^\pm/\sqrt{1+|C_i^\pm|^2}$ with

$$\begin{aligned} C_1^+ = -C_2^- &= \frac{-2i\Gamma_{12}^* M_2}{M_1^2 - M_2^2 + \sqrt{S}} \,, \\ C_1^- = -C_2^+ &= \frac{-2i\Gamma_{12} M_2}{M_1^2 - M_2^2 + \sqrt{S}} \,. \end{aligned} \tag{8.32}$$

The states $\psi_{1,2}^\pm$ evolve with time and decay into a lepton pair and antilepton pair [1]. Assuming $(M_1^2 - M_2^2)^2 \gg 4|\Gamma_{12}M_2|^2$, the lepton asymmetries generated are given by [23]

$$\begin{aligned} \varepsilon_i = \frac{1}{8\pi^2(M_1^2 - M_2^2)^2} \sum_{k,l} \{ &\mathrm{Im}\,[\mu_1\mu_2^* f_{1kl} f_{2kl}^*] \\ &+ \mathrm{Im}\,[(\mu_3)_1(\mu_3)_2^* f_{1kl} f_{2kl}^*]\} \left[\frac{M_i}{\Gamma_i}\right] . \end{aligned} \tag{8.33}$$

For the case $M_1 > M_2$, when the temperature of the universe cools down below M_1, ψ_1 decays away to create a lepton asymmetry. However, this asymmetry is washed out by lepton number nonconserving interactions of ψ_2 and the subsequent decay of ψ_2 at a temperature below M_2 sustains. The lepton asymmetry then gets converted to baryon asymmetry in the presence of the anomalous $B + L$ violating processes before the electroweak phase transition. The approximate final baryon asymmetry generated is given by

$$\frac{n_B}{s} \sim \frac{\varepsilon_2}{3g^* K (\ln K)^{0.6}}, \tag{8.34}$$

where $K \equiv \Gamma_2(M_2/T = 1)/H(M_2/T = 1)$ is a parameter measuring the deviation from thermal equilibrium at $T = M_2$, with the Hubble rate defined by $H = 1.66 {g_*}^{1/2}(T^2/M_{\mathrm{Pl}})$, where g_* corresponds to the number of relativistic degrees of freedom.

[1] Note that ξ_a and ξ_a^* are CP conjugate states, while $\psi_i^\pm$ are not.

Other than the decays and the inverse decays of triplet scalars, one needs to incorporate the gauge scatterings $\psi\bar{\psi} \leftrightarrow F\bar{F}, \phi\bar{\phi}, G\bar{G}$ (F corresponds to SM fermions and G corresponds to gauge bosons) and $\Delta L = 2$ scattering processes $ll \leftrightarrow \phi * \phi^*$ and $l\phi \leftrightarrow \bar{l}\phi^*$ into the Boltzmann equation analysis of the asymmetry. Including the above washout processes, it turns out that $M_\xi \gtrsim 10^{11}$ GeV is required in order to generate the correct asymmetry [114]. However, for a quasi-degenerate spectrum of scalar triplets the resonance effect can enhance the CP-asymmetry by a large amount and a successful leptogenesis scenario can be attained for a much smaller value of triplet scalar mass. A detailed analysis of the resonant leptogenesis is beyond the scope of this work and an account of the same can be found in Refs. [115, 116], where an absolute bound of $M_\xi \gtrsim 1.6$ TeV is obtained for a successful leptogenesis scenario.

In model B, the type III seesaw scheme is realized and the right-handed neutrinos enter together with the neutral component of the heavy fermion triplet in the neutrino mass matrix. As a consequence, the light neutrino masses, mixing and leptogenesis are not that tightly coupled as in the case of type I seesaw, where the constraints on the right-handed neutrino mass M_R can clash with the constraints coming from the textures of light neutrino masses and mixings. In the type III seesaw mechanism given in Eq. (8.15), we have six heavy Majorana neutrinos instead of the three heavy Majorana neutrinos in type I seesaw. This can give rise to three pseudo-Dirac pairs of neutrinos with one or more pairs having degenerate masses. The six heavy two component neutrinos have the form of the mass matrix given by [53]

$$\begin{pmatrix} \tilde{N}_i^c & \tilde{\Sigma}_i^0 \end{pmatrix} \begin{pmatrix} 0 & M_i\delta_{ij} \\ M_i\delta_{ij} & \tilde{M}_{\Sigma ij} \end{pmatrix} \begin{pmatrix} \tilde{N}_j^c \\ \tilde{\Sigma}_j^0 \end{pmatrix}. \tag{8.35}$$

Now the degenerate lightest pair of pseudo-Dirac neutrinos or equivalently, two Majorana neutrinos $N_\pm \simeq (\tilde{N}_1^c \pm \tilde{\Sigma}_1^0)/\sqrt{2}$ with masses $M_\pm \simeq \pm M_1 + \frac{1}{2}\tilde{M}_{\Sigma 11}$ can decay into light neutrino and Higgs doublet via the Yukawa term $Y_{i\pm}(N_\pm \nu_i)\Phi$, where

$$Y_{i\pm} \simeq \frac{(\tilde{Y}_{i1} \pm (\tilde{F}_2)_{i1})}{\sqrt{2}} \mp \frac{\tilde{M}_{11}}{4M_1}\frac{(\tilde{Y}_{i1} \mp (\tilde{F}_2)_{i1})}{\sqrt{2}}. \tag{8.36}$$

The asymmetry generated by the decays of $N_\pm$ is given by

$$\varepsilon_1 = \frac{1}{4\pi}\frac{\mathrm{Im}\left[\sum_j (Y_{j+}Y_{j-}^*)\right]^2}{\sum_j \left(|Y_{j+}|^2 + |Y_{j-}|^2\right)} I(M_-^2/M_+^2), \tag{8.37}$$

where $I(M_-^2/M_+^2)$ comes from the absorptive part of the decay amplitude, with $I(x) = \sqrt{x}[1-(1+x)\ln(1+(1/x))+1/(1-x)]$. Using the new basis parametrization $N_i^c = U_{ij}\tilde{N}_j^c$ and $\Sigma_{0i} = V_{ij}\tilde{\Sigma}_{0j}$ with the matrix $(F_1)_{ij}$ diagonal, where

$$U = \begin{pmatrix} u_{11} & \lambda u_{12} & \lambda u_{13} \\ \lambda u_{21} & u_{22} & u_{23} \\ \lambda u_{31} & u_{32} & u_{33} \end{pmatrix}, \tag{8.38}$$

with $u_{ij} \sim 1$ and

$$\tilde{F}_2 u = \begin{pmatrix} \lambda^2 f_{11} & \lambda f_{12} & \lambda f_{13} \\ \lambda f_{21} & f_{22} & f_{23} \\ \lambda f_{31} & f_{32} & f_{33} \end{pmatrix} v_u, \tag{8.39}$$

the asymmetry can be put in the form [53]

$$\varepsilon_1 = \frac{\lambda^2}{4\pi}\frac{(|u_{31}|^2 - |f_{31}|^2)\,\mathrm{Im}(u_{31}^* f_{31})}{|u_{31}|^2 + |f_{31}|^2 + |f_{21}|^2} I. \tag{8.40}$$

The lepton asymmetry of the universe is computed using

$$Y_L = \frac{n_B}{s} \sim \frac{\varepsilon_2 d}{3g^* K(\ln K)^{0.6}}, \tag{8.41}$$

where d is the washout parameter. In this case, for a hierarchical mass spectrum of triplets the lower bound on triplet mass for a successful leptogenesis scenario is given by $M_\Sigma \gtrsim 3\times 10^{10}$ [362, 363] and to have TeV scale leptogenesis one must assume a quasi-degenerate spectrum of fermion triplets giving resonant enhancement as in the case of scalar triplets, giving TeV scale bound on M_Σ [115, 364].

8.3 Collider signatures

The triplet fields ξ and Σ can be produced at the LHC if their masses are of the order of TeV. Therefore LHC gives a unique opportunity to verify the mechanism of neutrino mass generation if any of these heavy states or their signatures are observed. To this end, we give a very brief summery of the production and observability of the triplet fields in the two models discussed above. A quantitative exploration of the discovery potential of these new fields is beyond the scope of this work and here we mainly concentrate on a qualitative account of the likely scenarios.

The members of the scalar triplet field can be produced at the LHC via the channels

$$\begin{aligned} q\bar{q} &\rightarrow Z^*/\gamma^* \rightarrow \xi^{++}\xi^{--}, \\ q_1\bar{q}_2 &\rightarrow W^{\pm *} \rightarrow \xi^{++}\xi^{\mp}, \\ q\bar{q} &\rightarrow Z^*/\gamma^* \rightarrow \xi^{+}\xi^{-}. \end{aligned} \tag{8.42}$$

In the above three channels the interactions are fixed by the triplet gauge couplings and hence the production cross sections only depend on the scalar masses. In addition to the above three channels, there are additional channels where the scalar triplet field can be produced in association with $W^{\pm}$ or quarks,

$$\begin{aligned} q_1\bar{q}_2 &\rightarrow W^{\pm *} \rightarrow \xi^{++}W^{\mp}, \\ q_1q_2 &\rightarrow W^{\pm *}W^{\pm *}q_3q_4 \rightarrow \xi^{\pm\pm}q_3q_4, \\ q_1q_2 &\rightarrow Z^*Z^*q_3q_4 \rightarrow \xi^{\pm\pm}q_3q_4, \\ q_1q_2 &\rightarrow \gamma^*\gamma^*q_3q_4 \rightarrow \xi^{\pm\pm}q_3q_4. \end{aligned} \tag{8.43}$$

The associated production with $W^{\pm}$ and single production via $W^{\pm}W^{\pm}$ fusion involve the $\xi^{\pm\pm}W^{\pm}W^{\pm}$ vertex, which is suppressed by a factor of v_3/v_1. The $\gamma\gamma$ and ZZ fusion processes are also very suppressed compared to the pair production cross section.

The possible $\xi^{\pm\pm}$ decay modes are

$$\begin{aligned} \xi^{\pm\pm} &\rightarrow l_i^{\pm}l_j^{\pm}, \\ \xi^{\pm\pm} &\rightarrow W^{\pm}W^{\pm}, \\ \xi^{\pm\pm} &\rightarrow \xi^{\pm}W^{\pm}, \\ \xi^{\pm\pm} &\rightarrow \xi^{\pm}\xi^{\pm}, \end{aligned} \tag{8.44}$$

where $l_i = e, \mu, \tau$ for $i = 1, 2, 3$. The decay mode into a pair of leptons has been extensively discussed in the literature because it provides clear multi-lepton final state signatures for the pair production of doubly charged Higgs field with a very small SM background [365]. The possible two body decay modes of $\xi^{\pm}$ are

$$\begin{aligned} \xi^{\pm} &\rightarrow l_i^{\pm}\nu_j, \\ \xi^{\pm} &\rightarrow W^{\pm}Z, \\ \xi^{\pm} &\rightarrow u_j\bar{d}_k, \bar{u}_j d_k, \end{aligned} \tag{8.45}$$

with the last two decay modes again suppressed by a factor v_3/v_1. Thus the production of scalar triplet fields can give rise to several possible final states. The final states can be classified according to the number of charged leptons as (a) $l^+l^+l^-l^-X$, (b) $l^\pm l^\pm l^\mp X$, (c) $l^\pm l^\pm X$, (d) $l^+l^-j_\tau X$, (e) $l^\pm j_\tau j_\tau j_\tau X$, where l corresponds to electrons or muons (not necessarily all of the same flavor), j_τ corresponds to a tau jet and X represents additional jets [365]. The unique signature of model A is the decay mode $\xi^{++} \to \eta^+\eta^+$, if kinematically allowed.

Similarly, in model B the dominant partonic production channels of the charged and neutral components of the fermion triplet are given by

$$\begin{aligned} q\bar{q} &\to Z^*/\gamma^* \to \Sigma^+\Sigma^-, \\ q_1\bar{q}_2 &\to W^{\pm *} \to \Sigma^\pm\Sigma^0. \end{aligned} \tag{8.46}$$

The decay modes of $\Sigma^\pm$, Σ^0 are

$$\begin{aligned} \Sigma^\pm &\to l^\pm Z, \\ \Sigma^\pm &\to l^\pm \Phi, \\ \Sigma^\pm &\to \bar{\nu}W^+, \nu W^-, \\ \Sigma^0 &\to l^\pm W^\mp, \\ \Sigma^0 &\to \nu Z, \\ \Sigma^0 &\to \nu\Phi. \end{aligned} \tag{8.47}$$

Here the final states with different number of leptons can be classified as (a) six leptons, (b) five leptons, (c) $l^\pm l^\pm l^\pm l^\mp X$, (d) $l^+l^+l^-l^-X$, (e) $l^\pm l^\pm l^\pm X$, (f) $l^\pm l^\pm l^\mp X$, (g) l^+l^-X, (h) l^+l^-jjjjX and (i) $l^\pm jjjjX$ [365, 366]. The unique signatures of the type III seesaw mechanism such as six lepton and five lepton final states can be used to distinguish it from the type II seesaw scheme at the LHC.

8.4 Summary of the chapter

We have discussed the realization of mass varying neutrinos in an extension of the usual triplet Higgs model by including an extra Higgs doublet (η) and an extension of the SM with fermion triplets (Σ_R). We found that both scenarios can accommodate neutrino dark energy with a dynamical neutrino mass related to the acceleron field, in the former scenario with TeV scale triplet Higgs fields (ξ) and an additional doublet Higgs field (η) and in the latter scenario with TeV scale fermion triplets Σ. We have also discussed the possible leptogenesis mechanisms for simultaneously generating the observed baryon asymmetry of the universe in both scenarios. Finally, the TeV scale new fields in both models give unique and highly predictive collider signatures, testable in the current run of LHC.

Chapter 9

Scope for future studies

In this thesis we have studied several models beyond the SM in the contexts of LHC phenomenology, neutrino masses, flavor anomalies associated with B-decays and gauge coupling unification. We have also studied the possibility of explaining the matter-antimatter asymmetry via baryogenesis (leptogenesis) mechanisms in many models beyond the SM. We also explored the possibility of explaining the abundance of dark matter together with the matter-antimatter asymmetry of the universe via a cogenesis mechanism and the realization of neutrino dark energy in a few models beyond the standard model.

Two of the chapters of this thesis are devoted to the study of the Left-Right Symmetric Model (LRSM), which is one of the most popular candidates for extensions of the SM. We have discussed how the observation of a TeV scale W_R will rule out all conventional high scale or resonant possibilities of leptogenesis. Thus, if indeed LHC observes a TeV scale W_R then it will be very interesting to find some post-electroweak phase transition mechanism to explain the baryon asymmetry of the Universe. In this context, the experiments to observe the neutron-antineutron oscillations [202, 203] or the $(B-L)$ violating proton decay [59] will play a crucial role in confirming such possibilities. Consequently, a detailed and critical study of these mechanisms essential in understanding the matter-antimatter asymmetry of the universe.

The LRSM framework with vector-like fermions is a very interesting idea to explore in more detail. Irrespective of the diphoton signal, it can provide a very rich phenomenology corresponding to the fermion masses and mixing, particularly for the neutrinos and can have interesting implications for baryogenesis and the potential dark matter sector. Another interesting aspect is the details of the flavor sector of such models which is very interesting in the presence of vector-like new fields.

On the other hand, the low energy subgroups of E_6 are also very interesting candidates for physics beyond the SM. These models predict a number of new exotic particles and gauge bosons, giving rise to a very rich LHC and neutrino physics phenomenology. The particle content of these models includes leptoquarks, which can naturally address a number of flavor anomalies including the ones associated with B-decays. Thus if the B-decay anomalies are confirmed in future B-physics experiments then it will be interesting to study the flavor structure of these models in detail. From the point of view of leptogenesis the Alternative Left-Right Symmetric Model provides a unique opportunity to implement high scale leptogenesis in contrast to the conventional LRSMs, which suffer from strong gauge washout processes for a TeV scale W_R.

Finally, the cogenesis mechanisms provide a unique way to correlate two of the most puzzling topics in cosmology and particle physics: the matter-antimatter asymmetry of the universe and the dark matter abundance. Thus, it will be interesting to seek new frameworks beyond the SM which can allow a natural realization of the cogenesis mechanism and to test these ideas at the colliders and dark matter detection experiments. The idea of neutrino dark energy is very interesting because it relates the neutrino mass scale to the existence of the dark energy. Thus, it will be interesting to explore different mechanisms of neutrino masses in this context and to explore the associated collider phenomenology.

Chapter 10

Epilogue

In this thesis we have studied several interesting extensions of the SM in light of different LHC signals and flavor anomalies exploring neutrino masses, associated rare decays, gauge coupling unification and the possibility of explaining the matter-antimatter asymmetry via baryogenesis (leptogenesis) mechanisms. As this epilogue is being written, several potential signals reported at the end of first run have either disappeared or weakened, whereas some of the signals remain tantalizing hints of new physics. In this chapter we synthesize the current status of several different signals discussed in this thesis and various features of the various proposed extensions that are still valid.

After collecting more data both ATLAS and CMS collaborations have confirmed that the 750 GeV diphoton excess appears to have been a statistical fluctuation [367, 368]. The signals corresponding to searches for the diboson and dijet resonances have also weakened severely [369–375]. On the other hand the anomalies discussed in the flavor sector, particularly the ones associated with B-decays are persistent with new measurements at the B-factories and remain tantalizing hints of new physics. The LHC signals often played a guiding role which motivated several of the studies in this thesis. However, even if the signals have disappeared or weakened, the models studied remain very interesting due to the associated phenomenological and cosmological implications. Moreover, the LHC signal studies in the context of these extensions beyond the SM remain efficient landmark for future new physics searches, which can be readily adopted for any similar kind of future excess signals at LHC or next generation colliders.

Few of the chapters of this thesis are devoted to the study of the Left-Right Symmetric Model (LRSM), which is one of the most popular candidates for extensions of the SM. We have discussed how the observation of a TeV scale W_R will rule out all conventional high scale or resonant possibilities of leptogenesis. Thus, if indeed LHC observes a few TeV scale W_R in future then it will be very interesting to go back to this analysis to verify the falsifiability of leptogenesis mechanism. Similarly, irrespective of the diphoton signal, the discussed LRSM framework with vector-like fermions can provide a very rich phenomenology corresponding to the fermion masses and mixing, particularly for the neutrinos and can have interesting implications for baryogenesis and the potential dark matter sector. On the other hand, the low energy subgroups of E_6 are also very interesting candidates for physics beyond the SM. Irrespective of the $eejj$, diphoton, diboson signals, these models predict a number of new exotic particles and gauge bosons, giving rise to a very rich LHC and neutrino physics phenomenology. For example following Ref. [250] and several other E_6 motivated studies related to the diphoton excess, in Ref. [376] the phenomenology of extra Z-bosons, new vector-like fermions, sterile neutrinos, and neutral scalars in addition to the SM Higgs boson have been updated and extended. Also the relevance of such models to the present searches at LHC has been discussed and the diagnostics for heavy Z boson have been discussed in detail. The particle content of these models includes leptoquarks, which we have shown that can naturally address a number of flavor anomalies including the ones associated with B-decays. Thus if the persistent B-decay anomalies are confirmed in future B-physics experiments then these will be very interesting options for physics beyond the SM. From the point of view of leptogenesis the Alternative Left-Right Symmetric Model provides a unique opportunity to implement high scale leptogenesis in contrast to the conventional LRSMs, which suffer from strong gauge washout processes for a TeV scale W_R.

Bibliography

[1] S. L. Glashow, *Partial Symmetries of Weak Interactions*, *Nucl. Phys.* **22** (1961) 579–588.

[2] A. Salam, *Weak and Electromagnetic Interactions*, *Conf. Proc.* **C680519** (1968) 367–377.

[3] S. Weinberg, *A Model of Leptons*, *Phys. Rev. Lett.* **19** (1967) 1264–1266.

[4] P. W. Anderson, *Plasmons, Gauge Invariance, and Mass*, *Phys. Rev.* **130** (1963) 439–442.

[5] F. Englert and R. Brout, *Broken Symmetry and the Mass of Gauge Vector Mesons*, *Phys. Rev. Lett.* **13** (1964) 321–323.

[6] P. W. Higgs, *Broken Symmetries and the Masses of Gauge Bosons*, *Phys. Rev. Lett.* **13** (1964) 508–509.

[7] G. S. Guralnik, C. R. Hagen and T. W. B. Kibble, *Global Conservation Laws and Massless Particles*, *Phys. Rev. Lett.* **13** (1964) 585–587.

[8] P. W. Higgs, *Spontaneous Symmetry Breakdown without Massless Bosons*, *Phys. Rev.* **145** (1966) 1156–1163.

[9] N. Cabibbo, *Unitary Symmetry and Leptonic Decays*, *Phys. Rev. Lett.* **10** (1963) 531–533.

[10] M. Kobayashi and T. Maskawa, *CP Violation in the Renormalizable Theory of Weak Interaction*, *Prog. Theor. Phys.* **49** (1973) 652–657.

[11] PARTICLE DATA GROUP collaboration, K. A. Olive et al., *Review of Particle Physics*, *Chin. Phys.* **C38** (2014) 090001.

[12] S. Weinberg, *Baryon and Lepton Nonconserving Processes*, *Phys. Rev. Lett.* **43** (1979) 1566–1570.

[13] F. Wilczek and A. Zee, *Operator Analysis of Nucleon Decay*, *Phys. Rev. Lett.* **43** (1979) 1571–1573.

[14] S. Weinberg, *Varieties of Baryon and Lepton Nonconservation*, *Phys. Rev.* **D22** (1980) 1694.

[15] H. A. Weldon and A. Zee, *Operator Analysis of New Physics*, *Nucl. Phys.* **B173** (1980) 269–290.

[16] P. Minkowski, *$\mu \to e\gamma$ at a Rate of One Out of 10^9 Muon Decays?*, *Phys. Lett.* **B67** (1977) 421–428.

[17] M. Gell-Mann, P. Ramond and R. Slansky, *Complex Spinors and Unified Theories*, *Conf. Proc.* **C790927** (1979) 315–321, [1306.4669].

[18] T. Yanagida, *HORIZONTAL SYMMETRY AND MASSES OF NEUTRINOS*, *Conf. Proc.* **C7902131** (1979) 95–99.

[19] R. N. Mohapatra and G. Senjanovic, *Neutrino Mass and Spontaneous Parity Violation*, *Phys. Rev. Lett.* **44** (1980) 912.

[20] J. Schechter and J. W. F. Valle, *Neutrino Masses in SU(2) x U(1) Theories*, *Phys. Rev.* **D22** (1980) 2227.

[21] R. N. Mohapatra and G. Senjanovic, *Neutrino Masses and Mixings in Gauge Models with Spontaneous Parity Violation*, *Phys. Rev.* **D23** (1981) 165.

[22] J. Schechter and J. W. F. Valle, *Neutrino Decay and Spontaneous Violation of Lepton Number*, *Phys. Rev.* **D25** (1982) 774.

[23] E. Ma and U. Sarkar, *Neutrino masses and leptogenesis with heavy Higgs triplets*, *Phys. Rev. Lett.* **80** (1998) 5716–5719, [hep-ph/9802445].

[24] G. Lazarides and Q. Shafi, *R symmetry in minimal supersymmetry standard model and beyond with several consequences*, *Phys. Rev.* **D58** (1998) 071702, [hep-ph/9803397].

[25] W. Grimus, R. Pfeiffer and T. Schwetz, *A Four neutrino model with a Higgs triplet*, *Eur. Phys. J.* **C13** (2000) 125–132, [hep-ph/9905320].

[26] T. Hambye, E. Ma and U. Sarkar, *Supersymmetric triplet Higgs model of neutrino masses and leptogenesis*, *Nucl. Phys.* **B602** (2001) 23–38, [hep-ph/0011192].

[27] R. Foot, H. Lew, X. G. He and G. C. Joshi, *Seesaw Neutrino Masses Induced by a Triplet of Leptons*, *Z. Phys.* **C44** (1989) 441.

[28] E. Ma, *Pathways to naturally small neutrino masses*, *Phys. Rev. Lett.* **81** (1998) 1171–1174, [hep-ph/9805219].

[29] A. Zee, *A Theory of Lepton Number Violation, Neutrino Majorana Mass, and Oscillation*, *Phys. Lett.* **B93** (1980) 389.

[30] L. Wolfenstein, *A Theoretical Pattern for Neutrino Oscillations*, *Nucl. Phys.* **B175** (1980) 93–96.

[31] A. Zee, *Quantum Numbers of Majorana Neutrino Masses*, *Nucl. Phys.* **B264** (1986) 99–110.

[32] K. S. Babu, *Model of 'Calculable' Majorana Neutrino Masses*, *Phys. Lett.* **B203** (1988) 132–136.

[33] E. Ma, *Verifiable radiative seesaw mechanism of neutrino mass and dark matter*, *Phys. Rev.* **D73** (2006) 077301, [hep-ph/0601225].

[34] L. M. Krauss, S. Nasri and M. Trodden, *A Model for neutrino masses and dark matter*, *Phys. Rev.* **D67** (2003) 085002, [hep-ph/0210389].

[35] M. Aoki, S. Kanemura and O. Seto, *Neutrino mass, Dark Matter and Baryon Asymmetry via TeV-Scale Physics without Fine-Tuning*, *Phys. Rev. Lett.* **102** (2009) 051805, [0807.0361].

[36] M. Gustafsson, J. M. No and M. A. Rivera, *Predictive Model for Radiatively Induced Neutrino Masses and Mixings with Dark Matter*, Phys. Rev. Lett. **110** (2013) 211802, [1212.4806].

[37] S. Kanemura and H. Sugiyama, *Dark matter and a suppression mechanism for neutrino masses in the Higgs triplet model*, Phys. Rev. **D86** (2012) 073006, [1202.5231].

[38] S. Nasri and S. Moussa, *Model for small neutrino masses at the TeV scale*, Mod. Phys. Lett. **A17** (2002) 771–778, [hep-ph/0106107].

[39] P.-H. Gu and U. Sarkar, *Radiative Neutrino Mass, Dark Matter and Leptogenesis*, Phys. Rev. **D77** (2008) 105031, [0712.2933].

[40] S. Kanemura, T. Matsui and H. Sugiyama, *Loop Suppression of Dirac Neutrino Mass in the Neutrinophilic Two Higgs Doublet Model*, Phys. Lett. **B727** (2013) 151–156, [1305.4521].

[41] J. C. Pati and A. Salam, *Is Baryon Number Conserved?*, Phys. Rev. Lett. **31** (1973) 661–664.

[42] J. C. Pati and A. Salam, *Unified Lepton-Hadron Symmetry and a Gauge Theory of the Basic Interactions*, Phys. Rev. **D8** (1973) 1240–1251.

[43] J. C. Pati and A. Salam, *Lepton Number as the Fourth Color*, Phys. Rev. **D10** (1974) 275–289.

[44] R. N. Mohapatra and J. C. Pati, *A Natural Left-Right Symmetry*, Phys. Rev. **D11** (1975) 2558.

[45] G. Senjanovic and R. N. Mohapatra, *Exact Left-Right Symmetry and Spontaneous Violation of Parity*, Phys. Rev. **D12** (1975) 1502.

[46] R. N. Mohapatra and R. E. Marshak, *Local B-L Symmetry of Electroweak Interactions, Majorana Neutrinos and Neutron Oscillations*, Phys. Rev. Lett. **44** (1980) 1316–1319.

[47] G. Senjanovic, *Spontaneous Breakdown of Parity in a Class of Gauge Theories*, *Nucl. Phys.* **B153** (1979) 334–364.

[48] G. R. Dvali, G. Lazarides and Q. Shafi, *Mu problem and hybrid inflation in supersymmetric SU(2)-L x SU(2)-R x U(1)-(B-L)*, *Phys. Lett.* **B424** (1998) 259–264, [hep-ph/9710314].

[49] K. S. Babu, J. C. Pati and F. Wilczek, *Fermion masses, neutrino oscillations, and proton decay in the light of Super-Kamiokande*, *Nucl. Phys.* **B566** (2000) 33–91, [hep-ph/9812538].

[50] B. Brahmachari, E. Ma and U. Sarkar, *Truly minimal left right model of quark and lepton masses*, *Phys. Rev. Lett.* **91** (2003) 011801, [hep-ph/0301041].

[51] U. Sarkar, *Parity in left-right symmetric models*, *Phys. Lett.* **B594** (2004) 308–314, [hep-ph/0403276].

[52] S. M. Barr, *A Different seesaw formula for neutrino masses*, *Phys. Rev. Lett.* **92** (2004) 101601, [hep-ph/0309152].

[53] C. H. Albright and S. M. Barr, *Leptogenesis in the type III seesaw mechanism*, *Phys. Rev.* **D69** (2004) 073010, [hep-ph/0312224].

[54] C. H. Albright and S. M. Barr, *Resonant leptogenesis in a predictive SO(10) grand unified model*, *Phys. Rev.* **D70** (2004) 033013, [hep-ph/0404095].

[55] B. R. Desai, G. Rajasekaran and U. Sarkar, *An SO(10) GUT with see-saw masses for all fermions*, *Phys. Lett.* **B626** (2005) 167–174, [hep-ph/0411099].

[56] U. Sarkar, *Minimal supersymmetric SO(10) GUT with doublet Higgs*, *Phys. Lett.* **B622** (2005) 118–123, [hep-ph/0409019].

[57] H. Georgi and S. L. Glashow, *Unity of All Elementary Particle Forces*, *Phys. Rev. Lett.* **32** (1974) 438–441.

[58] H. Georgi, H. R. Quinn and S. Weinberg, *Hierarchy of Interactions in Unified Gauge Theories*, *Phys. Rev. Lett.* **33** (1974) 451–454.

[59] J. C. Pati, A. Salam and U. Sarkar, *Delta B = - Delta L, neutron —¿ e- pi+, e- K+, mu- pi+ and mu- K+ DECAY modes in SU(2)-L X SU(2)-R X SU(4)-C or SO(10)*, *Phys. Lett.* **B133** (1983) 330–336.

[60] R. N. Mohapatra, *UNIFICATION AND SUPERSYMMETRY. THE FRONTIERS OF QUARK - LEPTON PHYSICS*. Springer, Berlin, 1986, 10.1007/978-1-4757-1928-4.

[61] U. Sarkar, *Particle and astroparticle physics*. Series in high energy physics, cosmology, and gravitation. Taylor & Francis, New York, USA, 2008.

[62] R. Slansky, *Group Theory for Unified Model Building*, *Phys. Rept.* **79** (1981) 1–128.

[63] S. P. Martin, *A Supersymmetry primer*, `hep-ph/9709356`.

[64] J. Wess and B. Zumino, *Supergauge Transformations in Four-Dimensions*, *Nucl. Phys.* **B70** (1974) 39–50.

[65] J. Wess and J. Bagger, *Supersymmetry and supergravity*. 1992.

[66] L. Girardello and M. T. Grisaru, *Soft Breaking of Supersymmetry*, *Nucl. Phys.* **B194** (1982) 65.

[67] P. Fayet and J. Iliopoulos, *Spontaneously Broken Supergauge Symmetries and Goldstone Spinors*, *Phys. Lett.* **B51** (1974) 461–464.

[68] P. Fayet, *Supergauge Invariant Extension of the Higgs Mechanism and a Model for the electron and Its Neutrino*, *Nucl. Phys.* **B90** (1975) 104–124.

[69] L. O'Raifeartaigh, *Spontaneous Symmetry Breaking for Chiral Scalar Superfields*, *Nucl. Phys.* **B96** (1975) 331–352.

[70] A. D. Sakharov, *Violation of CP Invariance, c Asymmetry, and Baryon Asymmetry of the Universe*, *Pisma Zh. Eksp. Teor. Fiz.* **5** (1967) 32–35.

[71] M. Yoshimura, *Unified Gauge Theories and the Baryon Number of the Universe*, *Phys. Rev. Lett.* **41** (1978) 281–284.

[72] D. Toussaint, S. B. Treiman, F. Wilczek and A. Zee, *Matter - Antimatter Accounting, Thermodynamics, and Black Hole Radiation*, *Phys. Rev.* **D19** (1979) 1036–1045.

[73] S. Dimopoulos and L. Susskind, *On the Baryon Number of the Universe*, *Phys. Rev.* **D18** (1978) 4500–4509.

[74] J. R. Ellis, M. K. Gaillard and D. V. Nanopoulos, *Baryon Number Generation in Grand Unified Theories*, *Phys. Lett.* **B80** (1979) 360.

[75] S. Weinberg, *Cosmological Production of Baryons*, *Phys. Rev. Lett.* **42** (1979) 850–853.

[76] M. Yoshimura, *Origin of Cosmological Baryon Asymmetry*, *Phys. Lett.* **B88** (1979) 294–298.

[77] S. M. Barr, G. Segre and H. A. Weldon, *The Magnitude of the Cosmological Baryon Asymmetry*, *Phys. Rev.* **D20** (1979) 2494.

[78] D. V. Nanopoulos and S. Weinberg, *Mechanisms for Cosmological Baryon Production*, *Phys. Rev.* **D20** (1979) 2484.

[79] M. E. Shaposhnikov, *Baryon Asymmetry of the Universe in Standard Electroweak Theory*, *Nucl. Phys.* **B287** (1987) 757–775.

[80] M. E. Shaposhnikov, *Structure of the High Temperature Gauge Ground State and Electroweak Production of the Baryon Asymmetry*, *Nucl. Phys.* **B299** (1988) 797–817.

[81] N. Turok and J. Zadrozny, *Dynamical generation of baryons at the electroweak transition*, *Phys. Rev. Lett.* **65** (1990) 2331–2334.

[82] L. D. McLerran, M. E. Shaposhnikov, N. Turok and M. B. Voloshin, *Why the baryon asymmetry of the universe is approximately 10**-10*, *Phys. Lett.* **B256** (1991) 451–456.

[83] A. D. Dolgov, *NonGUT baryogenesis*, *Phys. Rept.* **222** (1992) 309–386.

[84] A. Yu. Ignatiev, N. V. Krasnikov, V. A. Kuzmin and A. N. Tavkhelidze, *Universal CP Noninvariant Superweak Interaction and Baryon Asymmetry of the Universe*, *Phys. Lett.* **B76** (1978) 436–438.

[85] A. M. Kazarian, S. V. Kuzmin and M. E. Shaposhnikov, *Cosmological lower bound on the EDM of the electron*, *Phys. Lett.* **B276** (1992) 131–134.

[86] V. A. Kuzmin, V. A. Rubakov and M. E. Shaposhnikov, *On the Anomalous Electroweak Baryon Number Nonconservation in the Early Universe*, *Phys. Lett.* **B155** (1985) 36.

[87] F. R. Klinkhamer and N. S. Manton, *A Saddle Point Solution in the Weinberg-Salam Theory*, *Phys. Rev.* **D30** (1984) 2212.

[88] I. Affleck and M. Dine, *A New Mechanism for Baryogenesis*, *Nucl. Phys.* **B249** (1985) 361–380.

[89] M. Dine, L. Randall and S. D. Thomas, *Baryogenesis from flat directions of the supersymmetric standard model*, *Nucl. Phys.* **B458** (1996) 291–326, [hep-ph/9507453].

[90] M. Fukugita and T. Yanagida, *Baryogenesis Without Grand Unification*, *Phys. Lett.* **B174** (1986) 45–47.

[91] G. 't Hooft, *Symmetry Breaking Through Bell-Jackiw Anomalies*, *Phys. Rev. Lett.* **37** (1976) 8–11.

[92] G. 't Hooft, *Computation of the Quantum Effects Due to a Four-Dimensional Pseudoparticle*, *Phys. Rev.* **D14** (1976) 3432–3450.

[93] P. B. Arnold, D. Son and L. G. Yaffe, *The Hot baryon violation rate is O (alpha-w**5 T**4)*, *Phys. Rev.* **D55** (1997) 6264–6273, [hep-ph/9609481].

[94] P. B. Arnold, D. T. Son and L. G. Yaffe, *Effective dynamics of hot, soft nonAbelian gauge fields. Color conductivity and log(1/alpha) effects*, *Phys. Rev.* **D59** (1999) 105020, [hep-ph/9810216].

[95] D. Bodeker, *On the effective dynamics of soft nonAbelian gauge fields at finite temperature*, *Phys. Lett.* **B426** (1998) 351–360, [hep-ph/9801430].

[96] D. Bodeker, *From hard thermal loops to Langevin dynamics*, *Nucl. Phys.* **B559** (1999) 502–538, [hep-ph/9905239].

[97] S. Yu. Khlebnikov and M. E. Shaposhnikov, *The Statistical Theory of Anomalous Fermion Number Nonconservation*, *Nucl. Phys.* **B308** (1988) 885–912.

[98] J. A. Harvey and M. S. Turner, *Cosmological baryon and lepton number in the presence of electroweak fermion number violation*, *Phys. Rev.* **D42** (1990) 3344–3349.

[99] P. Langacker, R. D. Peccei and T. Yanagida, *Invisible Axions and Light Neutrinos: Are They Connected?*, *Mod. Phys. Lett.* **A1** (1986) 541.

[100] M. A. Luty, *Baryogenesis via leptogenesis*, *Phys. Rev.* **D45** (1992) 455–465.

[101] H. Murayama, H. Suzuki, T. Yanagida and J. Yokoyama, *Chaotic inflation and baryogenesis by right-handed sneutrinos*, *Phys. Rev. Lett.* **70** (1993) 1912–1915.

[102] A. Acker, H. Kikuchi, E. Ma and U. Sarkar, *CP violation and leptogenesis*, *Phys. Rev.* **D48** (1993) 5006–5008, [hep-ph/9305290].

[103] W. Buchmuller and M. Plumacher, *Baryon asymmetry and neutrino mixing*, *Phys. Lett.* **B389** (1996) 73–77, [hep-ph/9608308].

[104] M. Flanz, E. A. Paschos and U. Sarkar, *Baryogenesis from a lepton asymmetric universe*, *Phys. Lett.* **B345** (1995) 248–252, [hep-ph/9411366].

[105] M. Flanz, E. A. Paschos, U. Sarkar and J. Weiss, *Baryogenesis through mixing of heavy Majorana neutrinos*, *Phys. Lett.* **B389** (1996) 693–699, [hep-ph/9607310].

[106] A. Pilaftsis, *CP violation and baryogenesis due to heavy Majorana neutrinos*, *Phys. Rev.* **D56** (1997) 5431–5451, [hep-ph/9707235].

[107] E. Roulet, L. Covi and F. Vissani, *On the CP asymmetries in Majorana neutrino decays*, *Phys. Lett.* **B424** (1998) 101–105, [hep-ph/9712468].

[108] W. Buchmuller and M. Plumacher, *CP asymmetry in Majorana neutrino decays*, *Phys. Lett.* **B431** (1998) 354–362, [hep-ph/9710460].

[109] M. Flanz and E. A. Paschos, *Further considerations on the CP asymmetry in heavy Majorana neutrino decays*, *Phys. Rev.* **D58** (1998) 113009, [hep-ph/9805427].

[110] T. Hambye, J. March-Russell and S. M. West, *TeV scale resonant leptogenesis from supersymmetry breaking*, *JHEP* **07** (2004) 070, [hep-ph/0403183].

[111] A. Pilaftsis and T. E. J. Underwood, *Resonant leptogenesis*, *Nucl. Phys.* **B692** (2004) 303–345, [hep-ph/0309342].

[112] R. Rangarajan and H. Mishra, *Leptogenesis with heavy Majorana neutrinos revisited*, *Phys. Rev.* **D61** (2000) 043509, [hep-ph/9908417].

[113] S. Davidson and A. Ibarra, *A Lower bound on the right-handed neutrino mass from leptogenesis*, *Phys. Lett.* **B535** (2002) 25–32, [hep-ph/0202239].

[114] T. Hambye, M. Raidal and A. Strumia, *Efficiency and maximal CP-asymmetry of scalar triplet leptogenesis*, *Phys. Lett.* **B632** (2006) 667–674, [hep-ph/0510008].

[115] A. Strumia, *Sommerfeld corrections to type-II and III leptogenesis*, *Nucl. Phys.* **B809** (2009) 308–317, [0806.1630].

[116] D. Aristizabal Sierra, M. Dhen and T. Hambye, *Scalar triplet flavored leptogenesis: a systematic approach*, *JCAP* **1408** (2014) 003, [1401.4347].

[117] J. R. Ellis, J. S. Hagelin, D. V. Nanopoulos, K. A. Olive and M. Srednicki, *Supersymmetric Relics from the Big Bang*, *Nucl. Phys.* **B238** (1984) 453–476.

[118] K. Griest, *Cross-Sections, Relic Abundance and Detection Rates for Neutralino Dark Matter*, *Phys. Rev.* **D38** (1988) 2357.

[119] A. Bottino, V. de Alfaro, N. Fornengo, G. Mignola and M. Pignone, *On the neutralino as dark matter candidate. 1. Relic abundance.*, *Astropart. Phys.* **2** (1994) 67–76, [hep-ph/9309218].

[120] T. Falk, K. A. Olive and M. Srednicki, *Heavy sneutrinos as dark matter*, *Phys. Lett.* **B339** (1994) 248–251, [hep-ph/9409270].

[121] V. A. Bednyakov, H. V. Klapdor-Kleingrothaus and S. G. Kovalenko, *Possible constraints on SUSY model parameters from direct dark matter search*, *Phys. Lett.* **B329** (1994) 5–9, [hep-ph/9401271].

[122] V. A. Bednyakov, H. V. Klapdor-Kleingrothaus and S. G. Kovalenko, *Superlight neutralino as a dark matter particle candidate*, *Phys. Rev.* **D55** (1997) 503–514, [hep-ph/9608241].

[123] E. Ma, *Common origin of neutrino mass, dark matter, and baryogenesis*, *Mod. Phys. Lett.* **A21** (2006) 1777–1782, [hep-ph/0605180].

[124] WMAP collaboration, G. Hinshaw et al., *Nine-Year Wilkinson Microwave Anisotropy Probe (WMAP) Observations: Cosmological Parameter Results*, *Astrophys. J. Suppl.* **208** (2013) 19, [1212.5226].

[125] PLANCK collaboration, P. A. R. Ade et al., *Planck 2015 results. XIII. Cosmological parameters*, 1502.01589.

[126] H. Davoudiasl, D. E. Morrissey, K. Sigurdson and S. Tulin, *Hylogenesis: A Unified Origin for Baryonic Visible Matter and Antibaryonic Dark Matter*, *Phys. Rev. Lett.* **105** (2010) 211304, [1008.2399].

[127] K. Kohri, A. Mazumdar, N. Sahu and P. Stephens, *Probing Unified Origin of Dark Matter and Baryon Asymmetry at PAMELA/Fermi*, *Phys. Rev.* **D80** (2009) 061302, [0907.0622].

[128] P.-H. Gu and U. Sarkar, *Common Origin of Visible and Dark Universe*, *Phys. Rev.* **D81** (2010) 033001, [0909.5463].

[129] H. An, S.-L. Chen, R. N. Mohapatra and Y. Zhang, *Leptogenesis as a Common Origin for Matter and Dark Matter*, *JHEP* **03** (2010) 124, [0911.4463].

[130] E. J. Chun, *Leptogenesis origin of Dirac gaugino dark matter*, *Phys. Rev.* **D83** (2011) 053004, [1009.0983].

[131] P.-H. Gu, M. Lindner, U. Sarkar and X. Zhang, *WIMP Dark Matter and Baryogenesis*, *Phys. Rev.* **D83** (2011) 055008, [1009.2690].

[132] B. Dutta and J. Kumar, *Asymmetric Dark Matter from Hidden Sector Baryogenesis*, *Phys. Lett.* **B699** (2011) 364–367, [1012.1341].

[133] A. Falkowski, J. T. Ruderman and T. Volansky, *Asymmetric Dark Matter from Leptogenesis*, *JHEP* **05** (2011) 106, [1101.4936].

[134] J. March-Russell and M. McCullough, *Asymmetric Dark Matter via Spontaneous Co-Genesis*, *JCAP* **1203** (2012) 019, [1106.4319].

[135] K. Petraki, M. Trodden and R. R. Volkas, *Visible and dark matter from a first-order phase transition in a baryon-symmetric universe*, *JCAP* **1202** (2012) 044, [1111.4786].

[136] K. Kamada and M. Yamaguchi, *Asymmetric Dark Matter from Spontaneous Cogenesis in the Supersymmetric Standard Model*, *Phys. Rev.* **D85** (2012) 103530, [1201.2636].

[137] N. Blinov, D. E. Morrissey, K. Sigurdson and S. Tulin, *Dark Matter Antibaryons from a Supersymmetric Hidden Sector*, *Phys. Rev.* **D86** (2012) 095021, [1206.3304].

[138] H. Kuismanen and I. Vilja, *Baryon asymmetry and dark matter from soft leptogenesis*, *Phys. Rev.* **D87** (2013) 015005, [1210.4335].

[139] P. Fileviez Perez and M. B. Wise, *Baryon Asymmetry and Dark Matter Through the Vector-Like Portal*, *JHEP* **05** (2013) 094, [1303.1452].

[140] W.-Z. Feng and P. Nath, *Cogenesis in a universe with vanishing $B - L$ within a gauged $U(1)_x$ extension*, *Phys. Lett.* **B731** (2014) 43–50, [1312.1334].

[141] M. Dhuria, C. Hati and U. Sarkar, *Moduli induced cogenesis of baryon asymmetry and dark matter*, *Phys. Lett.* **B756** (2016) 376–383, [1508.04144].

[142] J. I. Kapusta, *Neutrino superfluidity*, *Phys. Rev. Lett.* **93** (2004) 251801, [hep-th/0407164].

[143] S. Antusch, J. Kersten, M. Lindner and M. Ratz, *Dynamical electroweak symmetry breaking by a neutrino condensate*, *Nucl. Phys.* **B658** (2003) 203–216, [hep-ph/0211385].

[144] J. R. Bhatt and U. Sarkar, *Majorana Neutrino Superfluidity and Stability of Neutrino Dark Energy*, *Phys. Rev.* **D80** (2009) 045016, [0805.2482].

[145] G. Barenboim, *Inflation might be caused by the right: Handed neutrino*, *JHEP* **03** (2009) 102, [0811.2998].

[146] R. Horvat, P. Minkowski and J. Trampetic, *Dark consequences from light neutrino condensations*, *Phys. Lett.* **B671** (2009) 51–54, [0809.0582].

[147] J. R. Bhatt, B. R. Desai, E. Ma, G. Rajasekaran and U. Sarkar, *Neutrino Condensate as Origin of Dark Energy*, *Phys. Lett.* **B687** (2010) 75–78, [0911.5012].

[148] M. Azam, U. Sarkar and J. R. Bhatt, *Experimental signatures of cosmological neutrino condensation*, *Phys. Lett.* **B697** (2011) 7–10, [1008.5214].

[149] P. Gu, X. Wang and X. Zhang, *Dark energy and neutrino mass limits from baryogenesis*, *Phys. Rev.* **D68** (2003) 087301, [hep-ph/0307148].

[150] R. Fardon, A. E. Nelson and N. Weiner, *Dark energy from mass varying neutrinos*, *JCAP* **0410** (2004) 005, [astro-ph/0309800].

[151] H. Li, Z.-g. Dai and X.-m. Zhang, *Testing mass varying neutrino with short gamma ray burst*, *Phys. Rev.* **D71** (2005) 113003, [hep-ph/0411228].

[152] V. Barger, P. Huber and D. Marfatia, *Solar mass-varying neutrino oscillations*, *Phys. Rev. Lett.* **95** (2005) 211802, [hep-ph/0502196].

[153] A. W. Brookfield, C. van de Bruck, D. F. Mota and D. Tocchini-Valentini, *Cosmology with massive neutrinos coupled to dark energy*, *Phys. Rev. Lett.* **96** (2006) 061301, [astro-ph/0503349].

[154] A. Ringwald and L. Schrempp, *Probing Neutrino Dark Energy with Extremely High-Energy Cosmic Neutrinos*, *JCAP* **0610** (2006) 012, [astro-ph/0606316].

[155] R. Barbieri, L. J. Hall, S. J. Oliver and A. Strumia, *Dark energy and right-handed neutrinos*, *Phys. Lett.* **B625** (2005) 189–195, [hep-ph/0505124].

[156] R. Takahashi and M. Tanimoto, *Model of mass varying neutrinos in SUSY*, *Phys. Lett.* **B633** (2006) 675–680, [hep-ph/0507142].

[157] R. Fardon, A. E. Nelson and N. Weiner, *Supersymmetric theories of neutrino dark energy*, *JHEP* **03** (2006) 042, [hep-ph/0507235].

[158] E. Ma and U. Sarkar, *Connecting dark energy to neutrinos with an observable higgs triplet*, *Phys. Lett.* **B638** (2006) 356–358, [hep-ph/0602116].

[159] N. Afshordi, M. Zaldarriaga and K. Kohri, *On the stability of dark energy with mass-varying neutrinos*, *Phys. Rev.* **D72** (2005) 065024, [astro-ph/0506663].

[160] O. E. Bjaelde, A. W. Brookfield, C. van de Bruck, S. Hannestad, D. F. Mota, L. Schrempp et al., *Neutrino Dark Energy – Revisiting the Stability Issue*, *JCAP* **0801** (2008) 026, [0705.2018].

[161] C. Wetterich, *Growing neutrinos and cosmological selection*, *Phys. Lett.* **B655** (2007) 201–208, [0706.4427].

[162] D. F. Mota, V. Pettorino, G. Robbers and C. Wetterich, *Neutrino clustering in growing neutrino quintessence*, *Phys. Lett.* **B663** (2008) 160–164, [0802.1515].

[163] J. R. Bhatt, P.-H. Gu, U. Sarkar and S. K. Singh, *Left-right symmetric model of neutrino dark energy*, *Phys. Lett.* **B663** (2008) 83–85, [0711.2728].

[164] A. Hektor, L. Marzola, M. Raidal and H. Veermae, *A new mechanism for dark energy: the adaptive screening*, *JHEP* **01** (2015) 101, [1407.0389].

[165] C. Hati and U. Sarkar, *Neutrino dark energy and leptogenesis with TeV scale triplets*, *Eur. Phys. J.* **C76** (2016) 236, [1511.02874].

[166] CMS collaboration, V. Khachatryan et al., *Search for heavy neutrinos and* W *bosons with right-handed couplings in proton-proton collisions at* $\sqrt{s} = 8$ *TeV*, *Eur. Phys. J.* **C74** (2014) 3149, [1407.3683].

[167] CMS collaboration, *Search for Pair-production of First Generation Scalar Leptoquarks in pp Collisions at* $\sqrt{s} = 8$ *TeV*, Tech. Rep. CMS-PAS-EXO-12-041, CERN, Geneva, 2014.

[168] ATLAS collaboration, G. Aad et al., *Search for high-mass diboson resonances with boson-tagged jets in proton-proton collisions at* $\sqrt{s} = 8$ *TeV with the ATLAS detector*, *JHEP* **12** (2015) 055, [1506.00962].

[169] CMS collaboration, V. Khachatryan et al., *Search for massive resonances in dijet systems containing jets tagged as W or Z boson decays in pp collisions at* $\sqrt{s}$ *= 8 TeV*, *JHEP* **08** (2014) 173, [1405.1994].

[170] CMS collaboration, V. Khachatryan et al., *Search for massive resonances decaying into pairs of boosted bosons in semi-leptonic final states at* $\sqrt{s} = 8$ *TeV*, *JHEP* **08** (2014) 174, [1405.3447].

[171] ATLAS collaboration, G. Aad et al., *Search for new phenomena in the dijet mass distribution using* $p - p$ *collision data at* $\sqrt{s} = 8$ *TeV with the ATLAS detector*, *Phys. Rev.* **D91** (2015) 052007, [1407.1376].

[172] CMS collaboration, V. Khachatryan et al., *Search for resonances and quantum black holes using dijet mass spectra in proton-proton collisions at* $\sqrt{s} = 8$ *TeV*, *Phys. Rev.* **D91** (2015) 052009, [1501.04198].

[173] CMS collaboration, C. Collaboration, *Search for massive WH resonances decaying to* $\ell\nu\mathrm{b}\bar{\mathrm{b}}$ *final state in the boosted regime at* $\sqrt{s} = 8$ *TeV*, .

[174] CMS collaboration, C. Collaboration, *Search for new physics in high mass diphoton events in proton-proton collisions at 13TeV*, .

[175] T. A. collaboration, *Search for resonances decaying to photon pairs in 3.2 fb^{-1} of pp collisions at $\sqrt{s}$ = 13 TeV with the ATLAS detector*, .

[176] J. Ellis and D. S. Hwang, *Does the 'Higgs' have Spin Zero?*, *JHEP* **09** (2012) 071, [1202.6660].

[177] BABAR collaboration, J. P. Lees et al., *Evidence for an excess of $\bar{B} \to D^{(*)}\tau^-\bar{\nu}_\tau$ decays*, *Phys. Rev. Lett.* **109** (2012) 101802, [1205.5442].

[178] BABAR collaboration, J. P. Lees et al., *Measurement of an Excess of $\bar{B} \to D^{(*)}\tau^-\bar{\nu}_\tau$ Decays and Implications for Charged Higgs Bosons*, *Phys. Rev.* **D88** (2013) 072012, [1303.0571].

[179] BELLE collaboration, M. Huschle et al., *Measurement of the branching ratio of $\bar{B} \to D^{(*)}\tau^-\bar{\nu}_\tau$ relative to $\bar{B} \to D^{(*)}\ell^-\bar{\nu}_\ell$ decays with hadronic tagging at Belle*, *Phys. Rev.* **D92** (2015) 072014, [1507.03233].

[180] LHCB collaboration, R. Aaij et al., *Measurement of the ratio of branching fractions $\mathcal{B}(\bar{B}^0 \to D^{*+}\tau^-\bar{\nu}_\tau)/\mathcal{B}(\bar{B}^0 \to D^{*+}\mu^-\bar{\nu}_\mu)$*, *Phys. Rev. Lett.* **115** (2015) 111803, [1506.08614].

[181] BELLE collaboration, A. Abdesselam et al., *Measurement of the branching ratio of $\bar{B}^0 \to D^{*+}\tau^-\bar{\nu}_\tau$ relative to $\bar{B}^0 \to D^{*+}\ell^-\bar{\nu}_\ell$ decays with a semileptonic tagging method*, 1603.06711.

[182] LHCB collaboration, R. Aaij et al., *Test of lepton universality using $B^+ \to K^+\ell^+\ell^-$ decays*, *Phys. Rev. Lett.* **113** (2014) 151601, [1406.6482].

[183] LHCB collaboration, R. Aaij et al., *Measurement of Form-Factor-Independent Observables in the Decay $B^0 \to K^{*0}\mu^+\mu^-$*, *Phys. Rev. Lett.* **111** (2013) 191801, [1308.1707].

[184] C. Bobeth, G. Hiller and G. Piranishvili, *Angular distributions of $\bar{B} \to \bar{K}\ell^+\ell^-$ decays*, *JHEP* **12** (2007) 040, [0709.4174].

[185] MUON G-2 collaboration, G. W. Bennett et al., *Measurement of the negative muon anomalous magnetic moment to 0.7 ppm*, *Phys. Rev. Lett.* **92** (2004) 161802, [hep-ex/0401008].

[186] MUON G-2 collaboration, G. W. Bennett et al., *Final Report of the Muon E821 Anomalous Magnetic Moment Measurement at BNL*, *Phys. Rev.* **D73** (2006) 072003, [hep-ex/0602035].

[187] F. F. Deppisch, T. E. Gonzalo, S. Patra, N. Sahu and U. Sarkar, *Signal of Right-Handed Charged Gauge Bosons at the LHC?*, *Phys. Rev.* **D90** (2014) 053014, [1407.5384].

[188] F. F. Deppisch, T. E. Gonzalo, S. Patra, N. Sahu and U. Sarkar, *Double beta decay, lepton flavor violation, and collider signatures of left-right symmetric models with spontaneous D-parity breaking*, *Phys. Rev.* **D91** (2015) 015018, [1410.6427].

[189] J. Gluza and T. Jelinski, *Heavy neutrinos and the pp?lljj CMS data*, *Phys. Lett.* **B748** (2015) 125–131, [1504.05568].

[190] J. Brehmer, J. Hewett, J. Kopp, T. Rizzo and J. Tattersall, *Symmetry Restored in Dibosons at the LHC?*, *JHEP* **10** (2015) 182, [1507.00013].

[191] D. Chang, R. N. Mohapatra and M. K. Parida, *Decoupling Parity and SU(2)-R Breaking Scales: A New Approach to Left-Right Symmetric Models*, *Phys. Rev. Lett.* **52** (1984) 1072.

[192] E. Ma, S. Sarkar and U. Sarkar, *Scale of SU(2)(R) symmetry breaking and leptogenesis*, *Phys. Lett.* **B458** (1999) 73–78, [hep-ph/9812276].

[193] F. F. Deppisch, J. Harz and M. Hirsch, *Falsifying High-Scale Leptogenesis at the LHC*, *Phys. Rev. Lett.* **112** (2014) 221601, [1312.4447].

[194] F. F. Deppisch, J. Harz, M. Hirsch, W.-C. Huang and H. Pas, *Falsifying High-Scale Baryogenesis with Neutrinoless Double Beta Decay and Lepton Flavor Violation*, *Phys. Rev.* **D92** (2015) 036005, [1503.04825].

[195] J.-M. Frere, T. Hambye and G. Vertongen, *Is leptogenesis falsifiable at LHC?*, *JHEP* **01** (2009) 051, [0806.0841].

[196] P. S. Bhupal Dev, C.-H. Lee and R. N. Mohapatra, *Leptogenesis Constraints on the Mass of Right-handed Gauge Bosons*, *Phys. Rev.* **D90** (2014) 095012, [1408.2820].

[197] P. S. Bhupal Dev, C.-H. Lee and R. N. Mohapatra, *TeV Scale Lepton Number Violation and Baryogenesis*, *J. Phys. Conf. Ser.* **631** (2015) 012007, [1503.04970].

[198] M. Dhuria, C. Hati, R. Rangarajan and U. Sarkar, *The $eejj$ Excess Signal at the LHC and Constraints on Leptogenesis*, *JCAP* **1509** (2015) 035, [1502.01695].

[199] M. Dhuria, C. Hati, R. Rangarajan and U. Sarkar, *Falsifying leptogenesis for a TeV scale $W_R^\pm$ at the LHC*, *Phys. Rev.* **D92** (2015) 031701, [1503.07198].

[200] M. Doi, *Lepton number violating e- W+ –¿ e+ W- and e- e- –¿ W- W- processes in the left-right gauge model*, *Prog. Theor. Phys.* **101** (1999) 639–660.

[201] M. Dhuria, C. Hati, R. Rangarajan and U. Sarkar, *Explaining the CMS $eejj$ and e missing $\mathrm{p_T}$ jj excess and leptogenesis in superstring inspired E_6 models*, *Phys. Rev.* **D91** (2015) 055010, [1501.04815].

[202] R. N. Mohapatra and R. E. Marshak, *PHENOMENOLOGY OF NEUTRON OSCILLATIONS*, *Phys. Lett.* **B94** (1980) 183.

[203] D. G. Phillips, II et al., *Neutron-Antineutron Oscillations: Theoretical Status and Experimental Prospects*, *Phys. Rept.* **612** (2016) 1–45, [1410.1100].

[204] A. Strumia, *Interpreting the 750 GeV digamma excess: a review*, 2016. 1605.09401.

[205] P. S. Bhupal Dev and R. N. Mohapatra, *Unified explanation of the $eejj$, diboson and dijet resonances at the LHC*, *Phys. Rev. Lett.* **115** (2015) 181803, [1508.02277].

[206] F. F. Deppisch, L. Graf, S. Kulkarni, S. Patra, W. Rodejohann, N. Sahu et al., *Reconciling the 2 TeV Excesses at the LHC in a Linear Seesaw Left-Right Model*, *Phys. Rev.* **D93** (2016) 013011, [1508.05940].

[207] F. F. Deppisch, C. Hati, S. Patra, P. Pritimita and U. Sarkar, *Implications of the diphoton excess on left?right models and gauge unification*, *Phys. Lett.* **B757** (2016) 223–230, [1601.00952].

[208] D. Guadagnoli, R. N. Mohapatra and I. Sung, *Gauged Flavor Group with Left-Right Symmetry*, *JHEP* **04** (2011) 093, [1103.4170].

[209] G. C. Joshi and R. R. Volkas, *Extended weak isospin and fermion masses in a unified model*, *Phys. Rev.* **D45** (1992) 1711–1719.

[210] G. Aldazabal, L. E. Ibanez and F. Quevedo, *A D^- brane alternative to the MSSM*, *JHEP* **02** (2000) 015, [hep-ph/0001083].

[211] J. P. Conlon, A. Maharana and F. Quevedo, *Towards Realistic String Vacua*, *JHEP* **05** (2009) 109, [0810.5660].

[212] S. Patra, *Neutrinoless double beta decay process in left-right symmetric models without scalar bidoublet*, *Phys. Rev.* **D87** (2013) 015002, [1212.0612].

[213] P. S. B. Dev, R. N. Mohapatra and Y. Zhang, *Quark Seesaw Vectorlike Fermions and Diphoton Excess*, 1512.08507.

[214] Q.-H. Cao, S.-L. Chen and P.-H. Gu, *Strong CP Problem, Neutrino Masses and the 750 GeV Diphoton Resonance*, 1512.07541.

[215] A. Dasgupta, M. Mitra and D. Borah, *Minimal Left-Right Symmetry Confronted with the 750 GeV Di-photon Excess at LHC*, 1512.09202.

[216] R. Franceschini, G. F. Giudice, J. F. Kamenik, M. McCullough, A. Pomarol, R. Rattazzi et al., *What is the gamma gamma resonance at 750 GeV?*, 1512.04933.

[217] S. D. McDermott, P. Meade and H. Ramani, *Singlet Scalar Resonances and the Diphoton Excess*, 1512.05326.

[218] J. M. Arnold, B. Fornal and M. B. Wise, *Simplified models with baryon number violation but no proton decay*, *Phys. Rev.* **D87** (2013) 075004, [1212.4556].

[219] E. Ma, *Particle Dichotomy and Left-Right Decomposition of E(6) Superstring Models*, *Phys. Rev.* **D36** (1987) 274.

[220] ATLAS collaboration, G. Aad et al., *Search for new phenomena in final states with an energetic jet and large missing transverse momentum in pp collisions at $\sqrt{s}$ =8 TeV with the ATLAS detector*, *Eur. Phys. J.* **C75** (2015) 299, [1502.01518].

[221] CMS collaboration, V. Khachatryan et al., *Search for dark matter, extra dimensions, and unparticles in monojet events in proton–proton collisions at $\sqrt{s} = 8$ TeV*, *Eur. Phys. J.* **C75** (2015) 235, [1408.3583].

[222] A. Falkowski, O. Slone and T. Volansky, *Phenomenology of a 750 GeV Singlet*, 1512.05777.

[223] M. Heikinheimo, M. Raidal and C. Spethmann, *Testing Right-Handed Currents at the LHC*, *Eur. Phys. J.* **C74** (2014) 3107, [1407.6908].

[224] J. A. Aguilar-Saavedra and F. R. Joaquim, *Closer look at the possible CMS signal of a new gauge boson*, *Phys. Rev.* **D90** (2014) 115010, [1408.2456].

[225] B. A. Dobrescu and A. Martin, *Interpretations of anomalous LHC events with electrons and jets*, *Phys. Rev.* **D91** (2015) 035019, [1408.1082].

[226] B. Allanach, S. Biswas, S. Mondal and M. Mitra, *Explaining a CMS $eejj$ Excess With $\mathcal{R}-$parity Violating Supersymmetry and Implications for Neutrinoless Double Beta Decay*, *Phys. Rev.* **D91** (2015) 011702, [1408.5439].

[227] B. C. Allanach, S. Biswas, S. Mondal and M. Mitra, *Resonant slepton production yields CMS $eejj$ and ep_Tjj excesses*, *Phys. Rev.* **D91** (2015) 015011, [1410.5947].

[228] S. Biswas, D. Chowdhury, S. Han and S. J. Lee, *Explaining the lepton non-universality at the LHCb and CMS within a unified framework*, *JHEP* **02** (2015) 142, [1409.0882].

[229] F. S. Queiroz, K. Sinha and A. Strumia, *Leptoquarks, Dark Matter, and Anomalous LHC Events*, *Phys. Rev.* **D91** (2015) 035006, [1409.6301].

[230] B. Allanach, A. Alves, F. S. Queiroz, K. Sinha and A. Strumia, *Interpreting the CMS $\ell^+\ell^- jj \not{E}_T$ Excess with a Leptoquark Model*, *Phys. Rev.* **D92** (2015) 055023, [1501.03494].

[231] W.-Y. Keung and G. Senjanovic, *Majorana Neutrinos and the Production of the Right-handed Charged Gauge Boson*, *Phys. Rev. Lett.* **50** (1983) 1427.

[232] P. Candelas, G. T. Horowitz, A. Strominger and E. Witten, *Vacuum Configurations for Superstrings*, *Nucl. Phys.* **B258** (1985) 46–74.

[233] B. R. Greene, *String theory on Calabi-Yau manifolds*, in *Fields, strings and duality. Proceedings, Summer School, Theoretical Advanced Study Institute in Elementary Particle Physics, TASI'96, Boulder, USA, June 2-28, 1996*, pp. 543–726, 1996. hep-th/9702155.

[234] M. B. Green and J. H. Schwarz, *Anomaly Cancellation in Supersymmetric D=10 Gauge Theory and Superstring Theory*, *Phys. Lett.* **B149** (1984) 117–122.

[235] M. B. Green, J. H. Schwarz and E. Witten, *SUPERSTRING THEORY. VOL. 1: INTRODUCTION*. 1988.

[236] M. B. Green, J. H. Schwarz and E. Witten, *SUPERSTRING THEORY. VOL. 2: LOOP AMPLITUDES, ANOMALIES AND PHENOMENOLOGY*. 1988.

[237] TWIST collaboration, J. F. Bueno et al., *Precise measurement of parity violation in polarized muon decay*, *Phys. Rev.* **D84** (2011) 032005, [1104.3632].

[238] G. Beall, M. Bander and A. Soni, *Constraint on the Mass Scale of a Left-Right Symmetric Electroweak Theory from the K(L) K(S) Mass Difference*, *Phys. Rev. Lett.* **48** (1982) 848.

[239] A. Maiezza, M. Nemevsek, F. Nesti and G. Senjanovic, *Left-Right Symmetry at LHC*, *Phys. Rev.* **D82** (2010) 055022, [1005.5160].

[240] Y. Zhang, H. An, X. Ji and R. N. Mohapatra, *General CP Violation in Minimal Left-Right Symmetric Model and Constraints on the Right-Handed Scale*, *Nucl. Phys.* **B802** (2008) 247–279, [0712.4218].

[241] G. Senjanovic and V. Tello, *Right Handed Quark Mixing in Left-Right Symmetric Theory*, *Phys. Rev. Lett.* **114** (2015) 071801, [1408.3835].

[242] G. Ecker, W. Grimus and H. Neufeld, *The Neutron Electric Dipole Moment in Left-right Symmetric Gauge Models*, *Nucl. Phys.* **B229** (1983) 421–444.

[243] E. Ma, *D0 - Anti-d0 Mixing in the New Left-right Model*, *Mod. Phys. Lett.* **A3** (1988) 319.

[244] J. F. Gunion, J. L. Hewett, E. Ma, T. G. Rizzo, V. D. Barger, N. Deshpande et al., *Signatures for a New Supersymmetric Left-right Gauge Model From Superstrings*, *Int. J. Mod. Phys.* **A2** (1987) 1199.

[245] F. Aversa, S. Bellucci, M. Greco and P. Chiappetta, *Production of W(R) and W(I) bosons from superstring inspired E(6) models at hadron colliders*, *Phys. Lett.* **B254** (1991) 478–484.

[246] M. Diemoz, F. Ferroni, E. Longo and G. Martinelli, *Parton Densities from Deep Inelastic Scattering to Hadronic Processes at Super Collider Energies*, *Z. Phys.* **C39** (1988) 21.

[247] D. London and J. L. Rosner, *Extra Gauge Bosons in E(6)*, *Phys. Rev.* **D34** (1986) 1530.

[248] T. G. Rizzo, *Production of Flavor Changing Gauge Bosons From* $E(6)$ *at* e^+e^- *Hadron Colliders*, *Phys. Rev.* **D38** (1988) 71–77.

[249] B. C. Allanach, C. H. Kom and H. Pas, *Large Hadron Collider probe of supersymmetric neutrinoless double beta decay mechanism*, *Phys. Rev. Lett.* **103** (2009) 091801, [0902.4697].

[250] C. Hati, *Explaining the diphoton excess in Alternative Left-Right Symmetric Model*, *Phys. Rev.* **D93** (2016) 075002, [1601.02457].

[251] M. Dhuria and G. Goswami, *Perturbativity, vacuum stability and inflation in the light of 750 GeV diphoton excess*, 1512.06782.

[252] M. Bauer and M. Neubert, *Flavor Anomalies, the Diphoton Excess and a Dark Matter Candidate*, 1512.06828.

[253] LHC Higgs Cross Section Working Group collaboration, J. R. Andersen et al., *Handbook of LHC Higgs Cross Sections: 3. Higgs Properties*, 1307.1347.

[254] B. C. Allanach, P. S. B. Dev and K. Sakurai, *ATLAS diboson excess could be an R-parity violating dismuon excess*, *Phys. Rev.* **D93** (2016) 035010, [1511.01483].

[255] G.-C. Cho, S. Kaneko and A. Omote, *Decay of Charged Higgs boson in TeV scale supersymmetric seesaw model*, *Phys. Lett.* **B652** (2007) 325–330, [hep-ph/0611240].

[256] T. Hambye, E. Ma, M. Raidal and U. Sarkar, *Allowable low-energy E(6) subgroups from leptogenesis*, *Phys. Lett.* **B512** (2001) 373–378, [hep-ph/0011197].

[257] M. Dhuria, C. Hati and U. Sarkar, *Explaining the CMS excesses, baryogenesis and neutrino masses in E_6 motivated $U(1)_N$ model*, *Phys. Rev.* **D93** (2016) 015001, [1507.08297].

[258] P. Krawczyk and S. Pokorski, *Strongly Coupled Charged Scalar in B and t Decays*, *Phys. Rev. Lett.* **60** (1988) 182.

[259] J. Kalinowski, *Semileptonic Decays of B Mesons into $\tau\nu_\tau$ in a Two Higgs Doublet Model*, *Phys. Lett.* **B245** (1990) 201–206.

[260] W.-S. Hou, *Enhanced charged Higgs boson effects in B- —¿ tau anti-neutrino, mu anti-neutrino and b —¿ tau anti-neutrino + X*, *Phys. Rev.* **D48** (1993) 2342–2344.

[261] M. Tanaka, *Charged Higgs effects on exclusive semitauonic B decays*, *Z. Phys.* **C67** (1995) 321–326, [hep-ph/9411405].

[262] J. F. Kamenik and F. Mescia, *$B \to D\tau\nu$ Branching Ratios: Opportunity for Lattice QCD and Hadron Colliders*, *Phys. Rev.* **D78** (2008) 014003, [0802.3790].

[263] U. Nierste, S. Trine and S. Westhoff, *Charged-Higgs effects in a new B —¿ D tau nu differential decay distribution*, *Phys. Rev.* **D78** (2008) 015006, [0801.4938].

[264] M. Tanaka and R. Watanabe, *Tau longitudinal polarization in B -¿ D tau nu and its role in the search for charged Higgs boson*, *Phys. Rev.* **D82** (2010) 034027, [1005.4306].

[265] S. Fajfer, J. F. Kamenik and I. Nisandzic, *On the $B \to D^*\tau\bar{\nu}_\tau$ Sensitivity to New Physics*, *Phys. Rev.* **D85** (2012) 094025, [1203.2654].

[266] Y. Sakaki and H. Tanaka, *Constraints on the charged scalar effects using the forward-backward asymmetry on $B^- \to D^{(*)}\tau\bar{\nu}_\tau$*, *Phys. Rev.* **D87** (2013) 054002, [1205.4908].

[267] S. Fajfer, J. F. Kamenik, I. Nisandzic and J. Zupan, *Implications of Lepton Flavor Universality Violations in B Decays*, *Phys. Rev. Lett.* **109** (2012) 161801, [1206.1872].

[268] A. Datta, M. Duraisamy and D. Ghosh, *Diagnosing New Physics in $b \to c\,\tau\,\nu_\tau$ decays in the light of the recent BaBar result*, *Phys. Rev.* **D86** (2012) 034027, [1206.3760].

[269] J. A. Bailey et al., *Refining new-physics searches in $B- > D\tau\nu$ decay with lattice QCD*, *Phys. Rev. Lett.* **109** (2012) 071802, [1206.4992].

[270] D. Becirevic, N. Kosnik and A. Tayduganov, $\bar{B} \to D\tau\bar{\nu}_\tau$ *vs.* $\bar{B} \to D\mu\bar{\nu}_\mu$, *Phys. Lett.* **B716** (2012) 208–213, [1206.4977].

[271] M. Tanaka and R. Watanabe, *New physics in the weak interaction of* $\bar{B} \to D^{(*)}\tau\bar{\nu}$, *Phys. Rev.* **D87** (2013) 034028, [1212.1878].

[272] M. Freytsis, Z. Ligeti and J. T. Ruderman, *Flavor models for* $\bar{B} \to D^{(*)}\tau\bar{\nu}$, *Phys. Rev.* **D92** (2015) 054018, [1506.08896].

[273] S. Bhattacharya, S. Nandi and S. K. Patra, *Optimal-observable analysis of possible new physics in* $B \to D^{(*)}\tau\nu_\tau$, *Phys. Rev.* **D93** (2016) 034011, [1509.07259].

[274] A. Celis, M. Jung, X.-Q. Li and A. Pich, *Sensitivity to charged scalars in* $\boldsymbol{B \to D^{(*)}\tau\nu_\tau}$ *and* $\boldsymbol{B \to \tau\nu_\tau}$ *decays*, *JHEP* **01** (2013) 054, [1210.8443].

[275] P. Ko, Y. Omura and C. Yu, $B \to D^{(*)}\tau\nu$ *and* $B \to \tau\nu$ *in chiral U(1)' models with flavored multi Higgs doublets*, *JHEP* **03** (2013) 151, [1212.4607].

[276] A. Crivellin, C. Greub and A. Kokulu, *Explaining* $B \to D\tau\nu$, $B \to D^*\tau\nu$ *and* $B \to \tau\nu$ *in a 2HDM of type III*, *Phys. Rev.* **D86** (2012) 054014, [1206.2634].

[277] N. G. Deshpande and A. Menon, *Hints of R-parity violation in B decays into* $\tau\nu$, *JHEP* **01** (2013) 025, [1208.4134].

[278] I. Dorsner, S. Fajfer, J. F. Kamenik and N. Kosnik, *Can scalar leptoquarks explain the f(D(s)) puzzle?*, *Phys. Lett.* **B682** (2009) 67–73, [0906.5585].

[279] Y. Sakaki, M. Tanaka, A. Tayduganov and R. Watanabe, *Testing leptoquark models in* $\bar{B} \to D^{(*)}\tau\bar{\nu}$, *Phys. Rev.* **D88** (2013) 094012, [1309.0301].

[280] A. Greljo, G. Isidori and D. Marzocca, *On the breaking of Lepton Flavor Universality in B decays*, *JHEP* **07** (2015) 142, [1506.01705].

[281] I. Dorsner, S. Fajfer, N. Kosnik and I. Nisandzic, *Minimally flavored colored scalar in* $\bar{B} \to D^{(*)}\tau\bar{\nu}$ *and the mass matrices constraints*, *JHEP* **11** (2013) 084, [1306.6493].

[282] P. Biancofiore, P. Colangelo and F. De Fazio, *On the anomalous enhancement observed in $B \to D^{(*)}\tau\bar{\nu}_\tau$ decays*, *Phys. Rev.* **D87** (2013) 074010, [1302.1042].

[283] Y.-Y. Fan, Z.-J. Xiao, R.-M. Wang and B.-Z. Li, *The $B \to D^{(*)}l\nu_l$ decays in the pQCD approach with the Lattice QCD input*, 1505.07169.

[284] C. Hati, G. Kumar and N. Mahajan, *$\bar{B} \to D^{(*)}\tau\bar{\nu}$ excesses in ALRSM constrained from B, D decays and $D^0 - \bar{D}^0$ mixing*, *JHEP* **01** (2016) 117, [1511.03290].

[285] K. Hagiwara, A. D. Martin and M. F. Wade, *EXCLUSIVE SEMILEPTONIC B MESON DECAYS*, *Nucl. Phys.* **B327** (1989) 569–594.

[286] M. Neubert, *Model independent extraction of V(cb) from semileptonic decays*, *Phys. Lett.* **B264** (1991) 455–461.

[287] B. A. Dobrescu and A. S. Kronfeld, *Accumulating evidence for nonstandard leptonic decays of D_s mesons*, *Phys. Rev. Lett.* **100** (2008) 241802, [0803.0512].

[288] J. Barranco, D. Delepine, V. Gonzalez Macias and L. Lopez-Lozano, *Constraining New Physics with D meson decays*, *Phys. Lett.* **B731** (2014) 36–42, [1303.3896].

[289] H. F. A. Group. http://www.slac.stanford.edu/xorg/hfag/charm/CHARM15/results_mix_cpv.html.

[290] E. Golowich, J. Hewett, S. Pakvasa and A. A. Petrov, *Implications of D^0 - $\bar{D}^0$ Mixing for New Physics*, *Phys. Rev.* **D76** (2007) 095009, [0705.3650].

[291] K. Agashe and M. Graesser, *R-parity violation in flavor changing neutral current processes and top quark decays*, *Phys. Rev.* **D54** (1996) 4445–4452, [hep-ph/9510439].

[292] Y. Grossman, Z. Ligeti and E. Nardi, *New limit on inclusive $B \to X_s$ anti-neutrino neutrino decay and constraints on new physics*, *Nucl. Phys.* **B465** (1996) 369–398, [hep-ph/9510378].

[293] A. J. Buras, J. Girrbach-Noe, C. Niehoff and D. M. Straub, $B \to K^{(*)}\nu\overline{\nu}$ *decays in the Standard Model and beyond*, *JHEP* **02** (2015) 184, [1409.4557].

[294] D. Das, C. Hati, G. Kumar and N. Mahajan, *Towards a unified explanation of* $R_{D^{(*)}}$*,* R_K *and* $(g-2)_\mu$ *anomalies in a L-R model*, 1605.06313.

[295] R. Alonso, B. Grinstein and J. Martin Camalich, $SU(2) \times U(1)$ *gauge invariance and the shape of new physics in rare* B *decays*, *Phys. Rev. Lett.* **113** (2014) 241802, [1407.7044].

[296] G. Hiller and M. Schmaltz, R_K *and future* $b \to s\ell\ell$ *physics beyond the standard model opportunities*, *Phys. Rev.* **D90** (2014) 054014, [1408.1627].

[297] M. Bauer and M. Neubert, *Minimal Leptoquark Explanation for the* $R_{D^{(*)}}$ *,* R_K *, and* $(g-2)_g$ *Anomalies*, *Phys. Rev. Lett.* **116** (2016) 141802, [1511.01900].

[298] LSND collaboration, A. Aguilar-Arevalo et al., *Evidence for neutrino oscillations from the observation of anti-neutrino(electron) appearance in a anti-neutrino(muon) beam*, *Phys. Rev.* **D64** (2001) 112007, [hep-ex/0104049].

[299] MiniBooNE collaboration, A. A. Aguilar-Arevalo et al., *Event Excess in the MiniBooNE Search for* $\bar{\nu}_\mu \to \bar{\nu}_e$ *Oscillations*, *Phys. Rev. Lett.* **105** (2010) 181801, [1007.1150].

[300] G. Mention, M. Fechner, T. Lasserre, T. A. Mueller, D. Lhuillier, M. Cribier et al., *The Reactor Antineutrino Anomaly*, *Phys. Rev.* **D83** (2011) 073006, [1101.2755].

[301] T. A. Mueller et al., *Improved Predictions of Reactor Antineutrino Spectra*, *Phys. Rev.* **C83** (2011) 054615, [1101.2663].

[302] P. Huber, *On the determination of anti-neutrino spectra from nuclear reactors*, *Phys. Rev.* **C84** (2011) 024617, [1106.0687].

[303] J. Kopp, P. A. N. Machado, M. Maltoni and T. Schwetz, *Sterile Neutrino Oscillations: The Global Picture*, *JHEP* **05** (2013) 050, [1303.3011].

[304] J. M. Conrad, C. M. Ignarra, G. Karagiorgi, M. H. Shaevitz and J. Spitz, *Sterile Neutrino Fits to Short Baseline Neutrino Oscillation Measurements*, *Adv. High Energy Phys.* **2013** (2013) 163897, [1207.4765].

[305] Intensity Frontier Neutrino Working Group collaboration, A. de Gouvea et al., *Working Group Report: Neutrinos*, in *Community Summer Study 2013: Snowmass on the Mississippi (CSS2013) Minneapolis, MN, USA, July 29-August 6, 2013*, 2013. 1310.4340.

[306] M. Archidiacono, N. Fornengo, C. Giunti, S. Hannestad and A. Melchiorri, *Sterile neutrinos: Cosmology versus short-baseline experiments*, *Phys. Rev.* **D87** (2013) 125034, [1302.6720].

[307] E. Ma, *Neutrino masses in an extended gauge model with E(6) particle content*, *Phys. Lett.* **B380** (1996) 286–290, [hep-ph/9507348].

[308] J. L. Rosner, *Three sterile neutrinos in E6*, *Phys. Rev.* **D90** (2014) 035005, [1404.5198].

[309] A. S. Joshipura and U. Sarkar, *Phenomenologically Consistent Discrete Symmetries in Superstring Theories*, *Phys. Rev. Lett.* **57** (1986) 33.

[310] E. Ma, *EXOTIC BARYON NUMBER NONCONSERVATION: ANOTHER E(6) SUPERSTRING VARIATION*, *Phys. Rev. Lett.* **60** (1988) 1363.

[311] E. Ma and M. Raidal, *Three active and two sterile neutrinos in an E(6) model of diquark baryogenesis*, *J. Phys.* **G28** (2002) 95–102, [hep-ph/0012366].

[312] J. Hisano, N. Nagata and Y. Omura, *Interpretations of the ATLAS Diboson Resonances*, *Phys. Rev.* **D92** (2015) 055001, [1506.03931].

[313] K. Cheung, W.-Y. Keung, P.-Y. Tseng and T.-C. Yuan, *Interpretations of the ATLAS Diboson Anomaly*, *Phys. Lett.* **B751** (2015) 188–194, [1506.06064].

[314] B. A. Dobrescu and Z. Liu, *W' Boson near 2 TeV: Predictions for Run 2 of the LHC*, *Phys. Rev. Lett.* **115** (2015) 211802, [1506.06736].

[315] Y. Gao, T. Ghosh, K. Sinha and J.-H. Yu, *SU(2) $\times$ SU(2) $\times$ U(1) interpretations of the diboson and Wh excesses*, *Phys. Rev.* **D92** (2015) 055030, [1506.07511].

[316] Q.-H. Cao, B. Yan and D.-M. Zhang, *Simple non-Abelian extensions of the standard model gauge group and the diboson excesses at the LHC*, *Phys. Rev.* **D92** (2015) 095025, [1507.00268].

[317] T. Abe, R. Nagai, S. Okawa and M. Tanabashi, *Unitarity sum rules, three-site moose model, and the ATLAS 2 TeV diboson anomalies*, *Phys. Rev.* **D92** (2015) 055016, [1507.01185].

[318] J. Heeck and S. Patra, *Minimal Left-Right Symmetric Dark Matter*, *Phys. Rev. Lett.* **115** (2015) 121804, [1507.01584].

[319] B. C. Allanach, B. Gripaios and D. Sutherland, *Anatomy of the ATLAS diboson anomaly*, *Phys. Rev.* **D92** (2015) 055003, [1507.01638].

[320] T. Abe, T. Kitahara and M. M. Nojiri, *Prospects for Spin-1 Resonance Search at 13 TeV LHC and the ATLAS Diboson Excess*, *JHEP* **02** (2016) 084, [1507.01681].

[321] B. A. Dobrescu and Z. Liu, *Heavy Higgs bosons and the 2 TeV W′ boson*, *JHEP* **10** (2015) 118, [1507.01923].

[322] H. S. Fukano, S. Matsuzaki and K. Yamawaki, *Conformal Barrier for New Vector Bosons Decay to the Higgs*, *Mod. Phys. Lett.* **A31** (2016) 1630009, [1507.03428].

[323] H. S. Fukano, M. Kurachi, S. Matsuzaki, K. Terashi and K. Yamawaki, *2 TeV Walking Technirho at LHC?*, *Phys. Lett.* **B750** (2015) 259–265, [1506.03751].

[324] A. Thamm, R. Torre and A. Wulzer, *Composite Heavy Vector Triplet in the ATLAS Diboson Excess*, *Phys. Rev. Lett.* **115** (2015) 221802, [1506.08688].

[325] A. Carmona, A. Delgado, M. Quiros and J. Santiago, *Diboson resonant production in non-custodial composite Higgs models*, *JHEP* **09** (2015) 186, [1507.01914].

[326] C.-W. Chiang, H. Fukuda, K. Harigaya, M. Ibe and T. T. Yanagida, *Diboson Resonance as a Portal to Hidden Strong Dynamics*, *JHEP* **11** (2015) 015, [1507.02483].

[327] G. Cacciapaglia, A. Deandrea and M. Hashimoto, *Scalar Hint from the Diboson Excess?*, *Phys. Rev. Lett.* **115** (2015) 171802, [1507.03098].

[328] V. Sanz, *On the Compatibility of the Diboson Excess with a gg-Initiated Composite Sector*, *Adv. High Energy Phys.* **2016** (2016) 3279568, [1507.03553].

[329] A. Alves, A. Berlin, S. Profumo and F. S. Queiroz, *Dirac-fermionic dark matter in $U(1)_X$ models*, *JHEP* **10** (2015) 076, [1506.06767].

[330] J. A. Aguilar-Saavedra, *Triboson interpretations of the ATLAS diboson excess*, *JHEP* **10** (2015) 099, [1506.06739].

[331] C.-H. Chen and T. Nomura, *2 TeV Higgs boson and diboson excess at the LHC*, *Phys. Lett.* **B749** (2015) 464–468, [1507.04431].

[332] L. A. Anchordoqui, I. Antoniadis, H. Goldberg, X. Huang, D. Lust and T. R. Taylor, *Stringy origin of diboson and dijet excesses at the LHC*, *Phys. Lett.* **B749** (2015) 484–488, [1507.05299].

[333] C. Petersson and R. Torre, *ATLAS diboson excess from low scale supersymmetry breaking*, *JHEP* **01** (2016) 099, [1508.05632].

[334] J. Erler, P. Langacker, S. Munir and E. Rojas, *Improved Constraints on Z-prime Bosons from Electroweak Precision Data*, *JHEP* **08** (2009) 017, [0906.2435].

[335] T. Hambye, *Leptogenesis at the TeV scale*, *Nucl. Phys.* **B633** (2002) 171–192, [hep-ph/0111089].

[336] CDMS collaboration, R. Agnese et al., *Silicon detector results from the first five-tower run of CDMS II*, *Phys. Rev.* **D88** (2013) 031104, [1304.3706].

[337] CoGeNT collaboration, C. E. Aalseth et al., *CoGeNT: A Search for Low-Mass Dark Matter using p-type Point Contact Germanium Detectors*, *Phys. Rev.* **D88** (2013) 012002, [1208.5737].

[338] XENON100 collaboration, E. Aprile et al., *Dark Matter Results from 225 Live Days of XENON100 Data*, *Phys. Rev. Lett.* **109** (2012) 181301, [1207.5988].

[339] R. Allahverdi, B. Dutta and Y. Gao, *keV Photon Emission from Light Nonthermal Dark Matter*, *Phys. Rev.* **D89** (2014) 127305, [1403.5717].

[340] G. Kane, K. Sinha and S. Watson, *Cosmological Moduli and the Post-Inflationary Universe: A Critical Review*, *Int. J. Mod. Phys.* **D24** (2015) 1530022, [1502.07746].

[341] B. S. Acharya, P. Kumar, K. Bobkov, G. Kane, J. Shao and S. Watson, *Non-thermal Dark Matter and the Moduli Problem in String Frameworks*, *JHEP* **06** (2008) 064, [0804.0863].

[342] R. Allahverdi, M. Cicoli, B. Dutta and K. Sinha, *Nonthermal dark matter in string compactifications*, *Phys. Rev.* **D88** (2013) 095015, [1307.5086].

[343] H. Baer, K.-Y. Choi, J. E. Kim and L. Roszkowski, *Dark matter production in the early Universe: beyond the thermal WIMP paradigm*, *Phys. Rept.* **555** (2015) 1–60, [1407.0017].

[344] N. Blinov, J. Kozaczuk, A. Menon and D. E. Morrissey, *Confronting the moduli-induced lightest-superpartner problem*, *Phys. Rev.* **D91** (2015) 035026, [1409.1222].

[345] R. Allahverdi, B. Dutta and K. Sinha, *Baryogenesis and Late-Decaying Moduli*, *Phys. Rev.* **D82** (2010) 035004, [1005.2804].

[346] R. Allahverdi, B. Dutta and K. Sinha, *Cladogenesis: Baryon-Dark Matter Coincidence from Branchings in Moduli Decay*, *Phys. Rev.* **D83** (2011) 083502, [1011.1286].

[347] R. Allahverdi, B. Dutta, R. N. Mohapatra and K. Sinha, *A Supersymmetric Model for Dark Matter and Baryogenesis Motivated by the Recent CDMS Result*, *Phys. Rev. Lett.* **111** (2013) 051302, [1305.0287].

[348] R. Kitano, H. Murayama and M. Ratz, *Unified origin of baryons and dark matter*, *Phys. Lett.* **B669** (2008) 145–149, [0807.4313].

[349] K. Ishiwata, *Axino Dark Matter in Moduli-induced Baryogenesis*, *JHEP* **09** (2014) 122, [1407.1827].

[350] M. Kawasaki and K. Nakayama, *Baryon Asymmetry in Heavy Moduli Scenario*, *Phys. Rev.* **D76** (2007) 043502, [0705.0079].

[351] G. Kane, J. Shao, S. Watson and H.-B. Yu, *The Baryon-Dark Matter Ratio Via Moduli Decay After Affleck-Dine Baryogenesis*, *JCAP* **1111** (2011) 012, [1108.5178].

[352] T. Banks, D. B. Kaplan and A. E. Nelson, *Cosmological implications of dynamical supersymmetry breaking*, *Phys. Rev.* **D49** (1994) 779–787, [hep-ph/9308292].

[353] C. P. Burgess, M. Cicoli and F. Quevedo, *String Inflation After Planck 2013*, *JCAP* **1311** (2013) 003, [1306.3512].

[354] G. F. Giudice and A. Masiero, *A Natural Solution to the mu Problem in Supergravity Theories*, *Phys. Lett.* **B206** (1988) 480–484.

[355] A. Brignole, L. E. Ibanez and C. Munoz, *Soft supersymmetry breaking terms from supergravity and superstring models*, *Adv. Ser. Direct. High Energy Phys.* **21** (2010) 244–268, [hep-ph/9707209].

[356] Y. Grossman, T. Kashti, Y. Nir and E. Roulet, *Leptogenesis from supersymmetry breaking*, *Phys. Rev. Lett.* **91** (2003) 251801, [hep-ph/0307081].

[357] G. D'Ambrosio, G. F. Giudice and M. Raidal, *Soft leptogenesis*, *Phys. Lett.* **B575** (2003) 75–84, [hep-ph/0308031].

[358] Y. Nir, *CP violation*, *Conf. Proc.* **C9207131** (1992) 81–136.

[359] M. L. Graesser, I. M. Shoemaker and L. Vecchi, *Asymmetric WIMP dark matter*, *JHEP* **10** (2011) 110, [1103.2771].

[360] K. Petraki and R. R. Volkas, *Review of asymmetric dark matter*, *Int. J. Mod. Phys.* **A28** (2013) 1330028, [1305.4939].

[361] E. Ma, *Neutrino mass from triplet and doublet scalars at the TeV scale*, *Phys. Rev.* **D66** (2002) 037301, [hep-ph/0204013].

[362] T. Hambye, Y. Lin, A. Notari, M. Papucci and A. Strumia, *Constraints on neutrino masses from leptogenesis models*, *Nucl. Phys.* **B695** (2004) 169–191, [hep-ph/0312203].

[363] W. Fischler and R. Flauger, *Neutrino Masses, Leptogenesis, and Unification in the Absence of Low Energy Supersymmetry*, *JHEP* **09** (2008) 020, [0805.3000].

[364] D. Aristizabal Sierra, J. F. Kamenik and M. Nemevsek, *Implications of Flavor Dynamics for Fermion Triplet Leptogenesis*, *JHEP* **10** (2010) 036, [1007.1907].

[365] F. del Aguila and J. A. Aguilar-Saavedra, *Distinguishing seesaw models at LHC with multi-lepton signals*, *Nucl. Phys.* **B813** (2009) 22–90, [0808.2468].

[366] R. Franceschini, T. Hambye and A. Strumia, *Type-III see-saw at LHC*, *Phys. Rev.* **D78** (2008) 033002, [0805.1613].

[367] ATLAS collaboration, T. A. collaboration, *Search for scalar diphoton resonances with 15.4 fb^{-1} of data collected at $\sqrt{s}$=13 TeV in 2015 and 2016 with the ATLAS detector*, .

[368] CMS collaboration, V. Khachatryan et al., *Search for high-mass diphoton resonances in proton-proton collisions at 13 TeV and combination with 8 TeV search*, *Phys. Lett.* **B767** (2017) 147–170, [1609.02507].

[369] CMS collaboration, C. Collaboration, *Search for massive resonances decaying into WW, WZ, ZZ, qW and qZ in the dijet final state at* $\sqrt{s} = 13$ TeV, .

[370] CMS collaboration, A. M. Sirunyan et al., *Search for massive resonances decaying into WW, WZ or ZZ bosons in proton-proton collisions at* $\sqrt{s} = 13$ *TeV*, *JHEP* **03** (2017) 162, [1612.09159].

[371] CMS collaboration, C. Collaboration, *Search for massive resonances decaying into WW, WZ, ZZ, qW and qZ in the dijet final state at* $\sqrt{s} = 13$ TeV *using 2016 data*, .

[372] CMS collaboration, C. Collaboration, *Search for new diboson resonances in the dilepton + jets final state at* $\sqrt{s} = 13$ TeV *with 2016 data*, .

[373] CMS collaboration, A. M. Sirunyan et al., *Search for anomalous couplings in boosted* $\mathrm{WW}/\mathrm{WZ} \to \ell\nu\mathrm{q}\bar{\mathrm{q}}$ *production in proton-proton collisions at* $\sqrt{s} = 8$ *TeV*, 1703.06095.

[374] ATLAS collaboration, M. Aaboud et al., *Search for new phenomena in dijet events using 37 fb*$^{-1}$ *of pp collision data collected at* $\sqrt{s}$ *=13 TeV with the ATLAS detector*, 1703.09127.

[375] CMS collaboration, C. Collaboration, *Searches for dijet resonances in pp collisions at* $\sqrt{s} = 13$ TeV *using data collected in 2016.*, .

[376] A. Joglekar and J. L. Rosner, *Searching for signatures of* E_6, 1607.06900.

List of Publications

Publications in refereed journals

1. D. Das, **C. Hati**, G. Kumar and N. Mahajan
   Towards a unified explanation of $R_{D^{(*)}}$, R_K *and* $(g-2)_\mu$ *anomalies in a left-right model with leptoquarks*,
   To appear in Phys. Rev. D (2016), arXiv:1605.06313 [hep-ph].

2. **C. Hati**
   Explaining the diphoton excess in Alternative Left-Right Symmetric Model,
   Phys. Rev. D **93**, 075002 (2016), arXiv:1601.02457 [hep-ph].

3. F. F. Deppisch, **C. Hati**, S. Patra, P. Pritimita and U. Sarkar
   Implications of the diphoton excess on left-right models and gauge unification,
   Phys. Lett. B **757**, 223 (2016), arXiv:1601.00952 [hep-ph].

4. **C. Hati**, G. Kumar and N. Mahajan
   $\bar{B} \to D^{(*)}\tau\bar{\nu}$ *excesses in ALRSM constrained from* B, D *decays and* $D^0 - \bar{D}^0$ *mixing*,
   JHEP **01**, 117 (2016), arXiv:1511.03290 [hep-ph].

5. **C. Hati** and U. Sarkar
   Neutrino dark energy and leptogenesis with TeV scale triplets,
   Eur. Phys. J. C **76**, 236 (2016), arXiv:1511.02874 [hep-ph].

6. M. Dhuria, **C. Hati** and U. Sarkar
   Moduli induced cogenesis of baryon asymmetry and dark matter,
   Phys. Lett. B **756**, 376 (2016), arXiv:1508.04144 [hep-ph].

7. M. Dhuria, **C. Hati** and U. Sarkar
Explaining the CMS excesses, baryogenesis and neutrino masses in E_6 motivated $U(1)_N$ model,
Phys. Rev. D **93**, 015001 (2016), arXiv:1507.08297 [hep-ph].

8. M. Dhuria, **C. Hati**, R. Rangarajan and U. Sarkar
Falsifying leptogenesis for a TeV scale $W_R^{\pm}$ at the LHC,
Phys. Rev. D **92**, 031701 (Rapid Communication) (2015), arXiv:1503.07198 [hep-ph].

9. M. Dhuria, **C. Hati**, R. Rangarajan and U. Sarkar
The $eejj$ Excess Signal at the LHC and Constraints on Leptogenesis,
JCAP **1509**, 035 (2015), arXiv:1502.01695 [hep-ph].

10. M. Dhuria, **C. Hati**, R. Rangarajan and U. Sarkar
Explaining the CMS $eejj$ and e missing p_T jj excess and leptogenesis in superstring inspired E_6 models,
Phys. Rev. D **91**, 055010 (2015), arXiv:1501.04815 [hep-ph].

Preprints under review

1. F. F. Deppisch, **C. Hati**, S. Patra, U. Sarkar and J. W. F. Valle
331 Models and Grand Unification: From Minimal SU(5) to Minimal SU(6),
arXiv:1608.05334 [hep-ph].

2. A. Dasgupta, **C. Hati**, S. Patra and U. Sarkar
A minimal model of TeV scale WIMPy leptogenesis,
arXiv:1605.01292 [hep-ph].

Publications attached with thesis

1. M. Dhuria, **C. Hati**, R. Rangarajan and U. Sarkar
   Falsifying leptogenesis for a TeV scale $W_R^{\pm}$ *at the LHC*,
   Phys. Rev. D **92**, 031701 (Rapid Communication) (2015).
   doi: 10.1103/PhysRevD.92.031701

2. M. Dhuria, **C. Hati** and U. Sarkar
   Explaining the CMS excesses, baryogenesis and neutrino masses in E_6 *motivated* $U(1)_N$ *model*,
   Phys. Rev. D **93**, 015001 (2016).
   doi: 10.1103/PhysRevD.93.015001

3. F. F. Deppisch, **C. Hati**, S. Patra, P. Pritimita and U. Sarkar
   Implications of the diphoton excess on left-right models and gauge unification,
   Phys. Lett. B **757**, 223 (2016).
   doi: 10.1016/j.physletb.2016.03.081

PHYSICAL REVIEW D **92,** 031701(R) (2015)

Falsifying leptogenesis for a TeV scale $W_R^{\pm}$ at the LHC

Mansi Dhuria,[1,*] Chandan Hati,[1,2,†] Raghavan Rangarajan,[1,‡] and Utpal Sarkar[1,§]

[1]*Physical Research Laboratory, Navrangpura, Ahmedabad 380 009, India*
[2]*Indian Institute of Technology Gandhinagar, Chandkheda, Ahmedabad 382 424, India*

(Received 31 March 2015; published 18 August 2015)

We point out that the discovery of a right-handed charged gauge boson $W_R^{\pm}$ with mass of around a few TeV, for example through a signal of two leptons and two jets that has been reported by CMS to have a 2.8σ local excess or through a signal of a resonance decaying into a pair of standard model (SM) gauge bosons showing a local excess of 3.4σ (2.5σ global) reported by ATLAS search, will rule out all possibilities of leptogenesis in all classes of the left-right symmetric extensions of the Standard Model (LRSM) with both triplet and doublet Higgs scalars due to the unavoidable fast gauge mediated $B-L$ violating interactions $e_R^{\pm} W_R^{\mp} \rightarrow e_R^{\mp} W_R^{\pm}$. Our conclusions are very general in the sense that they do not necessarily demand for a lepton number violating detection signal of $W_R^{\pm}$.

DOI: 10.1103/PhysRevD.92.031701 PACS numbers: 12.60.Cn, 11.30.Fs, 13.85.Rm, 98.80.Cq

The Left-Right Symmetric Model (LRSM) [1] is one of the most popular candidates for extensions of the Standard Model (SM) of particle physics. In LRSM the Standard Model gauge group is extended at higher energies to

$$\mathcal{G}_{LR} \equiv SU(3)_c \times SU(2)_L \times SU(2)_R \times U(1)_{B-L}$$

where $B-L$ is the difference between baryon (B) and lepton (L) numbers. Left-right symmetry breaking predicts the existence of a massive right-handed charged gauge boson ($W_R^{\pm}$). In this paper, we point out that if $W_R^{\pm}$ has a mass of a few TeV and can be detected at the LHC, it will have profound consequences for our understanding of the baryon asymmetry of the Universe. This is a unique situation where by observing $W_R^{\pm}$ at the LHC, we can make a very strong statement about our origin, that is regarding the baryon asymmetry of the Universe. One of the most attractive mechanisms to generate the baryon asymmetry is leptogenesis, in which a lepton asymmetry is created before the electroweak phase transition, which then gets converted to the baryon asymmetry in the presence of $(B+L)$ violating anomalous processes [2]. Detection of a TeV scale $W_R^{\pm}$ at the LHC would imply violation of $(B-L)$ at a lower energy, which will rule out all scenarios of leptogenesis. In this context we must mention that an excess of 2.8σ level was observed in the energy bin $1.8\ \text{TeV} < M_{lljj} < 2.1\ \text{TeV}$ in the two leptons two jets channel at the LHC by the CMS experiment [3], which can be interpreted as due to $W_R^{\pm}$ decay by embedding the conventional LRSM with $g_L \neq g_R$ in $SO(10)$ [4] and with $g_L = g_R$ by taking into account the CP phases and nondegenerate masses of heavy neutrinos [5]. More recently, the ATLAS search has also reported a resonance that decays to a pair of SM gauge bosons to show a local excess of 3.4σ (2.5σ global) in the WZ final state at approximately 2 TeV [6], which can naturally be explained by a W_R in the LRSM framework with a coupling $g_R \sim 0.4$ [7].

In the LRSM the fermion sector transforms under the gauge group $\mathcal{G}_{LR}$ as:

$$l_L:\ (1,2,1,-1), \qquad l_R:\ (1,1,2,-1),$$
$$Q_L:\ \left(3,2,1,\frac{1}{3}\right), \qquad Q_R:\ \left(3,1,2,\frac{1}{3}\right). \tag{1}$$

In a popular version of the LRSM, the Higgs sector consists of one bidoublet Φ and two triplet $\Delta_{L,R}$ complex scalar fields with the transformations

$$\Phi:\ (1,2,2,0), \qquad \Delta_L:\ (1,3,1,2), \qquad \Delta_R:\ (1,1,3,2). \tag{2}$$

The left-right symmetry is spontaneously broken to reproduce the Standard Model and the smallness of the neutrino masses can be taken care of by the seesaw mechanism [8]. The symmetry breaking pattern follows the scheme

$$\mathcal{G}_{LR} \overset{\langle\Delta_R\rangle}{\rightarrow} SU(3)_C \times SU(2)_L \times U(1)_Y \equiv \mathcal{G}_{\rm SM}$$
$$\overset{\langle\Phi\rangle}{\rightarrow} SU(3)_C \times U(1)_{\rm EM} \equiv \mathcal{G}_{\rm EM}. \tag{3}$$

In the first stage of symmetry breaking the right-handed triplet Δ_R acquires a Vacuum Expectation Value (VEV) $\langle\Delta_R\rangle = \frac{1}{\sqrt{2}} v_R$ which breaks the $SU(2)_R$ symmetry and gives masses to the $W_R^{\pm}$, Z_R bosons. The electroweak symmetry is broken by the bidoublet Higgs Φ, which gives masses to the charged fermions and the gauge bosons $W_L^{\pm}$ and Z_L. The Δ_L gets an induced seesaw tiny VEV, which can give a Majorana mass to the left-handed neutrinos. The generators of the broken gauge groups are then related to

*mansi@prl.res.in
†chandan@prl.res.in
‡raghavan@prl.res.in
§utpal@prl.res.in

the electric charge by the modified Gell-Mann-Nishijima formula $Q = T_{3L} + T_{3R} + \frac{B-L}{2}$.

In a variant of the LRSM with triplet Higgs scalars, one considers only doublet Higgs scalars to break all the symmetries. This scenario is more popular in all superstring inspired models. Here the Higgs sector consists of doublet scalars

$$\Phi\colon\ (1,2,2,0), \qquad H_L\colon\ (1,2,1,1), \qquad H_R\colon\ (1,1,2,1), \tag{4}$$

and there is one additional singlet fermion field S_R (1,1,1,0) in addition to the fermions mentioned in Eq. (1). The doublet Higgs scalar H_R acquires a VEV to break the left-right symmetry and results in mixing of S with right-handed neutrinos, giving rise to one light Majorana neutrino, and one heavy pseudo-Dirac neutrino or two Majorana neutrinos.

In the conventional LRSM, the left-right symmetry is broken at a fairly high scale, $M_R > 10^{10}$ GeV. First, the gauge coupling unification requires this scale to be high, and second, thermal leptogenesis in this scenario gives a comparable bound. One often introduces a parity odd scalar and gives a large VEV to this field. This is called D-parity breaking, which may then allow $g_L \neq g_R$ even before the left-right symmetry breaking, and hence, this allows gauge coupling unification with TeV scale M_R. This is true for both triplet and doublet models of LRSM. Embedding the LRSM in an $SO(10)$ GUT framework, the violation of D-parity at a high scale can explain the CMS TeV scale W_R signal for $g_R \approx 0.6 g_L$ [4].

For a TeV scale $W_R^\pm$, all leptogenesis models may be classified into two groups:

(i) A lepton asymmetry is generated at a very high scale either in the context of D-parity breaking LRSM or through some other interactions, both thermal and nonthermal.

(ii) A lepton asymmetry is generated at the TeV scale with resonant enhancement, when the left-right symmetry breaking phase transition is taking place.

These discussions are valid for the LRSM with both triplet as well as doublet Higgs scalars. We use the reference of the two variants of the LRSM mentioned above to study the lepton number violating washout processes and demonstrate that all these possible scenarios of leptogenesis are falsifiable for a TeV scale W_R. In models with high-scale leptogenesis with $T > 10^9$ GeV, the low energy $B-L$ breaking is associated with giving mass to the $W_R^\pm$, which allows gauge interactions that wash out all the baryon asymmetry before the electroweak phase transition is over. On the other hand, the same lepton number violating gauge interactions will slow down the generation of the lepton asymmetry for resonant leptogenesis at the TeV scale, so that generation of the required baryon asymmetry of the universe is not possible for TeV scale $W_R^\pm$.

The most stringent constraints on the $W_R^\pm$ mass for successful high-scale leptogenesis for a hierarchical neutrino mass spectrum ($M_{N_{3R}} \gg M_{N_{2R}} \gg M_{N_{1R}} = m_{N_R}$) come from the $SU(2)_R$ interactions [9]. To have successful leptogenesis in the case $M_{N_R} > M_{W_R}$ the out-of-equilibrium condition for the scattering process $e_R^- + W_R^+ \to N_R \to e_R^+ + W_R^-$ gives

$$M_{N_R} \gtrsim 10^{16}\ \text{GeV} \tag{5}$$

with $m_{W_R}/m_{N_R} \gtrsim 0.1$. Now for the case $M_{W_R} > M_{N_R}$ leptogenesis can happen either at $T \simeq M_{N_R}$ or at $T > M_{W_R}$ but at less than the $B-L$ breaking scale. Considering the out-of equilibrium condition for the scattering process $e_R^\pm e_R^\pm \to W_R^\pm W_R^\pm$ through N_R exchange one obtains the constraint

$$M_{W_R} \gtrsim 3 \times 10^6\ \text{GeV}(M_{N_R}/10^2\ \text{GeV})^{2/3}. \tag{6}$$

Thus observing a W_R signal with a mass in the TeV range for hierarchical neutrino masses rules out the high-scale leptogenesis scenario. In Refs. [10], the constraints obtained from the observation of lepton number violating processes and neutrinoless double beta decay were studied to rule out typical scenarios of high-scale thermal leptogenesis, particularly leptogenesis models with right-handed neutrinos with mass greater than the mass scale observed at the LHC by the CMS experiment. The possibility of generating the required lepton asymmetry with a considerably low value of the W_R mass has been discussed in the context of the resonant leptogenesis scenario [11]. In the LRSM, it has been pointed out that successful low-scale leptogenesis with a quasidegenerate right-handed neutrinos mass spectrum, requires an absolute lower bound of 18 TeV on the W_R mass [12]. Recently, it was reported that just the right amount of lepton asymmetry can be produced even for a substantially lower value of the W_R mass ($M_{W_R} > 3$ TeV) [13] by considering relatively large Yukawa couplings, which has been updated to 13.1 TeV after a more careful analysis in Ref. [14]. In Refs. [12,13], the lepton number violating gauge scattering processes such as $N_R e_R \to \bar{u}_R d_R$, $N_R \bar{u}_R \to e_R d_R$, $N_R d_R \to e_R u_R$ and $N_R N_R \to e_R \bar{e}_R$ have been analyzed in detail. However, lepton number violating scattering processes with external W_R have been ignored on the account of the fact that for a heavy W_R, there will be a relative suppression of $e^{-m_{W_R}/m_{N_R}}$ in comparison to the processes with no external W_R. Now if the W_R mass is a few TeV's as suggested by the excess signal at the LHC reported by the CMS experiment then one has to take the latter processes seriously.

In Ref. [15], we had first pointed out that the lepton number violating washout processes ($e_R^\pm e_R^\pm \to W_R^\pm W_R^\pm$ and $e_R^\pm W_R^\mp \to e_R^\mp W_R^\pm$) can be mediated by doubly charged Higgs scalars in the conventional LRSM. Following that, in Ref. [14] only this channel was considered, and for a particular class of type-I seesaw model with relatively small

M_{N_R} it was found to have a small contribution, as expected for a large M_{W_R}/M_{N_R}. However the other gauge scattering processes in that scenario are strong enough to give a lower bound of 13.1 TeV on the W_R mass. In this paper, we explore the above lepton number violating scattering processes mediated by both Δ_R^{++} and N_R in a much more general context, where we have also taken into account the interference of these channels. The former channel has one gauge vertex and one Yukawa vertex, while for the latter channel both the vertices are gauge vertices, thus are highly unsuppressed compared to the processes involving Yukawa vertices. We find that the lepton number violating scattering process $e_R^{\pm}W_R^{\mp} \to e_R^{\mp}W_R^{\pm}$ mediated via both N_R and Δ_R^{++} can stay in equilibrium till the electroweak phase transition for a TeV scale W_R and wash out the lepton asymmetry.[1] Thus if one incorporates the above washout process in the Boltzmann equation for lepton number asymmetry, the mentioned lower limit on M_{W_R} for successful TeV-scale resonant leptogenesis will further go up. In the later variant of LRSM mentioned above the doubly charged Higgs is not there, however, the lepton number violating scattering processes mediated via N_R are still present and will wash out the lepton asymmetry.

In the LRSM, the charged current interaction involving the right-handed neutrino and the right-handed gauge boson is given by

$$\mathcal{L}_N = \frac{1}{2\sqrt{2}} g_R J_{R\mu} W_R^{-\mu} + \text{H.c.} \tag{7}$$

where $J_{R\mu} = \bar{e}_R\gamma_\mu(1+\gamma_5)N_R$. The Lagrangian for the right-handed Higgs triplet is given by

$$\mathcal{L}_{\Delta_R} \supset (D_{R\mu}\vec{\Delta}_R)^\dagger (D_R^\mu \vec{\Delta}_R), \tag{8}$$

where $\vec{\Delta}_R = (\Delta_R^{++}, \Delta_R^{+}, \Delta_R^{0})$ in the spherical basis and the covariant derivative is defined as $D_{R\mu} = \partial_\mu - ig_R(T_R^j A_{R\mu}^j) - ig' B_\mu$. The $A_{R\mu}^j$ and B_μ are gauge fields associated with $SU(2)_R$ and $U(1)_{B-L}$ groups with the gauge couplings given by g_R and g', respectively. After spontaneous breaking of the left-right symmetry by giving VEV to the neutral Higgs field Δ_R^0 i.e. $\langle \Delta_R^0 \rangle = \frac{1}{\sqrt{2}} v_R$, the interaction between the doubly charged Higgs triplet and the gauge boson W_R will be given by [16]

$$\mathcal{L}_{\Delta_R} \supset \left(-\frac{v_R}{\sqrt{2}}\right) g_R^2 W_{\mu R}^{-} W_R^{-\mu} \Delta_R^{++} + \text{H.c.} \tag{9}$$

The Yukawa interaction between the lepton doublet $\psi_{eR} = (N_R, e_R)^T$ and the Higgs triplet $\vec{\Delta}_R$ will be given by

$$\mathcal{L}_Y = h_{ee}^R \overline{(\psi_{eR})^c} (i\tau_2 \vec{\tau}.\vec{\Delta}_R)\psi_{eR} + \text{H.c.}, \tag{10}$$

where τ's are the Pauli matrices. By giving a VEV to the neutral Higgs triplet field, the Yukawa coupling can be expressed as $h_{ee}^R = \frac{M_{N_R}}{2v_R}$ where M_{N_R} corresponds to mass of the Majorana neutrino (N_R).

The Feynman diagrams of the lepton number violating scattering process induced by the above interactions are shown in Fig. 1. Utilizing the interactions in Eqs. (7)–(10), the differential scattering cross section for the $e_R^{\mp}(p)W_R^{\pm}(k) \to e_R^{\pm}(p')W_R^{\mp}(k')$ process is given by [16]

$$\frac{d\sigma_{e_R W_R}^{e_R W_R}}{dt} = \frac{1}{384\pi M_{W_R}^4 (s - M_{W_R}^2)^2} \Lambda_{e_R W_R}^{e_R W_R}(s,t,u), \tag{11}$$

where

$$\Lambda_{e_R W_R}^{e_R W_R}(s,t,u) = \Lambda_{e_R W_R}^{e_R W_R}(s,t,u)\big|_{N_R} + \Lambda_{e_R W_R}^{e_R W_R}(s,t,u)\big|_{\Delta_R^{++}} \tag{12}$$

and

$$\begin{aligned}\Lambda_{e_R W_R}^{e_R W_R}(s,t,u)\big|_{N_R} = g_R^4 \Bigg\{ &-t\left|M_{N_R}\left(\frac{s}{s-M_{N_R}^2} + \frac{u}{u-M_{N_R}^2}\right)\right|^2 \\ &-4M_{W_R}^2(su - M_{W_R}^4)(s-u)^2\left|\frac{M_{N_R}}{(s-M_{N_R}^2)(u-M_{N_R}^2)}\right|^2 \\ &-4M_{W_R}^4 t\left(\left|\frac{m_{N_R}}{(s-M_{N_R}^2)}\right|^2 + \left|\frac{M_{N_R}}{(u-M_{N_R}^2)}\right|^2\right)\Bigg\},\end{aligned} \tag{13}$$

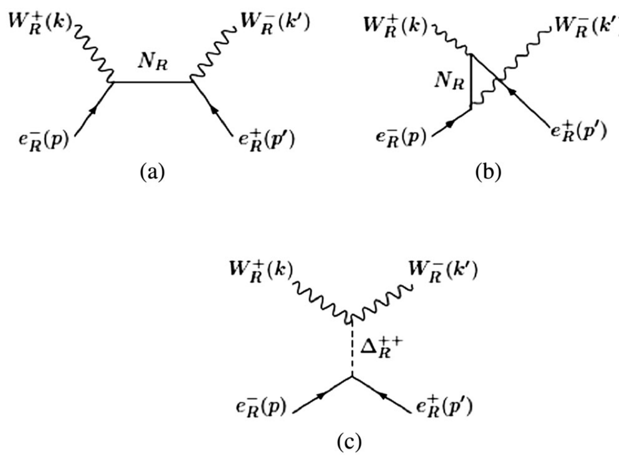

FIG. 1. Feynman diagrams for $e_R^- W_R^+ \to e_R^+ W_R^-$ scattering process (a,b) mediated by right handed neutrino N_R and (c) mediated by doubly charged Higgs scalar Δ_R^{++}. The Feynman diagrams for $e_R^- e_R^- \to W_R^- W_R^-$ are the same as above with appropriate change in direction of the external lines.

[1] Note that the other scattering process is doubly phase space suppressed at a temperature below the W_R mass and hence we will not consider it for leptogenesis at $T \lesssim M_{W_R}$.

$$\Lambda^{e_R W_R}_{e_R W_R}(s,t,u)|_{\Delta_R^{++}} = 4g_R^4(-t)\left\{\frac{(s+u)^2+8M_{W_R}^4}{(t-M_{\Delta_R}^2)^2}|M_{N_R}|^2 + \frac{(s+u)}{t-M_{\Delta_R}^2}|M_{N_R}|^2\left(\frac{s}{s-M_{N_R}^2}+\frac{u}{u-M_{N_R}^2}\right) + \frac{4M_{W_R}^4}{t-M_{\Delta_R}^2}|M_{N_R}|^2\left(\frac{1}{s-M_{N_R}^2}+\frac{1}{u-M_{N_R}^2}\right)\right\}, \quad (14)$$

where we have neglected any mixing between W_L and W_R. Note that on the right-hand side of Eq. (14) the first term represents the Higgs scalar exchange itself while the last two terms correspond to the interference between the Higgs scalar exchange and the N_R exchange mechanisms. The relation between Mandelstem variables $s=(p+k)^2$, $t=(p-p')^2$ and $u=(p-k')^2$ and scattering angle θ is given by

$$\begin{pmatrix} st \\ su - M_{W_R}^4 \end{pmatrix} = -\frac{1}{2}(s-M_{W_R}^2)^2(1\mp\cos\theta). \quad (15)$$

The differential scattering cross section for the $e_R^\pm(p)e_R^\pm(p') \to W_R^\pm(k)W_R^\pm(k')$ process is given by [16]

$$\frac{d\sigma^{e_R e_R}_{W_R W_R}}{dt} = \frac{1}{512\pi M_{W_R}^4 s^2}\Lambda^{e_R e_R}_{W_R W_R}(s,t,u), \quad (16)$$

where

$$\Lambda^{e_R e_R}_{W_R W_R}(s,t,u) = \Lambda^{e_R e_R}_{W_R W_R}(s,t,u)|_{N_R} + \Lambda^{e_R e_R}_{W_R W_R}(s,t,u)|_{\Delta_R^{++}}. \quad (17)$$

The expressions of $\Lambda^{e_R e_R}_{W_R W_R}(s,t,u)$ in this case are obtained by interchanging $s \leftrightarrow t$ in $\Lambda^{e_R W_R}_{e_R W_R}(s,t,u)$: $\Lambda^{e_R e_R}_{W_R W_R}(t,s,u) = -\Lambda^{e_R W_R}_{e_R W_R}(s,t,u)$. In this case, the Mandelstem variables $t=(p-k)^2$ and $u=(p-k')^2$ are related to $s=(p+p')^2$ and scattering angle θ by

$$\begin{pmatrix} t \\ u \end{pmatrix} = -\frac{s}{2}\left(1-\frac{2M_{W_R}^2}{s}\right)\left\{1\mp\sqrt{1-\left(\frac{2M_{W_R}^2}{s-2M_{W_R}^2}\right)^2}\cos\theta\right\}. \quad (18)$$

During the period $v_R > T > M_{W_R}$, both the lepton number violating processes are very fast without any suppression. To get an idea of the effectiveness of these scattering processes in wiping out the lepton asymmetry, we estimate the parameter

$$K \equiv \frac{n\langle\sigma|v|\rangle}{H}, \quad (19)$$

for both the processes, where n is the number density of relativistic species and is given by $n = 2\times\frac{3\zeta(3)}{4\pi^2}T^3$, H is the Hubble rate given by $H \simeq 1.7 g_*^{1/2}T^2/M_{\rm Pl}$, where $g_* \sim 100$ corresponds to the number of relativistic degrees of freedom, and $\langle\sigma|v|\rangle$ is the thermally averaged cross section. In order to obtain a rough estimate of v_R, let us draw an analogy with the Standard Model, where we have $\langle\phi\rangle = \frac{v_L}{\sqrt{2}}$ where $v_L = 246$ GeV, and $M_{W_L} \sim 80$ GeV. Now in the LRSM scenario, where we have $\langle\Delta_R^0\rangle = \frac{v_R}{\sqrt{2}}$ breaking the left-right symmetry and $M_{W_R} = g_R v_R$. Then taking $g_R \sim g_L$, we have $\frac{\langle\phi\rangle}{M_{W_L}} = \frac{\langle\Delta_R^0\rangle}{M_{W_R}} \approx 3$.

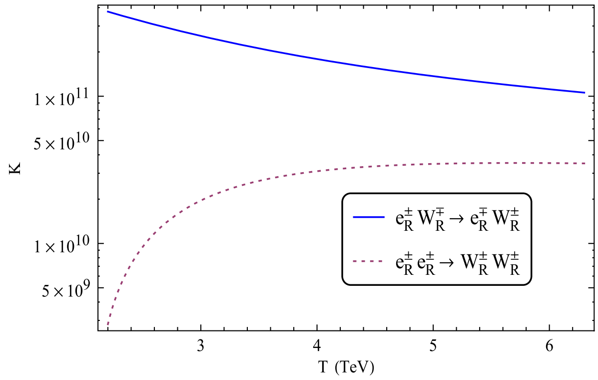

FIG. 2 (color online). Plot showing K as a function of temperature (T) with $M_{W_R} = 2.1$ TeV for the scattering processes $e_R^\pm W_R^\mp \to e_R^\mp W_R^\pm$ and $e_R^\pm e_R^\pm \to W_R^\pm W_R^\pm$ (including both Δ_R^{++} and N_R mediated diagrams) for $v_R > T > M_{W_R}$.

Using the differential cross-section given in Eqs. (11) and (16), we plot the behavior of K as a function of temperature in the range $3M_{W_R} > T > M_{W_R}$ for $M_{W_R} = 2.1$ TeV (in the mass range of CMS excess) in Fig. 2. The high value of K in Fig. 2 for both the processes implies that these scattering processes are very fast in washing out lepton asymmetry for $T \gtrsim M_{W_R}$. In the variant of LRSM with doublet Higgs scalars the scattering processes cannot be mediated via a doubly charged Higgs scalar. However, these lepton number violating scattering processes can still be mediated via heavy neutrinos, which washes out the lepton asymmetry in this scenario for $T \gtrsim M_{W_R}$.

For $T < M_{W_R}$, the process $e_R^\pm W_R^\mp \to e_R^\mp W_R^\pm$ is more important 1 Below we will estimate a lower bound on T until which the latter process stays in equilibrium below $T = M_{W_R}$. The cross section of this process as a function of temperature T can be obtained from Eq. (11). The scattering rate is given by[2] $\Gamma = \bar{n}\langle\sigma v_{\rm rel}\rangle$. At a temperature $T < M_{W_R}$ the number density $\bar{n} = g(\frac{TM_{W_R}}{2\pi})^{3/2}\exp(-\frac{M_{W_R}}{T})$ accounts for the Boltzmann suppression of the scattering rate. The condition for the scattering process to be in thermal equilibrium is $\Gamma > H$. Using $M_{N_R} \lesssim M_{W_R}$ and $v_{\rm rel} = 1$ we plot the temperature until which the scattering

[2]We have ignored any finite temperature effects to simplify the analysis. These effects are small and do not change our conclusions.

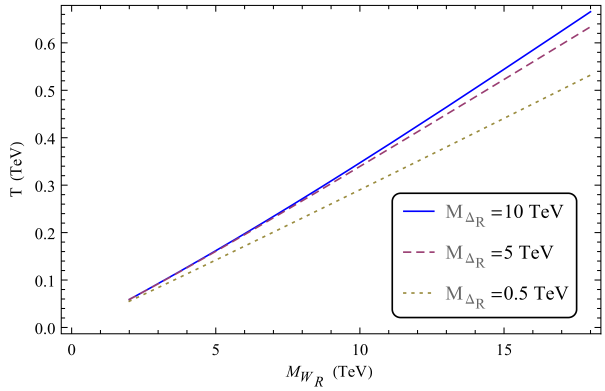

FIG. 3 (color online). Plots showing the out-of-equilibrium temperature (T) of the scattering process $e_R^{\pm}W_R^{\mp} \to e_R^{\mp}W_R^{\pm}$ (mediated via Δ_R^{++} and N_R fields) as a function of M_{W_R} for three different values of M_{Δ_R} and $M_{N_R} \sim M_{W_R}$.

process $e_R^{\pm}W_R^{\mp} \to e_R^{\mp}W_R^{\pm}$ stays in equilibrium as a function of the M_{W_R} in Fig. 3 for three different values of M_{Δ_R}. We have chosen the lowest value of M_{Δ_R} to be 500 GeV in accordance with the recent search limits on the doubly charged Higgs boson mass [17]. The plot clearly shows that unless M_{W_R} is significantly larger than the TeV scale, the scattering process $e_R^{\pm}W_R^{\mp} \to e_R^{\mp}W_R^{\pm}$ will stay in equilibrium till a temperature close to the electroweak phase transition and will continue to wash out the lepton asymmetry until that temperature. In the LRSM scenario with doublet Higgs scalars, the lepton number violating scattering processes mediated only via heavy neutrinos will continue to wash out the asymmetry until the electroweak phase transition, pushing up the lower limit on the W_R mass for a successful leptogenesis scenario far beyond the W_R signal range reported by the CMS experiment, ruling out the possibility of generating the observed baryon asymmetry from TeV scale resonant leptogenesis as well.

To conclude, for the high-scale leptogenesis scenario ($T \gtrsim M_{W_R}$), in both the variants of the LRSM the lepton number violating scattering processes ($e_R^{\pm}e_R^{\pm} \to W_R^{\pm}W_R^{\pm}$ and $e_R^{\pm}W_R^{\mp} \to e_R^{\mp}W_R^{\pm}$) are very efficient in wiping out the lepton asymmetry, while for a TeV scale resonant leptogenesis scenario the latter process will stay in equilibrium until the electroweak phase transition, washing out the lepton asymmetry for $T < M_{W_R}$. Hence we rule out the possibility of successful leptogenesis for $W_R^{\pm}$ with mass in the TeV range

(i) in all possible high-scale leptogenesis scenarios for the LRSM variants with (i) triplet Higgs and (ii) doublet Higgs, and
(ii) in TeV scale resonant leptogenesis scenarios for LRSM variants with (i) triplet Higgs and (ii) doublet Higgs.

Complementing the above results, we have also explored the low-energy subgroups of superstring motivated E_6 model in recent works. In one of the supersymmetric low-energy subgroups of the E_6 (known as the Alternative Left-Right Symmetric Model) one can allow for high-scale leptogenesis, and explain the excess signal at the LHC reported by the CMS experiment from resonant slepton decay. However, the excess signal cannot be explained by right-handed gauge boson decay while allowing leptogenesis, in both supersymmetric and non-supersymmetric low-energy subgroups of superstring motivated E_6 model [18]. Thus, in light of the above, if the two leptons and two jets excess at the LHC reported by the CMS experiment is indeed due to $W_R^{\pm}$ decay, then one needs to resort to a post-electroweak phase transition mechanism to explain the baryon asymmetry of the Universe and in this context, the experiments to observe the neutron-antineutron oscillation [19] or $(B-L)$ violating proton decay [20] will play a crucial role in confirming such possibilities.

[1] J. C. Pati and A. Salam, Lepton number as the fourth color, Phys. Rev. D **10**, 275 (1974); R. N. Mohapatra and J. C. Pati, A natural left-right symmetry, Phys. Rev. D **11**, 2558 (1975); G. Senjanovic and R. N. Mohapatra, Exact left-right symmetry and spontaneous violation of parity, Phys. Rev. D **12**, 1502 (1975).

[2] M. Fukugita and T. Yanagida, Baryogenesis without grand unification, Phys. Lett. B **174**, 45 (1986); for recent reviews see e.g. S. Davidson, E. Nardi, and Y. Nir, Leptogenesis, Phys. Rep. **466**, 105 (2008); C. S. Fong, E. Nardi, and A. Riotto, Leptogenesis in the Universe, Adv. High Energy Phys. **2012**, 158303 (2012).

[3] V. Khachatryan *et al.* (CMS Collaboration), Search for heavy neutrinos and W bosons with right-handed couplings in proton-proton collisions at $\sqrt{s} = 8$ TeV, Eur. Phys. J. C **74**, 3149 (2014).

[4] F. F. Deppisch, T. E. Gonzalo, S. Patra, N. Sahu, and U. Sarkar, Signal of right-handed charged gauge bosons at the LHC?, Phys. Rev. D **90**, 053014 (2014); Double beta decay, lepton flavor violation, and collider signatures of left-right symmetric models with spontaneous D-parity breaking, Phys. Rev. D **91**, 015018 (2015).

[5] J. Gluza and T. Jelinski, Heavy neutrinos and the $pp \to lljj$ CMS data, Phys. Lett. B **748**, 125 (2015).

[6] G. Aad *et al.* (ATLAS Collaboration), Search for high-mass diboson resonances with boson-tagged jets in proton-proton collisions at $\sqrt{s} = 8$ TeV with the ATLAS detector, arXiv:1506.00962.

[7] J. Brehmer, J. Hewett, J. Kopp, T. Rizzo, and J. Tattersall, Symmetry restored in Dibosons at the LHC?, arXiv:1507.00013.

[8] P. Minkowski, $\mu \to e\gamma$ at a rate of one out of 1-billion muon decays?, Phys. Lett. **67B**, 421 (1977); M. Gell-Mann, P. Ramond, and R. Slansky, Complex spinors and unified theories, Conf. Proc. C 790927 (1979), p. 315; T. Yanagida, Horizontal symmetry and masses of neutrinos, Conf. Proc. C 7902131 (1979), p. 95; R. N. Mohapatra and G. Senjanovic, Neutrino Mass and Spontaneous Parity Violation, Phys. Rev. Lett. **44**, 912 (1980); Neutrino masses and mixings in gauge models with spontaneous parity violation, Phys. Rev. D **23**, 165 (1981).

[9] E. Ma, S. Sarkar, and U. Sarkar, Scale of SU(2)(R) symmetry breaking and leptogenesis, Phys. Lett. B **458**, 73 (1999).

[10] F. F. Deppisch, J. Harz, and M. Hirsch, Falsifying High-Scale Leptogenesis at the LHC, Phys. Rev. Lett. **112**, 221601 (2014); F. F. Deppisch, J. Harz, M. Hirsch, W. C. Huang, and H. Päs, Falsifying high-scale baryogenesis with Neutrinoless double beta decay and lepton flavor violation, arXiv:1503.04825 [Phys. Rev. D (to be published)].

[11] M. Flanz, E. A. Paschos, and U. Sarkar, Baryogenesis from a lepton asymmetric universe, Phys. Lett. B **345**, 248 (1995); M. Flanz, E. A. Paschos, U. Sarkar, and J. Weiss, Baryogenesis through mixing of heavy Majorana neutrinos, Phys. Lett. B **389**, 693 (1996); A. Pilaftsis, *CP* violation and baryogenesis due to heavy Majorana neutrinos, Phys. Rev. D **56**, 5431 (1997); E. Roulet, L. Covi, and F. Vissani, On the *CP* asymmetries in Majorana neutrino decays, Phys. Lett. B **424**, 101 (1998); W. Buchmuller and M. Plumacher, *CP* asymmetry in Majorana neutrino decays, Phys. Lett. B **431**, 354 (1998); M. Flanz and E. A. Paschos, Further considerations on the *CP* asymmetry in heavy Majorana neutrino decays, Phys. Rev. D **58**, 113009 (1998); T. Hambye, J. March-Russell, and S. M. West, TeV scale resonant leptogenesis from supersymmetry breaking, J. High Energy Phys. 07 (2004) 070; A. Pilaftsis and T. E. J. Underwood, Resonant leptogenesis, Nucl. Phys. **B692**, 303 (2004).

[12] J. M. Frere, T. Hambye, and G. Vertongen, Is leptogenesis falsifiable at LHC?, J. High Energy Phys. 01 (2009) 051.

[13] P. S. Bhupal Dev, C. H. Lee, and R. N. Mohapatra, Leptogenesis constraints on the mass of right-handed gauge bosons, Phys. Rev. D **90**, 095012 (2014).

[14] P. S. Bhupal Dev, C. H. Lee, and R. N. Mohapatra, TeV scale lepton number violation and baryogenesis, arXiv:1503.04970.

[15] M. Dhuria, C. Hati, R. Rangarajan, and U. Sarkar, The $eejj$ excess signal at the LHC and constraints on leptogenesis, arXiv:1502.01695.

[16] M. Doi, Lepton number violating $e^-W^+ \to e^+W^-$ and $e^-e^- \to W^-W^-$ processes in the left-right gauge model, Prog. Theor. Phys. **101**, 639 (1999).

[17] K. A. Olive *et al.* (Particle Data Group Collaboration), Review of particle physics, Chin. Phys. C **38**, 090001 (2014).

[18] M. Dhuria, C. Hati, R. Rangarajan, and U. Sarkar, Explaining the CMS $eejj$ and ep_Tjj excess and leptogenesis in superstring inspired E_6 models, Phys. Rev. D **91**, 055010 (2015).

[19] R. N. Mohapatra and R. E. Marshak, Phenomenology of neutron oscillations, Phys. Lett. **94B**, 183 (1980); D. G. Phillips, II *et al.*, Neutron-Antineutron oscillations: Theoretical status and experimental prospects, arXiv:1410.1100.

[20] J. C. Pati, A. Salam, and U. Sarkar, $\Delta B = -\Delta L$, neutron $\to e^-\Pi^+, e^-\mathrm{K}^+, \mu^-\Pi^+$ and $\mu^-\mathrm{K}^+$ decay modes in $\mathrm{SU}(2)_\mathrm{L} \times \mathrm{SU}(2)_\mathrm{R} \times \mathrm{SU}(4)^{\mathrm{col}}$ or $\mathrm{SO}(10)$, Phys. Lett. **133B**, 330 (1983).

PHYSICAL REVIEW D **93,** 015001 (2016)

Explaining the CMS excesses, baryogenesis, and neutrino masses in a E_6 motivated $U(1)_N$ model

Mansi Dhuria,[1,*] Chandan Hati,[1,2,†] and Utpal Sarkar[1,‡]

[1]*Physical Research Laboratory, Navrangpura, Ahmedabad 380 009, India*
[2]*Indian Institute of Technology Gandhinagar, Chandkheda, Ahmedabad 382 424, India*
(Received 10 August 2015; published 7 January 2016)

We study the superstring inspired E_6 model motivated $U(1)_N$ extension of the supersymmetric standard model to explore the possibility of explaining the recent excess CMS events and the baryon asymmetry of the Universe in eight possible variants of the model. In light of the hints from short-baseline neutrino experiments at the existence of one or more light sterile neutrinos, we also study the neutrino mass matrices dictated by the field assignments and the discrete symmetries in these variants. We find that all the variants can explain the excess CMS events via the exotic slepton decay, while for a standard choice of the discrete symmetry four of the variants have the feature of allowing high scale baryogenesis (leptogenesis). For one other variant three body decay induced soft baryogenesis mechanism is possible which can induce baryon number violating neutron-antineutron oscillation. We also point out a new discrete symmetry which has the feature of ensuring proton stability and forbidding tree level flavor changing neutral current processes while allowing for the possibility of high scale leptogenesis for two of the variants. On the other hand, neutrino mass matrix of the $U(1)_N$ model variants naturally accommodates three active and two sterile neutrinos which acquire masses through their mixing with extra neutral fermions giving rise to interesting textures for neutrino masses.

DOI: 10.1103/PhysRevD.93.015001

I. INTRODUCTION

One of the simplest and well motivated extensions of the Standard Model (SM) gauge group $SU(3)_c \times SU(2)_L \times U(1)_Y$ is the $U(1)_N$ extension of the supersymmetric SM motivated by the superstring theory inspired E_6 model. This model, realizing the implementation of supersymmetry and the extension of the SM gauge group to a larger symmetry group, offers an attractive possibility of TeV-scale physics beyond the SM, testable at the LHC. On the other hand, small neutrino masses explaining the solar and atmospheric neutrino oscillations data and a mechanism for generating the observed baryon asymmetry of the Universe can be naturally accommodated in this model.

The presence of new exotic fields in addition to the SM fields and new interactions involving the new gauge boson Z' provides a framework to explore the associated rich phenomenology which can be tested at the LHC. To this end, we must mention that recently the CMS Collaboration at the LHC have reported excesses in the searches for the right-handed gauge boson W_R at a center of mass energy of $\sqrt{s} = 8$ TeV and 19.7 fb^{-1} of integrated luminosity [1] and dileptoquark production at a center of mass energy of $\sqrt{s} = 8$ TeV and 19.6 fb^{-1} of integrated luminosity [2]. In the former the final state $eejj$ was used to probe $pp \to W_R \to eN_R \to eejj$ and in the energy bin 1.8 TeV $< m_{\mathrm{eejj}} <$ 2.2 TeV a 2.8σ local excess have been reported accounting for 14 observed events with 4 expected background events from the SM. In the search for dileptoquark production, 2.4σ and 2.6σ local excesses in $eejj$ and $e\not{p}_T jj$ channels respectively have been reported corresponding to 36 observed events with $20.49 \pm 2.4 \pm 2.45$ (systematic errors) expected SM background events and 18 observed events with $7.54 \pm 1.20 \pm 1.07$ (systematic errors) expected SM background events respectively [2].

Attempts have been made to explain the above CMS excesses in the context of left-right symmetric model (LRSM). The $eejj$ excess have been explained from W_R decay for LRSM with $g_L = g_R$ by taking into account the CP phases and nondegenerate masses of heavy neutrinos in Ref. [3], and also by embedding the conventional LRSM with $g_L \neq g_R$ in the $SO(10)$ gauge group in Refs. [4]. In these models, the lepton asymmetry can get generated either through the lepton number violating decay of right-handed Majorana neutrinos [5] or heavy Higgs triplet scalars [6]. However, the conventional LRSM models (even after embedding it in higher gauge groups) are not consistent with the canonical mechanism of leptogenesis in the range of the mass of W_R (~2 TeV) corresponding to the $eejj$ excess at the LHC reported by the CMS [7–9].

The $eejj$ excess has also been discussed in the context of W_R and Z' production and decay in Ref. [10] and in the context of pair production of vectorlike leptons in Refs. [11]. In Ref. [12], a scenario connecting leptoquarks to dark matter was proposed accounting for the recent

*mansi@prl.res.in
†chandan@prl.res.in
‡utpal@prl.res.in

excess seen by CMS. In Refs. [13,14], the excess events have been shown to occur in R-parity violating processes via the resonant production of a slepton. In Ref. [15], the three effective low-energy subgroups of the superstring inspired E_6 model with a low energy $SU(2)_{(R)}$ were studied and a R-parity conserving scenario was proposed in which both the $eejj$ and $e\not{p}_T jj$ signals can be produced from the decay of an exotic slepton in two of the effective low-energy subgroups of the superstring inspired E_6 model, out of which one subgroup (known as the alternative left-right symmetric model [16]) allows for the possibility of having successful high-scale leptogenesis.

In this Letter, we systematically study the E_6 motivated $U(1)_N$ extension of the supersymmetric SM gauge group to explain the excess CMS events and simultaneously explain the baryon asymmetry of the Universe via baryogenesis (leptogenesis). To this end, we impose discrete symmetries to the above gauge group which ensures proton stability, forbids the tree level flavor changing neutral current (FCNC) processes and dictates the form of the neutrino mass matrix in the variants of the $U(1)_N$ model. We find that all the variants can explain the excess CMS events via the exotic slepton decay, while for a standard choice of the discrete symmetry some of them have the feature of allowing high scale baryogenesis (leptogenesis) via the decay of a heavy Majorana baryon (lepton) and some are not consistent with such mechanisms. We have pointed out the possibility of the three body decay induced soft baryogenesis mechanism which can induce baryon number violating neutron-antineutron ($n-\bar{n}$) oscillation [17] in one such variant, on the other hand, we have also explored a new discrete symmetry for these variants which has the feature of ensuring proton stability and forbidding tree level FCNC processes while allowing for the possibilities of high scale leptogenesis through the decay of a heavy Majorana lepton. We also comment on the more recent ATLAS and CMS diboson and dijet excesses in the context of $U(1)_N$ model and other alternatives that can address these excesses. In light of the hints from short-baseline neutrino experiments [18] at the existence of one or more light sterile neutrinos which can interact only via mixing with the active neutrinos, we have explored the neutrino mass matrix of the $U(1)_N$ model variants which naturally contains three active and two sterile neutrinos [19]. These neutrinos acquire masses through their mixing with extra neutral fermions giving rise to interesting textures for neutrino masses governed by the field assignments and the imposed discrete symmetries.

The outline of the article is as follows. In Sec. II, we review the E_6 model motivated $U(1)_N$ extension of supersymmetric standard model and the transformations of the various superfields under the gauge group. In Sec. III, we discuss the imposition of discrete symmetries and give the variants of the $U(1)_N$ model and the corresponding superpotentials. In Sec. IV we discuss the possibility of producing $eejj$ and $e\not{p}_T jj$ events from the decay of an exotic slepton. In Sec. V, we comment on the possibility of explaining the recent diboson and dijet excesses reported by the ATLAS and CMS Collaborations in the context of $U(1)_N$ model and in general. In Sec. VI, we explore the possible mechanisms of baryogenesis (leptogenesis) for the different variants of the $U(1)_N$ model. In Sec. VII, we study the neutral fermionic mass matrices and the resultant structure of the neutrino mass matrices. In Sec. VIII we conclude with our results.

II. $U(1)_N$ EXTENSION OF SUPERSYMMETRIC STANDARD MODEL

In the heterotic superstring theory with $E_8 \times E_8'$ gauge group the compactification on a Calabi-Yau manifold leads to the breaking of E_8 to $SU(3) \times E_6$ [20,21]. The flux breaking of E_6 can result in different low-energy effective subgroups of rank-5 and rank-6. One such possibility is realized in the $U(1)_N$ model. The rank-6 group E_6 can be broken down to low-energy gauge groups of rank-5 or rank-6 with one or two additional $U(1)$ in addition to the SM gauge group. For example E_6 contains the subgroup $SO(10) \times U(1)_\psi$ while $SO(10)$ contains the subgroup $SU(5) \times U(1)_\chi$. In fact some mechanisms can break the E_6 group directly into the rank-6 gauge scheme

$$E_6 \to SU(3)_C \times SU(2)_L \times U(1)_Y \times U(1)_\psi \times U(1)_\chi. \quad (1)$$

These rank-6 schemes can further be reduced to rank-5 gauge group with only one additional $U(1)$ which is a linear combination of $U(1)_\psi$ and $U(1)_\chi$

$$Q_\alpha = Q_\psi \cos\alpha + Q_\chi \sin\alpha, \quad (2)$$

where

$$Q_\psi = \sqrt{\frac{3}{2}}(Y_L - Y_R), \qquad Q_\chi = \sqrt{\frac{1}{10}}(5T_{3R} - 3Y). \quad (3)$$

For a particular choice of $\tan\alpha = \sqrt{\frac{1}{15}}$ the right-handed counter part of neutrino superfield (N^c) can transform trivially under the gauge group and the corresponding $U(1)$ gauge extension to the SM is denoted as $U(1)_N$. The trivial transformation of N^c can allow a large Majorana mass of N^c in the $U(1)_N$ model thus providing attractive possibility of baryogenesis (leptogenesis).

Let us consider one of the maximal subgroups of E_6 given by $SU(3)_C \times SU(3)_L \times SU(3)_R$. The fundamental 27 representation of E_6 under this subgroup is given by

$$27 = (3,3,1) + (3^*,1,3^*) + (1,3^*,3). \quad (4)$$

The matter superfields of the first family are assigned as:

TABLE I. Transformations of the various superfields of the 27 representation under $SU(3)_C \times SU(2)_L \times U(1)_Y \times U(1)_N$.

	$SU(3)_c$	$SU(2)_L$	Y_L	T_{3R}	Y_R	$U(1)_Y$	$U(1)_N$
Q	3	2	$\frac{1}{6}$	0	0	$\frac{1}{6}$	$\frac{1}{\sqrt{40}}$
u^c	3^*	1	0	$-\frac{1}{2}$	$-\frac{1}{6}$	$-\frac{2}{3}$	$\frac{1}{\sqrt{40}}$
d^c	3^*	1	0	$\frac{1}{2}$	$-\frac{1}{6}$	$\frac{1}{3}$	$\frac{2}{\sqrt{40}}$
L	1	2	$-\frac{1}{6}$	0	$-\frac{1}{3}$	$-\frac{1}{2}$	$\frac{2}{\sqrt{40}}$
e^c	1	1	$\frac{1}{3}$	$\frac{1}{2}$	$\frac{1}{6}$	1	$\frac{1}{\sqrt{40}}$
h	3	1	$-\frac{1}{3}$	0	0	$-\frac{1}{3}$	$-\frac{2}{\sqrt{40}}$
h^c	3^*	1	0	0	$\frac{1}{3}$	$\frac{1}{3}$	$-\frac{3}{\sqrt{40}}$
X	1	2	$-\frac{1}{6}$	$-\frac{1}{2}$	$\frac{1}{6}$	$-\frac{1}{2}$	$-\frac{3}{\sqrt{40}}$
X^c	1	2	$-\frac{1}{6}$	$\frac{1}{2}$	$\frac{1}{6}$	$\frac{1}{2}$	$-\frac{2}{\sqrt{40}}$
n	1	1	$\frac{1}{3}$	0	$-\frac{1}{3}$	0	$\frac{5}{\sqrt{40}}$
N^c	1	1	$\frac{1}{3}$	$-\frac{1}{2}$	$\frac{1}{6}$	0	0

$$\begin{pmatrix} u \\ d \\ h \end{pmatrix} + \begin{pmatrix} u^c & d^c & h^c \end{pmatrix} + \begin{pmatrix} E^c & \nu & \nu_E \\ N_E^c & e & E \\ e^c & N^c & n \end{pmatrix}, \quad (5)$$

where $SU(3)_L$ operates vertically and $SU(3)_R$ operates horizontally. Now if the $SU(3)_L$ gets broken to $SU(2)_L \times U(1)_{Y_L}$ and the $SU(3)_R$ gets broken to $U(1)_{T_{3R}} \times U(1)_{Y_R}$ via the flux mechanism then the resulting gauge symmetry is given by $SU(3)_C \times SU(2)_L \times U(1)_Y \times U(1)_N$, where the $U(1)_N$ charge assignment is given by

$$Q_N = \sqrt{\frac{1}{40}}(6Y_L + T_{3R} - 9Y_R), \quad (6)$$

and the electric charge is given by

$$Q = T_{3L} + Y, \qquad Y = Y_L + T_{3R} + Y_R. \quad (7)$$

The transformations of the various superfields of the fundamental 27 representation of E_6 under $SU(3)_C \times SU(2)_L \times U(1)_Y \times U(1)_N$ and the corresponding assignments of Y_L, T_{3R} and Y_R are listed in Table I, where $Q = (u, d)$, $L = (\nu_e, e)$, $X = (\nu_E, E)$ and $X^c = (E^c, N_E^c)$.

III. DISCRETE SYMMETRIES AND VARIANTS OF $U(1)_N$ MODEL

The presence of the extra particles in this model can have interesting phenomenological consequences; however, they can also cause serious problems regarding fast proton decay, tree level flavor changing neutral current (FCNC) and neutrino masses. Considering the decomposition of $27 \times 27 \times 27$ there are 11 possible superpotential terms. The most general superpotential can be written as

$$\begin{aligned} W &= W_0 + W_1 + W_2, \\ W_0 &= \lambda_1 Q u^c X^c + \lambda_2 Q d^c X + \lambda_3 L e^c X \\ &\quad + \lambda_4 S h h^c + \lambda_5 S X X^c + \lambda_6 L N^c X^c + \lambda_7 d^c N^c h, \\ W_1 &= \lambda_8 Q Q h + \lambda_9 u^c d^c h^c, \\ W_2 &= \lambda_{10} Q L h^c + \lambda_{11} u^c e^c h. \end{aligned} \quad (8)$$

The first five terms of W_0 give masses to the usual SM particles and the new heavy particles h, h^c, X and X^c. The last term of W_0 i.e. LN^cX^c can generate a nonzero Dirac neutrino mass and in some scenarios it is desirable to have the coupling λ_6 very small or vanishing, so that the three neutrinos pick up small masses. Now the rest five terms corresponding to W_1 and W_2 cannot all be there together as it would induce rapid proton decay. Imposition of a discrete symmetry can forbid such terms and give a sufficiently long-lived proton [22]. We will impose a $Z_2^B \times Z_2^H$ discrete symmetry, where the first $Z_2^B = (-1)^{3B}$ prevents rapid proton decay and the second discrete symmetry Z^H distinguishes between the Higgs and matter supermultiplets and suppress the tree level FCNC processes.

Under $Z_2^B = (-1)^{3B}$ we have

$$\begin{aligned} Q, u^c, d^c &: \ -1 \\ L, e^c, X, X^c, S &: \ +1, \end{aligned} \quad (9)$$

now depending on the assignments of h, h^c and N^c one can have different variants of the model. Such different possibilities are listed in Table II.

In the models where h, h^c are even under Z_2^B the superfields $h(B = -2/3)$ and $h^c(B = 2/3)$ are diquarks while for the rest $h(B = 1/3, L = 1)$ and $h^c(B = -1/3, L = -1)$ are leptoquarks. N^c with the assignment $Z_2^B = -1$ are baryons and the assignment $Z_2^B = +1$ are leptons. In addition to the trilinear terms listed in Table II there can be bilinear terms such as LX^c and N^cN^c. The former can give rise to nonzero neutrino mass and the latter can give heavy Majorana baryon (lepton) N^c mass. Model 1 is similar to model 5 of Ref. [23] and model A of Ref. [24]. Model 2 is same as model B of Ref. [24]. Model 8 is quite different from the ones that have been discussed in connection with leptogenesis in the literature (e.g. [25]). Here the matter superfields X, X^c carry nonzero $B - L$ quantum numbers and the tree level FCNC processes are forbidden.

A. Model 1

In this model we take the second discrete symmetry Z_2^H to be $Z_2^L = (-1)^L$ following Ref. [24], and it is imposed as follows

$$\begin{aligned} L, e^c, X_{1,2}, X_{1,2}^c, S_{1,2} &: \ -1 \\ Q, u^c, d^c, N^c, h, h^c, S_3, X_3, X_3^c &: \ +1. \end{aligned} \quad (10)$$

TABLE II. Possible transformations of h, h^c and N^c under Z_2^B and the allowed superpotential terms.

Model	h, h^c	N^c	Allowed trilinear terms
1	$+1$	-1	W_0 ($\lambda_6 = 0$), W_1
2	$+1$	-1 for $N^c_{1,2}$, $+1$ for N^c_3	W_0 ($\lambda_6 = 0$ for $N^c_{1,2}$, $\lambda_7 = 0$ for N^c_3),W_1
3	-1	$+1$	W_0, W_2
4	-1	$+1$ for $N^c_{1,2}$, -1 for N^c_3	W_0 ($\lambda_6 = \lambda_7 = 0$ for N^c_3), W_2
5	$+1$	$+1$ for $N^c_{1,2}$, -1 for N^c_3	W_0 ($\lambda_6 = 0$ for N^c_3, $\lambda_7 = 0$ for $N^c_{1,2}$), W_1
6	$+1$	$+1$	W_0 ($\lambda_7 = 0$), W_1
7	-1	-1	W_0 ($\lambda_6 = \lambda_7 = 0$), W_2
8	-1	-1 for $N^c_{1,2}$, $+1$ for N^c_3	W_0 ($\lambda_6 = \lambda_7 = 0$ for $N^c_{1,2}$), W_2

The neutral Higgs superfields S_3, X_3 and X_3^c have zero lepton numbers and can pick up vacuum expectation values (VEVs) while the presence of the bilinear terms $LX^c_{1,2}$ imply that $X^c_{1,2}$ have $L = -1$ and $X_{1,2}$ have $L = 1$. In this model N^c is a baryon with $B = 1$ and it acquires a Majorana mass from the bilinear term mN^cN^c. The complete superpotential of model 1 is given by

$$\begin{aligned} W = {} & \lambda_1^{ij} Q_j u_i^c X_3^c + \lambda_2^{ij} Q_j d_i^c X_3 + \lambda_3 L_j e_i^c X_3 + \lambda_4^{ij} S_3 h_i h_j^c \\ & + \lambda_5^{3ab} S_3 X_a X_b^c + \lambda_5^{a3b} S_a X_3 X_b^c + \lambda_5^{ab3} S_a X_b X_3^c \\ & + \lambda_5^{333} S_3 X_3 X_3^c + \lambda_7^{ijk} d_i^c h_j N_k^c + \mu^{ia} L_i X_a^c \\ & + m_N^{ij} N_i^c N_j^c + W_1, \end{aligned} \tag{11}$$

where i, j, k are flavor indices which run over all 3 flavors and a, $b = 1$, 2.[1]The form of the superpotential clearly shows that the up-type quarks couple to X_3^c only while the down-type quarks and the charged leptons couple to X_3 only, resulting in the suppression of the FCNC processes at the tree level.

B. Model 2

Here the second discrete symmetry Z_2^L is imposed as follows

$$\begin{aligned} L, e^c, X_{1,2}, X^c_{1,2}, S_{1,2}, N^c_3 &: \; -1 \\ Q, u^c, d^c, N^c_{1,2}, h, h^c, S_3, X_3, X_3^c &: \; +1. \end{aligned} \tag{12}$$

In this model $N^c_{1,2}$ are baryons with $B = 1$ but N_3^c is a lepton and can give mass to one of the neutrinos via the term $LN_3^cX_3^c$. The complete superpotential of model 2 is given by

$$\begin{aligned} W = {} & \lambda_1^{ij} Q_j u_i^c X_3^c + \lambda_2^{ij} Q_j d_i^c X_3 + \lambda_3 L_j e_i^c X_3 + \lambda_4^{ij} S_3 h_i h_j^c \\ & + \lambda_5^{3ab} S_3 X_a X_b^c + \lambda_5^{a3b} S_a X_3 X_b^c + \lambda_5^{ab3} S_a X_b X_3^c \\ & + \lambda_5^{333} S_3 X_3 X_3^c + \lambda_6^{i} L_i N_3^c X_3^c + \lambda_7^{ija} d_i^c h_j N_a^c + \mu^{ia} L_i X_a^c \\ & + m_N^{ab} N_a^c N_b^c + m_N^{33} N_3^c N_3^c + W_1. \end{aligned} \tag{13}$$

[1]We will use this notation hereafter in this article. The indices i, j, k run over 1,2,3, while the indices a, b run over 1,2.

C. Model 3

Under the second discrete symmetry $Z_2^H = Z_2^L = (-1)^L$ the superfields transform as follows

$$\begin{aligned} L, e^c, X_{1,2}, X^c_{1,2}, S_{1,2}, N^c, h, h^c &: \; -1 \\ Q, u^c, d^c, S_3, X_3, X_3^c &: \; +1. \end{aligned} \tag{14}$$

In this model all the N^cs are leptons. The complete superpotential of model 4 is given by

$$\begin{aligned} W = {} & \lambda_1^{ij} Q_j u_i^c X_3^c + \lambda_2^{ij} Q_j d_i^c X_3 + \lambda_3 L_j e_i^c X_3 + \lambda_4^{ij} S_3 h_i h_j^c \\ & + \lambda_5^{3ab} S_3 X_a X_b^c + \lambda_5^{a3b} S_a X_3 X_b^c + \lambda_5^{ab3} S_a X_b X_3^c \\ & + \lambda_5^{333} S_3 X_3 X_3^c + \lambda_6^{ij3} L_i N_j^c X_3^c + \lambda_7^{ijk} d_i^c h_j N_k^c \\ & + \mu^{ia} L_i X_a^c + m_N^{ij} N_i^c N_j^c + W_2. \end{aligned} \tag{15}$$

D. Model 4

Here the second discrete symmetry Z_2^H is again chosen to be $(-1)^L$ giving the transformations of the superfields as follows

$$\begin{aligned} L, e^c, X_{1,2}, X^c_{1,2}, S_{1,2}, N^c_{1,2}, h, h^c &: \; -1 \\ Q, u^c, d^c, N_3^c, S_3, X_3, X_3^c &: \; +1. \end{aligned} \tag{16}$$

$N^c_{1,2}$ are leptons while N_3^c is a baryon. The complete superpotential of model 2 is given by

$$\begin{aligned} W = {} & \lambda_1^{ij} Q_j u_i^c X_3^c + \lambda_2^{ij} Q_j d_i^c X_3 + \lambda_3 L_j e_i^c X_3 + \lambda_4^{ij} S_3 h_i h_j^c \\ & + \lambda_5^{3ab} S_3 X_a X_b^c + \lambda_5^{a3b} S_a X_3 X_b^c + \lambda_5^{ab3} S_a X_b X_3^c \\ & + \lambda_5^{333} S_3 X_3 X_3^c + \lambda_6^{ia3} L_i N_a^c X_3^c + \lambda_7^{ija} d_i^c h_j N_a^c \\ & + \mu^{ia} L_i X_a^c + m_N^{ab} N_a^c N_b^c + m_N^{33} N_3^c N_3^c + W_2. \end{aligned} \tag{17}$$

E. Models 5 and 6

In model 5 if we choose the second discrete symmetry Z_2^H to be $Z_2^L = (-1)^L$ then the superfields transform as follows

$$L, e^c, X_{1,2}, X^c_{1,2}, S_{1,2}, N^c_{1,2}: \ -1$$
$$Q, u^c, d^c, N^c_3, h, h^c, S_3, X_3, X^c_3: \ +1, \tag{18}$$

which forbids the terms $\lambda_6 L_i N^c_a X^c_b$ (λ_7 is already vanishing for $N^c_{1,2}$ from the imposition of the first discrete symmetry Z^B_2) and thus the possibility of high scale baryogenesis (via leptogenesis) through the decay of Majorana N^c gets ruled out. However there can be soft baryogenesis through three body decays which can induce $n-\bar{n}$ oscillation. We will elaborate on this in Sec. VI. With the above choice of second discrete symmetry given in Eq. (18) the complete superpotential for model 5 is given by

$$\begin{aligned} W = {} & \lambda^{ij}_1 Q_j u^c_i X^c_3 + \lambda^{ij}_2 Q_j d^c_i X_3 + \lambda_3 L_j e^c_i X_3 + \lambda^{ij}_4 S_3 h_i h^c_j \\ & + \lambda^{3ab}_5 S_3 X_a X^c_b + \lambda^{a3b}_5 S_a X_3 X^c_b + \lambda^{ab3}_5 S_a X_b X^c_3 \\ & + \lambda^{333}_5 S_3 X_3 X^c_3 + \lambda^{ia}_6 L_i N^c_a X^c_3 + \lambda^{ij3}_7 d^c_i h_j N^c_3 + \mu^{ia} L_i X^c_a \\ & + m^{ab}_N N^c_a N^c_b + m^{33}_N N^c_3 N^c_3 + W_1. \end{aligned} \tag{19}$$

We find that in this model it is possible to allow high scale leptogenesis through the decay of Majorana N^c by a clever choice of the second discrete symmetry such that it can distinguish between the matter and Higgs superfields and also suppress the unwanted FCNC processes at the tree level. One such choice can be Z^E_2 which is associated with most of the exotic states. We define the transformation properties of the various superfields under $Z^H_2 = Z^E_2$ as follows

$$X_{1,2}, X^c_{1,2}, S_{1,2}, N^c: \ -1$$
$$L, e^c, Q, u^c, d^c, h, h^c, S_3, X_3, X^c_3: \ +1, \tag{20}$$

Thus for this choice also X_3, X^c_3 and S_3 are the Higgs superfields that acquire VEVs. Since up-type quarks couple to X^c_3 only and down-type quarks and charged SM leptons couple to only X_3 the FCNC processes at the tree level are suppressed. The complete superpotential of model 5 with the assignments in Eq. (20) reduces to

$$\begin{aligned} W' = {} & \lambda^{ij}_1 Q_j u^c_i X^c_3 + \lambda^{ij}_2 Q_j d^c_i X_3 + \lambda_3 L_j e^c_i X_3 + \lambda^{ij}_4 S_3 h_i h^c_j \\ & + \lambda^{3ab}_5 S_3 X_a X^c_b + \lambda^{a3b}_5 S_a X_3 X^c_b + \lambda^{ab3}_5 S_a X_b X^c_3 \\ & + \lambda^{333}_5 S_3 X_3 X^c_3 + \lambda^{iab}_6 L_i N^c_a X^c_b \\ & + m^{ab}_N N^c_a N^c_b + m^{33}_N N^c_3 N^c_3 + W_1. \end{aligned} \tag{21}$$

In model 6 also, the similar assignments for the superfields as given in Eq. (20) holds good and the complete superpotential is similar to Eq. (21) except the λ_6 term which now reads $\lambda^{ija}_6 L_i N^c_j X^c_a$.

F. Models 7 and 8

Taking second discrete symmetry to be $Z^H_2 = (-1)^L$ the superfields transform as follows

$$L, e^c, X_{1,2}, X^c_{1,2}, S_{1,2}, h, h^c: \ -1$$
$$Q, u^c, d^c, N^c, S_3, X_3, X^c_3: \ +1. \tag{22}$$

In this model all the N^cs are baryons. The complete superpotential of model 7 is given by

$$\begin{aligned} W = {} & \lambda^{ij}_1 Q_j u^c_i X^c_3 + \lambda^{ij}_2 Q_j d^c_i X_3 + \lambda_3 L_j e^c_i X_3 + \lambda^{ij}_4 S_3 h_i h^c_j \\ & + \lambda^{3ab}_5 S_3 X_a X^c_b + \lambda^{a3b}_5 S_a X_3 X^c_b + \lambda^{ab3}_5 S_a X_b X^c_3 \\ & + \lambda^{333}_5 S_3 X_3 X^c_3 + \mu^{ia} L_i X^c_a + m^{ij}_N N^c_i N^c_j + W_2. \end{aligned} \tag{23}$$

Note that the λ_6 and λ_7 terms which are essential for baryogenesis through N^c decay (as discussed in Sec. VI) are forbidden by the Z^B_2 symmetry irrespective of what Z^H_2 one chooses. For model 8 also one can write down the superfield transformations and the superpotential. In this case the mass term for N^c is given by $m^{ab}_N N^c_a N^c_b + m^{33}_N N^c_3 N^c_3$ and the terms $\lambda^{i33}_6 L_i N^c_3 X^c_3$, $\lambda^{ij3}_7 d^c_i h_j N^c_3$ are present in addition to the terms given in Eq. (23).

IV. EXPLAINING THE CMS *eejj* (AND *e$\not{p}_T$jj*) EXCESS(ES)

An inspection of Table II and the corresponding allowed superpotential terms reveals that all the models listed there contain the terms $\lambda_2 Q_i d^c_j X_3$ and $\lambda_3 L_i e^c_j X_3$ in the superpotential ($\tilde{N}^c_E$ and $\tilde{\nu}_E$ acquires VEVs and $SU(2)\times U(1)_Y$ gets broken to $U(1)_{\rm EM}$) and can give rise to $eejj$ signal from the exotic slepton $\tilde{E}$ decay. $\tilde{E}$ can be resonantly produced in pp collisions, which then subsequently decays to a charged lepton and neutrino, followed by interactions of the neutrino producing an $eejj$ signal. The process leading to $eejj$ signal is given in Fig. 1.

The models where h and h^c are leptoquarks (Models 3, 4, 7 and 8 in Table II) can produce both $eejj$ and $e\not{p}_T jj$ signals from the decay of scalar superpartner(s) of the exotic particle(s). Both events can be produced in the above scenarios via (i) resonant production of the exotic slepton $\tilde{E}$ (ii) and pair production of scalar leptoquarks $\tilde{h}$. The processes involving exotic slepton decay leading to both $eejj$ and $e\not{p}_T jj$ signals are given in Fig. 2. The superpotential terms involved in these processes are $\lambda_{10} Q L h^c$ and $\lambda_{11} u^c e^c h$ in addition the two terms responsible for the first signal. The partonic cross section of slepton production is given by [26]

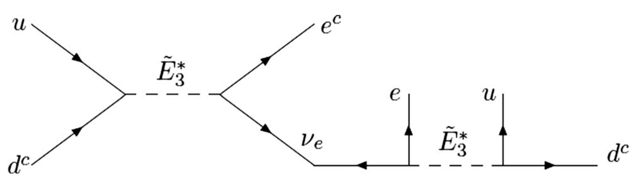

FIG. 1. Feynman diagram for a single exotic particle $\tilde{E}$ production leading to $eejj$ signal.

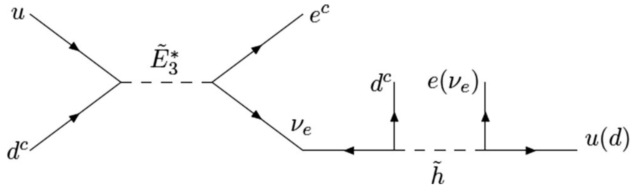

FIG. 2. Feynman diagram for exotic slepton $\tilde{E}$ production leading to both $eejj$ and $e\not{p}_T jj$ signal.

$$\hat{\sigma} = \frac{\pi}{12\hat{s}} |\lambda_2|^2 \delta\left(1 - \frac{m_{\tilde{E}}^2}{\hat{s}}\right), \tag{24}$$

where $\hat{s}$ is the partonic center of mass energy, and $m_{\tilde{E}}$ is the mass of the resonant slepton. The total cross section is approximated to be [26]

$$\sigma(pp \to eejj) \propto \frac{|\lambda_2|^2}{m_{\tilde{E}}^3} \times \beta_1 \tag{25}$$

and

$$\sigma(pp \to e\not{p}_T jj) \propto \frac{|\lambda_2|^2}{m_{\tilde{E}}^3} \times \beta_2, \tag{26}$$

where β_1 is the branching fraction for the decay of $\tilde{E}$ to $eejj$ and β_2 is the branching fraction for the decay to $e\not{p}_T jj$. $\beta_{1,2}$ and the coupling λ_2 are the free parameters. The cross section for the processes can be calculated as a function of the exotic slepton mass and bounds for the value of the mass of the exotic slepton can be obtained by matching the theoretically calculated excess events with the ones observed at the LHC at a center of mass energy $\sqrt{s} = 8$ TeV. Thus, the $U(1)_N$ models can explain the excess $eejj$ (and $e\not{p}_T jj$) signal(s) at the LHC via resonant exotic slepton decay.

V. MORE RECENT ATLAS AND CMS DIBOSON AND DIJET EXCESSES

Very recently, the ATLAS and CMS collaborations have reported a number of diboson and dijet excesses over the SM expectations near the invariant mass region 1.8–2.0 TeV. The search for diboson production has been reported by the ATLAS Collaboration to show a 3.4σ excess at $\sim$2 TeV in boosted jets of WZ channel amounting to a global 2.5σ excess over the SM expectation [27]. The method of jet substructure has been used to discriminate the hadronic decays of W and Z bosons from QCD dijets and due to overlaps in the jet masses of the gauge bosons many events can also be interpreted as ZZ or WW resonances, yielding 2.9σ and 2.6σ excesses in two channels respectively. On the other hand, the CMS has reported a 1.4σ excess at $\sim$1.9 TeV in their search for diboson production without discriminating between the W- and Z-tagged jets [28] and a 1.5σ excess at $\sim$1.8 TeV in the search for diboson production with a leptonically tagged Z [29]. In the search for dijet resonances the ATLAS and CMS Collaborations have reported excesses at 1.8 TeV with 2.2σ and 1σ significance levels respectively [30,31]. The CMS has also reported a 2.1σ excess in the energy bin 1.8 to 1.9 TeV in the resonant HW production channel [32].

Several phenomenological explanations have been proposed addressing these excesses [33–55]. In the framework of simple extensions of the SM, a heavy W' with mass $\sim$2 TeV produced via $q\bar{q}$ annihilation can explain the excess in WZ channel via its mixing with the SM W for a mixing angle grater than 10^{-2}. While a heavy Z' can mix with the SM Z and then decay into W^+W^- to explain the excess in the W^+W^- channel. Assuming that the SM Z_1 boson mixes with Z_2 via a mixing angle ϕ_z to give the mass eigenstates Z and Z'

$$\begin{pmatrix} Z_1 \\ Z_2 \end{pmatrix} = \begin{pmatrix} \cos\phi_z & -\sin\phi_z \\ \sin\phi_z & \cos\phi_z \end{pmatrix} \begin{pmatrix} Z \\ Z' \end{pmatrix}, \tag{27}$$

the relevant vertex for the Z' can be written as

$$\begin{aligned} \mathcal{V}_{Z'WW}\colon\ & g\cos\theta_w \sin\phi_z[(p_{Z'} - p_{W^+})^\beta g^{\mu\alpha} \\ & + (p_{W^+} - p_{W^-})^\mu g^{\alpha\beta} + (p_{W^-} - p_{Z'})^\alpha g^{\mu\beta}] \\ & \times \varepsilon_\mu(p_{Z'})\varepsilon_\alpha(p_{W^+})\varepsilon_\beta(p_{W^-}), \end{aligned} \tag{28}$$

where $\cos\phi_z \simeq 1$ is assumed. The partial decay width of Z' into W^+W^- is given by

$$\begin{aligned} \Gamma_{Z'W^+W^-} = {} & \sin^2\phi_z \left(\frac{g^2\cos^2\theta_w}{192\pi} \frac{M_{Z'}^5}{M_W^4}\right)\left(1 - \frac{M_W^2}{M_{Z'}^2}\right)^{3/2} \\ & \times \left(1 + 20\frac{M_W^2}{M_{Z'}^2} + 12\frac{M_W^4}{M_{Z'}^4}\right). \end{aligned} \tag{29}$$

For Z', the seven—eight events around the 2 TeV peak gives the benchmark $\sigma(Z') \times B(Z' \to W^+W^-) \simeq 5$–6 fb. However, the semileptonic channel of the W^+W^- decay puts an upper limit on $\sigma(Z') \times B(Z' \to W^+W^-) \simeq 3$ fb at 95% confidence level [29]. Ignoring this slight inconsistency one can obtain a range of values for g' and $\sin\phi_z$ which can explain the excess. It turns out that to explain the excess one must have $\sin\phi_z \gtrsim 10^{-3}$ [35]. However from electroweak precision data $\sin\phi_z$ corresponding to Z_N in our model is constrained $\sin\phi_z \lesssim 7 \times 10^{-4}$ [56]. Thus, all the excess events cannot be addressed via the Z_N decay. For a leptophobic Z' the mixing angle can be relaxed to 8×10^{-3}, which is close to the required value to explain the diboson anomaly [35].

It is also interesting to note that the ATLAS diboson excess can also be explained with a 2 TeV sgoldstino scalar assuming that the SUSY breaking scale is in the few TeV range as pointed out in Ref. [55]. Our model being a supersymmetric one can also entertain such a possibility.

Lastly, since the $U(1)_N$ model is a low energy subgroup of the superstring motivated E_6 group, it is also possible to rely on additional anomalous $U(1)$ fields coming from stringy construct, for example the D-brane compactifications it was shown in Ref. [54] that under the assumption of a low string scale, the dibosn and dijet excesses can be addressed by an anomalous $U(1)$ field with very small couplings to the leptons.

VI. BARYOGENESIS (LEPTOGENESIS) IN $U(1)_N$ MODELS

Some of the variants of low-energy $U(1)_N$ subgroup of E_6 model allows for the possibility of explaining baryogenesis (leptogenesis) from the decay of heavy Majorana particle N^c. In order to generate the baryon asymmetry of the Universe from N^c decay the conditions that must be satisfied are (i) violation of $B-L$ from Majorana mass of N^c, (ii) complex couplings must give rise to sufficient CP violation and (iii) the out-of-equilibrium condition given by

$$\Gamma_N < H(T = m_N) = \sqrt{\frac{4\pi^3 g_*}{45}}\frac{T^2}{M_{\rm Pl}}, \tag{30}$$

must be satisfied, where Γ_N is the decay width of Majorana N^c, $H(T)$ is the Hubble rate, g_* is the effective number of relativistic degrees of freedom at temperature T and $M_{\rm Pl}$ is the Planck mass. This implies that N^c cannot transform nontrivially under the low-energy subgroup $G = SU(3)_C \times SU(2)_L \times U(1)_Y \times U(1)_N$, which is readily satisfied in some variants of $U(1)_N$ model (see Table I). Thus the out-of-equilibrium decay of heavy N^c can give rise to high-scale baryogenesis (leptogenesis).

Models 1 and 2 have distinctive features of allowing direct baryogenesis via decay of heavy Majorana baryon N^c [24]. In both schemes, $N^c_{k(a)}$ decays to $B-L=B=-1$ final states $d^c_i\tilde{h}_j$, $\tilde{d}^c{}_i h_j$ and to their conjugate states with $B-L=B=1$, via the interaction term λ_7^{ijk} (λ_7^{ija}) in Eqs. (11) and (13). In both cases, the CP violation comes from the complex Yukawa coupling λ_7^{ijk} (λ_7^{ija}) given in Eqs. (11) and (13). The asymmetry is generated from interference between tree level decays and one-loop vertex and self-energy diagrams. The one-loop vertex and self-energy diagrams are shown in Fig. 3.

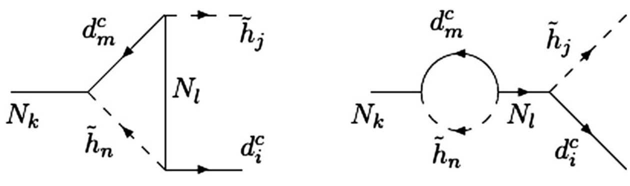

FIG. 3. One-loop diagrams for N_k decay which interferes with the tree level decay to provide CP violation.

The asymmetry is given by

$$\epsilon^k = \frac{1}{24\pi}\frac{\sum_{i,j,l,m,n}\mathrm{Im}[\lambda_7^{ijk}\lambda_7^{inl*}\lambda_7^{mjl*}\lambda_7^{mnk}]}{\sum_{i,j}\lambda_7^{ijk*}\lambda_7^{ijk}} \times\left[\mathcal{F}_V\left(\frac{M^2_{N_l}}{M^2_{N_k}}\right) + 3\mathcal{F}_S\left(\frac{M^2_{N_l}}{M^2_{N_k}}\right)\right], \tag{31}$$

where

$$\mathcal{F}_V = \frac{2\sqrt{x}}{x-1}, \qquad \mathcal{F}_S = \sqrt{x}\ln\left(1+\frac{1}{x}\right). \tag{32}$$

$\mathcal{F}_V$ corresponds to a one-loop function for a vertex diagram and $\mathcal{F}_S$ corresponds to a one-loop function for a self-energy diagram. The baryon to entropy ratio generated by decays of N_k is given by $n_B/s \sim \epsilon n_\gamma/s \sim (\epsilon/g_*)(45/\pi^4)$, where n_γ is number density of photons per comoving volume and g_* corresponds to the number of relativistic degrees of freedom. By considering $\lambda^7_{ijk} \sim 10^{-3}$ in model 1, one can generate $n_B/s \sim 10^{-10}$ for maximal CP violation. Similarly, one needs $\lambda_7^{ija} \sim 10^{-3}$ to satisfy required bound on n_B/s in model 2.

In models 3 and 4, $N^c_{1,2}$ (N^c) are Majorana leptons and hence a $B-L$ asymmetry is created via the decay of heavy N^c which then gets converted to the baryon asymmetry of the Universe in the presence of the $B+L$ violating anomalous processes before the electroweak phase transition. In these two cases, $N^c_{k(a)}$ decays to the final states $d^c_i\tilde{h}_j$, $\tilde{d}^c{}_i h_j$ with $B-L=-1$ and to their conjugate states with $B-L=1$, via the interaction term λ_7^{ija} (λ_7^{ijk}) in Eqs. (17) and (15). The one-loop diagrams that can interfere with the tree level $N_a(N_k)$ decays to provide the required CP violation are again the diagrams given in Fig. 3. However in these scenarios a $B-L$ asymmetry is created from the decay of Majorana N^c in contrast to the B asymmetry created in models 1 and 2. Again utilizing the general expression for calculating asymmetry parameter as given in Eq. (31), one needs $\lambda_7^{ija}(\lambda_7^{ijk}) \sim 10^{-3}$ in order to satisfy $n_B/s \sim 10^{-10}$ bound in both models 3 and 4.

For models 5 and 6, we have discussed two possible choices for the second discrete symmetries in Sec. III. In model 5, $N^c_{1,2}$ are leptons and N^c_3 is a baryon while in model 6 all the N^c's are leptons. For the first choice of second discrete symmetry $Z_2^H = Z_2^L$ the form of the superpotential [Eq. (19) for model 5] clearly shows that one cannot generate the baryon asymmetry of the Universe from high scale leptogenesis via the decay of heavy Majorana N^c in these models. However, the term $\lambda_7^{ij3}d^c_i h_j N^c_3$ can give rise to baryogenesis at TeV scale or below if one consider soft supersymmetry (SUSY) breaking terms in model 5. The relevant soft SUSY terms in the Lagrangian is given by

$$\mathcal{L} \sim m^2_{\tilde{h}_i}\tilde{h}_i^\dagger\tilde{h}_i + m^2_{\tilde{Q}_l}\tilde{Q}_l^\dagger\tilde{Q}_l + A^{ilm}\tilde{h}_i\tilde{Q}_l\tilde{Q}_m + \cdots, \tag{33}$$

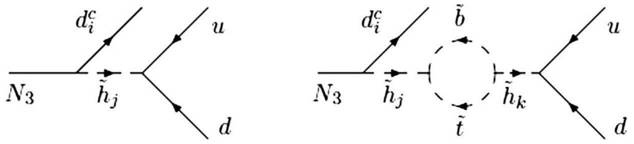

FIG. 4. The tree level and one-loop diagrams for N_3 decay giving rise to baryogenesis in model 5.

where i corresponds to the different generations of leptoquarks and $Q_{l(m)} = (u_l, d_l)$, l, $m = 1, 2, 3$, corresponds to three generations of superpartners of the Standard Model quarks. The Feynman diagrams for the tree level process and the one-loop process interfering with it to provide the CP violation are shown in Fig. 4. The asymmetry parameter in this case is given by [57]

$$\epsilon = A_{N_3} \sum_{i,j,k} \left[\mathrm{Im}[\lambda_7^{ij3*} \lambda_7^{ik3} \mathcal{A}^{j33*} \mathcal{A}^{k33}] \left(\frac{|\lambda_8^{j11}|^2}{m^2_{\tilde{h}_j}} - \frac{|\lambda_8^{k11}|^2}{m^2_{\tilde{h}_k}} \right) + \mathrm{Im}[\lambda_7^{ij3*} \lambda_7^{ik3} \lambda_8^{j11} \lambda_8^{k11*}] \left(\frac{|\mathcal{A}^{j33}|^2}{m^2_{\tilde{h}_1}} - \frac{|\mathcal{A}^{k33}|^2}{m^2_{\tilde{h}_1}} \right) + \mathrm{Im}[\mathcal{A}^{j33} \mathcal{A}^{k33*} \lambda_8^{j11} \lambda_8^{k11*}] \left(\frac{|\lambda_7^{ij3}|^2}{m^2_{\tilde{h}_j}} - \frac{|\lambda_7^{ik3}|^2}{m^2_{\tilde{h}_k}} \right) \right], \tag{34}$$

where $A_{N_3} = \frac{1}{\Gamma_{N_3}} \frac{1}{(2\pi)^3} \frac{1}{12} \frac{\pi}{4\pi^2} \frac{M^5_{N_3}}{m^2_{\tilde{h}_j} m^2_{\tilde{h}_k}}$ and Γ_{N_3} is the total decay width of N_3. Thus, by considering the soft SUSY breaking terms [given in Eq. (33)] of TeV scale, one can generate required amount of baryon asymmetry for particular values of Yukawa couplings.

This can also induce neutron-antinutron $(n - \bar{n})$ oscillation violating baryon number by two units $(\Delta B = 2)$ [17].

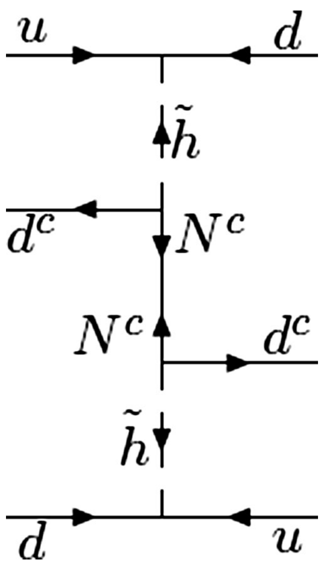

FIG. 5. $n - \bar{n}$ oscillation induced by effective six-quark interaction.

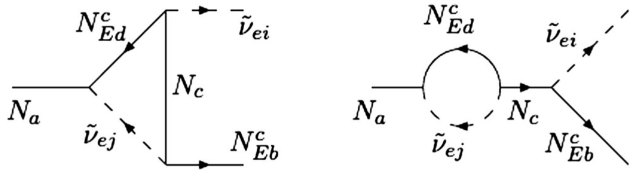

FIG. 6. One-loop diagrams for N_a decay which interferes with the tree level decay to provide CP violation.

The effective six-quark interaction inducing $n - \bar{n}$ oscillation is shown in Fig. 5. In fact, models 1 and 2 can also induce $n - \bar{n}$ oscillation in a similar fashion. However in model 6 all the N^cs are leptons and hence in this model a scheme for baryogenesis similar to above is not possible.

Now if we choose the second discrete symmetry to be $Z_2^H = Z_2^E$ in models 5 and 6 [see Eq. (20)] then it is possible to allow high scale leptogenesis via the decay of heavy Majorana N^c. In these two models $N^c_{a(j)}$ decays to the final states $\nu_{e_i} \tilde{N}^c_{E_b}$, $\tilde{\nu}_{e_i} N^c_{E_b}$, $e_i \tilde{E}^c_b$, $\tilde{e}_i E^c_b$ with $B - L = -1$ and to their conjugate states with $B - L = 1$, via the interaction term λ_7^{iab} (λ_7^{ijb}) in Eq. (21). Here we take advantage of the fact that Z_2^E symmetry forbids bilinear term like LX^c, and consequently X^c need not to carry any lepton number, it can simply have the assignment $B = L = 0$. The one-loop diagrams for $N_a(N_j)$ decays that can interfere with the tree level decay diagrams to provide the required CP violation are given in Fig. 6.

For models 7 and 8 the imposition of the Z_2^B symmetry implies vanishing λ_6 and λ_7 for two or more generations of N^c. Thus in these models no matter what kind of Z_2^H we choose sufficient CP violation cannot be produced and consequently the possibility of baryogenesis (leptogenesis) from the decay of heavy Majorana N^c is ruled out. Thus one needs to resort to some other mechanism to generate the baryon asymmetry of the Universe.

VII. NEUTRINO MASSES

In all the variants of $U(1)_N$ model that we have considered in Sec. III, the scalar component of S_3 acquires a VEV to break the $U(1)_N$. The fermionic component of S_3 pairs up with the gauge fermion to form a massive Dirac particle. However the fields $S_{1,2}$ still remains massless and can give rise to an interesting neutrino mass matrix structure.

In model 1, the field $N^c_{1,2,3}$ are baryons and hence they do not entertain the possibility of canonical seesaw mechanism of generating mass for neutrinos. However, the bilinear terms $\mu^{ia} L_i X^c_a$ can give rise to four nonzero masses for $\nu_{e,\mu,\tau}$ and $S_{1,2}$ as noted in Ref. [24]. The 9×9 mass matrix for the neutral fermionic fields of this model $\nu_{e,\mu,\tau}$, $S_{1,2}$, $\nu_{E_{1,2}}$ and $N^c_{E_{1,2}}$ is given by

$$\mathcal{M}^1 = \begin{pmatrix} 0 & 0 & 0 & \mu^{ia} \\ 0 & 0 & \lambda_5^{ab3} v_2 & \lambda_5^{a3b} v_1 \\ 0 & \lambda_5^{ba3} v_2 & 0 & M_a \delta_{ab} \\ (\mu^T)^{ai} & \lambda_5^{b3a} v_1 & M_a \delta_{ab} & 0 \end{pmatrix}, \qquad (35)$$

where v_1 and v_2 are the VEVs acquired by $\tilde{\nu}_{E_3}$ and $\tilde{N}^c_{E_3}$ respectively, and $M_{1,2}$ corresponds to the mass eigenvalues of the neutral fields $X_{1,2}$ and $X^c_{1,2}$. We will further assume that the field $\nu_{E_{1,2}}$ pairs up with the charge conjugate states to obtain heavy Dirac mass. Thus in Eq. (35) four of the nine fields are very heavy with masses M_1, M_1, M_2 and M_2 to a good approximation. This becomes apparent once we diagonalize $\mathcal{M}^1$ in M_a by a rotation about the 3-4 axis to get

$$\mathcal{M}'^1 = \begin{pmatrix} 0 & 0 & \mu^{ia}/\sqrt{2} & \mu^{ia}/\sqrt{2} \\ 0 & 0 & (\lambda_5^{ab3} v_2 + \lambda_5^{a3b} v_1)/\sqrt{2} & (-\lambda_5^{ab3} v_2 + \lambda_5^{a3b} v_1)/\sqrt{2} \\ (\mu^T)^{ai}/\sqrt{2} & (\lambda_5^{ba3} v_2 + \lambda_5^{b3a} v_1)/\sqrt{2} & M_a \delta_{ab} & 0 \\ (\mu^T)^{ai}/\sqrt{2} & (-\lambda_5^{ba3} v_2 + \lambda_5^{b3a} v_1)/\sqrt{2} & 0 & -M_a \delta_{ab} \end{pmatrix}. \qquad (36)$$

Then we readily obtain the 5×5 reduced mass matrix for the three neutrinos and $S_{1,2}$ given by

$$\mathcal{M}^1_\nu = \begin{pmatrix} 0 & \mu^{ic} \lambda_5^{cb3} v_2 M_c^{-1} \\ \lambda_5^{ac3} \mu^{cj} v_2 M_c^{-1} & (\lambda_5^{ac3} \lambda_5^{c3b} + \lambda_5^{a3c} \lambda_5^{cb3}) v_1 v_2 M_c^{-1} \end{pmatrix}, \qquad (37)$$

where the repeated dummy indices are summed over. Note that one neutrino remains massless in this model, two of the active neutrinos acquire small masses and the remaining eigenvalues correspond to sterile neutrino states. From Eq. (37) it follows that the bilinear terms $\mu L X_c$ and the sterile neutrinos are essential for the nonzero active neutrino masses in this model. The fields $N^c_{1,2,3}$, which are responsible for creating the baryon asymmetry of the Universe do not enter the neutrino mass matrix anywhere and hence the neutrino masses in this model do not have any direct connection with the baryon asymmetry. To have the active neutrino masses of the order 10^{-4} eV one can choose the sterile neutrino mass of the order 1 eV and the off diagonal entries in Eq. (37) to be of the order 10^{-2} eV. In this model the oscillations between the three active neutrinos and two sterile neutrinos is natural, and this allows the possibility of accommodating the LSND results [18]. The mixing between $S_{1,2}$ and the heavy neutral leptons ν_E, N^c_E can give rise to the decays $E_{1,2} \to W^- S_{1,2}$, $E^c_{1,2} \to W^+ S_{1,2}$, $\nu_{E_{1,2}} \to Z S_{1,2}$ and $N^c_{1,2} \to Z S_{1,2}$, which will compete with the decays arising from the Yukawa couplings $E_{1,2} \to H^- S_{1,2}$, $E^c_{1,2} \to H^+ S_{1,2}$, $\nu_{E_{1,2}} \to H^0 S_{1,2}$ and $N^c_{1,2} \to H^0 S_{1,2}$, where $H^+(H^0)$ are physical admixture of $\tilde{E}_3(\tilde{\nu}_{E_3})$ and $\tilde{E}^c_3(\tilde{N}^c_{E_3})$.

In model 2, N^c_3 is a lepton and hence the term $\lambda_6^{i33} L_i N^c_3 X^c_3$ in the superpotential given in Eq. (13) can give rise to a seesaw mass for one active neutrino, while the other two active neutrinos can acquire masses from Eq. (37) as before. Thus in this model all three neutrinos can be massive instead of two in model 1. Note that this model can allow the neutrino mass texture where one of the active neutrinos can have mass much larger compared to the other two, which can naturally give atmospheric neutrino oscillations with a Δm^2 orders of magnitude higher than Δm^2 for solar neutrino oscillations.

In the case of model 3 all three N^c fields are leptons and the 12×12 mass matrix for the neutral fermions spanning $\nu_{e,\mu,\tau}$, $S_{1,2}$, $N^c_{1,2,3}$, $\nu_{E_{1,2}}$ and $N^c_{E_{1,2}}$ is given by

$$\mathcal{M}^3 = \begin{pmatrix} 0 & 0 & \lambda_6^{ij3} v_2 & 0 & \mu^{ia} \\ 0 & 0 & 0 & \lambda_5^{ab3} v_2 & \lambda_5^{a3b} v_1 \\ \lambda_6^{ji3} v_2 & 0 & M_{N_i} \delta_{ij} & 0 & 0 \\ 0 & \lambda_5^{ba3} v_2 & 0 & 0 & M_a \delta_{ab} \\ (\mu^T)^{ai} & \lambda_5^{b3a} v_1 & 0 & M_a \delta_{ab} & 0 \end{pmatrix}. \qquad (38)$$

This gives the reduced 5×5 matrix for three active and two sterile neutrinos as follows

$$\mathcal{M}^3_\nu = \begin{pmatrix} \lambda_6^{ik3} \lambda_6^{kj3} v_2^2 M_{N_k}^{-1} & \mu^{ic} \lambda_5^{cb3} v_2 M_c^{-1} \\ \lambda_5^{ac3} \mu^{cj} v_2 M_c^{-1} & (\lambda_5^{ac3} \lambda_5^{c3b} + \lambda_5^{a3c} \lambda_5^{cb3}) v_1 v_2 M_c^{-1} \end{pmatrix}. \qquad (39)$$

This clearly shows that in this model active neutrinos can acquire seesaw masses even in the absence of the bilinear term $\mu L X^c$ and the sterile neutrinos. As we have discussed in Sec. VI, the out-of-equilibrium decay of N^c creates the lepton asymmetry in this model; thus, M_N can be constrained from the requirement of successful leptogenesis. However one still has some room left to play with λ_5, μ and M_a, which can give rise to interesting neutrino mass textures. In model 4, the fields $N^c_{1,2}$ are leptons while N^c_3 is a baryon and hence the 11×11 mass matrix spanning $\nu_{e,\mu,\tau}$, $S_{1,2}$, $N^c_{1,2}$, $\nu_{E_{1,2}}$ and $N^c_{E_{1,2}}$ will reduce to a 5×5 matrix similar to Eq. (39), except the (1,1) entry which is now given by $\lambda_6^{ic3}\lambda_6^{cj3}v_2^2M^{-1}_{N_c}$. Thus it follows that two of the active neutrinos can acquire masses even without the bilinear term μLX^c and the sterile neutrinos.

For models 5 and 6 we have discussed two possible choices for the second discrete symmetry Z_2^H in Sec. III. In the former model $N^c_{1,2}$ are leptons and N^c_3 is a baryon while in the latter model all $N^c_{1,2,3}$ are leptons. In model 5, for the first choice i.e. $Z_2^B = Z_2^L$ the 11×11 mass matrix for the neutral fermions spanning $\nu_{e,\mu,\tau}$, $S_{1,2}$, $N^c_{1,2}$, $\nu_{E_{1,2}}$ is given by

$$\mathcal{M}^5 = \begin{pmatrix} 0 & 0 & \lambda_6^{id3}v_2 & 0 & \mu^{ia} \\ 0 & 0 & 0 & \lambda_5^{ab3}v_2 & \lambda_5^{a3b}v_1 \\ \lambda_6^{di3}v_2 & 0 & M_{N_d}\delta_{dg} & 0 & 0 \\ 0 & \lambda_5^{ba3}v_2 & 0 & 0 & M_a\delta_{ab} \\ (\mu^T)^{ai} & \lambda_5^{b3a}v_1 & 0 & M_a\delta_{ab} & 0 \end{pmatrix}, \tag{40}$$

which can be reduced to 5×5 matrix for three active and two sterile neutrinos

$$\mathcal{M}^3_\nu = \begin{pmatrix} \lambda_6^{ic3}\lambda_6^{cj3}v_2^2M^{-1}_{N_c} & \mu^{ic}\lambda_5^{cb3}v_2M_c^{-1} \\ \lambda_5^{ac3}(\mu^T)^{cj}v_2M_c^{-1} & (\lambda_5^{ac3}\lambda_5^{c3b}+\lambda_5^{a3c}\lambda_5^{cb3})v_1v_2M_c^{-1} \end{pmatrix}, \tag{41}$$

which is similar to the form in model 4 and hence similar conclusions follow. Model 6 gives a reduced mass matrix similar to model 3 given in Eq. (39).

For the second choice in model 5, i.e. $Z_2^B = Z_2^E$ the 11×11 mass matrix for the neutral fermions is given by

$$\mathcal{M}^5 = \begin{pmatrix} 0 & 0 & 0 & 0 & 0 \\ 0 & 0 & 0 & \lambda_5^{ab3}v_2 & \lambda_5^{a3b}v_1 \\ 0 & 0 & M_{N_d}\delta_{dg} & 0 & 0 \\ 0 & \lambda_5^{ba3}v_2 & 0 & 0 & M_a\delta_{ab} \\ 0 & \lambda_5^{b3a}v_1 & 0 & M_a\delta_{ab} & 0 \end{pmatrix}, \tag{42}$$

which clearly shows that the active neutrinos are massless in this case while the sterile neutrinos acquire masses $(\lambda_5^{ac3}\lambda_5^{c3b}+\lambda_5^{a3c}\lambda_5^{cb3})v_1v_2M_c^{-1}$. The masslessness of the active neutrinos is a consequence of the exotic discrete Z_2^E symmetry which forbids the mixing among the exotic and nonexotic neutral fermion fields defined in Eq. (20). The situation is similar for $Z_2^B = Z_2^E$ in model 6 also.

The analysis of mass matrix for models 7 and 8 are exactly similar to model 1 and 2 respectively with similar conclusions.

VIII. CONCLUSIONS

We have studied the variants of effective low-energy $U(1)_N$ model motivated by the superstring inspired E_6 group in presence of discrete symmetries ensuring proton stability and forbidding tree level flavor changing neutral current processes. Our aim was to explore the eight possible variants to explain the excess $eejj$ and ep_Tjj events that have been observed by CMS at the LHC and to simultaneously explain the baryon asymmetry of the Universe via baryogenesis (leptogenesis). We have also studied the neutrino mass matrices governed by the field assignments and the discrete symmetries in these variants.

We find that all the variants can produce an $eejj$ excess signal via exotic slepton decay, while, the models where h and h^c are leptoquarks (models 3, 4, 7 and 8) both $eejj$ and ep_Tjj signals can be produced simultaneously. While the constraints coming from the electroweak precision data on the mixing angle between Z_N and the SM Z makes it difficult to address the recent diboson and dijet excesses reported by ATLAS and CMS Collaborations in the framework of $U(1)_N$ model. For the choice $Z_2^H = Z_2^L = (-1)^L$ as the second discrete symmetry, two of the variants (models 1 and 2) offers the possibility of direct baryogenesis at high scale via decay of heavy Majorana baryon, while two other (models 3 and 4) can accommodate high-scale leptogenesis. For the above choice of the second discrete symmetry none of the other variants are consistent with high-scale baryogenesis (leptogenesis), however, model 5 allows for the possibility of baryogenesis at TeV scale or below by considering soft supersymmetry breaking terms and this mechanism can induce baryon number violating $n-\bar{n}$ oscillation. On the other hand we have also pointed out a new choice for the second discrete symmetry which has the feature of ensuring proton stability and forbidding tree level FCNC processes, while allowing for the possibility of high scale leptogenesis for models 5 and 6. Studying the neutrino mass matrices for the $U(1)_N$ model variants we find that these variants can naturally give three active and two sterile neutrinos and accommodate the LSND results. These neutrinos acquire masses through their mixing with extra neutral fermions and can give rise to interesting neutrino mass textures where the results for the atmospheric and solar neutrino oscillations can be naturally explained.

[1] V. Khachatryan *et al.* (CMS Collaboration), Eur. Phys. J. C **74**, 3149 (2014).
[2] CMS Collaboration (CMS Collaboration), Report No. CMS-PAS-EXO-12-041.
[3] J. Gluza and T. Jelinski, Phys. Lett. B **748**, 125 (2015).
[4] F. F. Deppisch, T. E. Gonzalo, S. Patra, N. Sahu, and U. Sarkar, Phys. Rev. D **90**, 053014 (2014); **91**, 015018 (2015).
[5] M. Fukugita and T. Yanagida, Phys. Lett. B **174**, 45 (1986); For recent reviews see, e.g., S. Davidson, E. Nardi, and Y. Nir, Phys. Rep. **466**, 105 (2008); C. S. Fong, E. Nardi, and A. Riotto, Adv. High Energy Phys. **2012**, 158303 (2012).
[6] E. Ma and U. Sarkar, Phys. Rev. Lett. **80**, 5716 (1998); G. Lazarides and Q. Shafi, Phys. Rev. D **58**, 071702 (1998); T. Hambye, E. Ma, and U. Sarkar, Nucl. Phys. **B602**, 23 (2001).
[7] M. Dhuria, C. Hati, R. Rangarajan, and U. Sarkar, Phys. Rev. D **92**, 031701 (2015).
[8] M. Dhuria, C. Hati, R. Rangarajan, and U. Sarkar, J. Cosmol. Astropart. Phys. 09 (2015) 035.
[9] E. Ma, S. Sarkar, and U. Sarkar, Phys. Lett. B **458**, 73 (1999).
[10] J. A. Aguilar-Saavedra and F. R. Joaquim, Phys. Rev. D **90**, 115010 (2014).
[11] B. A. Dobrescu and A. Martin, Phys. Rev. D **91**, 035019 (2015).
[12] F. S. Queiroz, K. Sinha, and A. Strumia, Phys. Rev. D **91**, 035006 (2015); B. Allanach, A. Alves, F. S. Queiroz, K. Sinha, and A. Strumia, Phys. Rev. D **92**, 055023 (2015).
[13] B. Allanach, S. Biswas, S. Mondal, and M. Mitra, Phys. Rev. D **91**, 011702 (2015); B. C. Allanach, S. Biswas, S. Mondal, and M. Mitra, Phys. Rev. D **91**, 015011 (2015).
[14] S. Biswas, D. Chowdhury, S. Han, and S. J. Lee, J. High Energy Phys. 02 (2015) 142.
[15] M. Dhuria, C. Hati, R. Rangarajan, and U. Sarkar, Phys. Rev. D **91**, 055010 (2015).
[16] E. Ma, Phys. Rev. D **36**, 274 (1987).
[17] R. N. Mohapatra and R. E. Marshak, Phys. Rev. Lett. **44**, 1316 (1980); **44(E)**, 1643 (1980); R. N. Mohapatra and R. E. Marshak, Phys. Lett. **94B**, 183 (1980); D. G. Phillips, II *et al.*, arXiv:1410.1100.
[18] A. Aguilar-Arevalo *et al.* (LSND Collaboration), Phys. Rev. D **64**, 112007 (2001); A. A. Aguilar-Arevalo *et al.* (MiniBooNE Collaboration), Phys. Rev. Lett. **98**, 231801 (2007); **102**, 101802 (2009); **105**, 181801 (2010); G. Mention, M. Fechner, T. Lasserre, T. A. Mueller, D. Lhuillier, M. Cribier, and A. Letourneau, Phys. Rev. D **83**, 073006 (2011); T. A. Mueller, D. Lhuillier, M. Fallot, A. Letourneau, S. Cormon, M. Fechner, L. Giot, T. Lasserre *et al.*, Phys. Rev. C **83**, 054615 (2011); P. Huber, Phys. Rev. C **84**, 024617 (2011); **85**, 029901 (2012); J. Kopp, P. A. N. Machado, M. Maltoni, and T. Schwetz, J. High Energy Phys. 05 (2013) 050; J. M. Conrad, C. M. Ignarra, G. Karagiorgi, M. H. Shaevitz, and J. Spitz, Adv. High Energy Phys. **2013**, 163897 (2013); A. de Gouvea *et al.* (Intensity Frontier Neutrino Working Group Collaboration), arXiv:1310.4340; M. Archidiacono, N. Fornengo, C. Giunti, S. Hannestad, and A. Melchiorri, Phys. Rev. D **87**, 125034 (2013).
[19] E. Ma, Phys. Lett. B **380**, 286 (1996); J. L. Rosner, Phys. Rev. D **90**, 035005 (2014).
[20] P. Candelas, G. T. Horowitz, A. Strominger, and E. Witten, Nucl. Phys. **B258**, 46 (1985).
[21] B. R. Greene, arXiv:hep-th/9702155.
[22] A. S. Joshipura and U. Sarkar, Phys. Rev. Lett. **57**, 33 (1986).
[23] E. Ma, Phys. Rev. Lett. **60**, 1363 (1988).
[24] E. Ma and M. Raidal, J. Phys. G **28**, 95 (2002).
[25] T. Hambye, E. Ma, M. Raidal, and U. Sarkar, Phys. Lett. B **512**, 373 (2001).
[26] B. C. Allanach, C. H. Kom, and H. Pas, Phys. Rev. Lett. **103**, 091801 (2009).
[27] G. Aad *et al.* (ATLAS Collaboration), arXiv:1506.00962.
[28] V. Khachatryan *et al.* (CMS Collaboration), J. High Energy Phys. 08 (2014) 173.
[29] V. Khachatryan *et al.* (CMS Collaboration), J. High Energy Phys. 08 (2014) 174.
[30] G. Aad *et al.* (ATLAS Collaboration), Phys. Rev. D **91**, 052007 (2015).
[31] V. Khachatryan *et al.* (CMS Collaboration), Phys. Rev. D **91**, 052009 (2015).
[32] CMS Collaboration (CMS Collaboration), Report No. CMS-PAS-EXO-14-010.
[33] J. Brehmer, J. Hewett, J. Kopp, T. Rizzo, and J. Tattersall, J. High Energy Phys. 10 (2015) 182.
[34] J. Hisano, N. Nagata, and Y. Omura, Phys. Rev. D **92**, 055001 (2015).
[35] K. Cheung, W. Y. Keung, P. Y. Tseng, and T. C. Yuan, Phys. Lett. B **751**, 188 (2015).
[36] B. A. Dobrescu and Z. Liu, Phys. Rev. Lett. **115**, 211802 (2015).
[37] Y. Gao, T. Ghosh, K. Sinha, and J. H. Yu, Phys. Rev. D **92**, 055030 (2015).
[38] Q. H. Cao, B. Yan, and D. M. Zhang, Phys. Rev. D **92**, 095025 (2015).
[39] T. Abe, R. Nagai, S. Okawa, and M. Tanabashi, Phys. Rev. D **92**, 055016 (2015).
[40] J. Heeck and S. Patra, Phys. Rev. Lett. **115**, 121804 (2015).
[41] B. C. Allanach, B. Gripaios, and D. Sutherland, Phys. Rev. D **92**, 055003 (2015).
[42] T. Abe, T. Kitahara, and M. M. Nojiri, arXiv:1507.01681.
[43] B. A. Dobrescu and Z. Liu, J. High Energy Phys. 10 (2015) 118.
[44] H. S. Fukano, S. Matsuzaki, and K. Yamawaki, arXiv:1507.03428.
[45] H. S. Fukano, M. Kurachi, S. Matsuzaki, K. Terashi, and K. Yamawaki, Phys. Lett. B **750**, 259 (2015).
[46] A. Thamm, R. Torre, and A. Wulzer, Phys. Rev. Lett. **115**, 221802 (2015).
[47] A. Carmona, A. Delgado, M. Quirs, and J. Santiago, J. High Energy Phys. 09 (2015) 186.
[48] C. W. Chiang, H. Fukuda, K. Harigaya, M. Ibe, and T. T. Yanagida, J. High Energy Phys. 11 (2015) 015.
[49] G. Cacciapaglia, A. Deandrea, and M. Hashimoto, Phys. Rev. Lett. **115**, 171802 (2015).
[50] V. Sanz, arXiv:1507.03553.
[51] A. Alves, A. Berlin, S. Profumo, and F. S. Queiroz, J. High Energy Phys. 10 (2015) 076.
[52] J. A. Aguilar-Saavedra, J. High Energy Phys. 10 (2015) 099.
[53] C. H. Chen and T. Nomura, Phys. Lett. B **749**, 464 (2015).
[54] L. A. Anchordoqui, I. Antoniadis, H. Goldberg, X. Huang, D. Lust, and T. R. Taylor, Phys. Lett. B **749**, 484 (2015).
[55] C. Petersson and R. Torre, arXiv:1508.05632v2.
[56] J. Erler, P. Langacker, S. Munir, and E. Rojas, J. High Energy Phys. 08 (2009) 017.
[57] T. Hambye, Nucl. Phys. **B633**, 171 (2002).

Physics Letters B 757 (2016) 223–230

Contents lists available at ScienceDirect

Physics Letters B

www.elsevier.com/locate/physletb

Implications of the diphoton excess on left–right models and gauge unification

Frank F. Deppisch [a], Chandan Hati [b,c], Sudhanwa Patra [d,*], Prativa Pritimita [d], Utpal Sarkar [b]

[a] Department of Physics and Astronomy, University College London, London WC1E 6BT, United Kingdom
[b] Physical Research Laboratory, Navrangpura, Ahmedabad 380 009, India
[c] Indian Institute of Technology Gandhinagar, Chandkheda, Ahmedabad 382 424, India
[d] Center of Excellence in Theoretical and Mathematical Sciences, Siksha 'O' Anusandhan University, Bhubaneswar-751030, India

ARTICLE INFO

Article history:
Received 19 January 2016
Received in revised form 10 March 2016
Accepted 30 March 2016
Available online 4 April 2016
Editor: M. Cvetič

ABSTRACT

The recent diphoton excess signal at an invariant mass of 750 GeV can be interpreted in the framework of left–right symmetric models with additional scalar singlets and vector-like fermions. We propose a minimal scenario for such a purpose. Extending the LRSM framework to include these new vector-like fermionic fields, on the other hand, results in interesting phenomenological implications for the LRSM fermion masses and mixing. Furthermore, existence of such vector-like fermions can also have interesting implications for baryogenesis and the dark matter sector. The introduction of a real bi-triplet scalar which contains a potential DM candidate will allow the gauge couplings to unify at $\approx 10^{17.7}$ GeV.

1. Introduction

The CMS and ATLAS Collaborations have recently reported a roughly 3σ excess in the diphoton channel at an invariant mass of about 750 GeV in the first 3 fb^{-1} of collected data from Run 2 of the LHC at 13 TeV [1,2]. The Landau–Yang theorem forbids the possibility of a massive spin one resonance decaying to $\gamma\gamma$. The leading interpretations of the excess within the context of new physics scenarios therefore consist of postulating a fundamental spin zero or spin two particle with mass of about 750 GeV. However no enhancements have been seen in the dijet, $t\bar{t}$, diboson or dilepton channels posing a clear challenge to the possible interpretations of this excess. The absence of a peaked $\gamma\gamma$ angular distribution in the observed events towards the beam direction disfavours [3] the spin two hypothesis and the spin zero resonance interpretation seems more favourable from a theoretical point of view.

A large number of interpretations of the diphoton signal in terms of physics beyond the Standard Model have been proposed in the literature [4–136]. One of the possibilities that has been largely explored in the literature is a scalar or pseudo-scalar resonance produced through gluon–gluon fusion and decaying to $\gamma\gamma$ via loop diagrams with circulating fermions or bosons. A new resonance coupling with the Standard Model (SM) t quark or $W^{\pm}$ can give rise to such loop diagrams, however, they will be highly suppressed at the large $\gamma\gamma$ invariant masses and the dominant decay channel would have to be $t\bar{t}$ or W^+W^-. Hence the observation of the $\gamma\gamma$ resonance at 750 GeV (much greater than the electroweak symmetry breaking scale) hints towards the existence of vector-like fermions around that mass scale. Given that both the ATLAS and CMS Collaborations have suggested signal events consistent with each other at a tempting 3σ statistical significance level, hinting towards a new physics scenario, it is important to explore the possible model framework that can naturally accommodate such vector-like fermions.

From a theoretical stand point, a framework that can explain the diphoton excess while being consistent with other searches for new physics is particularly intriguing. To this end, one must mention the results reported by the CMS Collaboration in the first run of LHC for the right-handed gauge boson W_R search at $\sqrt{s} = 8$ TeV and 19.7 fb^{-1} of integrated luminosity [137]. A 2.8σ local excess was reported in the $eejj$ channel in the energy range 1.8 TeV $< m_{eejj} < 2.2$ TeV, hinting at a right handed gauge counterpart of the SM $SU(2)_L$ broken around the TeV scale. The Left–Right Symmetric Model (LRSM) framework with $g_R \neq g_L$ can explain such signal with the possibility of being embedded into a ultraviolet complete higher gauge group [138–141]. It is thus an interesting exercise to

* Corresponding author.
E-mail addresses: f.deppisch@ucl.ac.uk (F.F. Deppisch), chandan@prl.res.in (C. Hati), sudha.astro@gmail.com (S. Patra), pratibha.pritimita@gmail.com (P. Pritimita), utpal@prl.res.in (U. Sarkar).

http://dx.doi.org/10.1016/j.physletb.2016.03.081

explore the possibility of naturally accommodating the $\gamma\gamma$ excess also in such a framework.

In this paper, we explore the possibility of extending the standard LRSM framework with vector-like fermions and singlet scalars which can explain the diphoton signal. Adding such new vector-like fermionic fields, on the other hand, results in interesting phenomenological implications for the LRSM fermion masses and mixing. Moreover, existence of such vector-like fermions can have interesting implications for baryogenesis and the potential dark matter sector. In gauged flavour groups with left–right symmetry [142] or quark-lepton symmetric models [143], vector-like fermions are naturally accommodated while in LRSMs originating from D-brane or heterotic string compactifications also often include vector-like fermions [144,145]. We propose a minimal LRSM that hosts such vector-like fermions and which can explain the diphoton signal. We also explore the possible fermion masses and mixing phenomenology and the implications of these vector-like particles in baryogenesis and the dark matter sector.

The plan of rest of this paper is as follows. In section 2, we discuss the LRSM accommodating new vector-like fermions and the implications on masses and mixing of the fermions. In section 3, we discuss the general aspects of the diphoton signal in the context of a scalar resonance decaying to $\gamma\gamma$ through circulating vector-like fermions in the loop. In section 4, we explore the possibility of obtaining a gauge coupling unification including the new vector like fields. In section 5, we discuss the implications of the vector-like fermions for baryogenesis and the dark matter sector. In section 6, we summarize and make concluding remarks.

2. Left–right symmetric model framework

The left–right symmetric extension of the SM has the basic gauge group given by

$$\mathcal{G}_{L,R} \equiv SU(3)_C \times SU(2)_L \times SU(2)_R \times U(1)_{B-L}, \tag{1}$$

where $B-L$ is the difference between baryon and lepton number. The electric charge is related to the third component of isospin in the $SU(2)_{L,R}$ gauge groups and the $B-L$ charge as

$$Q = T_{3L} + T_{3R} + 1/2(B-L). \tag{2}$$

The quarks and leptons transform under the LRSM gauge group as

$$q_L = \begin{pmatrix} u_L \\ d_L \end{pmatrix} \equiv [2,1,\frac{1}{3},3], \quad q_R = \begin{pmatrix} u_R \\ d_R \end{pmatrix} \equiv [1,2,\frac{1}{3},3],$$
$$\ell_L = \begin{pmatrix} \nu_L \\ e_L \end{pmatrix} \equiv [2,1,-1,1], \quad \ell_R = \begin{pmatrix} \nu_R \\ e_R \end{pmatrix} \equiv [1,2,-1,1],$$

where the gauge group representations are written in the form $[SU(2)_L, SU(2)_R, B-L, SU(3)_C]$.

Originally the left–right symmetric extension of the SM [146–151], was introduced to give a natural explanation for parity violation seen in radioactive beta decay and to consistently address the light neutrino masses via seesaw mechanism [152–156]. The latter form doublets with the right handed charged fermions under the $SU(2)_R$ gauge group. If $SU(2)_R$ breaks at around the TeV scale, LRSMs offer a rich interplay between high energy collider signals and low energy processes such as neutrinoless double beta decay and lepton flavour violation [157]. The principal prediction of this scenario is a TeV scale right-handed gauge boson W_R. The CMS and ATLAS Collaborations had reported several excesses at around 2 TeV in Run 1 of the LHC, pointing towards such a possibility. From the first results of Run 2, no dijet and diboson excesses have been reported (more data is required to exclude the diboson excesses reported in run 1), the relatively "cleaner" $eejj$ channel signal is still present hinting at a 2 TeV W_R. In light of the diphoton excess it is important to revisit the LRSM framework to explore the possibility of accommodating such signal and the possible implications.

Table 1
LRSM representations of extended field content.

Field	$SU(2)_L$	$SU(2)_R$	$B-L$	$SU(3)_C$
q_L	2	1	1/3	3
q_R	1	2	1/3	3
ℓ_L	2	1	−1	1
ℓ_R	1	2	−1	1
$U_{L,R}$	1	1	4/3	3
$D_{L,R}$	1	1	−2/3	3
$E_{L,R}$	1	1	−2	1
$N_{L,R}$	1	1	0	1
H_L	2	1	1	1
H_R	1	2	1	1
S	1	1	0	1

As already mentioned in the introduction and discussed in section 3, the 750 GeV diphoton excess can be explained through the resonant production and decay of a scalar or pseudoscalar particle. To this end, we propose a simple left–right symmetric model with a scalar singlet S and vector-like fermions added to the minimal particle content of left–right symmetric models.[1]

We extend the standard LRSM framework to include isosinglet vector-like copies of LRSM fermions. This kind of a vector-like fermion spectrum is very naturally embedded in gauged flavour groups with left–right symmetry [142] or quark-lepton symmetric models [143]. The field content of this model and the relevant transformations under the LRSM gauge group are shown in Table 1.

The relevant Yukawa part of the Lagrangian is given by

$$\begin{aligned}\mathcal{L} = &-\sum_X (\lambda_{SXX} S\bar{X}X + M_X \bar{X}X) \\ &- (\lambda_U^L \tilde{H}_L \bar{q}_L U_R + \lambda_U^R \tilde{H}_R \bar{q}_R U_L \\ &+ \lambda_D^L H_L \bar{q}_L D_R + \lambda_D^R H_R \bar{q}_R D_L \\ &+ \lambda_E^L H_L \bar{\ell}_L E_R + \lambda_E^R H_R \bar{\ell}_R E_L \\ &+ \lambda_N^L \tilde{H}_L \bar{\ell}_L N_R + \lambda_N^R \tilde{H}_R \bar{\ell}_R N_L + \text{h.c.}),\end{aligned} \tag{3}$$

where the summation is over $X = U, D, E, N$ and we suppress flavour and colour indices on the fields and couplings. $\tilde{H}_{L,R}$ denotes $\tau_2 H^*_{L,R}$, where τ_2 is the usual second Pauli matrix.

The vacuum expectation values (VEVs) of the Higgs doublets $H_R(1,2,-1)$ and $H_L(2,1,-1)$ break the LRSM gauge group to the SM gauge group and the SM gauge group to $U(1)_{\text{EM}}$ respectively, with an ambiguity of parity breaking, which can either be broken at the TeV scale or at a much higher scale M_P. In the latter case, the Yukawa couplings can be different for right-type and left-type Yukawa terms because of the renormalization group running below M_P, $\lambda_X^R \neq \lambda_X^L$. Hence, we distinguish the left and right handed couplings explicitly with the subscripts L and R. We use the VEV normalizations $\langle H_L \rangle = (0, v_L)^T$ and $\langle H_R \rangle = (0, v_R)^T$ with $v_L = 175$ GeV and v_R constrained by searches for the heavy right-handed W_R boson at colliders and at low energies, $v_R \gtrsim 1-3$ TeV (depending on the right-handed gauge coupling). Due to the absence of a bidoublet Higgs scalar, normal Dirac mass terms for the SM fermions are absent and the charged fermion mass matrices assume a seesaw structure. However, if one does not want to de-

[1] We assume the resonance to be a new singlet scalar and it can easily be generalized to a pseudoscalar case.

pend on a "universal" seesaw structure, a Higgs bidoublet Φ can be introduced along with $H_{L,R}$.

After symmetry breaking, the mass matrices for the fermions are given by

$$M_{uU} = \begin{pmatrix} 0 & \lambda_U^L v_L \\ \lambda_U^R v_R & M_U \end{pmatrix}, \quad M_{dD} = \begin{pmatrix} 0 & \lambda_D^L v_L \\ \lambda_D^R v_R & M_D \end{pmatrix},$$
$$M_{eE} = \begin{pmatrix} 0 & \lambda_E^L v_L \\ \lambda_E^R v_R & M_E \end{pmatrix}, \quad M_{\nu N} = \begin{pmatrix} 0 & \lambda_N^L v_L \\ \lambda_N^R v_R & M_N \end{pmatrix}. \tag{4}$$

The mass eigenstates can be found by rotating the mass matrices via left and right orthogonal transformations $O^{L,R}$ (we assume all parameters to be real). For example, the up quark diagonalization yields $O_U^{LT} \cdot M_{uU} \cdot O_U^R = \mathrm{diag}(\hat{m}_u, \hat{M}_U)$. Up to leading order in $\lambda_U^L v_L$, the resulting up-quark masses are

$$\hat{M}_U \approx \sqrt{M_U^2 + (\lambda_U^R v_R)^2}, \quad \hat{m}_u \approx \frac{(\lambda_U^L v_L)(\lambda_U^R v_R)}{\hat{M}_U}, \tag{5}$$

and the mixing angles $\theta_U^{L,R}$ parametrizing $O_U^{L,R}$,

$$\tan(2\theta_U^L) \approx \frac{2(\lambda_U^L v_L) M_U}{M_U^2 + (\lambda_U^R v_R)^2}, \quad \tan(2\theta_U^R) \approx \frac{2(\lambda_U^R v_R) M_U}{M_U^2 - (\lambda_U^R v_R)^2}. \tag{6}$$

The other fermion masses and mixings are given analogously. For an order of magnitude estimate one may approximate the phenomenologically interesting regime with the limit $\lambda_U^R v_R \to M_U$ in which case the mixing angles approach $\theta_U^L \to \hat{m}_u/\hat{M}_U$ and $\theta_U^R \to \pi/4$. This means that θ_U^L is negligible for all fermions but the top quark and its vector partner [90].

We here neglect the flavour structure of the Yukawa couplings $\lambda_X^{L,R}$ and λ_{SXX} which will determine the observed quark and leptonic mixing. The hierarchy of SM fermion masses can be generated by either a hierarchy in the Yukawa couplings or in the masses of the vector like fermions.

As described above, the light neutrino masses are of Dirac-type as well, analogously given by

$$\hat{m}_\nu = \frac{\lambda_N^L \lambda_N^R v_L v_R}{M_N}. \tag{7}$$

It is natural to assume that $M_N \gg v_R$, as the vector like N is a singlet under the model gauge group. In this case, the scenario predicts naturally light Dirac neutrinos [142].

3. Diphoton signal from a scalar resonance

One may attempt to interpret the diphoton excess at as the resonant production of the singlet scalar S with mass $M_S = 750$ GeV. Considering the possible production mechanisms for the resonance at 750 GeV it is interesting to note that the CMS and ATLAS did not report a signal in the ~ 20 fb^{-1} data at 8 TeV in Run 1. One possible interpretation of this can be that the resonance at 750 GeV is produced through a mechanism with a steeper energy dependence. Excluding the possibility of an associated production of this resonance, the most favourable mechanism is gluon–gluon fusion which we here also consider as the dominant production mechanism. Subsequently, the scalar with mass 750 GeV decays to two photons via a loop as well. The cross section can be expressed as

$$\sigma(pp \to \gamma\gamma) = \frac{C_{gg}}{M_S s} \Gamma_{gg} \mathrm{Br}_{\gamma\gamma}, \tag{8}$$

with the proton centre of mass energy $\sqrt{s}$ and the parton distribution integral $C_{gg} = 174$ at $\sqrt{s} = 8$ TeV and $C_{gg} = 2137$ at $\sqrt{s} = 13$ TeV [14]. One can obtain a best fit guess of the cross section by reconstructing the likelihood, assumed to be Gaussian, from the 95% C.L. expected and observed limits in an experimental search. For the diphoton excess, we use a best fit cross section value of 7 fb found by combining the 95% C.L. ranges from ATLAS and CMS at 13 TeV and 8 TeV for a resonance mass of 750 GeV [14].

Apart from the necessary decay modes of the scalar S i.e., $S \to gg$ and $S \to \gamma\gamma$, S may also decay to other particles; due to the necessary SM invariance and the fact that $M_S > m_Z$, $S \to \gamma\gamma$ necessitates the decays $S \to \gamma Z$ and ZZ which are suppressed by $2\tan^2\theta_W \approx 0.6$ and $\tan^4\theta_W \approx 0.1$ relative to $\Gamma(S \to \gamma\gamma)$ [14]. Furthermore, S in our model may also decay to SM fermions due to mixing with the heavy vector-like fermions. As described above, the mixing is only sizeable for the top and its vector partner. The total width is thereby given by $\Gamma_S \approx \Gamma_{gg} + 1.7 \times \Gamma_{\gamma\gamma} + \Gamma_{t\bar{t}}$.

We would like to stress that while the diphoton resonance undoubtedly is the motivation behind this work, the purpose of this paper is to construct a consistent LRSM framework that can naturally accommodate vector-like fermions taking the diphoton signal as a hint and explore the consequent phenomenology. One can find similar interpretations of the diphoton excess in [90,118,119] in models with a singlet scalar accompanied by vector-like fermions.

Production of a scalar resonance in gluon fusion via a loop of vector-like quarks and subsequent decay of scalar resonance to $\gamma\gamma$ via a loop of vector-like quarks and leptons. There are contributions to $\Gamma(S \to \gamma\gamma)$ from quark-like vector fermion $\psi_Q = U, D$ and lepton-like vector fermion $\psi_L = E$ propagating inside the loop. Apart from quark-like vector fermion contributing to the production of scalar through gluon fusion, there could be another top-quark mediated diagram via mixing with SM Higgs boson.

In the LRSM framework discussed in section 2, the vector-like degrees of freedom contribute to the loop leading to $S \to gg$ and $S \to \gamma\gamma$. The partial decay widths are given by [17]

$$\Gamma_{\gamma\gamma} = \frac{\alpha^2 M_S^3}{256\pi^3} \left| \sum_X \frac{N_X^C Q_X^2 \lambda'_{SXX}}{M_X} \mathcal{A}\left(\frac{m_S^2}{4M_X^2}\right) \right|^2,$$
$$\Gamma_{gg} = K \frac{\alpha_s^2 M_S^3}{128\pi^3} \left| \sum_X^C \frac{\lambda'_{SXX}}{M_X} \mathcal{A}\left(\frac{m_S^2}{4M_X^2}\right) \right|^2. \tag{9}$$

Here, the sums in $\Gamma_{\gamma\gamma}$ and Γ_{gg} are over all and coloured fermion species and flavours, respectively. N_X^C is the number of colour degrees of freedom of a species, i.e. 1 for leptonic vector-like fermions and 3 for quark-like fermions. Similarly, Q_X is the electric charge of the species. The effective coupling of S to a fermion species is $\lambda'_{SXX} = \lambda_{SXX}(O_X^R)_{1X}(O_X^L)_{1X}$, i.e. the coupling λ_{SXX} dressed with the corresponding left and right mixing matrix element. The value of the parameters $\alpha \approx 1/127$, $\alpha_s \approx 0.1$ and $K \approx 1.7$ [17] in which $A(x)$ is a loop function defined by

$$A(x) = \frac{2}{x^2}[x + (x-1) f(x)], \tag{10}$$

with

$$f(x) = \begin{cases} \arcsin^2\sqrt{x} & x \le 1 \\ -\frac{1}{4}\left[\ln\left(\frac{1+\sqrt{1-x}}{1-\sqrt{1-x}}\right) - i\pi\right]^2 & x > 1. \end{cases} \tag{11}$$

In addition, the decay of S to a pair of fermions (here only relevant for the top) is given by

$$\Gamma_{f\bar{f}} = \frac{N_f^C \lambda'^2_{Xff} M_S}{16\pi} \left(1 - \frac{4M_f^2}{M_S^2}\right)^{2/3}. \tag{12}$$

In order to arrive at an estimate for the diphoton production cross section, we assume that the vector fermion masses and couplings to S are degenerate (M_X, λ_{SXX}), except for the top partner

(M_T, λ_{STT}). In the limit of large vector fermion masses $M_X \gtrsim M_S/2$, we arrive at the approximation for the partial widths,

$$\frac{\Gamma_{gg}}{M_S} \approx 1.3 \times 10^{-4} \left(\frac{\lambda_{SXX} \cdot \text{TeV}}{M_X}\right)^2,$$
$$\frac{\Gamma_{\gamma\gamma}}{M_S} \approx 3.4 \times 10^{-7} \left(\frac{\lambda_{SXX}\text{TeV}}{M_X}\right)^2,$$
$$\frac{\Gamma_{t\bar{t}}}{M_S} \approx 1.3 \times 10^{-3} \left(\frac{\lambda_{TXX}\text{TeV}}{M_T}\right)^2. \tag{13}$$

As discussed in [14] in a model-independent fashion, the diphoton excess can be explained for $10^{-6} \lesssim \Gamma_{gg}/M_S \lesssim 2 \times 10^{-3}$ (the upper limit is due to the limit from dijet searches) and $\Gamma_{\gamma\gamma}/M_S \approx 10^{-6}$, as long as gg and $\gamma\gamma$ are the only decay modes of S. In order to achieve this, the top partner T needs to have a significantly weaker coupling or heavier mass than the rest of the vector fermions. Assuming the decay width to $t\bar{t}$ contributes negligibly to the total width, the diphoton cross section, Eq. (8) is

$$\sigma(pp \to \gamma\gamma) \approx 1.7 \text{ fb} \cdot \left(\frac{\lambda_{SXX} \cdot \text{TeV}}{M_X}\right)^2. \tag{14}$$

The experimentally suggested cross section $\sigma(pp \to \gamma\gamma) \approx 7$ fb can be achieved with $M_X/\lambda_{SXX} \approx 0.5$ TeV (and $\Gamma_{gg}/M_S \approx 5 \times 10^{-4}$ satisfying the dijet limit). In such a scenario, the total width of S is of the order $\Gamma_S \approx 0.5$ GeV, i.e. much smaller than the 45 GeV suggested by ATLAS if interpreted as a single particle resonance. $\Gamma_{\gamma\gamma}/\Gamma_{gg}$ can also be independently boosted by introducing a hierarchy with leptonic partners lighter than the quark partners. While certainly marginal and requiring a specific structure among the vector fermions, this demonstrates that the diphoton excess, apart from the broad width seen by ATLAS, can be accommodated in our model.

4. Gauge coupling unification

In the previous section, we have discussed how the inclusion of new vector-like fermions in LRSM can aptly explain the diphoton excess traced around 750 GeV at the LHC. Interestingly this framework can also be embedded in a non-SUSY grand unified theory like $SO(10)$ having left–right symmetry as its only intermediate symmetry breaking step with the breaking chain given as follows

$$SO(10) \xrightarrow{\langle\Sigma\rangle} \mathcal{G}_{2213P} \xrightarrow{\langle H_R\rangle} \mathcal{G}_{213} \xrightarrow{\langle H_L\rangle} \mathcal{G}_{13}. \tag{15}$$

The $SO(10)$ group breaks down to left–right symmetric group $\mathcal{G}_{2213P} \equiv SU(2)_L \times SU(2)_R \times U(1)_{B-L} \times SU(3) \times \mathcal{P}$ via a non-zero VEV of $\Sigma \subset 210_H$. Here, $\mathcal{P}$ is defined as the discrete left–right symmetry, a generalized parity symmetry or charge-conjugation symmetry. The vital step is to break the left–right gauge symmetry and this is attained with the help of the right-handed Higgs doublet H_R. Finally, the SM gauge group is spontaneously broken by its left-handed counterpart H_L. As described above we add another scalar singlet S in order to explain the diphoton signal though it is not contributing to the renormalization group (RG) evolution of the gauge couplings.

In addition to the particle content described in Table 1, we include a bi-triplet $\eta \equiv (3, 3, 0, 1)$ under $\mathcal{G}_{2213P}$ to achieve successful gauge unification. This can be confirmed by using the relevant RG equation for the gauge couplings g_i,

$$\mu \frac{\partial g_i}{\partial \mu} = \frac{b_i}{16\pi^2} g_i^3, \tag{16}$$

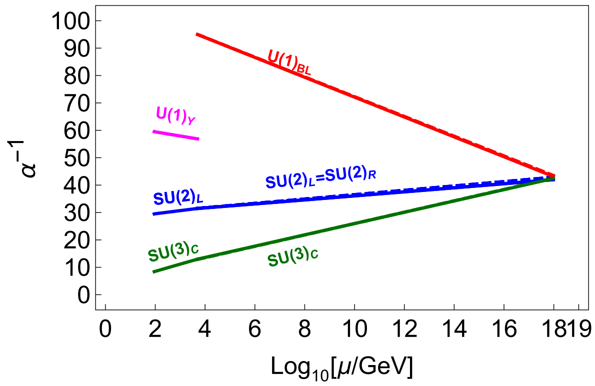

Fig. 1. Gauge coupling running in the considered model accommodating the diphoton excess, demonstrating successful gauge unification at the scale $M_{\text{GUT}} = 10^{17.75}$ GeV with an intermediate left–right symmetry breaking scale at 10 TeV. The dashed lines correspond to one loop RGE of gauge couplings while the two loop effects are displayed in solid lines.

where the one-loop beta-coefficients b_i are given by

$$b_i = -\frac{11}{3}\mathcal{C}_2(G) + \frac{2}{3}\sum_{R_f} T(R_f)\prod_{j\neq i} d_j(R_f) + \frac{1}{3}\sum_{R_s} T(R_s)\prod_{j\neq i} d_j(R_s). \tag{17}$$

Here, $\mathcal{C}_2(G)$ is the quadratic Casimir operator for gauge bosons in their adjoint representation,

$$\mathcal{C}_2(G) \equiv \begin{cases} N & \text{if } SU(N), \\ 0 & \text{if } U(1). \end{cases} \tag{18}$$

$T(R_f)$ and $T(R_s)$ are the traces of the irreducible representation $R_{f,s}$ for a given fermion and scalar, respectively,

$$T(R_{f,s}) \equiv \begin{cases} 1/2 & \text{if } R_{f,s} \text{ is fundamental}, \\ N & \text{if } R_{f,s} \text{ is adjoint}, \\ 0 & \text{if } U(1), \end{cases} \tag{19}$$

and $d(R_{f,s})$ is the dimension of a given representation $R_{f,s}$ under all $SU(N)$ gauge groups except the i-th gauge group under consideration. An additional factor of 1/2 should be multiplied in the case of a real Higgs representation. Using the above particle content, the beta-coefficients at one loop are found to be $b_{2L} = -19/6$, $b_Y = 41/10$, $b_{3C} = -7$ from the SM to the LR breaking scale and $b_{2L} = b_{2R} = -13/6$, $b_{BL} = 59/6$, $b_{3C} = -17/3$ from the LR breaking scale to the GUT scale. We have also evaluated the two loop contributions which give a very marginal deviation over one loop contributions. The resulting running of the gauge couplings at one loop and two loop orders are shown in Fig. 1 with the breaking scales

$$M_{\text{GUT}} = 10^{17.75} \text{ GeV}, \quad M_{\text{LR}} = 10 \text{ TeV}. \tag{20}$$

5. Implications for baryogenesis and dark matter

The vector-like fermions added to the spectrum of the LRSM framework can have very profound implications for a baryogenesis mechanism such as leptogenesis and the dark matter sector. While the proposal of high scale leptogenesis via singlet heavy Majorana neutrinos (or a heavy Higgs triplet) decay added to the SM is beyond the reach of the present and near future collider experiments, the LRSM scenario provides a window of opportunity for low TeV scale leptogenesis testable at the LHC. However, the observation of a 2 TeV W_R boson at the LHC, through confirmation of the 2.8σ signal of two leptons and two jets reported by the CMS Collaboration, would rule out the possibility of high scale as well as TeV scale resonant leptogenesis with the standard LRSM fields due to the unavoidable fast gauge mediated $B-L$ violating interactions [158–165].

On the other hand, the new vector-like fermions added to the LRSM to accommodate the diphoton excess can open a whole new world of possibilities. A particularly interesting possibility is the realization of baryogenesis and dark matter annihilation through a vector-like portal first explored in [166]. As an example, consider the following additional terms in the Lagrangian,

$$\mathcal{L} \supset -(\lambda_{XU} X \overline{u_R} U_L + \text{h.c.}) - m_X^2 X^\dagger X - \lambda_X (X^\dagger X)^2 - \lambda_{HX} H^\dagger H X^\dagger X, \tag{21}$$

where X is an inert doublet (a singlet complex) dark matter scalar field in the LR(SM) case. X is charged under some exotic global $U(1)_\chi$ symmetry, under which only the vector-like quarks and dark matter fields transform non-trivially. Thus, the introduction of a vector-like quarks can connect the dark matter to the usual LR(SM) quarks, which can be readily used to make a connection between the baryon asymmetry and dark matter, as pointed out in [166]. In rest of this section we focus on sketching the simpler case of the extended SM which can be expanded to the LRSM case by replacing the singlets with appropriate doublet representations. However, in the case of the LRSM some subtleties are present and we comment on them towards the end of this section. On the other hand, this idea can easily be generalized to accommodate a down-type quark portal or charged lepton portal (corresponding to a leptogenesis scenario of baryogenesis).

The basic idea behind the vector-like portal is to generate an asymmetry in the vector-like sector through baryogenesis, which then subsequently gets transferred to the SM baryons and the dark matter sector through the renormalizable couplings in Eq. (21). In addition one can introduce a scalar field Y with the couplings

$$\mathcal{L} \supset -(\lambda_{\nu Y} Y \nu_R \nu_R + \text{h.c.}) - m_Y^2 Y^\dagger Y - \lambda_Y (Y^\dagger Y)^2 - \lambda_{XY} X^\dagger X Y^\dagger Y, \tag{22}$$

which allows the annihilation of a pair of X into Y fields. The latter can subsequently decay into two singlet right handed neutrinos ensuring the asymmetric nature of the dark matter X relic density for a large enough annihilation cross section. Now turning to the question of how to generate the primordial asymmetry in the vector-like sector which defines the final dark matter asymmetry and baryon asymmetry, let us further add two types of heavy diquarks with the couplings

$$\mathcal{L} \supset \lambda_{\Delta U_L} \Delta_u U_L U_L + \lambda_{\Delta U_R} \Delta_u U_R U_R + \lambda_{\Delta d} \Delta_d d_R d_R + \lambda_\chi \Delta_u \Delta_d \Delta_d \chi + \text{h.c.}, \tag{23}$$

where $\Delta_u : (\bar{6}, 1, -4/3)$, $\Delta_d : (\bar{6}, 1, 2/3)$ and the field χ breaks the local $U(1)_\chi$ symmetry under which X and U have non-trivial charges denoted by $q_\chi(U)$ and $q_\chi(X)$. For the SM fields this charge is simply $B-L$, which right away gives $q_\chi(\Delta_d) = -2/3$. The rest of the charges are determined in terms of the free charge $q_\chi(U)$,

$$q_\chi(\Delta_u) = -2q_\chi(U), \quad q_\chi(\chi) = 2q_\chi(U) + 4/3, \quad q_\chi(X) = 1/3 - q_\chi(U). \tag{24}$$

In order to forbid the dangerous proton decay induced by the operators $\mathcal{O} = X^2, S^2, X^2S^2, X^4, S^4$ [167], one needs to satisfy the condition

$$q_\chi(\mathcal{O}) \neq n(2q_\chi(U) + 4/3), \quad \text{where } n = 0, \pm 1, \pm 2, \cdots. \tag{25}$$

From Eq. (23) it follows that after χ acquires a VEV to break the $U(1)_\chi$ symmetry, Δ_u has the decay modes

$$\Delta_u \to \Delta_d^* \Delta_d^*, \quad \Delta_u \to \bar{U}\bar{U}, \tag{26}$$

and a *CP* asymmetry (between the above modes and their conjugate modes) can be obtained by interference of the tree level diagrams with one loop self-energy diagrams with two generations of Δ_u. Finally, the asymmetry generated in the vector-like quarks gets transferred to the dark matter asymmetry and baryon asymmetry via the λ_{XU} term in Eq. (21). This mechanism gives a ratio between the dark matter relic density and the baryon asymmetry given by

$$\frac{\Omega_{DM}/m_X}{\Omega_B/M_p} = \frac{79}{28}, \tag{27}$$

and in this model a dark matter mass $m_X \sim 2$ GeV. A typical prediction of this model is neutron–antineutron oscillations induced by the up-type and two down-type diquarks through the mixing of vector-like up-type quarks with the usual up quarks. However, such oscillations will be suppressed by the mixing.

One can similarly construct a leptogenesis model involving vector-like charged leptons. In case of the LRSM a generalization of the above scheme is straightforward; however, the lepton number violating gauge scattering processes involving a low scale W_R can rapidly wash out any primordial asymmetry generated above the mass scale of W_R. In fact, some of these gauge processes can continue to significantly reduce the generation of lepton asymmetry below the mass scale of W_R, thus the vector-like quark portals seem to be more promising in this case. Other alternatives include mechanisms like neutron–antineutron oscillation or some alternative LRSM scheme such as the Alternative Left–Right Symmetric Model [168] where the dangerous gauge scatterings can be avoided by means of special gauge quantum number assignments of a heavy neutrino [169]. Also note that, in general, one can utilize the singlet neutral vector-like lepton as a dark matter candidate by ensuring the stability against decay into usual LRSM fermions. Finally, the real bi-triplet scalar field η introduced to achieve successful gauge unification can also be a potential dark matter candidate.

In passing, we would like to mention that attempts have been made in the literature to address the broadness of the resonance using an invisible component of the scalar width. This in turn gives a large monojet signal which has been constrained from run-1 monojet searches at ATLAS [170] and CMS [171], see for example Ref. [39]. However, the monojet search data seems to disfavour the required rates to explain the broadness of the resonance. In our model, S can couple to $XX^\dagger$ and $YY^\dagger$ etc. leading to decay of S into them, which produces missing energy final state. This mode can be constrained from monojet searches as long as $M_{X,Y} < M_S/2$. Even without the scalar S being directly coupled to X's, its decay can produce a pair jets and X's via the λ_{XU} coupling term in Eqn. (21), which can again be constrained using dijet searches at ATLAS and CMS. In the discussion above we assume that these constrains are respected if $M_{X,Y} < M_S/2$. While for the case $M_{X,Y} > M_S/2$, the monojet and the dijet constraints are no longer applicable since in this case S will decay via a loop of $X(Y)$'s.

6. Conclusions

We have considered a unified framework to explain the recent diphoton excess reported by ATLAS and CMS around 750 GeV. The addition of vector-like fermions and a singlet scalar S to LRSM but without a scalar bidoublet explains the fermion masses and mixing via a universal seesaw mechanism. The diphoton signal with $\sigma(pp \to S \to \gamma\gamma) \approx 4 - 12$ fb can be explained in this model with TeV scale vector fermions. The broad width suggested by the ATLAS excess cannot be understood, though.

We successfully embed this model within an SO(10) GUT framework by introducing a real bi-triplet scalar. This additional scalar, which contains a potential DM candidate, allows the gauge couplings to unify at the scale $10^{17.7}$ GeV. We also discuss further possibilities in this class of LRSM models with vector-like fermions for mechanisms of baryogenesis and DM.

Acknowledgements

FFD would like to thank Suchita Kulkarni for useful discussions. PP is grateful to the Department of Science and Technology (DST), Govt. of India INSPIRE Fellowship DST/INSPIRE Fellowship/2014/IF140299. The work of SP is partly supported by DST, India under the financial grant SB/S2/HEP-011/2013. The work US is supported partly by the JC Bose National Fellowship grant under DST, India.

References

[1] CMS Collaboration, J. Olsen, CMS physics results from Run 2 presented on Dec. 15th. 2015, Search for new physics in high mass diphoton events in proton–proton collisions at 13 TeV.
[2] ATLAS Collaboration, M. Kado, ATLAS physics results from Run 2 presented on Dec. 15th 2015, ATLAS-CONF-2015-081.
[3] J. Ellis, D.S. Hwang, Does the 'Higgs' have spin zero?, J. High Energy Phys. 09 (2012) 071, arXiv:1202.6660.
[4] S. Di Chiara, L. Marzola, M. Raidal, First interpretation of the 750 GeV diphoton resonance at the LHC, arXiv:1512.04939.
[5] A. Pilaftsis, Diphoton signatures from heavy axion decays at LHC, arXiv:1512.04931.
[6] S. Knapen, T. Melia, M. Papucci, K. Zurek, Rays of light from the LHC, arXiv:1512.04928.
[7] M. Backovic, A. Mariotti, D. Redigolo, Di-photon excess illuminates Dark Matter, arXiv:1512.04917.
[8] E. Molinaro, F. Sannino, N. Vignaroli, Strong dynamics or axion origin of the diphoton excess, arXiv:1512.05334.
[9] R.S. Gupta, S. Jäger, Y. Kats, G. Perez, E. Stamou, Interpreting a 750 GeV diphoton resonance, arXiv:1512.05332.
[10] J. Ellis, S.A.R. Ellis, J. Quevillon, V. Sanz, T. You, On the interpretation of a possible ~ 750 GeV particle decaying into $\gamma\gamma$, arXiv:1512.05327.
[11] T. Higaki, K.S. Jeong, N. Kitajima, F. Takahashi, The QCD axion from aligned axions and diphoton excess, arXiv:1512.05295.
[12] Y. Mambrini, G. Arcadi, A. Djouadi, The LHC diphoton resonance and dark matter, arXiv:1512.04913.
[13] D. Buttazzo, A. Greljo, D. Marzocca, Knocking on new physics' door with a scalar resonance, arXiv:1512.04929.
[14] R. Franceschini, G.F. Giudice, J.F. Kamenik, M. McCullough, A. Pomarol, R. Rattazzi, M. Redi, F. Riva, A. Strumia, R. Torre, What is the gamma gamma resonance at 750 GeV?, arXiv:1512.04933.
[15] A. Angelescu, A. Djouadi, G. Moreau, Scenarii for interpretations of the LHC diphoton excess: two Higgs doublets and vector-like quarks and leptons, arXiv:1512.04921.
[16] B. Bellazzini, R. Franceschini, F. Sala, J. Serra, Goldstones in diphotons, arXiv:1512.05330.
[17] S.D. McDermott, P. Meade, H. Ramani, Singlet scalar resonances and the diphoton excess, arXiv:1512.05326.
[18] M. Low, A. Tesi, L.-T. Wang, A pseudoscalar decaying to photon pairs in the early LHC run 2 data, arXiv:1512.05328.
[19] C. Petersson, R. Torre, The 750 GeV diphoton excess from the goldstino superpartner, arXiv:1512.05333.
[20] Q.-H. Cao, Y. Liu, K.-P. Xie, B. Yan, D.-M. Zhang, A boost test of anomalous diphoton resonance at the LHC, arXiv:1512.05542.
[21] A. Kobakhidze, F. Wang, L. Wu, J.M. Yang, M. Zhang, LHC diphoton excess explained as a heavy scalar in top-seesaw model, arXiv:1512.05585.
[22] P. Agrawal, J. Fan, B. Heidenreich, M. Reece, M. Strassler, Experimental considerations motivated by the diphoton excess at the LHC, arXiv:1512.05775.
[23] W. Chao, R. Huo, J.-H. Yu, The minimal scalar-stealth top interpretation of the diphoton excess, arXiv:1512.05738.
[24] S. Fichet, G. von Gersdorff, C. Royon, Scattering light by light at 750 GeV at the LHC, arXiv:1512.05751.
[25] D. Curtin, C.B. Verhaaren, Quirky explanations for the diphoton excess, arXiv:1512.05753.
[26] C. Csaki, J. Hubisz, J. Terning, The minimal model of a diphoton resonance: production without gluon couplings, arXiv:1512.05776.
[27] D. Aloni, K. Blum, A. Dery, A. Efrati, Y. Nir, On a possible large width 750 GeV diphoton resonance at ATLAS and CMS, arXiv:1512.05778.
[28] S.V. Demidov, D.S. Gorbunov, On sgoldstino interpretation of the diphoton excess, arXiv:1512.05723.
[29] J.M. No, V. Sanz, J. Setford, See-saw composite Higgses at the LHC: linking naturalness to the 750 GeV di-photon resonance, arXiv:1512.05700.
[30] Y. Bai, J. Berger, R. Lu, A 750 GeV dark pion: cousin of a dark G-parity-odd WIMP, arXiv:1512.05779.
[31] S. Matsuzaki, K. Yamawaki, 750 GeV diphoton signal from one-family walking technipion, arXiv:1512.05564.
[32] B. Dutta, Y. Gao, T. Ghosh, I. Gogoladze, T. Li, Interpretation of the diphoton excess at CMS and ATLAS, arXiv:1512.05439.
[33] D. Becirevic, E. Bertuzzo, O. Sumensari, R.Z. Funchal, Can the new resonance at LHC be a CP-odd Higgs boson?, arXiv:1512.05623.
[34] P. Cox, A.D. Medina, T.S. Ray, A. Spray, Diphoton excess at 750 GeV from a radion in the bulk-Higgs scenario, arXiv:1512.05618.
[35] R. Martinez, F. Ochoa, C.F. Sierra, Diphoton decay for a 750 GeV scalar dark matter, arXiv:1512.05617.
[36] L. Bian, N. Chen, D. Liu, J. Shu, A hidden confining world on the 750 GeV diphoton excess, arXiv:1512.05759.
[37] J. Chakrabortty, A. Choudhury, P. Ghosh, S. Mondal, T. Srivastava, Di-photon resonance around 750 GeV: shedding light on the theory underneath, arXiv:1512.05767.
[38] A. Ahmed, B.M. Dillon, B. Grzadkowski, J.F. Gunion, Y. Jiang, Higgs-radion interpretation of 750 GeV di-photon excess at the LHC, arXiv:1512.05771.
[39] A. Falkowski, O. Slone, T. Volansky, Phenomenology of a 750 GeV singlet, arXiv:1512.05777.
[40] Q.-H. Cao, C.B. Jackson, W.-Y. Keung, I. Low, J. Shu, The Higgs mechanism and loop-induced decays of a scalar into two Z bosons, Phys. Rev. D 81 (2010) 015010, arXiv:0911.3398.
[41] I. Low, J. Lykken, G. Shaughnessy, Have we observed the Higgs (imposter)?, Phys. Rev. D 86 (2012) 093012, arXiv:1207.1093.
[42] W. Chao, Symmetries behind the 750 GeV diphoton excess, arXiv:1512.06297.
[43] L.M. Carpenter, R. Colburn, J. Goodman, Supersoft SUSY models and the 750 GeV diphoton excess, beyond effective operators, arXiv:1512.06107.
[44] E. Megias, O. Pujolas, M. Quiros, On dilatons and the LHC diphoton excess, arXiv:1512.06106.
[45] A. Alves, A.G. Dias, K. Sinha, The 750 GeV S-cion: where else should we look for it?, arXiv:1512.06091.
[46] E. Gabrielli, K. Kannike, B. Mele, M. Raidal, C. Spethmann, H. Veermäe, A SUSY inspired simplified model for the 750 GeV diphoton excess, arXiv:1512.05961.
[47] J.S. Kim, J. Reuter, K. Rolbiecki, R.R. de Austri, A resonance without resonance: scrutinizing the diphoton excess at 750 GeV, arXiv:1512.06083.
[48] R. Benbrik, C.-H. Chen, T. Nomura, Higgs singlet as a diphoton resonance in a vector-like quark model, arXiv:1512.06028.
[49] G.M. Pelaggi, A. Strumia, E. Vigiani, Trinification can explain the di-photon and di-boson LHC anomalies, arXiv:1512.07225.
[50] A.E.C. Hernández, I. Nisandzic, LHC diphoton 750 GeV resonance as an indication of $SU(3)_c \times SU(3)_L \times U(1)_X$ gauge symmetry, arXiv:1512.07165.
[51] J. de Blas, J. Santiago, R. Vega-Morales, New vector bosons and the diphoton excess, arXiv:1512.07229.
[52] P.S.B. Dev, D. Teresi, Asymmetric Dark Matter in the Sun and the diphoton excess at the LHC, arXiv:1512.07243.
[53] S.M. Boucenna, S. Morisi, A. Vicente, The LHC diphoton resonance from gauge symmetry, arXiv:1512.06878.
[54] K. Kulkarni, Extension of νMSM model and possible explanations of recent astronomical and collider observations, arXiv:1512.06836.
[55] M. Chala, M. Duerr, F. Kahlhoefer, K. Schmidt-Hoberg, Tricking Landau–Yang: how to obtain the diphoton excess from a vector resonance, arXiv:1512.06833.
[56] M. Bauer, M. Neubert, Flavor anomalies, the diphoton excess and a dark matter candidate, arXiv:1512.06828.
[57] J.M. Cline, Z. Liu, LHC diphotons from electroweakly pair-produced composite pseudoscalars, arXiv:1512.06827.
[58] L. Berthier, J.M. Cline, W. Shepherd, M. Trott, Effective interpretations of a diphoton excess, arXiv:1512.06799.
[59] J.S. Kim, K. Rolbiecki, R.R. de Austri, Model-independent combination of diphoton constraints at 750 GeV, arXiv:1512.06797.
[60] X.-J. Bi, Q.-F. Xiang, P.-F. Yin, Z.-H. Yu, The 750 GeV diphoton excess at the LHC and dark matter constraints, arXiv:1512.06787.
[61] J.J. Heckman, 750 GeV diphotons from a D3-brane, arXiv:1512.06773.
[62] F.P. Huang, C.S. Li, Z.L. Liu, Y. Wang, 750 GeV diphoton excess from cascade decay, arXiv:1512.06732.

[63] J. Cao, C. Han, L. Shang, W. Su, J.M. Yang, Y. Zhang, Interpreting the 750 GeV diphoton excess by the singlet extension of the Manohar–Wise model, arXiv:1512.06728.
[64] F. Wang, L. Wu, J.M. Yang, M. Zhang, 750 GeV diphoton resonance, 125 GeV Higgs and muon g-2 anomaly in deflected anomaly mediation SUSY breaking scenario, arXiv:1512.06715.
[65] O. Antipin, M. Mojaza, F. Sannino, A natural Coleman–Weinberg theory explains the diphoton excess, arXiv:1512.06708.
[66] X.-F. Han, L. Wang, Implication of the 750 GeV diphoton resonance on two-Higgs-doublet model and its extensions with Higgs field, arXiv:1512.06587.
[67] R. Ding, L. Huang, T. Li, B. Zhu, Interpreting 750 GeV diphoton excess with R-parity violation supersymmetry, arXiv:1512.06560.
[68] I. Chakraborty, A. Kundu, Diphoton excess at 750 GeV: singlet scalars confront naturalness, arXiv:1512.06508.
[69] D. Barducci, A. Goudelis, S. Kulkarni, D. Sengupta, One jet to rule them all: monojet constraints and invisible decays of a 750 GeV diphoton resonance, arXiv:1512.06842.
[70] W.S. Cho, D. Kim, K. Kong, S.H. Lim, K.T. Matchev, J.-C. Park, M. Park, The 750 GeV diphoton excess may not imply a 750 GeV resonance, arXiv:1512.06824.
[71] T.-F. Feng, X.-Q. Li, H.-B. Zhang, S.-M. Zhao, The LHC 750 GeV diphoton excess in supersymmetry with gauged baryon and lepton numbers, arXiv:1512.06696.
[72] D. Bardhan, D. Bhatia, A. Chakraborty, U. Maitra, S. Raychaudhuri, T. Samui, Radion candidate for the LHC diphoton resonance, arXiv:1512.06674.
[73] H. Han, S. Wang, S. Zheng, Scalar explanation of diphoton excess at LHC, arXiv:1512.06562.
[74] M. Dhuria, G. Goswami, Perturbativity, vacuum stability and inflation in the light of 750 GeV diphoton excess, arXiv:1512.06782.
[75] S. Chang, A simple $U(1)$ gauge theory explanation of the diphoton excess, arXiv:1512.06426.
[76] C. Han, H.M. Lee, M. Park, V. Sanz, The diphoton resonance as a gravity mediator of dark matter, arXiv:1512.06376.
[77] M.T. Arun, P. Saha, Gravitons in multiply warped scenarios – at 750 GeV and beyond, arXiv:1512.06335.
[78] G. Li, Y.-n. Mao, Y.-L. Tang, C. Zhang, Y. Zhou, S.-h. Zhu, A loop-philic pseudoscalar, arXiv:1512.08255.
[79] H. Han, S. Wang, S. Zheng, Dark matter theories in the light of diphoton excess, arXiv:1512.07992.
[80] J.A. Casas, J.R. Espinosa, J.M. Moreno, The 750 GeV diphoton excess as a first light on supersymmetry breaking, arXiv:1512.07895.
[81] J. Zhang, S. Zhou, Electroweak vacuum stability and diphoton excess at 750 GeV, arXiv:1512.07889.
[82] J. Liu, X.-P. Wang, W. Xue, LHC diphoton excess from colorful resonances, arXiv:1512.07885.
[83] K. Das, S.K. Rai, The 750 GeV diphoton excess in a $U(1)$ hidden symmetry model, arXiv:1512.07789.
[84] H. Davoudiasl, C. Zhang, A 750 GeV messenger of dark conformal symmetry breaking, arXiv:1512.07672.
[85] M. Cvetič, J. Halverson, P. Langacker, String consistency, heavy exotics, and the 750 GeV diphoton excess at the LHC, arXiv:1512.07622.
[86] M. Badziak, Interpreting the 750 GeV diphoton excess in minimal extensions of two-Higgs-doublet models, arXiv:1512.07497.
[87] K.M. Patel, P. Sharma, Interpreting 750 GeV diphoton excess in SU(5) grand unified theory, arXiv:1512.07468.
[88] S. Moretti, K. Yagyu, The 750 GeV diphoton excess and its explanation in 2-Higgs doublet models with a real inert scalar multiplet, arXiv:1512.07462.
[89] J. Gu, Z. Liu, Running after diphoton, arXiv:1512.07624.
[90] P.S.B. Dev, R.N. Mohapatra, Y. Zhang, Quark seesaw vectorlike fermions and diphoton excess, arXiv:1512.08507.
[91] N. Bizot, S. Davidson, M. Frigerio, J.L. Kneur, Two Higgs doublets to explain the excesses $pp \to \gamma\gamma(750\text{ GeV})$ and $h \to \tau^{\pm}\mu^{\mp}$, arXiv:1512.08508.
[92] L.A. Anchordoqui, I. Antoniadis, H. Goldberg, X. Huang, D. Lust, T.R. Taylor, 750 GeV diphotons from closed string states, arXiv:1512.08502.
[93] F. Goertz, J.F. Kamenik, A. Katz, M. Nardecchia, Indirect constraints on the scalar di-photon resonance at the LHC, arXiv:1512.08500.
[94] X.-J. Bi, R. Ding, Y. Fan, L. Huang, C. Li, T. Li, S. Raza, X.-C. Wang, B. Zhu, A promising interpretation of diphoton resonance at 750 GeV, arXiv:1512.08497.
[95] W. Chao, Neutrino catalyzed diphoton excess, arXiv:1512.08484.
[96] J. Gao, H. Zhang, H.X. Zhu, Diphoton excess at 750 GeV: gluon–gluon fusion or quark–antiquark annihilation?, arXiv:1512.08478.
[97] J.E. Kim, Is an axizilla possible for di-photon resonance?, arXiv:1512.08467.
[98] Q.-H. Cao, Y. Liu, K.-P. Xie, B. Yan, D.-M. Zhang, The diphoton excess, low energy theorem and the 331 model, arXiv:1512.08441.
[99] C. Cai, Z.-H. Yu, H.-H. Zhang, The 750 GeV diphoton resonance as a singlet scalar in an extra dimensional model, arXiv:1512.08440.
[100] F. Wang, W. Wang, L. Wu, J.M. Yang, M. Zhang, Interpreting 750 GeV diphoton resonance in the NMSSM with vector-like particles, arXiv:1512.08434.
[101] J. Cao, F. Wang, Y. Zhang, Interpreting the 750 GeV diphoton excess within topflavor seesaw model, arXiv:1512.08392.
[102] H. An, C. Cheung, Y. Zhang, Broad diphotons from narrow states, arXiv:1512.08378.
[103] Y.-L. Tang, S.-h. Zhu, NMSSM extended with vector-like particles and the diphoton excess on the LHC, arXiv:1512.08323.
[104] M. Son, A. Urbano, A new scalar resonance at 750 GeV: towards a proof of concept in favor of strongly interacting theories, arXiv:1512.08307.
[105] J.-C. Park, S.C. Park, Indirect signature of dark matter with the diphoton resonance at 750 GeV, arXiv:1512.08117.
[106] A. Salvio, A. Mazumdar, Higgs stability and the 750 GeV diphoton excess, arXiv:1512.08184.
[107] D. Chway, R. Dermíšek, T.H. Jung, H.D. Kim, Glue to light signal of a new particle, arXiv:1512.08221.
[108] E. Ma, Diphoton revelation of the utilitarian supersymmetric standard model, arXiv:1512.09159.
[109] K. Kaneta, S. Kang, H.-S. Lee, Diphoton excess at the LHC Run 2 and its implications for a new heavy gauge boson, arXiv:1512.09129.
[110] A.E.C. Hernández, The 750 GeV diphoton resonance can cause the SM fermion mass and mixing pattern, arXiv:1512.09092.
[111] I. Low, J. Lykken, Implications of gauge invariance on a heavy diphoton resonance, arXiv:1512.09089.
[112] P.V. Dong, N.T.K. Ngan, Phenomenology of the simple 3–3–1 model with inert scalars, arXiv:1512.09073.
[113] S. Kanemura, N. Machida, S. Odori, T. Shindou, Diphoton excess at 750 GeV in an extended scalar sector, arXiv:1512.09053.
[114] S. Kanemura, K. Nishiwaki, H. Okada, Y. Orikasa, S.C. Park, R. Watanabe, LHC 750 GeV diphoton excess in a radiative seesaw model, arXiv:1512.09048.
[115] S.K. Kang, J. Song, Top-phobic heavy Higgs boson as the 750 GeV diphoton resonance, arXiv:1512.08963.
[116] C.-W. Chiang, M. Ibe, T.T. Yanagida, Revisiting scalar quark hidden sector in light of 750-GeV diphoton resonance, arXiv:1512.08895.
[117] Y. Hamada, T. Noumi, S. Sun, G. Shiu, An O(750) GeV resonance and inflation, arXiv:1512.08984.
[118] Q.-H. Cao, S.-L. Chen, P.-H. Gu, Strong CP problem, neutrino masses and the 750 GeV diphoton resonance, arXiv:1512.07541.
[119] A. Dasgupta, M. Mitra, D. Borah, Minimal left–right symmetry confronted with the 750 GeV di-photon excess at LHC, arXiv:1512.09202.
[120] W. Chao, The diphoton excess from an exceptional supersymmetric standard model, arXiv:1601.00633.
[121] C.W. Murphy, Vector leptoquarks and the 750 GeV diphoton resonance at the LHC, arXiv:1512.06976.
[122] J. Chang, K. Cheung, C.-T. Lu, Interpreting the 750 GeV di-photon resonance using photon-jets in hidden-valley-like models, arXiv:1512.06671.
[123] W.-C. Huang, Y.-L.S. Tsai, T.-C. Yuan, Gauged two Higgs doublet model confronts the LHC 750 GeV di-photon anomaly, arXiv:1512.07268.
[124] L. Marzola, A. Racioppi, M. Raidal, F.R. Urban, H. Veermäe, Non-minimal CW inflation, electroweak symmetry breaking and the 750 GeV anomaly, arXiv:1512.09136.
[125] S. Chakraborty, A. Chakraborty, S. Raychaudhuri, Diphoton resonance at 750 GeV in the broken MRSSM, arXiv:1512.07527.
[126] Y. Nakai, R. Sato, K. Tobioka, Footprints of new strong dynamics via anomaly, arXiv:1512.04924.
[127] K. Harigaya, Y. Nomura, Composite models for the 750 GeV diphoton excess, arXiv:1512.04850.
[128] K. Ghorbani, H. Ghorbani, The 750 GeV diphoton excess from a pseudoscalar in fermionic dark matter scenario, arXiv:1601.00602.
[129] L.J. Hall, K. Harigaya, Y. Nomura, 750 GeV diphotons: implications for supersymmetric unification, arXiv:1512.07904.
[130] X.-F. Han, L. Wang, L. Wu, J.M. Yang, M. Zhang, Explaining 750 GeV diphoton excess from top/bottom partner cascade decay in two-Higgs-doublet model extension, arXiv:1601.00534.
[131] N. Bonne, G. Moreau, Reproducing the Higgs boson data with vector-like quarks, Phys. Lett. B 717 (2012) 409–419, arXiv:1206.3360.
[132] A. Angelescu, A. Djouadi, G. Moreau, Vector-like top/bottom quark partners and Higgs physics at the LHC, arXiv:1510.07527.
[133] G. Moreau, Constraining extra-fermion(s) from the Higgs boson data, Phys. Rev. D 87 (1) (2013) 015027, arXiv:1210.3977.
[134] B.C. Allanach, P.S.B. Dev, S.A. Renner, K. Sakurai, Di-photon excess explained by a resonant sneutrino in R-parity violating supersymmetry, arXiv:1512.07645.
[135] U. Danielsson, R. Enberg, G. Ingelman, T. Mandal, The force awakens – the 750 GeV diphoton excess at the LHC from a varying electromagnetic coupling, arXiv:1601.00624.
[136] Y. Jiang, Y.-Y. Li, T. Liu, 750 GeV resonance in the gauged $U(1)'$-extended MSSM, arXiv:1512.09127.
[137] CMS Collaboration, V. Khachatryan, et al., Search for heavy neutrinos and W bosons with right-handed couplings in proton–proton collisions at $\sqrt{s} = 8$ TeV, Eur. Phys. J. C 74 (11) (2014) 3149, arXiv:1407.3683.

[138] F.F. Deppisch, T.E. Gonzalo, S. Patra, N. Sahu, U. Sarkar, Signal of right-handed charged gauge bosons at the LHC?, Phys. Rev. D 90 (5) (2014) 053014, arXiv:1407.5384.
[139] F.F. Deppisch, T.E. Gonzalo, S. Patra, N. Sahu, U. Sarkar, Double beta decay, lepton flavor violation, and collider signatures of left–right symmetric models with spontaneous D-parity breaking, Phys. Rev. D 91 (1) (2015) 015018, arXiv:1410.6427.
[140] P.S. Bhupal Dev, R.N. Mohapatra, Unified explanation of the $eejj$, diboson and dijet resonances at the LHC, Phys. Rev. Lett. 115 (18) (2015) 181803, arXiv:1508.02277.
[141] F.F. Deppisch, L. Graf, S. Kulkarni, S. Patra, W. Rodejohann, N. Sahu, U. Sarkar, Reconciling the 2 TeV excesses at the LHC in a linear seesaw left–right model, Phys. Rev. D 93 (2016) 013011, arXiv:1508.05940.
[142] D. Guadagnoli, R.N. Mohapatra, I. Sung, Gauged flavor group with left–right symmetry, J. High Energy Phys. 04 (2011) 093, arXiv:1103.4170.
[143] G.C. Joshi, R.R. Volkas, Extended weak isospin and fermion masses in a unified model, Phys. Rev. D 45 (1992) 1711–1719.
[144] G. Aldazabal, L.E. Ibanez, F. Quevedo, A D^- brane alternative to the MSSM, J. High Energy Phys. 02 (2000) 015, arXiv:hep-ph/0001083.
[145] J.P. Conlon, A. Maharana, F. Quevedo, Towards realistic string vacua, J. High Energy Phys. 05 (2009) 109, arXiv:0810.5660.
[146] J.C. Pati, A. Salam, Lepton number as the fourth color, Phys. Rev. D 10 (1974) 275–289.
[147] R. Mohapatra, J.C. Pati, A natural left–right symmetry, Phys. Rev. D 11 (1975) 2558.
[148] G. Senjanović, R.N. Mohapatra, Exact left–right symmetry and spontaneous violation of parity, Phys. Rev. D 12 (1975) 1502.
[149] G. Senjanović, Spontaneous breakdown of parity in a class of gauge theories, Nucl. Phys. B 153 (1979) 334–364.
[150] R.N. Mohapatra, G. Senjanović, Neutrino mass and spontaneous parity violation, Phys. Rev. Lett. 44 (1980) 912.
[151] R.N. Mohapatra, G. Senjanovic, Neutrino masses and mixings in gauge models with spontaneous parity violation, Phys. Rev. D 23 (1981) 165.
[152] P. Minkowski, $\mu \to e\gamma$ at a rate of one out of 10^9 muon decays?, Phys. Lett. B 67 (1977) 421–428.
[153] M. Gell-Mann, P. Ramond, R. Slansky, Complex spinors and unified theories, Conf. Proc. C790927 (1979) 315–321, arXiv:1306.4669.
[154] T. Yanagida, Horizontal symmetry and masses of neutrinos, Conf. Proc. C7902131 (1979) 95–99.
[155] J. Schechter, J.W.F. Valle, Neutrino masses in SU(2) $\times$ U(1) theories, Phys. Rev. D 22 (1980) 2227.
[156] J. Schechter, J.W.F. Valle, Neutrino decay and spontaneous violation of lepton number, Phys. Rev. D 25 (1982) 774.
[157] S. Patra, Neutrinoless double beta decay process in left–right symmetric models without scalar bidoublet, Phys. Rev. D 87 (1) (2013) 015002, arXiv:1212.0612.
[158] E. Ma, S. Sarkar, U. Sarkar, Scale of $SU(2)_R$ symmetry breaking and leptogenesis, Phys. Lett. B 458 (1999) 73–78, arXiv:hep-ph/9812276.
[159] J.-M. Frere, T. Hambye, G. Vertongen, Is leptogenesis falsifiable at LHC?, J. High Energy Phys. 01 (2009) 051, arXiv:0806.0841.
[160] F.F. Deppisch, J. Harz, M. Hirsch, W.-C. Huang, H. Pas, Falsifying high-scale baryogenesis with neutrinoless double beta decay and lepton flavor violation, Phys. Rev. D 92 (3) (2015) 036005, arXiv:1503.04825.
[161] F.F. Deppisch, J. Harz, M. Hirsch, Falsifying high-scale leptogenesis at the LHC, Phys. Rev. Lett. 112 (2014) 221601, arXiv:1312.4447.
[162] P.S. Bhupal Dev, C.-H. Lee, R.N. Mohapatra, Leptogenesis constraints on the mass of right-handed gauge bosons, Phys. Rev. D 90 (9) (2014) 095012, arXiv:1408.2820.
[163] M. Dhuria, C. Hati, R. Rangarajan, U. Sarkar, The $eejj$ excess signal at the LHC and constraints on leptogenesis, J. Cosmol. Astropart. Phys. 1509 (09) (2015) 035, arXiv:1502.01695.
[164] M. Dhuria, C. Hati, R. Rangarajan, U. Sarkar, Falsifying leptogenesis for a TeV scale $W_R^\pm$ at the LHC, Phys. Rev. D 92 (3) (2015) 031701, arXiv:1503.07198.
[165] P.S. Bhupal Dev, C.-H. Lee, R.N. Mohapatra, TeV scale lepton number violation and baryogenesis, J. Phys. Conf. Ser. 631 (1) (2015) 012007, arXiv:1503.04970.
[166] P. Fileviez Perez, M.B. Wise, Baryon asymmetry and dark matter through the vector-like portal, J. High Energy Phys. 05 (2013) 094, arXiv:1303.1452.
[167] J.M. Arnold, B. Fornal, M.B. Wise, Simplified models with baryon number violation but no proton decay, Phys. Rev. D 87 (2013) 075004, arXiv:1212.4556.
[168] E. Ma, Particle dichotomy and left–right decomposition of $E(6)$ superstring models, Phys. Rev. D 36 (1987) 274.
[169] M. Dhuria, C. Hati, R. Rangarajan, U. Sarkar, Explaining the CMS $eejj$ and $e\not{p}_T jj$ excess and leptogenesis in superstring inspired E_6 models, Phys. Rev. D 91 (5) (2015) 055010, arXiv:1501.04815.
[170] ATLAS Collaboration, G. Aad, et al., Search for new phenomena in final states with an energetic jet and large missing transverse momentum in pp collisions at $\sqrt{s} = 8$ TeV with the ATLAS detector, Eur. Phys. J. C 75 (7) (2015) 299, arXiv:1502.01518;
ATLAS Collaboration, G. Aad, et al., Eur. Phys. J. C 75 (9) (2015) 408 (Erratum).
[171] CMS Collaboration, V. Khachatryan, et al., Search for dark matter, extra dimensions, and unparticles in monojet events in proton–proton collisions at $\sqrt{s} = 8$ TeV, Eur. Phys. J. C 75 (5) (2015) 235, arXiv:1408.3583.